ISAS - INTERNATIONAL SCHOOL
FOR ADVANCED STUDIES

Rhythmic activity induced by pharmacological block of synaptic inhibition in the neonatal rat spinal cord.

Thesis submitted for the degree of "Doctor Philosophiae"

ACADEMIC YEAR 1996-97

CANDIDATE
Dr. Enrico Bracci

SUPERVISOR
Prof. Andrea Nistri

SISSA - SCUOLA
INTERNAZIONALE
SUPERIORE
DI STUDI AVANZATI
TRIESTE
Strada Costiera 11

TRIESTE

Table of contents

ACKNOWLEDGMENTS

I wish to express my gratitude to Professor A. Nistri for giving me the opportunity to perform this work and for his careful and stimulating supervision. I would like to thank Professors A. Cattaneo, E. Cherubini and A. Nistri for creating a propitious scientific environment at the Biophysics Sector of SISSA. I am indebted to Drs. L. Ballerini and M. Beato with whom I have fruitfully and pleasantly collaborated during my PhD course.

NOTE

Part of the data reported in the present thesis have been published in the articles listed below. In all cases the candidate personally performed the experimental work and data analysis, and contributed to paper writing.

- Ballerini L, **Bracci E** and Nistri A. Desensitization of AMPA receptors limits the amplitude of EPSPs and the excitability of motoneurons of the rat isolated spinal cord. Eur J Neurosci (1995). 7, 1229-1234.

- **Bracci E**, Ballerini L and Nistri A. Spontaneous rhythmic bursts induced by pharmacological block of inhibition in lumbar motoneurons of the neonatal rat spinal cord. J Neurophysiol (1996) 75, 640-647.

- **Bracci E**, Ballerini L and Nistri A. Localization of rhythmogenic networks responsible for spontaneous bursts induced by strychnine and bicuculline in the rat isolated spinal cord. J Neurosci (1996) 16, 7063-7076.

- Ballerini L, **Bracci E** and Nistri A. Pharmacological block of the elctrogenic sodium pump disrupts rhythmic bursting induced by strychnine and bicuculline in the neonatal rat spinal cord. J Neurophysiol (1997) 77, 17-23).

- **Bracci E**, Beato M and Nistri A. Afferent inputs modulate the activity of a rhythmic burst generator in the rat disinhibited spinal cord in vitro. J Neurophysiol (1997) (accepted January 1st 1997, in press).

ABSTRACT

The present study has investigated the spontaneous rhythmic activity induced in the in vitro neonatal rat spinal cord by pharmacological block of synaptic inhibition. Intracellular recordings from lumbar motoneurons under current-clamp conditions revealed that the $GABA_A$ receptor antagonist bicuculline (20 μM) elicited irregular paroxysmal bursting activity, while no bursting was observed in the presence of the glycine receptor antagonist strychnine (1 μM). Nevertheless, an extremely regular rhythmic bursting pattern was consistently observed when bicuculline and strychnine were simultaneously applied to the cord. Rhythmic bursts were large amplitude (>20 mV) depolarizing events appearing at a frequency of about 2/min. Individual bursts lasted for several s and comprised several intraburst oscillations at 2-6 Hz. The efficacy of bicuculline and strychnine antagonism was tested with exogenous application of GABA or glycine, that failed to affect dorsal root (DR) evoked motoneuron responses in the presence of the respective antagonist. Bursting activity persisted in the presence of the $GABA_B$ antagonist CGP 52 432 (10 μM). Under voltage-clamp conditions, rhythmic bursts were detected as rhythmic currents with inward polarity at negative holding potentials and outward polarity at positive holding potentials. These results suggest that bursts were synaptically generated on motoneurons via excitatory receptors. Simultaneous recordings from ventral roots revealed that bursting activity was strongly synchronized throughout all lumbar motoneurons. Nevertheless, antidromic stimulation of a motoneuronal population failed to affect bursting timecourse, suggesting that rhythmic bursts were produced by a premotoneuronal network. Glutamatergic transmission was shown to play a prominent role in such a network since bursts were suppressed by the non NMDA receptor antagonist CNQX (20 μM) and were abolished or slowed down by NMDA receptor antagonists APV (20 μM) or CPP (10 μM). In the presence of cyclothiazide, a selective blocker of AMPA receptor desensitization, bursting was accelerated and lost its sensitivity to NMDA receptor antagonists. Rhythmic bursts were accelerated up to cycle periods < 10 s by several agents that are also able to induce or accelerate locomotor activity, including 5-HT, NMDA or increases in extracellular potassium. Several cellular mechanisms potentially involved in rhythmogenesis were

tested in the disinhibited spinal cord. Apamin (0.4 μM), a selective blocker of calcium-activated potassium conductances shortened both cycle period and burst duration without changing their regular rhythmicity. Block of inward rectifier conductances by caesium (4 mM) reversibly hyperpolarized the motoneuron membrane potential and largely increased burst duration, while cycle period and rhythmicity remained unaltered. Ouabain (10 μM), strophanthidin (4 μM) or potassium-free solutions disrupted rhythmic bursting which was changed into irregularly occurring paroxysmal events of variable duration. These findings suggested that the electrogenic sodium pump operation played a prominent pacemaker role in the disinhibited spinal cord. The interaction of afferent synaptic inputs with the rhythmogenic network was also studied. Repetitive DR stimulations entrained bursts on a one-to-one basis when delivered at periods between 2 and 20 s. Within this range, evoked burst duration strongly decreased when the stimulation period was reduced; these data enlightened a strong plasticity of the rhythmogenic network. At stimulation period < 2s bursting activity became uncoupled from DR stimuli and resumed its spontaneous periodicity. Similar results were obtained with stimulation of the ventrolateral descending fibres. Localization of the rhythmogenic networks was investigated by means of selective lesions. Complete coronal spinal transection at L3 or L6 level did not block bursting recorded from L5 or L2 roots, respectively. Longitudinal midsagittal hemisection preserved bursting activity in both disconnected sides. Removal of dorsal horns did not affect burst frequency or left-to-right synchronicity while it reduced burst duration. An isolated ventral quadrant displayed enhanced burst frequency while bursts became very short events, suggesting that the oscillatory intraburst structure was dependent on a larger circuitry comprising either both ventral horns or one side of the spinal cord.

The present findings show that regular spinal rhythmicity does not require synaptic inhibition and raise the possibility that a mechanism based on excitatory processes could underlie rhythm generation during stereotyped motor activities. It is proposed that in the absence of synaptic inhibition bursts might arise from reciprocal excitation of a group of spinal interneurons and that an outward current generated by the electrogenic sodium pump in such interneurons might be responsible for maintenance of quiescent interburst intervals.

INTRODUCTION

1. Synchronous rhythmic behaviour is widespread in the mammalian central nervous system.

The ability to generate synchronized oscillatory activity appears to be a distinctive feature of the mammalian central nervous system (CNS), in which this kind of behaviour can be recorded under certain conditions from several neural structures. Rhythmic activity generated by assemblies of neurons can be detected by means of different recording techniques. Electroencephalographic recordings are used to detect surface field potentials arising from the collective activity of a large number of neurons. Intratissue extracellular recordings, in which an electrode is placed in close proximity to nerve cells or fibres, are used to detect the activity of a more limited number of neural units. Intracellular recordings, performed by means of sharp glass microelectrodes or patch-clamp electrodes, allow monitoring the timecourse of single neuron membrane potential (or transmembrane current if the membrane potential is clamped by an amplifier).

The introduction of intracellular recordings revealed that the single-neuron correlate of the electroencephalographic (EEG) waves is constituted by membrane potential oscillations comprising periodic patterns of action potentials (Steriade et al, 1993, Steriade et al, 1994; Bal et al, 1995). These oscillations take place synchronously in a large number of neurons: it is this feature that allows EEG techniques to detect this type of behaviour with distal electrodes, that can only monitor spatially-averaged population activity.

Traditionally, two different mechanisms by which a network of neurons can produce rhythmic behaviours are considered (Steriade et al, 1993). Rhythmic activity can be generated by a network of neurons by means of synaptic contacts between its elements

even if these elements are not intrinsically able to produce a similar rhythmic behaviour when synaptically isolated (network-driven rhythmicity). Alternatively, neurons provided with an intrinsic ability to produce membrane potential oscillations (due to particular voltage-dependent conductances) can be responsible for rhythmic pattern generation (pacemaker neuron-driven rhythmicity), like in the case of cardiac tissue, in which rhythmic contractions are generated by intrinsic cellular oscillations (Di Francesco et al, 1986). Even if the distinction between network-driven and pacemaker neuron-driven rhythmogenesis is often useful, it is important to note that synaptic contacts are always necessary to assure synchronization of individual oscillators, so that "oscillations of isolated neurons can be transformed by interaction with other neurons into less stereotyped rhythmic patterns" (Steriade et al, 1993). Furthermore, neuronal intrinsic membrane properties will ultimately affect network-driven activity, since they determine the input-output relation for any nerve cell, so that in certain cases it could be difficult to establish whether a neuron is actually generating its "intrinsic" oscillations within a rhythmic network.

As far as the forebrain is concerned, several rhythmic patterns can be detected during different behavioural states. In particular, different phases of sleep are accompanied by major changes in EEG recordings, that undergo a transition from low amplitude-fast frequency to large amplitude-low frequency activity when a mammal falls asleep. Thalamic and cortical networks are involved in the generation of the slow wave patterns that characterize resting sleep (reviewed by Steriade et al, 1994). Thalamic networks have been shown to produce "spindle waves" , i.e. waxing and waning bursts of oscillations (at 7-14 Hz) that characterize the early phase of sleep. These oscillations have been shown to arise from a dynamic interplay between thalamocortical and reticular thalamic neurons, connected by an excitatory-inhibitory synaptic loop that plays a major role in the generation of this behaviour (Bal et al, 1995; Lee and McCormick, 1996; Bal and McCormick 1996). Delta waves (1-4 Hz) appear in a later phase of sleep and arise in cortical layers II-V. Unlike spindle waves, that rely upon synaptic interactions, delta oscillations can also be produced by isolated neurons via an interplay of two intrinsic membrane currents (the hyperpolarization-activated cation current I_h and the transient, low-threshold calcium current I_t; Steriade et al, 1993);

even in this case, however, synaptic connections are obviously needed in order to ensure synchronization. Slow sleep oscillations (<1Hz) are also generated within cortical circuits and appear to be synaptically generated in pyramidal cells (Steriade et al, 1993).

Fast spontaneous oscillations (20-100 Hz) have been recorded in aroused animals in several parts of the cortex (following sensory stimulation) as well as in the hippocampus (reviewed by Engel et al, 1992; Jefferys et al, 1996); this type of evidence suggested that "the conventional notion of a totally desynchronized cortical activity upon arousal should be revised as fast rhythms are enhanced and synchronized within intracortical networks during brain activation" (Steriade et al, 1996). In the hippocampus, in addition to fast oscillations, the so called theta rhythm (4-12 Hz) seems to be a prominent feature, especially during spatial exploration (Bragin et al, 1995). As far as pathological conditions are concerned, rhythmic paroxysmal synchronization of neuronal activity is well known to take place during epileptic seizures (Dichter, 1988). Interestingly, a particular epileptic syndrome, namely absence seizures, is considered to be a "perversion" of spindle waves oscillations associated with a decreased functionality of fast synaptic inhibition (Bal et al 1995).

While important progress has been undoubtedly achieved in the understanding of the cellular and network mechanisms that underlie the generation of some of these patterns (Steriade et al, 1993; Contreras and Steriade 1996; Lee and McCormick, 1996; Bal and McCormick 1996), the overwhelming complexity of forebrain organization has so far prevented a satisfactory, widely accepted comprehension of the functional role of the various rhythmic patterns.

2. Central pattern generators underlie repetitive motor activities

An important class of rhythmic patterns in the CNS is the one expressed by motoneurons. Such patterns are generated by neuronal networks located in the spinal cord or in the brainstem and are related to the generation of stereotypic motor tasks such as mastication, respiration, locomotion, scratching etc. The basic features of such motor activities have been shown to be generated by central networks even in the absence of descending inputs and of sensory afferent feedback (for a review see

Grillner, 1981 and Rossignol, 1996), although this feedback is necessary to ensure correct adaptation of motor output to environmental changes (for a discussion see Katz, 1996). The neural networks able to produce rhythmic patterns of motor activity in the absence of sensory feedback are referred to as central pattern generators (CPGs). Unlike oscillatory patterns generated in the forebrain, the functional role of patterns generated by spinal (or brainstem) networks is generally well identified, since the corresponding motor activities can be easily observed at a macroscopical level in the intact animal. Nevertheless, the cellular and network mechanisms underlying central pattern generation in mammals are still unclear, nor it is clear whether a common rhythmogenic mechanism supports disparate motor patterns, as discussed in the following subheadings.

3. Organization of the spinal cord

The spinal cord is the most caudal structure of the central nervous system (CNS) and, with its cylindrical appearance, the one that most closely resembles in shape the embryonic neural tube from which the CNS develops. At its rostral end, the spinal cord borders with the most caudal part of the brainstem (the medulla), that can be viewed as an intracranial, enlarged extension of the spinal cord. Since it contains most of the motoneurons innervating the body muscles, the spinal cord plays a major role in the motor function of vertebrates, and is considered as the lower station of a hierarchical motor system including the brainstem and the motor cortex. By receiving proprioceptive and sensory input from internal organs, muscles and skin, the spinal cord also plays a crucial role in relaying and/or processing somatosensory information. Spinal networks are connected to supraspinal centers by ascending and descending pathways. Important relay stations of the ascending pathways from the spinal cord to the cerebral cortex are found in the brainstem and in the thalamus, while descending pathways involve, in addition to direct corticospinal tracts, the basal ganglia, the cerebellum and the brainstem (Brodal, 1981; Kuypers, 1981).

As far as the basic structure is concerned, the anatomical organization of the spinal cord appears to be the same in the different mammals in which it has been studied (Rexed, 1964). The spinal cord is contained in the vertebral column through which the

spinal nerves emerge via intervertebral foramina. Spinal nerves are mixed since they contain sensory and motor fibres. Sensory primary afferent fibres (whose cellular bodies are contained in the dorsal root ganglia outside the cord) enter the spinal cord at several levels from the dorsal aspect through the dorsal roots (DR). At the same levels, efferent motoneuronal axons leave the cord ventrally through the ventral roots (VR). VR and DR ipsilateral pairs fuse near the DR ganglia to form mixed spinal nerves. The spinal cord is subdivided into cervical, thoracic, lumbar and sacral segments. Two enlargements characterize the spinal cord at cervical and lumbar level, where a larger number of motoneurons innervating forelimbs and hindlimbs, respectively, is located. The outer part of the spinal cord is formed by white matter that mainly contains ascending (in the dorsal, lateral and ventral columns of the white matter) and descending axons (ventral columns); the inner region is formed by grey matter mainly containing the nerve cells. A cross section of the spinal cord (fig I.1, top) reveals the symmetrical, butterfly-shaped appearance of the grey matter, with each hemicord formed by one dorsal horn (elongated toward the point where dorsal roots enter the cord), an intermediate region and one large ventral horn. The schematic drawing of fig I.1 (bottom) also shows the nine laminae (1-10) in which the grey matter is divided, plus the grey matter surrounding the central canal (10). Such laminae, originally described by Rexed (1952), are characterized by different morphological features and their surfaces are roughly parallel to the ventral and dorsal surface of the cord; most of them extend longitudinally along the whole length of the cord, even though their shape can vary at the cervical and lumbar enlargements.

Motoneurons are the only neurons that make synaptic contacts with nonneural tissue (i.e. muscle fibres); motoneurons innervating a given muscle in the limbs or trunk lie clustered in individual motor nuclei; such nuclei are cigar-shaped, longitudinal structures located in the ventral part of the ventral horn (lamina 9); at lumbar level, motor nuclei expand medially and laterally, forming two or more distinct motor columns (see fig I.1, adapted from Paxinos and Watson, 1986). Two kinds of motoneurons are present in mammals (even if motoneurons with mixed features are also reported): *alpha* motoneurons, innervating extrafusal striated muscle fibres and producing muscular output force and *gamma* motoneurons that innervate intrafusal

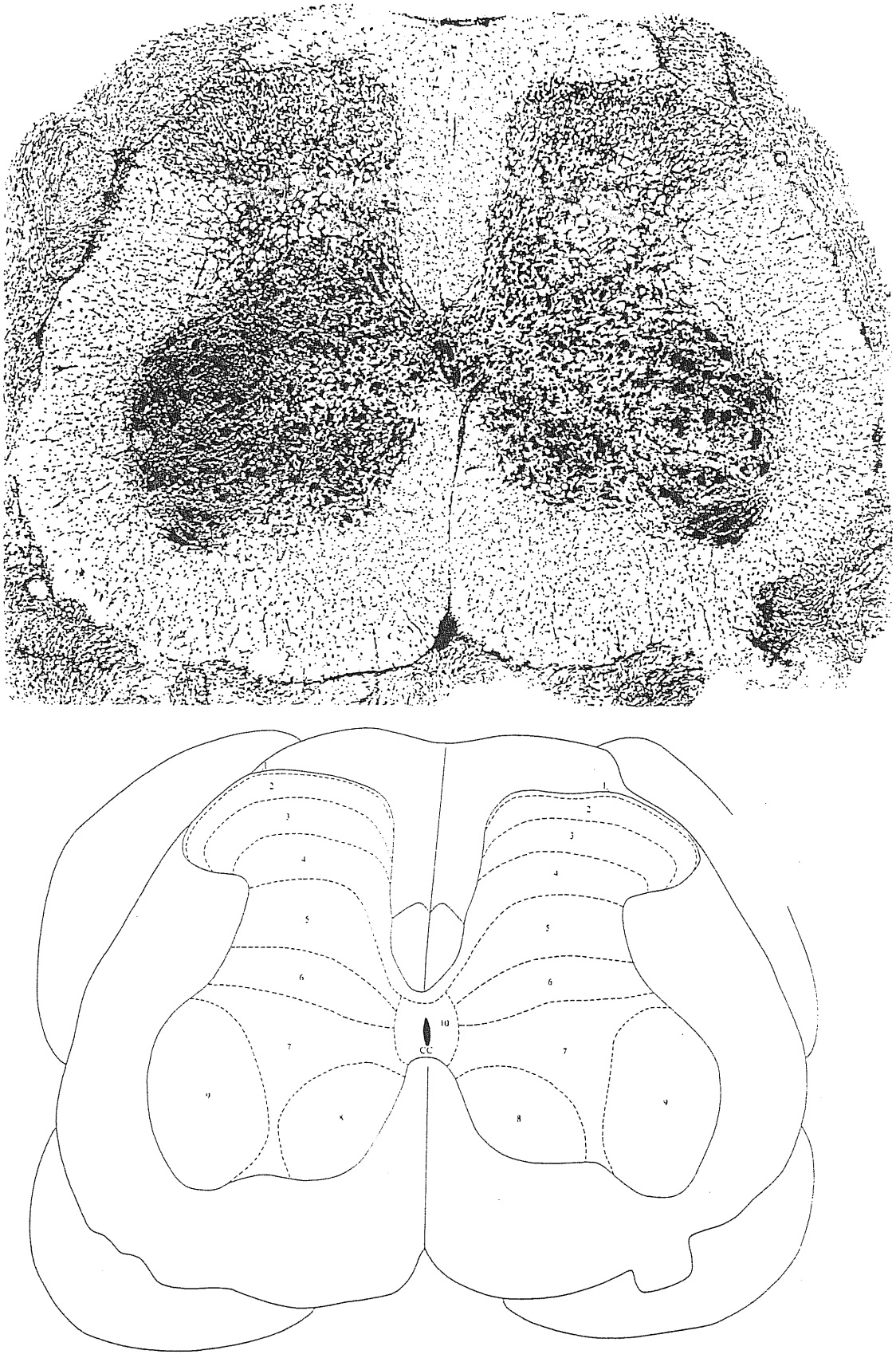

Fig I.1. *Cross section of the spinal cord at lumbar level.*
Cross section at L5 level of the spinal cord of an adult rat (top) and schematic drawing of laminae 1-10 (bottom). Motoneurons are mainly contained in laminae 9 and 8. CC: central canal. (Adapted from Paxinos and Watson, 1986).

muscle fibres within muscle spindle receptors and modulate the sensitivity to muscle displacement of group Ia or II afferents that innervate such receptors. Group Ia afferents convey centrally information about muscle length while group II afferents signal muscle length variation. Another important group of afferents (Ib) arises from Golgi tendon organs and signal muscle tension. The conduction velocity of myelinated fibres is proportional to fibre diameter (Hunt, 1954). Group Ia afferents are the fastest afferent fibres (90-120 m/s in the adult cat); group Ib afferents are slightly slower (70-90 m/s) and group II afferents conduct at 35-75 m/s (Hunt, 1954). Afferent fibres conveying somatic or pain sensation are also classified according to their diameter and conduction velocity: Aβ>Aδ>C. With the exception of C group, all these afferents are composed by myelinated fibres. The synapses of primary afferents on spinal (or brainstem) neurons are thought to be always of excitatory type (Burke, 1990). The only afferents that are thought to impinge monosynaptically on motoneurons are group Ia fibres (these fibres also excite several classes of interneurons in the dorsal and ventral laminae). In vitro experiments have shown that the excitatory action of Ia fibres on postsynaptic targets is mediated by the amino acid glutamate and that this neurotransmitter acts both on N-Methyl-D-Aspartate (NMDA) and non NMDA receptor subtypes (Pinco and Lev-Tov, 1993a). These glutamate-gated channels are permeable to cations but are responsible for excitatory post synaptic potentials (EPSPs) characterized by different timecourse and voltage dependence (Mayer and Westbrook, 1987; Jonas and Spruston 1994).

Group I and II fibres, as well as cutaneous afferents, are involved in several spinal reflexes that have been extensively investigated starting from the last century (reviewed by Baldissera et al, 1981). The study of mono- and polysynaptic reflex pathways has cast light over a number of relatively simple spinal circuits. These include (among others) the circuits mediating the *stretch reflex* (in which stretching a muscle excites Ia afferents that in turn excite motoneurons innervating the same muscle, thus promoting its contractions) *reciprocal inhibition,* in which Ia afferents arising from a given muscle excite a class of interneurons located in the intermediate laminae (Ia interneurons) that in turn inhibit motoneurons innervating antagonist muscles; *recurrent inhibition* of motoneurons by a group of interneurons (Renshaw cells), that are excited by

motoneuron axon collaterals (reviewed by Baldissera et al, 1981). The spinal circuits related to recurrent and reciprocal inhibition and elucidated by reflex studies are illustrated in the diagram of fig I.2 (adapted from Baldissera et al, 1981).

Synaptic inhibition of motoneurons by the interneurons activated in these reflex pathways has been shown to be mediated by the inhibitory amino acids glycine and GABA that act on ligand-gated channels (i.e. glycine and $GABA_A$ receptors) mainly permeable to chloride (Burke, 1990; Gao and Ziskind-Conhaim, 1995). Motoneuron terminals release acetylcholine at the neuromuscular junction (Dale et al, 1936; Matthews-Bellinger and Salpeter, 1978) and at synapses that they form onto interneurons and other motoneurons (Eccles and al, 1954). Stimulation of muscle or cutaneous afferents was found to reduce group Ia EPSPs in motoneurons without producing detectable inhibitory post synaptic potentials (IPSPs). This phenomenon is associated with a depolarization of the primary afferents (PAD) and is considered to be due to a presynaptic axo-axonic inhibition of the Ia terminals (Burke, 1990). Presynaptic inhibition is thought to be mediated by $GABA_A$ receptors that exert a depolarizing action on primary afferent terminals presumably due to the fact that the chloride equilibrium potential is more positive than the resting membrane potential in these terminals (Burke, 1990; Stuart and Redman 1992); an involvement of $GABA_B$ receptor subtypes, whose activation causes no depolarization in primary afferents, has also been shown and has been suggested to be due to reduced influx of calcium in the terminals (Burke, 1990). Presynaptic inhibition is fully abolished by the GABA antagonist picrotoxin (Nistri, 1983; Sivilotti and Nistri, 1991).

Despite the important progress achieved in the comprehension of reflex activity, a satisfactory understanding of the enormous complexity of the spinal organization is undoubtedly still far to come. Furthermore, the apparent simplicity of some spinal reflexes has been revealed to be deceptive; reflex pathways are not independent of each other: different reflexes may involve common classes of interneurons; furthermore these interneurons (and the reflexes to which they participate) can in turn be strongly modulated by supraspinal inputs or by other spinal networks such as central pattern generators (reviewed by Burke, 1990).

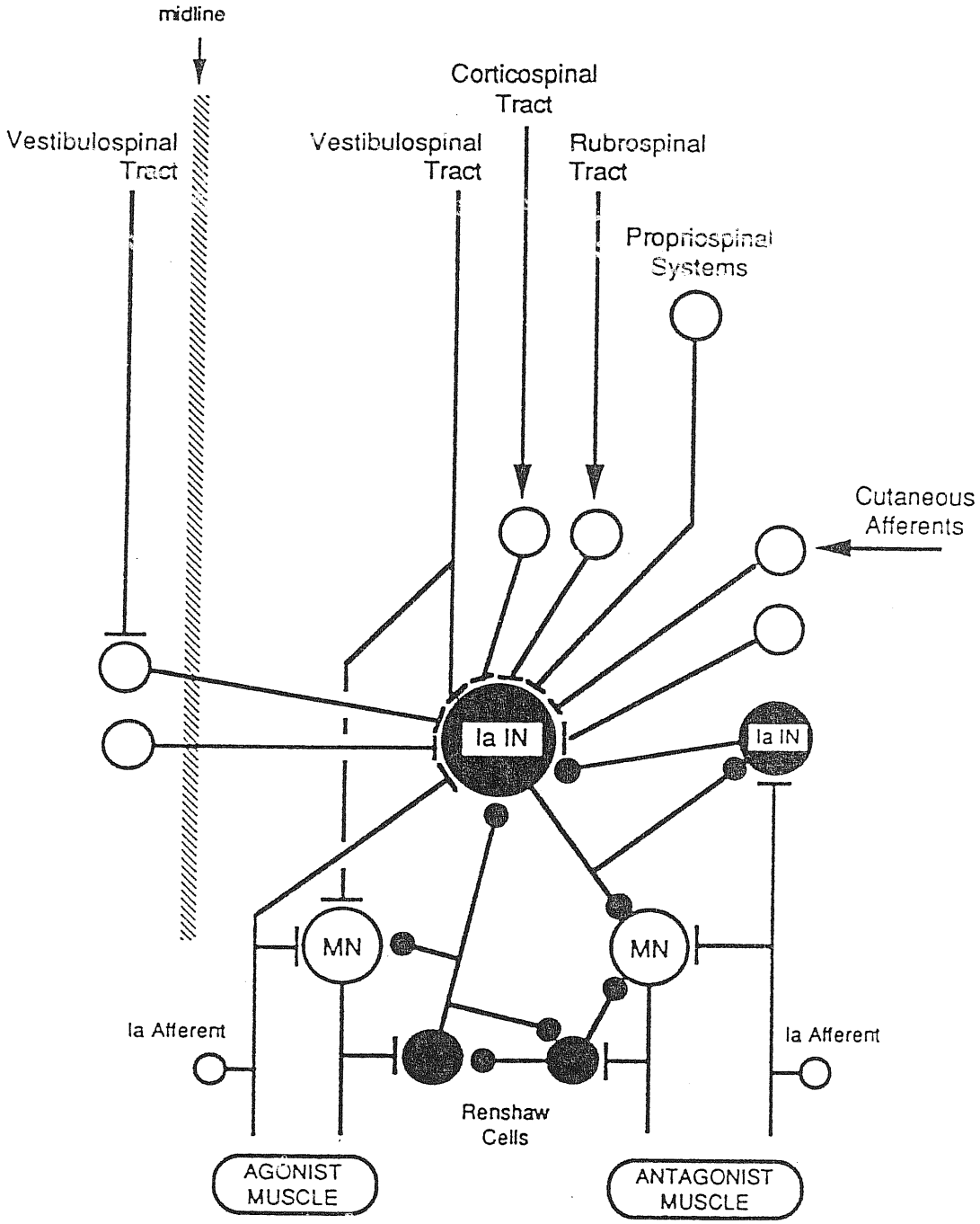

Fig I.2. *Descending and afferent synaptic inputs to an inhibitory interneuron.*
Oversimplified scheme showing the organization of descending and afferent synaptic inputs to an inhibitory interneuron (Ia IN) involved in reciprocal inhibition between antagonist motoneurons (MNs). Recurrent inhibition of motoneurons by Renshaw cells and its interaction with Ia IN is also partially illustrated. Open circles and bars denote excitatory neurons and synapses, respectively. Filled circles denote inhibitory neurons and synapses. (Adapted from Baldissera et al, 1981).

4. Spinal pattern generation studied in vivo.

At the end of the last century Sherrington (1898) observed that cats, dogs and monkeys can perform locomotion after a complete transection of the spinal cord and proposed that this activity was produced in mammals by a chain of reflexes, requiring afferent inputs for its maintenance. However, in 1911 Brown observed locomotor movements after spinal section in vivo even when dorsal roots are cut bilaterally, thus demonstrating the presence of an intrinsic spinal pattern generator responsible for locomotion. The hypothesis that the central program for locomotion can be fully expressed by spinal networks even in the absence of sensory feedback has been firmly established many years later in the cat. In this animal a well coordinated pattern of locomotor activity can be detected from peripheral nerves even after block of muscles by curare ("fictive locomotion" i.e. without real limb movement) or after section of DR fibres (Grillner, 1981, Pearson and Rossignol, 1991; Rossignol, 1996), two conditions under which afferent inputs cannot play a role in rhythmogenesis. Experiments on cats and rodents have also proved that coordinated locomotor or airstepping behaviour can be performed by spinal animals (i.e. with the spinal cord completely isolated from supraspinal structures) (reviewed by Rossignol, 1996). Thus, it is widely accepted that a central pattern generator entirely located within the spinal cord is responsible for the basic features of the locomotor program.

Central pattern generation is usually studied in vivo by means of muscle fibre recordings (electromyograms) or nerve recordings (in which the activity of several nerves supplying identified muscles is monitored). An example of simultaneous electromyograpic recordings from some extensor and flexor hindlimb muscles in an adult intact cat during treadmill locomotion at 0.4 m/s is presented in fig I.3 (adapted from Rossignol, 1996). While locomotion is roughly characterized by rhythmic alternating bursts of activity in flexor and extensor muscles within one limb, detailed phase-relations and burst duration of the numerous muscles subserving the ankle, the knee and the hip during one step cycle are complex (Rossignol, 1996; Kiehn and Kjaerulff, 1996). Another rhythmic pattern that has been studied is scratching, that, unlike locomotion, involves the use of only one hindlimb. During scratching the pattern of muscle activation is similar to but distinct from locomotion (Gelfand et al, 1988) and

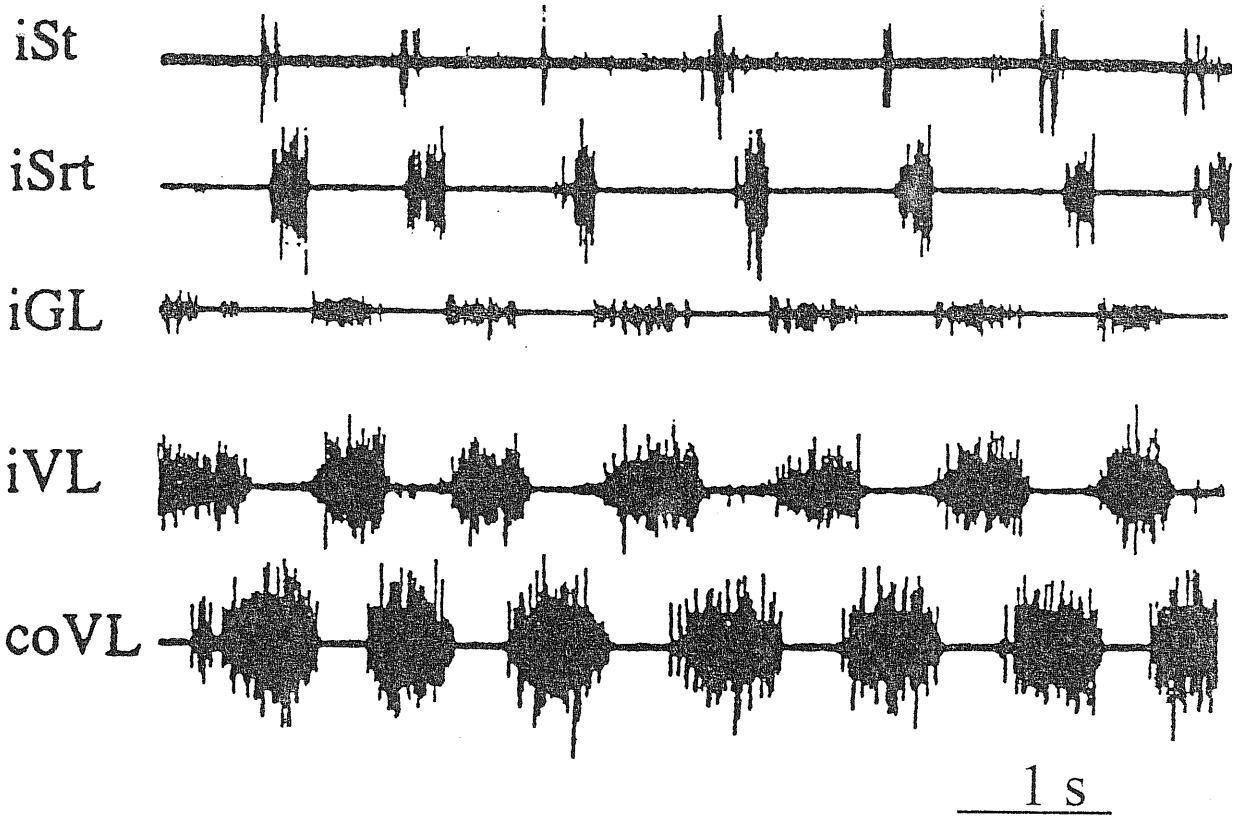

Fig I.3. *Electromyographic (EMG) recordings of coordinated locomotor activity.*
Electromyograms from the hindlimb muscles of a normal cat chronically implanted with EMG electrodes and walking on a treadmill at 0.4 m/s. iSt ipsilateral semitendinosus. iSrt: ipsilateral sartorius anterior. iGL: ipsilateral lateral gastrocnemius. iVL: ipsilateral vastus lateralis. coVL: contralateral vastus lateralis. (Adapted from Rossignol, 1996).

the circuitry responsible for this activity have been proposed to be in part overlapping with those responsible for locomotion (Rossignol, 1996).

A restricted area of the brainstem termed mesencephalic locomotor region (MLR) has been found to play an important role in the supraspinal control of locomotion. In fact, in the decerebrate cat, treadmill locomotion is induced by electrical stimulation of this region (Shik et al, 1966); under these conditions, locomotion speed can be increased by increasing stimulation intensity, but locomotion frequency is not simply related to the stimulation pattern. Chemical stimulation of the MLR by GABA antagonists has also been shown to induce locomotion (Garcia-Rill et al, 1985). These observations indicated that a descending synaptic input arising from the brainstem is converted in a rhythmic pattern by the spinal pattern generators. Further studies suggested that induction of locomotor behaviour may result from sequential activation of the medial reticular formation and ventrolateral spinal pathways by the MLR, although alternative pathways (involving the pontomedullary locomotor strip that link the MLR to propriospinal neurons) have also been considered (Rossignol, 1996).

The observation that stimulation of the MLR can evoke locomotion promptly stimulated investigators to check whether the descending command initiating locomotion can be mimicked by exogenous application of neurotransmitters or their agonists. Several agents have been found to be able to induce or boost locomotor activity. In particular, experiments on spinal cats have revealed that administration of the noradrenaline precursor L-DOPA (together with nialamide, a monoamine oxidase inhibitor; Grillner, 1981) or of the α-2 noradrenergic receptor agonist clonidine (Forssberg and Grillner, 1973) can evoke locomotion. Serotoninergic agonists can facilitate locomotion but fail to induce it in spinal cats in which clonidine can induce such a behaviour (Barbeau and Rossignol, 1991). Glutamate mediated transmission has been shown to play a central role in locomotion, since application of either NMDA or non-NMDA antagonists blocks brainstem-evoked locomotion and co-application of NMDA and a glutamate uptake blocker induces fictive locomotion (Douglas et al, 1993). These experiments have not clarified, however, whether glutamate receptors are necessary for the operation of central pattern generators, for the transmission of descending commands to such generators or for both.

The role played during locomotion by specific interneuronal classes involved in reflex pathways has been tested in paralyzed cats during MLR stimulation. By using selective antagonists of glycinergic or cholinergic transmission it has been concluded that Ia interneurons and Renshaw cells do not play an essential role in controlling locomotion, that has been suggested to result from a spinal network independent of motoneurons or Renshaw cell activity (Pratt and Jordan, 1987).

An important issue is whether the ability to produce centrally generated motor patterns is innate in mammals or whether it develops during early life possibly due to motor experience. Developmental studies performed on embryonic and neonatal cats have suggested that the basic motor program responsible for stereotypic activities is innate and that "the basic circuitry is present right at birth and its full manifestation is contingent upon the development of other intrinsic and extrinsic factors, a conclusion (also) reached by work on chick embryo and tadpoles in which developmental issues can be studied on a wider developmental scale" (Rossignol, 1996).

The cat has also been extensively used to investigate in vivo the complex issue concerning the modulation of locomotor activity by proprioceptive and sensory afferent inputs as well as the phase-dependent modulation of reflex activity during locomotion (reviewed by Rossignol, 1996). Fictive locomotion evoked by MLR stimulation has been shown to be entrained on a one-to-one basis by sinusoidal movements imposed to the hip joint, specifically due to periodic muscle stretch (Kriellaars et al, 1994). Furthermore, cutaneous reflexes have been found to be modulated during locomotion in a phase-dependent manner different for each individual muscle, so that a given muscle can be excited, inhibited or unaffected by the same stimulation during different phases of the step cycle (Drew and Rossignol, 1990).

Of particular relevance are experiments showing that mechanical constraint applied to one hindlimb during locomotion impairs the normal rhythmic activity of motoneurons supporting that hindlimb but not of motoneurons innervating the contralateral hindlimb (Edgerton et al, 1976; Grillner, 1981). The observation that rhythmic activity can take place in some motoneuronal pools while it is impaired in others have pushed these investigators to formulate the "unit burst generator" hypothesis, according to which each synergistic group of muscles acting on a particular joint is subserved by a specific

burst generator (i.e. a spinal network able to produce rhythmic bursting); different stereotypic motor behaviours such as locomotion, scratching, paw shake, etc. would then result from appropriate phase-coupling of several unit burst generators.

5. Spinal pattern generation studied in vitro.

Several vertebrate preparations maintained in vitro have also been found suitable for studying spinal rhythmogenesis. An important advantage of in vitro experimental conditions is that they allow a finely-tuned pharmacological control that is usually impossible in vivo (Rossingol, 1996).

Spinal pattern generation has been extensively studied in spinal preparations isolated from lower vertebrates (such as lamprey and frog embryo); these studies have provided a detailed knowledge of several cellular processes involved in spinal rhythmogenesis; since a comparable knowledge is still missing for the mammalian spinal cord, lower vertebrates provide an important experimental model for higher vertebrate function. In vitro preparations from birds (especially the chick embryo) have also provided important notions on spinal rhythmogenesis, and are particularly suitable for investigating the early lifetime development of motor functions. Recently, rodent spinal preparations in vitro have been introduced to study central pattern generation, thus allowing a more detailed investigation of the pharmacological sensitivity of the rhythm generating networks in mammals. Some important findings obtained with these preparations are summarized below.

Lamprey is a primitive fish in which swimming consists of a sinusoidal eel-like body movement during which each of the about 100 segments produces a rhythmic activation of body muscles characterized by left-right alternation (reviewed by Grillner et al 1991, 1995). Rhythmic activity of two adjacent segments displays a phase-delay of approximately 1% of the cycle period (independent from cycle duration), with the rostral segments bursting earlier during forward locomotion (and viceversa during backward swimming). In the lamprey spinal cord maintained in vitro, fictive swimming can be elicited by bath application of NMDA, α-amino-hydroxy-5-methyl-4-isoxazolepropionate (AMPA) or kainate, and can be recorded from ventral roots (as schematically illustrated

in fig I.4A, adapted from Grillner et al, 1991), in which rhythmic alternating bursts of motoneuronal activity are present. NMDA-induced pattern is slower (i.e. in the lower part of the physiological burst frequency range) than AMPA or kainate-induced rhythm (that is in the middle or upper part of the physiological burst frequency range; Schotland and Grillner, 1993), as illustrated in fig I.4B (adapted from Grillner et al, 1991). The basic rhythmogenic mechanism in the lamprey spinal cord appears to be contained within a few segments, since a reduced preparation consisting of two or three segments can still display rhythmic alternating bursting (Grillner et al, 1995). Longitudinal intersegmental coordination is believed to result from excitatory (mainly mediated by glutamate receptors) and inhibitory (mainly mediated by glycine and GABA receptors) coupling of the different segments; several models have been proposed to explain how such a coupling can produce a rostrocaudal phase delay (Tegner et al 1993; Hagevik and McClellan, 1994). The neural circuitries of segmental rhythmogenic networks have been widely studied and detailed diagrams have been proposed (as illustrated in fig I.4C, adapted from Grillner et al, 1991). Reciprocal inhibition between left and right neuronal pools (mediated by contralaterally projecting, glycinergic interneurons) is a prominent feature of these circuits and is believed to play a crucial role in rhythmogenesis (Grillner et al 1991). According to this view, when two (spontaneously active) pools of neurons are linked by reciprocal inhibition, alternating rhythmic activity is automatically generated (since only one pool can be active at a given time), as long as additional mechanisms that favour burst termination in the active pool (and consequent activation of the previously silent one) are considered (Grillner et al 1995). One of this mechanism could be delayed activation during a burst of a lateral inhibitory interneuron (LIN in fig I.4C) acting on the contralateral projecting interneuron (CCIN in fig I.4C) responsible for inhibition of the contralateral side (Grillner et al, 1991). Activity-dependent turning on of calcium-dependent potassium channels (Sah, 1996) has also been proposed to be involved in burst termination, since block of these channels by apamin decreases burst frequency (El Manira et al, 1994). Application of 5-HT during fictive swimming has also been found to decrease burst frequency, at least in part due to its inhibitory action on calcium-dependent potassium channels (Wikstrom et al, 1995). Lamprey spinal neurons display intrinsic membrane potential oscillations induced by application of NMDA and resistant

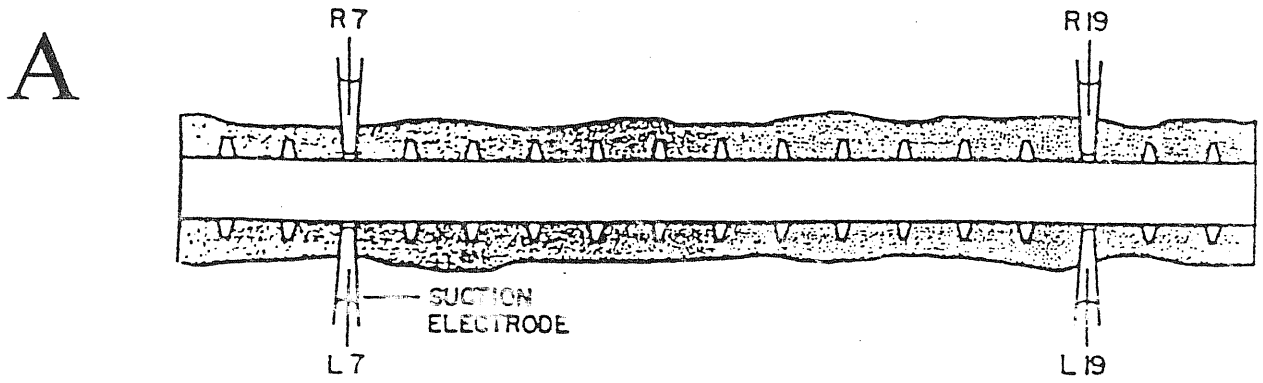

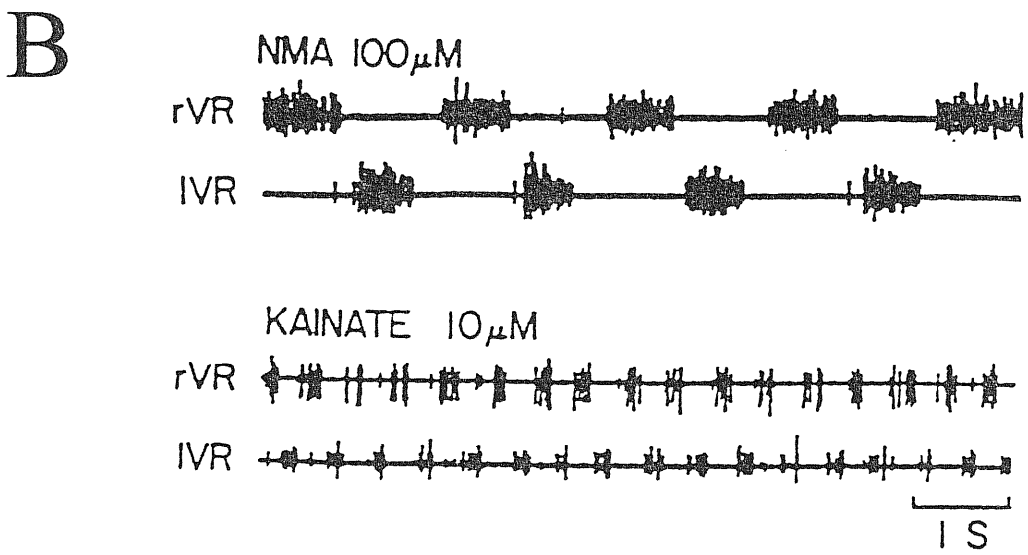

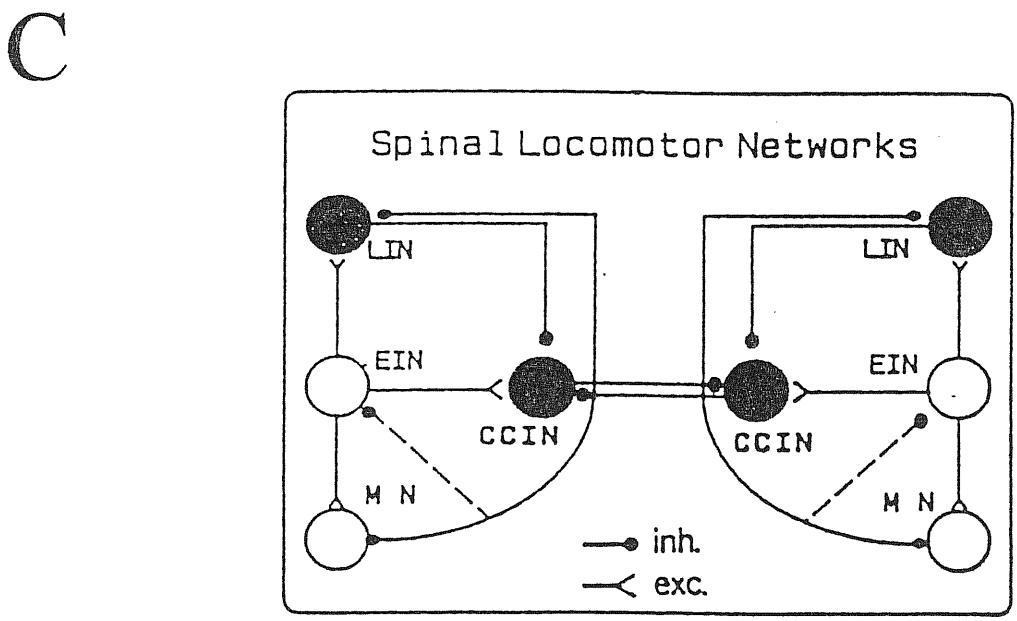

Fig I.4. *Fictive locomotion in the lamprey spinal cord in vitro.*
A: schematic drawing of a typical experimental configuration in which suction electrodes are applied to bilateral pairs of ventral roots 7 and 19. B: Alternating patterns recorded from left and right ventral roots of the same segment in the presence of 100 μM N-Methyl-Aspartate (NMA) or 10 μM kainate. C: diagram of synaptic connections in the segmental circuit. EIN: excitatory interneuron. CCIN: contralaterally, caudally projecting interneuron. LIN: lateral interneuron. MN: motoneuron. (Adapted from Grillner et al, 1991).

to the sodium channel blocker tetrodotoxin, that abolishes action potential-mediated synaptic transmission (Traven et al, 1993; Moore et al, 1993). Such intrinsic pacemaker properties are also considered important for lamprey rhythmogenesis and in particular for burst termination (Grillner et al 1995).

In the superfused, paralysed *Xenopus* embryo, episodes of fictive swimming can be elicited by sensory stimulation or excitatory amino acid agonists application and are characterized by rhythmic, left-right alternated activation of motoneurons (Dale and Roberts, 1984; Arshavsky et al, 1993; Soffe, 1996). Like in the lamprey spinal cord, glycinergic reciprocal inhibition is thought to play a crucial role in Xenopus embryo pattern generation (Dale 1995). Electrical synapses between motoneurons and mutual glutamatergic excitation of ipsilateral spinal neurons are also considered important factors for rhythmogenesis (Perrins and Roberts 1995; Roberts et al, 1995). Like in lamprey spinal cord, in the Xenopus embryo apamin sensitive potassium channels have been shown to contribute to burst cycle and motor episode termination (Wall and Dale, 1995). A recent report (Dale and Gilday, 1996) has shown that in the Xenopus embryo purinergic transmission is implicated in locomotor episodes maintenance and termination, since ATP (or a related substance) is released during swimming and reduces voltage-gated potassium currents, thus increasing the excitability of the spinal motor circuits. Adenosine, that is also produced during motor activity, reduces the voltage-gated calcium currents, and lowers the excitability of the motor circuits, thus opposing the actions of ATP. A gradually changing balance between ATP and adenosine therefore seems to underlie the run-down of the motor pattern for swimming. Another rhythmic activity that can be observed under fictive conditions in vitro in the Xenopus embryo is struggling. Although behaviourally distinct, swimming and struggling motor patterns appear to be generated by similar interneuronal mechanisms and the gradual transition from one to the other offers an interesting example of behavioural switch between two distinct motor activities under controlled pharmacological conditions (Soffe, 1993; Green and Soffe, 1996; Soffe 1996).

The *chick embryo* spinal cord isolated in vitro is also suitable to study pattern generation, since it displays spontaneous or stimulation-evoked episodes of rhythmic activity characterized by alternation between flexor and extensor motoneurons (Landmesser and O'Donovan, 1984), as illustrated in fig I.5 (adapted from Ho and O'Donovan, 1993) in which the typical bursting activity of femorotibialis (knee extensor) and sartorius (hip flexor) nerves during a motor episode is depicted. This preparation has provided important insights about localization and segmentalization of the rhythm generating networks (Ho and O'Donovan, 1993). In this system, the ability to express rhythmic activity has been found to be distributed along the rostrocaudal axis of the cord, while even a single, isolated segment can to perform rhythmic activity. The rostral lumbosacral segments display a greater rhythmogenic capacity than the caudal ones. A strong degree of synchronization for motoneuronal activity is present along the rostrocaudal axis, and appear to be mediated by propriospinal pathways travelling in the ventrolateral white matter and by synaptic interactions within the grey matter. Selective lesions have revealed that rhythmic activity with alternation persists in spinal cords in which the dorsal and medial halves have been removed or in an isolated ventral quadrant. A thin strip of lateral or ventral grey matter is still able to perform rhythmic activity, even if alternation is lost in this reduced preparation. These results suggest that rhythmogenesis and alternation are produced by anatomically distinct networks that can be affected separately. The neural substrate necessary for alternation appears to be located dorsomedial to the lateral motor column, while the capacity for rhythmogenesis is more widely distributed throughout the ventral grey matter (Ho and O'Donovan, 1993). The neurotransmitters involved in chick embryo spinal rhythmogenesis have also been investigated by means of local and bath application of several antagonists (Sernagor et al 1995). These studies have confirmed that alternation and rhythmogenesis are controlled by two distinct mechanisms (since for instance local application of the $GABA_A$ antagonist bicuculline to the ventral side of the cord converted a flexor-extensor alternating rhythm into a synchronous one without altering burst frequency). Furthermore it has been suggested that the synaptic drive from a premotor rhythm-generating network onto motoneurons is mediated by a circuit comprising GABA-ergic

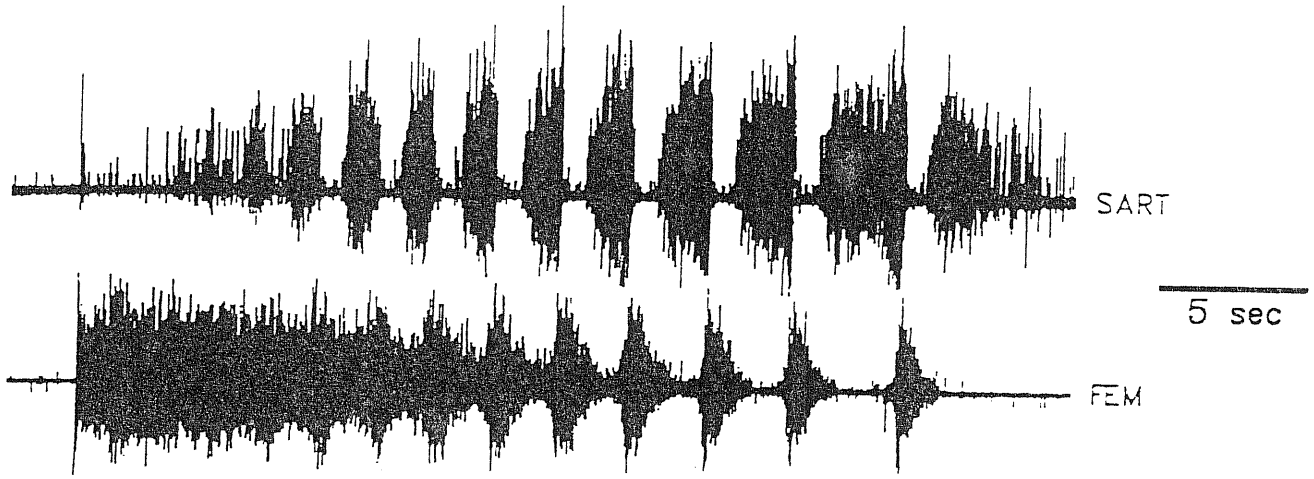

Fig I.5. *Motor activity in the chick embryo spinal cord.*

A typical episode of motor activity in the chick embryo spinal cord in vitro (evoked by single pulse stimulation of the dorsal surface of the thoracic cord). Rhythmic bursts appear in alternation in the sartorius nerve (SART) and in the femoralis nerve (FEM), both recorded with suction electrodes. (Adapted from Ho and O'Donovan, 1993).

and glutamatergic interneurons and responsible for flexor-extensor motoneurons phasing (Sernagor et al, 1995).

The *neonatal rat* spinal cord maintained in vitro remains viable for many hours when superfused with a saline solution that reproduces the composition of the cerebro-spinal fluid (Otsuka and Konishi, 1974). This preparation has been used to study central pattern generation since 1987, when Kudo and Yamada reported that bath-application of NMDA produces locomotor-like activity in a spinal cord-hindlimb preparation of neonatal rat. A brainstem-spinal cord preparation with hindlimb attached has also been shown to produce a locomotor output in response to electrical stimulation of the brainstem, with only minor changes occurring after dorsal root cut (Atsuta et al, 1991). A brainstem-spinal cord preparation, with the brainstem superfused separately from the spinal cord, has been shown to produce locomotor patterns after application of several agents (including the neuropeptide substance P and bicuculline) to the brainstem (Smith et al, 1988). Following these reports, fictive locomotion has been extensively studied in isolated spinal cord preparations of neonatal rat by means of recordings from bilateral pairs of lumbar ventral roots. A possible complication of this technique is that an individual ventral root often contains axons innervating antagonist muscles, so that a flexor-extensor alternating activity can be masked when recorded from ventral roots (Cowley and Schmidt, 1994a). A study based on peripheral nerves recordings has shown that although alternating patterns of rhythmic activity can be induced in lumbar ventral roots of the neonatal rat spinal cord by bath application of cholinergic, serotoninergic and glutamatergic agonists, these patterns are not always compatible with locomotion, since flexor-extensor alternation can be absent (Cowley and Schmidt 1994b). While acetylcholine- and NMDA- induced patterns (in the presence of edrophonium) have been found to be often incompatible with locomotion, 5-HT-induced patterns usually comprise locomotor-like flexor-extensor alternation. These findings have been extended and confirmed by an ample electromyographic study in which hip, knee and ankle flexors and extensors muscles have been monitored in a hindlimb-attached spinal cord preparation (Kiehn and Kjaerulff, 1996). Under these conditions, 5-HT-induced patterns in the neonatal rat display muscle phasing very

similar to that observed in adult mammals, as illustrated in fig I.6 (adapted from Kiehn and Kjaerulff, 1996). This study has also shown that L2 or L5 ventral roots mainly contain the axons of flexor or extensor motoneurons, respectively, and thus can be efficiently used for fictive locomotion monitoring (Kiehn and Kjaerulff 1996).

Alternating patterns induced by bath application of 5-HT or NMDA have been shown to display a strong frequency dependence on the concentration of these agents (Cazalets et al, 1992). In this study burst frequency has been shown to increase with increasing doses of 5-HT or NMDA in a range between 4 and 60 cycles/min. The effects of several doses of 5-HT are illustrated in the example of fig I.7A and in the plot of fig I.7B (adapted from Cazalets et al, 1992). A dose-dependent acceleration of fictive locomotion is also caused by raising extracellular potassium concentration from 2 to 6 mM (Sqalli-Houssaini et al, 1993). While patterns induced by individual application of 5-HT or NMDA are sometimes expressed only transiently, a very stable pattern can be elicited by coapplication of both agents, a cocktail that is now routinely used (Sqalli-Houssaini et al, 1993, Kjaerulff and Kiehn, 1996).

The presence of a dual control over the CPG, comprising a facilitating component mediated by glutamatergic synaptic transmission and an inhibitory component mediated by GABAergic processes has been proposed (Cazalets et al, 1994). This hypothesis is based on the observation that NMDA-induced patterns can be slowed down or blocked by bath application of GABA agonists (acting either on $GABA_A$ or $GABA_B$ receptors), while non saturating concentrations of the $GABA_A$ antagonist bicuculline speed up burst frequency.

A controversial issue is the one regarding the localization of the CPG responsible for locomotion. In the neonatal rat spinal cord in which locomotion is induced neurochemically, the fluorescent activity-marker sulphorhodamine labels neurons especially in the intermediate grey (laminae VI-VII) and in the area surrounding the central canal (lamina X) (in addition to motoneurons; Kjaerulff et al, 1994). Intracellular recordings from lamina VII interneurons have revealed that these cells receive a rhythmic synaptic input during fictive locomotion (MacLean et al, 1995). Lesion studies have shown that a flexor-extensor alternating pattern can still be observed after longitudinal sagittal hemisection of the cord and that both left-right and

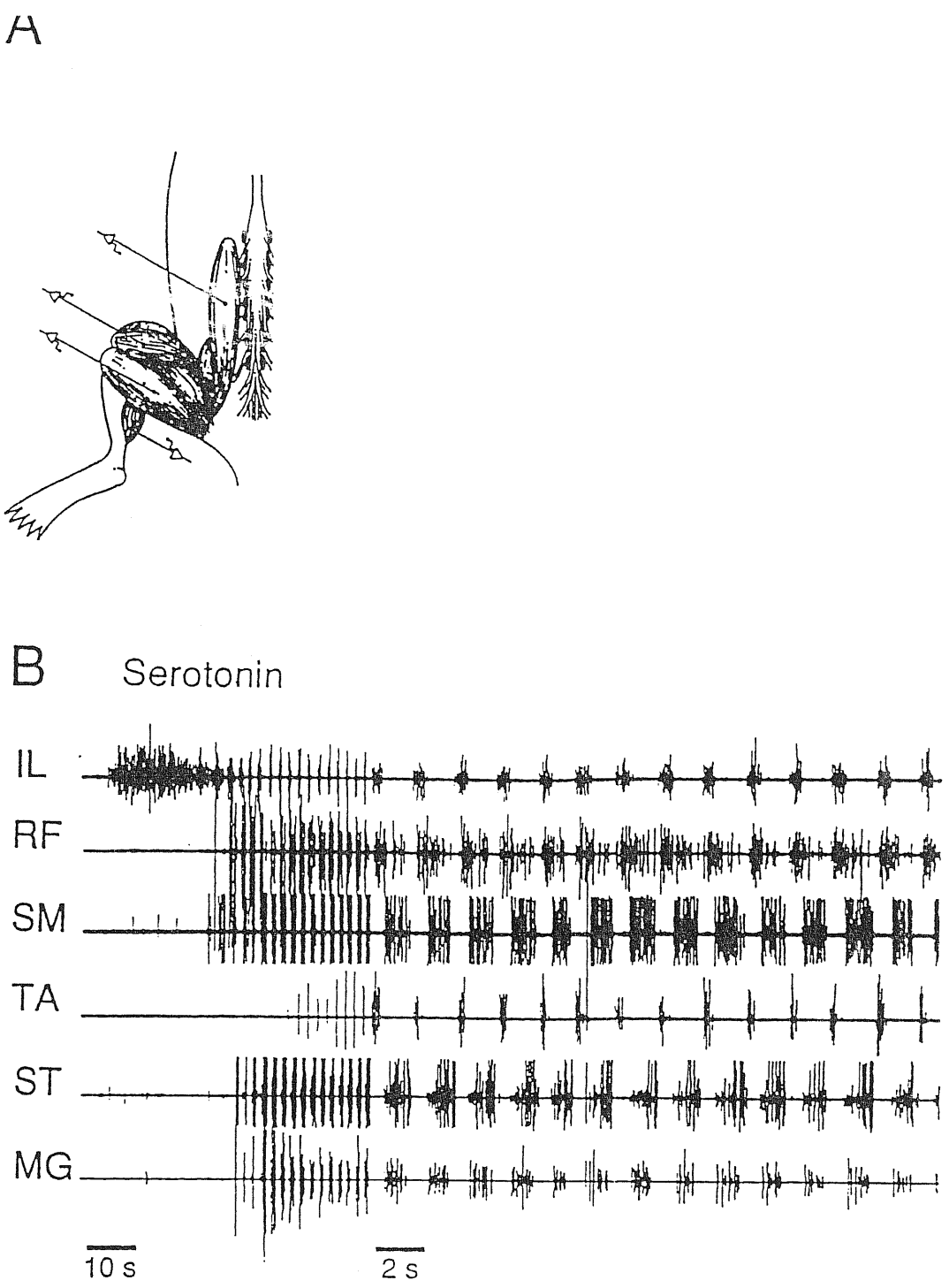

Fig I.6. *5-HT-induced electromyographic (EMG) pattern in the neonatal hindlimb-attached spinal cord preparation.*

A. Drawing of the preparation and of some muscles used for recordings (see amplifier symbols). B. EMG activity of different hindlimb muscles following 5-HT application (30 μM). Note change in timescale (the earlier stage of 5-HT application is presented at a lower time expansion). IL: iliopsoas. RF: rectus femoris. SM: semimebranosus. TA: tibialis anterioris. ST: semitendinosus. MG: medial gastrocnemius. (Adapted from Kiehn and Kjaerulff, 1996).

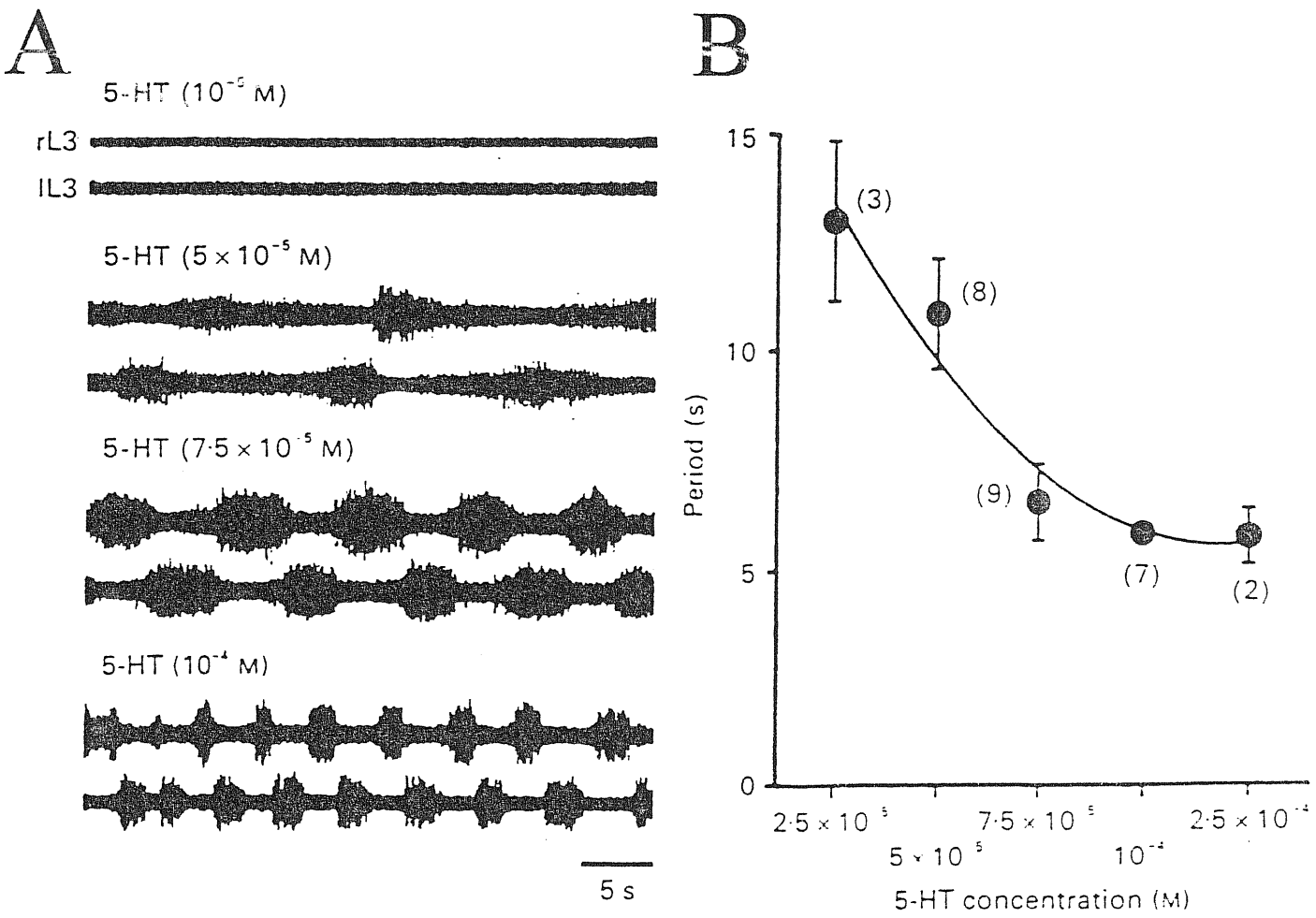

Fig I.7. *Dose-dependence of 5-HT induced-fictive locomotion.*

A. Bilateral recordings from left and right L3 ventral roots are used to monitor fictive locomotion frequency in the presence of different 5-HT concentrations. B. Plot illustrating that cycle period decreases from 12 to 6 s when 5-HT concentration is raised from 25 to 250 µM. (Adapted from Cazalets et al, 1992).

flexor-extensor alternation is preserved after removal of dorsal horns (Kudo et al, 1991; Kjaerulff, and Kiehn, 1996); furthermore the segments located caudally to L2 (as well as those located rostrally) have been shown to display rhythmogenic ability when surgically isolated (Kjaerulff, and Kiehn, 1996). These data are similar to those obtained in the chick embryo (Ho and O'Donovan, 1993) but in marked contrast with those of Cazalets et al (1995) that, by partitioning the spinal cord by vaseline walls and applying 5-HT and NMDA only to certain segments, have suggested that the network that organizes locomotion in the newborn rat is not segmentally distributed but is restricted to a specific part of the cord, namely the L1-L2 segments. According to these authors a CPG located in the upper lumbar segments is responsible both for rhythmogenesis and alternation and can transmit a coordinated motor output to the motoneurons of more caudal lumbar segments via monosynaptic connections. By means of vaseline barriers these authors have also studied the neurotransmitters involved in the synaptic drive from CPG to motoneurons and have concluded that it consists of alternating periods of synaptic inhibition (mediated by glycine) and excitation (mediated by NMDA and non-NMDA glutamate receptors) (Cazalets et al, 1996). Recent localization experiments have provided evidence in favour of a distributed nature of the networks responsible for locomotor activity along the rostrocaudal axis and have suggested that 5-HT and NMDA activated rhythmic networks are differently localized within lumbar segments (Cowley and Schmidt, 1997). The ability of afferent inputs to affect locomotor behaviour has been studied by means of DR or ventrolateral afferent stimulation. A short train of electrical stimulations of a DR (as well as selective activation of extensor afferents) has been shown to reset the cycle phase of fictive locomotion; entrainment of fictive locomotion with repetitive application of stimulation trains is possible only within a very narrow range of frequencies. Similarly, ventrolateral (VL) afferent (Magnuson et al, 1995) or bilateral DR (Sqalli-Houssaini et al, 1993) stimulations have been shown to affect fictive locomotion timecourse and to modify its frequency in a limited range around the spontaneous value.

6. Proposed mechanisms for spinal rhythmogenesis.

Despite the growing amount of data available about pharmacology and localization of the networks responsible for rhythmic pattern generation in the neonatal rat spinal cord, little is known about the neural mechanisms that underlie spinal rhythmogenesis in the mammalian spinal cord. In this regard, two popular hypotheses should be considered.

a) Following the original conjecture by Brown (1911), it has been proposed that pattern generation in the neonatal rat could result from *reciprocal inhibition* between antagonistic pools of neurons (*half-centers model*). According to this model rhythmogenesis and alternation are generated by a single mechanism (reciprocal inhibition), that keeps silent one pool of neurons while the other is active. As mentioned before, reciprocal inhibition between left and right neurons has been well documented in the spinal cord of lamprey and Xenopus embryo, for which detailed models of the half-center circuitry and neurotransmitters involved have been proposed (see fig I.4C for lamprey segmental circuits). A difference between the schemes proposed for lamprey and Xenopus embryo is that in the latter a positive-feedback mutual excitation between elements of the same pool has been included to explain burst maintenance (Roberts et al, 1995), while this feature is not apparent in lamprey models (Grillner et al, 1995). Several cellular factors (including rebound excitation mediated by voltage-dependent NMDA receptor channels, calcium-dependent potassium channels activation and presynaptic inhibitory mechanisms) are usually incorporated into models based on half centers in order to explain burst termination in the active pool and subsequent activity-switching to the antagonist pool. The concept of reciprocal inhibition between two half centers is particularly simple to apply to lower vertebrates in which swimming activity is characterized by simple left-right alternation of motoneuronal bursting at each segmental level. In mammals, where also flexor-extensor alternation on each side is present, reciprocal inhibition models have to consider that more than two pools should be linked by this kind of relation or, alternatively, that left-right alternation and extensor-flexor alternation may be produced by different mechanisms (Sernagor et al, 1995).

b) *Pacemaker neurons* (i.e. cells provided with intrinsic membrane properties that allow the generation of rhythmic activity even in the absence of synaptic inputs) have been proposed to play an important role in spinal pattern generation as well as in respiration (Grillner et al, 1991; Kiehn, 1991; Hultborn and Kiehn 1992; Feldman and Smith 1989). According to this hypothesis, a kernel of interconnected pacemaker neurons may be able to transmit a rhythmic output to the rest of the network. Spinal pacemaker neurons have been described in the lamprey spinal cord in the presence of exogenous NMDA. In this case membrane potential oscillations are generated through a dynamic interplay between voltage-dependent NMDA-gated channels (whose auto-regenerative opening is responsible for the depolarizing phase of the oscillation) and calcium-activated potassium channels (that repolarize the cell following calcium entry through NMDA receptors and voltage-dependent calcium channels), as described by Grillner et al (1991). In the neonatal rat spinal cord, interneurons performing intrinsic oscillations have been found at different laminar locations (Hochman et al 1994a; Kiehn et al 1996; see below for a description). The ability to generate *plateau potentials* (i.e. cellular depolarizations initiated by an external input but sustained by intrinsic membrane mechanisms) is another mechanism potentially involved in central pattern generation. This property can allow a neuron to amplify and/or prolong a synaptic signal (Kiehn, 1991). As in the case of pacemaker neurons, the ability to generate plateau potentials may depend on the presence of voltage-dependent inward currents. In fact, depolarization-gated conductances can give rise to a negative-slope region in the current-voltage relationship of these neurons. In turn, this property may be associated with the existence of a second dynamically-stable state, i.e. a membrane potential level (more positive than the resting one) at which there is no net current flux and to which the cell would return after small synaptic perturbations (Schwindt and Crill, 1984). Bistable behaviour has been shown to occur in vertebrate motoneurons (reviewed by Hultborn and Kiehn, 1992), and interneurons (Kiehn et al 1996). It is important to note that reciprocal inhibition and pacemaker neurons are not mutually exclusive hypotheses, and have been integrated in computational models (Grillner et al 1995).

In particular, turn off of NMDA dependent oscillations is thought to contribute to burst termination in the half centers of the lamprey spinal cord (Grillner et al 1991).

7. Reciprocal inhibition and pacemaker neurons in the neonatal rat spinal cord

In the neonatal rat spinal cord, fast synaptic inhibition is mainly mediated by GABAergic and glycinergic transmission (Young and Macdonald, 1983; Davidoff and Hackman, 1984). The currents gated by these amino acids are mostly mediated by chloride ions (Gao and Ziskind-Conhaim, 1995) and exert a depolarizing action on motoneurons during embryonic development and during the first days of postnatal life (Takahashi, 1984, Wu et al, 1992). At the level of interneuronal somatosensory pathways the action of these receptors appears to shift from an excitatory to an inhibitory function around embryonic days 18-19; in fact, starting from this age blockade of either $GABA_A$ or glycine receptors strongly increases DR-evoked polysynaptic responses of motoneurons both in amplitude and duration of (Wu et al, 1992) and destroys left-right alternation of NMDA-induced patterns (Kudo et al, 1991). These changes in the effects of $GABA_A$ and glycine receptors are probably due to a shift of reversal potential for Cl^- towards more negative values during embryonic development (Wu et al, 1992, Gao and Ziskind-Conhaim, 1995). For the neonatal rat spinal cord direct demonstration and identification of the synaptic processes mediating reciprocal inhibition are still lacking. Nonetheless, reciprocal inhibition between left and right sides is considered to be predominantly mediated by glycine receptors (Cazalets et al, 1994). GABAergic transmission has been proposed to exert, on the central pattern generator, an inhibitory action that can counterbalance the action of excitatory amino acids (Cazalets et al, 1994). However, other authors have suggested that $GABA_A$ receptors are also involved in reciprocal inhibition (Cowley and Schmidt, 1995).

As far as intrinsic oscillations are concerned, neurons endowed with such properties have been described in neonatal rat spinal slices in the area surrounding the central canal and have been proposed to play a role in spinal rhythmogenesis (Hochman et al, 1994a); in these cells pacemaker ability is maintained in the presence of tetrodotoxin and, like in lamprey spinal neurons, it depends on the presence of bath-applied NMDA, presumably due to the peculiar voltage dependence of these receptors. However, these

pacemaker properties have not been directly related to locomotor activity. Recently whole-cell recordings from rhythmically activated interneurons of laminae VII and X during fictive locomotion have been reported (Kiehn et al 1996). A small fraction of these cells has been found to display plateau potential properties and an even smaller fraction has been found to produce transient, intrinsic oscillations during washout of locomotion-inducing drugs.

As far as motoneurons are concerned, NMDA-induced, tetrodotoxin-resistant oscillations and plateau potentials have been reported in the neonatal rat (Hochman et al, 1994b), but it has not been possible to assess a direct involvement of these properties in locomotor activity.

Nevertheless, in the recent past several experimental findings have challenged the view of reciprocal inhibition and NMDA-dependent pacemaker neurons as the main rhythmogenic factors in the rat spinal cord.

In embryonic rat spinal cord, NMDA application elicits a synchronous rhythm in left and right VRs up to embryonic day 17 (E17), while left-right alternation appears only after E18; the early synchronous rhythm is insensitive to blockade of $GABA_A$ or glycine receptors, suggesting that inhibitory processes are not required for its generation (Kudo et al, 1991). Furthermore, during late embryonic stages at which alternation is present, application of glycine receptor antagonists converts it into a synchronous rhythm (Kudo et al, 1991). Similarly, left-right alternating patterns induced by 5-HT, NMDA or acetylcholine in the neonatal rat have been shown to be converted into left-right synchronous rhythmic patterns by pharmacological block of either $GABA_A$ or glycine receptors (Cowley and Schmidt, 1995); analogous results have also been reported for the lamprey spinal cord after block of glycine receptors (Cohen and Harris-Warrick, 1984; Alford et al, 1990; Hagevik and McClellan, 1994). A dissociation between alternation and rhythmogenesis suggests that reciprocal inhibition (that is expected to generate always alternating activity) is not required for spinal rhythmicity.

As far as pacemaker neurons are concerned, the observation that fictive locomotion can persist after removal of extracellular magnesium (Kiehn et al, 1996) or in the presence of NMDA antagonists (Beato et al, 1997), two conditions that should have impaired

the operation of NMDA receptor-dependent pacemaker neurons, suggests that such intrinsic properties are not required for spinal pattern generation in the rat spinal cord.

8. Block of synaptic inhibition

The observation mentioned above that pharmacological block of glycine or $GABA_A$ receptors converts alternating patterns into synchronous ones suggests that inhibitory synaptic processes are required for time-phasing of spinal patterns in different motoneuronal pools but raises a question about the functional role of inhibitory synaptic transmission for rhythmogenesis in the neonatal rat spinal cord. In this light it is important to note that pharmacological disinhibition has been shown to induce rhythmic behaviour in several CNS preparations.

In hippocampal slices in vitro synchronous bursting can be elicited by pharmacological block of $GABA_A$ receptors by picrotoxin (Hablitz 1984; Miles et al, 1984; Traub et al, 1993). Hippocampal bursts are usually initiated by a longer "primary" depolarization (accompanied by firing activity) and followed by several shorter "secondary" depolarizations appearing at decreasing frequency (Traub et al, 1993; Merlin et al, 1995). An example of this activity, in which bursts appear at regular intervals, is illustrated in fig I.8 (adapted from Merlin et al, 1995). These bursts are abolished by block of non NMDA glutamate receptors, while block of NMDA receptors abolishes secondary depolarizations while preserving the primary events (Lee and Hablitz, 1990; Traub et al, 1993). Excitation of a single neuron has been shown to be sufficient to initiate a synchronized population discharge (Miles and Wong, 1983). Recurrent excitatory connections between CA3 pyramidal neurons are believed to play an essential role in the genesis of these synchronous events (Traub et al, 1993; Taylor et al, 1995). Spontaneous-like events can also be evoked by antidromic stimulation of the Schaffer collaterals and entrainment at frequencies larger than the spontaneous one has been reported (Merlin et al, 1995). An interplay between mutual excitation of pyramidal neurones (mediated by glutamatergic synapses) and intrinsic membrane properties (generating oscillations in the dendrites of pyramidal neurons) has been proposed to underlie hippocampal bursting in the absence of synaptic inhibition (Traub et al, 1993). Bursting expressed by hippocampal slices in vitro has been related to epileptic seizures

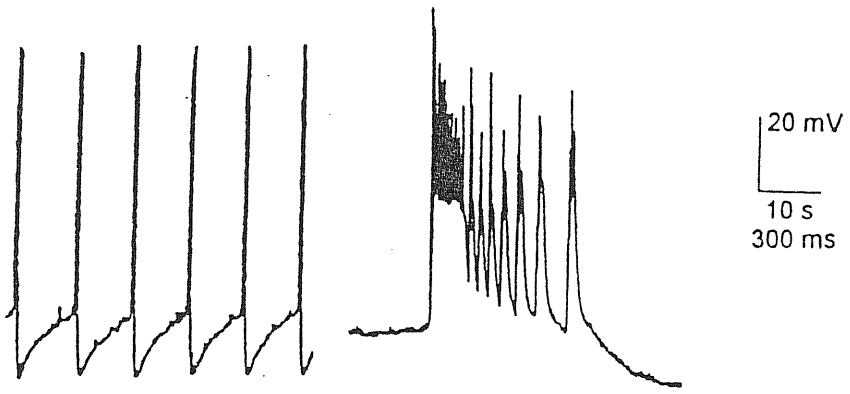

Fig I.8. *Rhythmic bursting activity induced by picrotoxin in the hippocampus.*
Intracellular recordings (under current-clamp conditions) from a CA3 hippocampal neuron in the presence of picrotoxin (50 μM). The faster timescale trace (right) depicts the structure of a single bursting event, characterized by a primary burst (i.e. the first and longer lasting depolarizing event), by several afterdischarges (i.e. repetitive depolarizations following the initial one) and by a large afterhyperpolarization (i.e. the persistent hyperpolarization that follows the last afterdischarge). (Adapted from Merlin et al, 1995).

as well as to physiologically-expressed hippocampal rhythms (Traub et al, 1993; Merlin et al, 1995; Taylor et al, 1995), although the functional role of this activity is still to be elucidated. Bursting activity induced by bicuculline has also been observed in vitro in the cerebral cortex (Hwa et al 1991). In a brainstem preparation in vitro, rhythmic respiratory output is not abolished by application of $GABA_A$ antagonists or chloride-free solution, a condition in which the chloride reversal potential is expected to shift toward a more positive value, thus eliminating the ability of synaptic inhibitory processes to produce membrane hyperpolarization (Feldman and Smith 1989).

In organotypic slice cultures of embryonic rat spinal cord, a preparation in which the synaptic organization present in a transverse plane of the cord is at least in part preserved, pharmacological block of synaptic inhibition mediated by $GABA_A$ and/or glycine receptors has been shown to convert random synaptic activity of motoneurons into rhythmic clusters of EPSPs (with an average frequency of 5 Hz) that are grouped into bursts separated by quiescent intervals lasting several seconds (Streit, 1993). This activity has been shown to be blocked by antagonists of non NMDA glutamate receptors but not of NMDA receptors, that decrease burst rate without affecting burst length; focal stimulation of spinal neurons elicits spontaneous-like bursts if delivered after a long quiescent interval, while low-amplitude, short bursts are evoked by stimulations applied immediately after the end of a spontaneous burst or by repetitive stimulations at 5 Hz. These findings, together with the observation that burst duration and burst amplitude were both positively correlated with the duration of the preceding quiescent interval, has suggested that frequency-dependent synaptic depression could play an important role in burst termination; on the other hand, burst initiation has been found to be independent of recovery from synaptic depression (Streit, 1993). This bursting activity has been proposed to be possibly related to spontaneous embryo motility (that is expressed before synaptic inhibition become functional) and to activity-dependent strengthening of spinal synapses (Streit, 1993).

In the cat spinal cord in vivo, intravenous or local application of penicillin (an agent that is known to antagonize GABAergic transmission) or strychnine (a glycine antagonist) induces motoneuronal paroxysmal bursting that has been studied as a spinal model of epileptic seizures (reviewed by Schwindt and Crill, 1984). While strychnine-

induced bursts have been shown to be merely driven by massive, synchronized synaptic inputs onto motoneurons, the longer penicillin-induced bursts (that can last several seconds) appear to be only triggered by excitatory synaptic inputs; their maintenance is rather accomplished by intrinsic membrane properties of motoneurons, that generate plateau potentials due to a transiently-induced change in their steady current-voltage (I-V) relation. This change is characterized by an increase in the negative slope of the I-V curve, that results in a region of net inward current. This condition gives rise to a second, depolarized stable level of the motoneuron membrane potential (as discussed above). This modification in the I-V curve has been suggested to result from reduction of a potassium outward current, due to potassium accumulation in the extracellular space following the initial synaptic depolarization and to the consequent positive shift of the potassium reversal potential. Such a condition would create a "vicious circle" in which the initial depolarization induces further persistence in a depolarized state (Scwindt and Crill, 1984).

A facilitation of locomotor activity in spinally transected cats has been reported to occur following application of the $GABA_A$ antagonist bicuculline (Robinson and Goldberger, 1985).

9. Aims of the present study

Many of the previously mentioned results show that the presence of synaptic inhibition within a neural network is not a necessary condition for the generation of rhythmic behaviour. The present study aimed at investigating whether rhythmogenesis can spontaneously occur in the intact neonatal rat spinal cord after pharmacological block of synaptic inhibition. Since the answer to this question turned out to be affirmative, an investigation into the neuronal mechanisms giving rise to this behaviour was undertaken.

Pharmacological block of synaptic inhibition provides an experimental simplification of the spinal circuitries that can help enlightening important features of spinal networks and their elements; furthermore, disinhibition can unmask those functional properties of the system that rely on excitatory synaptic transmission only. The present data, by

bridging new data to the field so far described, should contribute to clarify the poorly understood issue of spinal pattern generation.

Several issues concerning spinal rhythmogenesis in the absence of synaptic inhibition have been addressed in the course of the present study. After an initial assessment of the effective blockade of inhibitory synaptic processes, the experimental effort has been mainly aimed at answering the following questions:

a. Is this rhythmic activity expressed synchronously within motoneuronal pools innervating different ventral roots?
b. What kind of cellular and network mechanisms would underlie this rhythmic activity? In particular, to what extent can motoneurons contribute to rhythmic bursting? What is the role of NMDA and non NMDA glutamate receptor in the rhythmogenic network? What are the ionic membrane mechanisms specifically involved in this phenomenon?
c. What is the localization of the rhythmogenic networks at segmental and laminar level?
d. Is rhythmic bursting modulated by the agents that are known to induce and/or modulate other spinal rhythms such as fictive locomotion?
e. To what extent can the rhythmogenic network operation be affected by afferent synaptic inputs from physiologically relevant pathways such as dorsal roots or ventrolateral afferent fibres?

As a corollary to the experimental findings a tentative model will be proposed to explain rhythmic bursting in the disinhibited spinal cord in terms of cellular and synaptic events in a premotoneuronal network. A schematic diagram for the connections between rhythmogenic networks, afferent pathways and motoneurons will be presented. The possible functional link between the networks giving rise to rhythmic bursting in the absence of inhibition and those supporting fictive locomotion will be discussed on the basis of the experimental data.

METHODS

1. Dissection.

The spinal cord (from low thoracic segments to *cauda equina*) was isolated from neonatal rats (0-12 days old; P0-P12). For this purpose, the animal was anaesthetised with an intraperitoneal injection (0.4-0.6 ml) of urethane solution (10% in distilled water). When the animal lost the withdrawal reflex, it was rapidly decapitated with scissors; the forelimbs and the ventral part of the body were removed and the animal was eviscerated in order to expose the ventral aspect of the vertebral column. The remaining skin was also removed. At this stage the body was washed in cooled (4 °C) oxygenated artificial cerebrospinal fluid (ACSF; see below for composition) and fixed by pins (ventral side up) to the sylgard bottom of a small petri dish containing ACSF at the same temperature. Solution in the dish was continuously oxygenated and replaced every 2-4 min. The spinal cord was exposed by complete laminaectomy performed in the rostrocaudal direction with small scissors under a microscope. Meningeal tissue was removed from the exposed side, and dorsal and ventral roots were cut close to the cord, with the exception of those to be used for stimulation or recording (these roots were left as long as possible). Isolation of the cord was completed by removing the remaining meningeal tissue on the dorsal side.

2. Superfusion.

After dissection the spinal cord was pinned to the Sylgard bottom of a recording chamber (2 ml volume) and continuously superfused with ACSF fed by either gravity (from a fixed level of 25 cm maintained by a peristaltic pump) or directly by such a pump (5-8 ml/min). Gravity superfusion, that ensured constant flow also during drug application, was mainly used for intracellular experiments (see below) that required a

greater mechanical stability. Pump superfusion was used only for extracellular recordings.

The following ACSF composition (in mM) was used: NaCl 113, KCl 4.5, $MgCl_27H_2O$ 1, $CaCl_2$ 2, NaH_2PO_4 1, $NaHCO_3$ 25 and glucose 11, gassed with 95% O_2-5% CO_2; pH 7.4, at room temperature (20 °C). ACSF with this composition is also referred to as control solution. The preparation was always allowed to recover for at least 40 min before the experiment started.

In some experiments the concentration of chloride or potassium ions was changed. Low-chloride solution was obtained by equimolar substitution of NaCl with Na-isethionate. In this way the Cl^- concentration was reduced by 94% (from 120.5 to 7.5 mM) while the concentration of the other ions was unchanged.

Changes in external potassium concentration were obtained by setting the KCl concentration in the bath solution at 0 (potassium-free solution) 1, 2, 4 or 8 mM instead of the standard value (4.5 mM). These manipulations altered the chloride concentration by less than 7 %. Therefore no compensation of chloride concentration was performed.

3. Experimental configurations

The neonatal rat spinal cord was used either for intracellular recordings from motoneurons or for extracellular recordings from VRs (see below for recordings techniques).

For intracellular recording, the cord was pinned one side up and slightly rotated in order to leave the ventrolateral part (containing the motor nuclei) more accessible for penetration by the microelectrode, that was lowered vertically by means of a micromanipulator (Narishige MX-4). For simultaneous ventral root recordings the preparation was usually pinned ventral side up. Fig M.1 presents schematic drawings of the experimental set-up used for intracellular (A) or VR recording (B) experiments. For sake of clarity only a portion of the spinal cord is represented in these drawings in order to show the grey matter. The spinal cord is presented with an upside-up orientation in fig M.1A in order to make comparison with fig M.1B and with fig I.1 of the Introduction section more convenient.

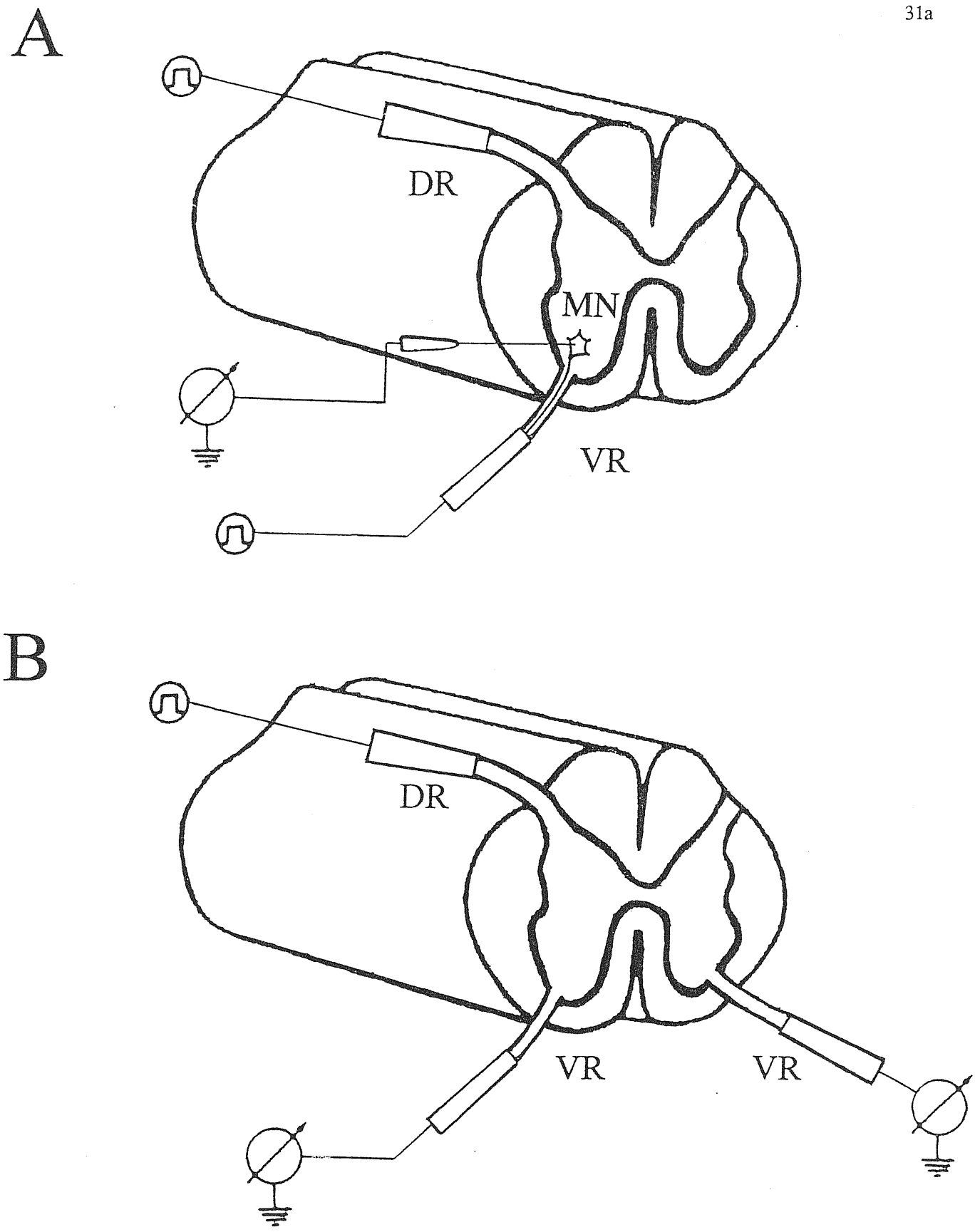

Fig M.1. *Schematic drawing of the experimental set-up used for intracellular or extracellular recordings.*
In order to give prominence to the spinal grey matter only a portion of the spinal cord (that was intact during experiments) is depicted. A. During intracellular recordings a lumbar motoneuron (MN) was recorded with a sharp microelectrode (depicted as a straight line entering the MN) connected to an amplifier (see voltmeter symbol). The corresponding ventral root (VR) was kept in a stimulating suction electrode (open box) in order to antidromically activate (step in a circle symbol) the MN axon (represented as a filament leaving the cell and entering the VR). An ipsilateral dorsal root (DR) at the same segmental level was also kept in a stimulating suction electrode in order to elicit mono and polysynaptic responses from the impaled MN. B. For extracellular recordings, left and right VRs at the same segmental level were usually recorded simultaneously with suction electrodes connected to an amplifier. One DR at the same segmental level was kept in a stimulating suction electrode in order to activate afferent fibres.

During intracellular experiments, one VR and one ipsilateral DR at the same segmental level were drawn into suction electrodes for antidromic or ortodromic stimulation, respectively, as shown in Fig M.1A (see below for stimulation procedures). For extracellular experiments, two lumbar VRs (usually right and left VRs at the same egmental level) were individually recorded with suction electrodes, while one DR was drawn into a third suction electrode for stimulation (fig M.1B). In some experiments an additional bipolar stimulating electrode was placed in contact with the ventrolateral surface of the spinal cord at cervical or thoracic level in order to stimulate ventrolateral descending fibres.

4. Electrical stimulation.

Miniature bipolar suction electrodes were used in order to deliver single or repetitive electrical stimuli to either DR or VR. Such electrodes were made by heating and pulling plastic cones or glass capillaries; one copper or tungsten wire was inserted within the suction electrode, while another one was attached externally to it (close to the suction electrode tip). The suction electrode tip diameter was chosen to closely fit the root to be stimulated. Brief electrical pulses (0.1 ms duration; 0.1-10 V amplitude) were applied in order to activate antidromically motor axons contained within VRs or to activate selectively low threshold DR afferent fibres (Kiehn et al, 1992).

Tests were carried out to monitor the afferent volley induced by DR stimulation. For this purpose, a 3 M NaCl-filled microelectrode was inserted at the site of entry of the dorsal root at a distance of 3.5±0.5 mm from the stimulating electrode. The afferent volley appeared as a biphasic waveform with the earliest detectable peak occurring at 0.5 ms from the start of the stimulus artefact (any faster components could not be resolved from the artefact). Such a peak corresponded to fibre activity with 6.3 m/s conduction velocity and was associated with ventral root responses having latencies < 4 ms.

Ventrolateral descending tracts were stimulated via a bipolar tungsten electrode consisting of two filaments insulated except that at their tip (0.026 mm diameter) and placed in contact with the spinal cord lateral surface at the level of the low thoracic cord (T11-T13). In this case stronger electrical pulses (0.1 ms duration and 5-40 V amplitude) were usually required to elicit motoneuronal responses (Pinco and Lev-Tov, 1994).

For each preparation, stimulation intensity was expressed as times threshold (× T), where T was the lower stimulation amplitude that was able to elicit an antidromic spike (for VR stimulation) or a detectable postsynaptic response (for DR or ventrolateral stimulation). On a sample of preparations used for repetitive stimulation protocols (see Results section) threshold was measured for DR (T=1.8±0.5 V; n=28) or ventrolateral (T=18±4 V; n= 11) stimulation.

When protocols requiring repetitive activation of fibres were applied, stimulation intervals were set with a Digitimer 400. During such protocols repetitive stimuli at a given period were usually applied for 5 min (though in some cases for up to 15 min).

5. Recording techniques.

a. Intracellular recordings.

Intracellular recordings from motoneurons were performed with sharp glass microelectrodes filled with 3 M KCl and connected via a 0.1× headstage (Axon Instruments) to an amplifier (Axoclamp 2A, Axon Instruments). Electrode resistance was 25-70 MΩ. Current-clamp recordings were performed either in bridge or in discontinuous current-clamp mode at 1.5-2 kHz. The sharp microelectrode was also used to inject current into the cell (via the Axoclamp circuits). Motoneuron input resistance was calculated as the ratio between the steady state hyperpolarization induced by injection of a negative current pulse (500 ms) to the amplitude of the current injected (usually 0.1 nA). Single-electrode voltage-clamp was performed with electrodes of resistance <30 MΩ using a switching frequency between voltage recording and current injection of 2.5-3 kHz and a gain ≥ 1nA/mV. Current and voltage signals were displayed on line on an oscilloscope (Hewlett & Packard 54600A), a chart recorder (Gould TA240) and a computer monitor (using PClamp software in Fetchex mode). Signals were also digitised (VR-10B, Instrutech Corporation) and recorded on videotape for off-line analysis. When stimulation protocols were used, data were usually also stored on-line in a computer hard-disk via PClamp software (in Clampex mode; sampling interval 36 μs- 1 ms).

Motoneurons were identified through antidromic stimulation: When the electrode was lowered into the ventral horn, single pulse stimulation at 0.5 Hz was applied to the ipsilateral homologous ventral root. When the electrode reached a motor nucleus, such a stimulation evoked a short-latency (1-2 ms) mono or biphasic field potential due to motoneuron population firing (Fulton and Walton, 1986a). At this stage electrode resistance was monitored by brief (10 ms) pulses of negative current (0.1 nA). Increase in the apparent electrode resistance was used as a diagnostic sign that the electrode touched the membrane of a motoneuron. The "clear" command of the amplifier was used in order to favour membrane penetration. After motoneuron impalement, ventral root stimulation elicited a short latency (≤2 ms, see fig R.2A-C of Results section) all-or-none overshooting antidromic action potential (Fulton and Walton, 1986a). Examples of this kind of responses are illustrated in fig R.2A-C of Results section. Only cells in which this kind of response could be consistently elicited were considered as identified motoneurons and included for analysis.

b. Ventral root recordings.

Ventral root recording was performed with miniature monopolar suction electrodes made by glass capillaries. A silver/silver-chloride pellet (World Precision Instruments) was inserted in the capillary (together with a suction tube) and connected to a low-noise battery-powered DC-coupled amplifier (DAM 50, World Precision Instruments), usually with 30 kHz lowpass filter. When slow drifts of the voltage signal made DC-coupling unsuitable for recording, AC-coupled (100 Hz-10 kHz passband) amplification was used. Signals were displayed on line on a chart recorder and tape-recorded for further analysis. An additional 20 Hz low pass filter was sometimes used. The tip of the suction electrode allowed entry of the entire length of VR and establishment of a seal between the tip and the cord surface. Under these conditions DC-coupled ventral root recording was suitable to detect not only firing activity but also slower membrane potential variations of the corresponding population of motoneurons. In fact, while firing activity usually appeared as biphasic signals under these recording conditions, slower polarization changes that took place simultaneously in a large number of motoneurons preserved the same polarity as those observed with intracellular techniques, as clearly demonstrated by comparison of

the stereotypical bursts recorded either from a single motoneuron or from a ventral root, as shown for instance in fig R.5 of Results section. This fig also shows that bursting activity could still be suitably detected when signals were AC coupled and/or lowpassed at 20 Hz (see Results).

6. Discrete lesions of the spinal cord

Lesions of the spinal cord were performed with a razor blade fragment under a microscope in order to determine the localization of the rhythmogenic networks in the absence of synaptic inhibition. When laminar lesions were performed, after electrophysiological recordings the preparation was fixed with tissue-freezing medium (Cryogel, Yung) and frozen at -80 °C; 60 μm slices were sectioned with a cryostat, stained with toluidine blue (1% in distilled water) and examined with a Zeiss Axiovert 135 microscope (5× magnification).

7. Drugs

Drugs were bath-applied via the superfusion solution. For this purpose, stock solutions of the agents (usually at concentrations 10^3 times larger than the final ones) were made in distilled water or dimethylsulphoxide (in this case the solvent bath concentration was ≤0.02%) and frozen in small aliquots (≤1 ml). The final concentration was obtained by dissolving an amount of the stock solution into the oxygenated ACSF. The following drugs were used:

-α-amino-3-hydroxy-5-methyl-4-isoxazolepropionate (AMPA)
-γ-aminobutyric acid (GABA)
-3-((RS)-2-carboxypiperazine-4-yl)-propyl-1-phosphonate (CPP)
-5-hydroxytryptamine (5-HT)
-6-cyano-7-nitroquinoxaline-2,3-dione (CNQX)
-apamin
-bicuculline methiodide (bicuculline)

-carbachol

-cyclothiazide

-glutamate

-glycine

-N-Methyl-D-aspartate (NMDA)

-N-Methyl-lignocaine iodide (QX 222)

-ouabain

-R-5-aminophosphonovalerate (APV)

-strophanthidin

-strychnine nitrate (strychnine)

-tetrodotoxin (TTX)

8. Data analysis

Quantitative analysis of bursting activity required a definition of several parameters. For intracellular and DC-coupled extracellular recordings, a burst was defined as a period of sustained membrane depolarization above a threshold, that was set at 5-25 times the standard deviation of the baseline noise (BSD, measured over 0.5-1 s during the quiescent period immediately before the onset of a burst) depending on signal-to-noise ratio conditions. Cycle period was defined as the time between the onset of one burst and the onset of the subsequent one. Burst duration was defined as the time during which the membrane potential remained above the preset threshold. Fig M.2 illustrates burst cycle period and duration measurement in a typical intracellular experiment in which the BSD was 0.37 mV and the threshold was set at 25×BSD. Definition of burst duration was chosen in an attempt to include only the portion of this event that was manifestly driven by synaptic currents. In fact, as shown in the example of fig M.2, when recorded intracellularly under current-clamp conditions an individual burst was characterized by a stereotypic oscillatory waveform (with superimposed action potentials) followed by a long afterdepolarization (characterized by the absence of detectable synaptic events) that persisted up to the onset of the following burst. Burst decay could be usually fitted by the sum of two exponential functions, one with a fast decay time constant (139±14 ms in

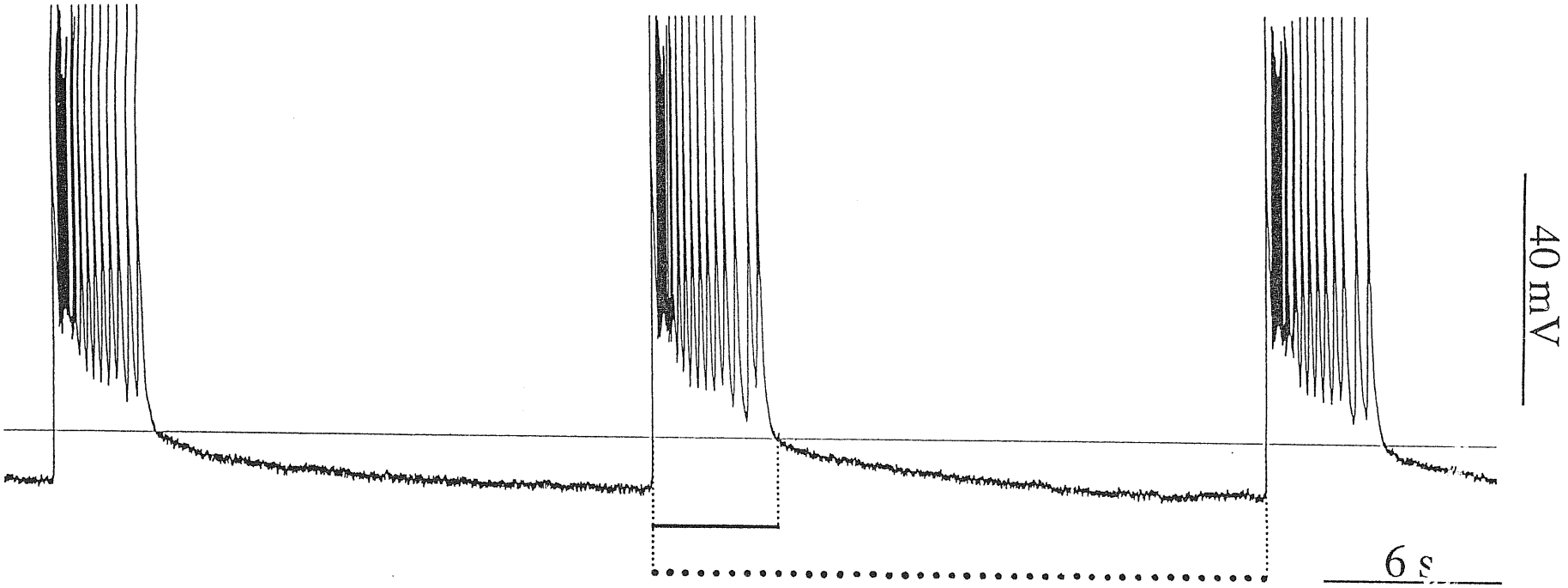

Fig M.2. Example of measurements of burst duration and cycle period during spontaneous bursting.

Original intracellular recordings (under current-clamp conditions) from a motoneuron during typical spontaneous bursting activity (comprising three burst episodes) are shown. The horizontal straight line represents the threshold level for burst detection (this level was set at 25 times the standard deviation of the baseline noise above the resting membrane potential attained immediately before the onset of a burst). Onset and offset of the central burst are indicated by vertical dotted lines. Burst duration (illustrated by the horizontal solid bar for the middle burst) is defined as the time during which the motoneuron membrane potential remained positive to the threshold level. Cycle period (illustrated by dotted horizontal line for the middle cycle) is defined as the interval between the onset of one burst and the onset of the following one.

the example of fig M.2) and one with a slow decay time constant (6.9±1.6 s in the example of fig M.2); the faster decay time constant corresponded to the falling phase of the last intraburst oscillation (see Results section for a description of intraburst structure), while the slower decay time constant corresponded to the persistent afterdepolarization. Under voltage-clamp conditions (see Results section), intraburst oscillations could be detected as rhythmic currents with a timecourse similar to that of current-clamp potential oscillations. Such rhythmic currents displayed an inward polarity at negative holding potentials, disappeared at 0 mV holding potential and were detected as outward currents at positive holding potentials (see fig R.8 of Results section). In this case burst decay could be fitted by a monoexponential function with a decay time constant similar to the faster decay time constant of current-clamp experiments (<150 ms). As explained in the Results section, these findings suggest that intraburst oscillations were mediated by excitatory synaptic events, whose timecourse was poorly affected by motoneuron membrane potential. On the other hand, under voltage-clamp conditions (regardless of holding potential in the range -80, +20 mV) it was not possible to detect any current corresponding to slowly decaying afterdepolarization observed under current-clamp conditions. These findings suggest that origin and nature of such an afterdepolarization, that remain obscure, were different from those of intraburst oscillations. For this reason the adopted burst definition consistently allowed inclusion of intraburst oscillation and exclusion of the slowly decaying depolarization.

Burst frequency was calculated as the inverse of the cycle period. In this way a frequency value (usually expressed as burst/min) was associated to each burst cycle. Therefore, an average value and a standard deviation could be calculated for burst frequency (as well as for cycle period) during a given treatment in each preparation.

Rise-time was measured from baseline to peak; only intracellular experiments were used for rise-time measurements. Burst amplitude was defined as the peak amplitude of the initial (and largest) burst depolarization, that was usually followed by several oscillations reaching less depolarized levels (see for instance fig R.4C of the Results section). Intraburst oscillations frequency was measured as the inverse of the peak-to-peak time interval. Voltage calibration is usually reported only for intracellular experiments.

Pooled data were expressed as mean ± standard deviation. Statistical differences between groups of data were analysed by using Student's *t* test. According to the in-use convention, two groups of data were considered significantly different when $P<0.05$. Regularity of bursting patterns was quantified by two parameters: the coefficient of variation of burst duration (CVd) and the coefficient of variation of cycle period (CVc), that were calculated in each preparation for a given treatment as the ratio between the standard deviation and the mean value of burst duration or cycle period and expressed as percent values.

RESULTS

1. Viability of the spinal cord.

After dissection, spinal cord viability was ascertained by means of electrophysiological tests. In healthy preparations, single pulse, above-threshold stimulation of one lumbar dorsal root elicited a reflex response in the ipsilateral ventral root at the same segmental level; furthermore, above-threshold stimulation of one VR (0.1 ms) elicited a mono or biphasic extracellular field potential in the motor nuclei; this response could be recorded with a sharp microelectrode in the ipsilateral ventral horn at the same segmental level of the stimulated VR. If these properties were missing the preparation was not used for experiments. Usually healthy spinal cords could be maintained in vitro for many hours (up to 12) without any apparent electrophysiological sign of deterioration. Only in 3 of the 212 spinal preparations that were used for the present study, a gradual rundown of DR- or VR-evoked responses prevented carrying out of the experimental protocols.

2. Spontaneous and evoked activity of motoneurons in control solution.

Intracellular recordings were performed from 97 motoneurons in 71 different preparations. On average, motoneuron membrane potential (in the absence of injected current) was -69±8 mV and motoneuron membrane input resistance was 40±14 MΩ.

In control solution, the spontaneous activity of motoneurons recorded with a sharp microelectrode consisted of frequent, depolarizing synaptic potentials occurring in a random fashion; not infrequently, a tendency for these synaptic potentials (that occasionally reached the threshold for action potential) to form clusters of activity was observed, as shown in the example of fig R.1 (for another example of spontaneous activity in control solution see also fig R.3A,C).

Antidromic stimulation of the corresponding VR elicited an action potential in the impaled motoneuron (fig R.2A); these evoked events were characterized by a latency

between the stimulus artefact and the onset of the spike ≤2 ms. On average, antidromic spike amplitude was 78±13 mV. These data are in accordance with previous reports (Fulton and Walton, 1986a, b). Gradual hyperpolarization of the motoneuron membrane potential by injection of a negative current resulted in an all-or-none reduction of the antidromic spike amplitude (compare fig R.2A, B with fig R.2C); this phenomenon is known to be due to failed invasion of the somato-dendritic compartment by antidromically travelling action potential (Eccles, 1964).

In control solution, DR stimulations evoked short latency (<10 ms) depolarizing synaptic potentials in motoneurons. These responses were similar to those previously described in the same preparation (Lev-Tov and Pinco, 1992; Pinco and Lev-Tov, 1993a), since they usually comprised both mono and polysynaptic components and displayed a marked frequency-dependent paired-pulse depression for intervals between 0.5 and 30 s. Fig R.2D and 2E illustrate two examples of such paired pulse depression of DR-evoked motoneuronal responses for 1 s interstimulus interval; in both cases DR stimulation intensity was set to evoke responses that did not reach firing threshold.

As previously described (Lev-Tov and Pinco, 1992; Pinco and Lev-Tov 1993b), DR-evoked responses (recorded from motoneurons or VRs) were mediated by both NMDA and non NMDA glutamate receptors and were fully abolished (n=8) by combined application of the NMDA receptor blocker 2-amino-5-phosphonovaleric acid (APV; 20 μM) and of the non-NMDA receptor blocker 6-cyano-7-nitroquinoxaline-2,3-dione (CNQX; 10-20 μM).

Stimulation of the ventrolateral fibres evoked depolarizing responses in lumbar VRs (latency ≤20 ms). As previously described (Elliott and Wallis, 1993; Pinco and Lev-Tov, 1994), such responses were strongly reduced in amplitude and area (by ≥90 %) by co-application of CNQX and APV (n=4).

3. Effects of pharmacological block of $GABA_A$ receptors in the spinal cord.

The present study was aimed at investigating the reorganization of spontaneous synaptic activity in the neonatal rat spinal cord after block of synaptic inhibition, with special interest in the possible development of rhythmic phenomena under these conditions.

Therefore, we firstly studied the effects of single pharmacological block of either $GABA_A$ and glycine receptors, that mediate the two main inhibitory processes in the spinal cord (Young and Macdonald, 1983; Davidoff and Hackman, 1984).

When the $GABA_A$ receptor antagonist bicuculline (20 μM, sufficient to saturate $GABA_A$ receptors; DeFeudis and Somoza 1977; Moehler and Okada 1977) was bath-applied to the spinal cord, spontaneous synaptic activity of motoneurons (recorded intracellularly) was changed into irregular paroxysmal bursting in 5/5 preparations tested. A typical example of the effects of bicuculline on spontaneous activity recorded from a lumbar motoneuron is illustrated in fig R.3A-B. In all preparations tested, bicuculline-induced bursts were initiated by a rapid depolarization (average rise time =336±87 ms) and followed by a plateau phase (lasting 5-40 s) characterized by superimposed high-frequency irregular activity. Bursts terminated with a slow decay phase (during which high-frequency activity waned). On average, burst duration was 34±21 s, with peak amplitude of 40±10 mV and frequency of 1.6±0.8 burst/min. Not infrequently two or more bursts coalesced together. On average, the values for CVd and CVi were 51±11 and 37±10 %, respectively, a finding which indicated their irregular duration and occurrence. The input resistance of motoneurons was not significantly changed in the presence of bicuculline; the resting membrane potential (measured during the interburst quiescent intervals) was also unchanged. Bicuculline-induced effects could be completely reversed within 10-20 min wash out (fig R.3C).

4. Effects of pharmacological block of glycine receptors in the spinal cord.

Bath application of the glycine antagonist strychnine (1 μM, sufficient to saturate glycine receptor; Becker et al. 1988; Schneider and Fyffe, 1992) did not induce spontaneous bursting of motoneurons in 10/12 preparations, in which it caused a marked reduction of the small amplitude depolarizing synaptic potentials (<10 mV) and the sporadic appearance of large-amplitude (>10 mV) depolarizing events, that occasionally reached the threshold for action potential firing. The different effects of bicuculline and strychnine on motoneuronal spontaneous activity are shown in the example of fig R.3. In this experiment strychnine was applied after 30 min bicuculline washout (fig R.3D), when the effects of bicuculline on spontaneous activity of the recorded motoneuron had fully

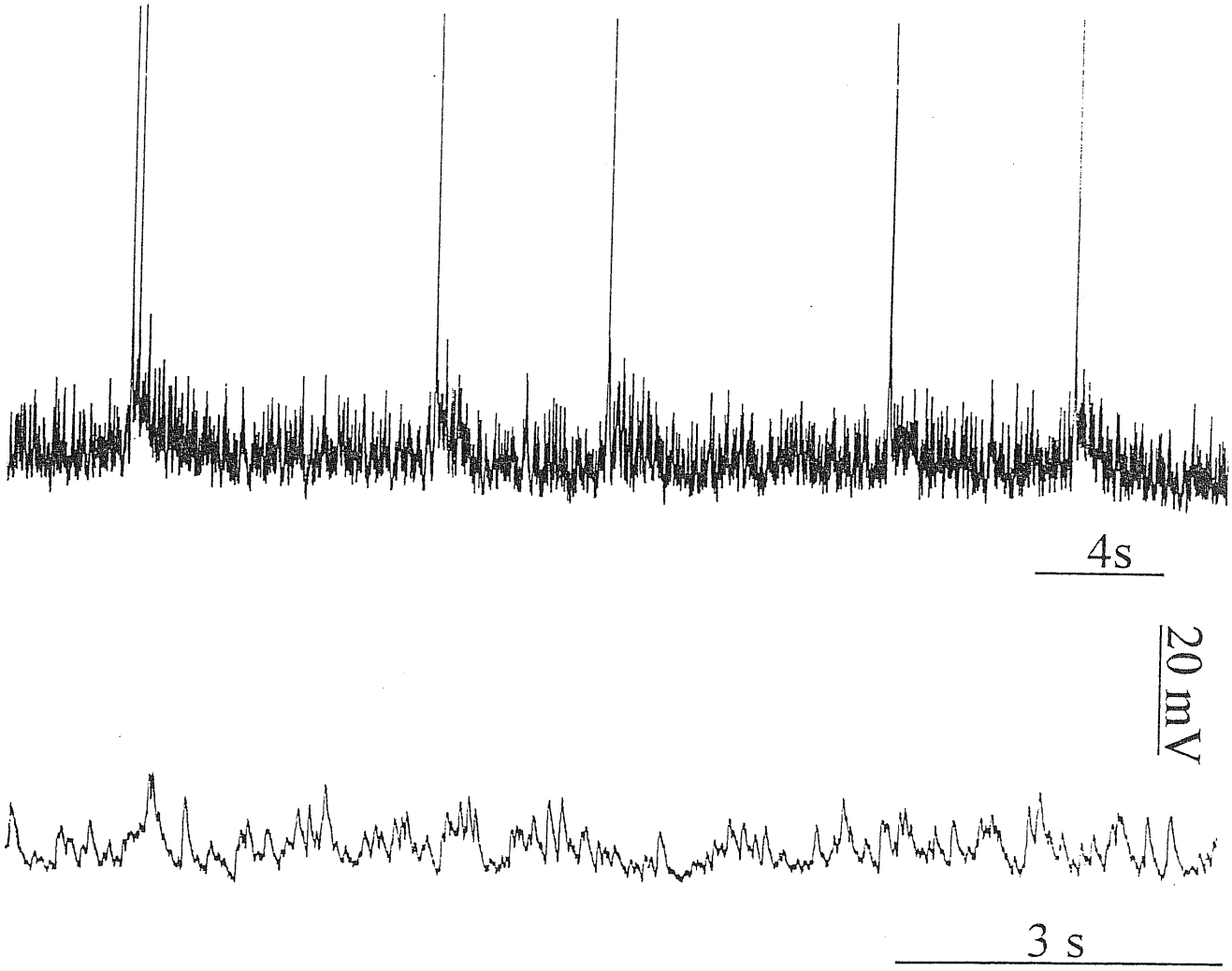

Fig R.1. *Spontaneous activity of single lumbar motoneuron in control solution.*

Top trace shows spontaneous synaptic activity of a motoneuron comprising irregularly-occurring clusters of depolarizing synaptic potentials (occasionally reaching firing threshold). Bottom trace shows spontaneous activity of the same cell on a faster timescale: individual depolarizing synaptic potential can be recognized. Resting potential: -69 mV. In the top trace spikes are truncated.

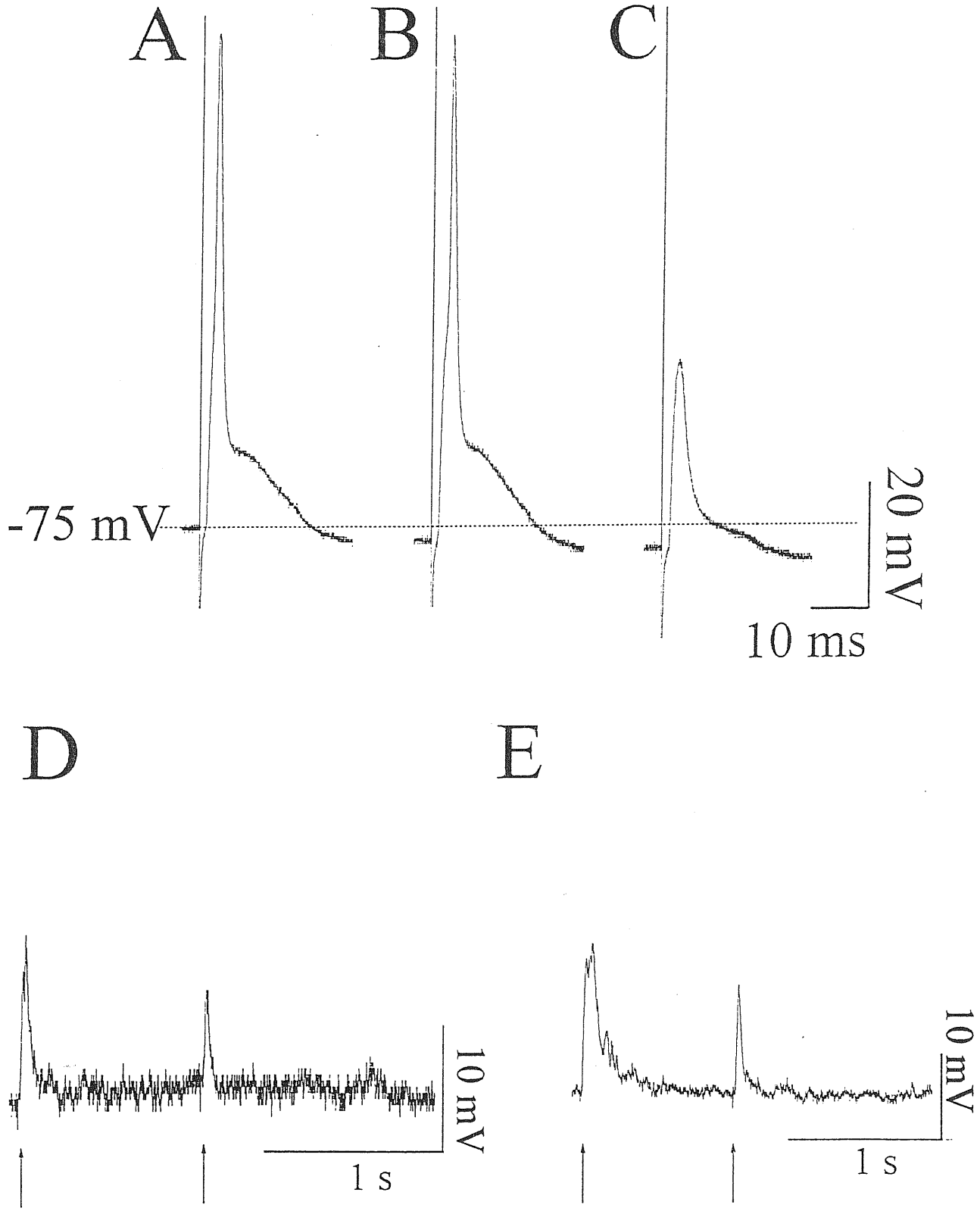

Fig R.2. *VR- and DR-evoked responses of motoneurons in control solution.*
A: Antidromic action potential elicited by single VR stimulation (see artefact) in a motoneuron with a resting membrane potential of -75 mV. B: when the cell is hyperpolarized by 3 mV through current injection a fully developed action potential can still be evoked by VR stimulation. C: further hyperpolarization (1.5 mV) produces a dramatic decrease in the amplitude of the VR-evoked event. D, E: effects of paired DR stimulations (1 s apart, indicated by arrows) on lumbar motoneurons of two different preparations. In both cases depolarizing synaptic response evoked by the second pulse is strongly depressed with respect to the one evoked by the first pulse. Resting potential: -72 mV (D) or -75 (E).

disappeared (fig R.3C). Only in 2/10 preparations application of strychnine evoked sporadic, irregular spontaneous bursting (not shown). Even when strychnine did not elicit spontaneous bursting, dorsal root stimulation elicited long-lasting burst-like events, as previously described (Wu et al, 1992; Pinco and Lev-Tov, 1993a). In none of the motoneurons tested strychnine elicited significant alterations in resting potential or input resistance.

5. Simultaneous block of $GABA_A$ and glycine receptors: rhythmic bursting.

When bicuculline and strychnine were co-applied, a highly regular bursting pattern developed in motoneurons. Such a bursting activity became stable after 10-15 min from the beginning of the application and then persisted as long as the application was maintained (up to 6 hours). Only in 2 out of 205 preparations to which strychnine and bicuculline were coapplied during intracellular or extracellular recordings, rhythmic bursting activity was not observed. A typical example of the effects caused by strychnine and bicuculline is shown in fig R.4, in which the spontaneous activity of a lumbar motoneuron before and after coapplication of these agents is illustrated. The early phase (0-10 min) of the application was characterized by paroxysmal, irregular bursts that lasted for several tenths of seconds. This activity gradually turned into regular rhythmic bursting. In the faster timescale trace of fig R.4 (middle) the clock-like burst occurrence (approximately 2 events/min) is apparent. Bursts were followed by a long-lasting afterdepolarization that often persisted till the onset of the next burst (see Methods section for definition of burst duration). The interburst interval was characterized by the absence of any detectable synaptic potential. A further timescale expansion comprising one individual burst is presented in the bottom trace of fig R.4 and reveals the typical structure of these events, characterized by a rapid depolarizing onset (about 100 ms from baseline to peak with an amplitude > 40mV) followed by a plateau phase (lasting 0.2-2 s) over which large-amplitude "intraburst" oscillations of the motoneuron membrane potential gradually developed. Such oscillations lasted for several seconds and were characterized by a decreasing frequency along the course of the burst (in the range 6-2 Hz). Firing activity was usually present during the plateau phase and during the rising

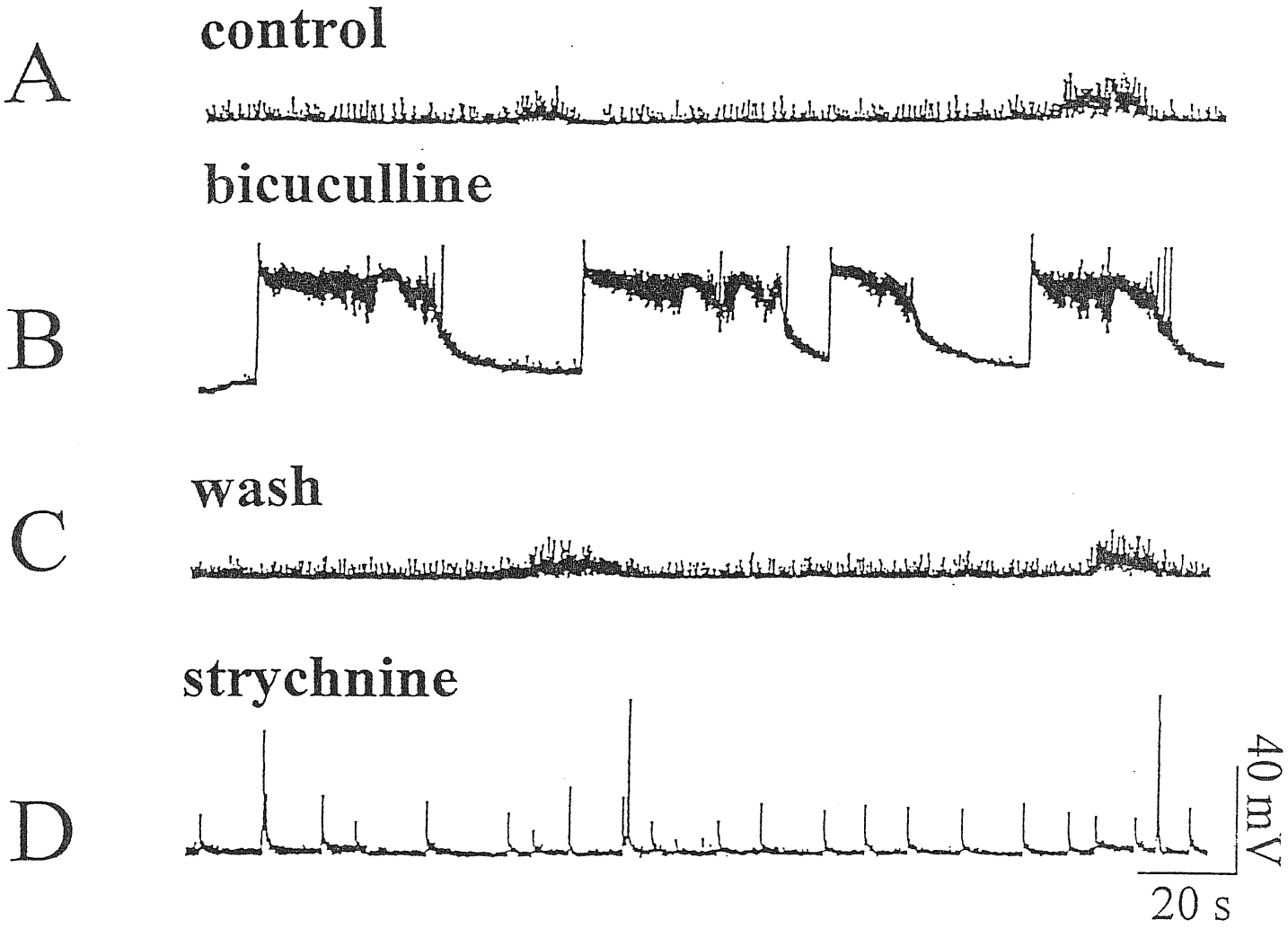

Fig R.3. *Spontaneous activity of motoneurons in the presence of bicuculline or strychnine.* Spontaneous synaptic activity in control solution (A) is changed into irregular bursting pattern (B) after 5 min bicuculline application, an effect reversible after 20 min washout (C). In the same cell subsequent strychnine application (D) depresses low-amplitude activity and produces irregularly occurring, large-amplitude synaptic potentials. Resting potential (-70 mV) was not changed by bicuculline or strychnine application.

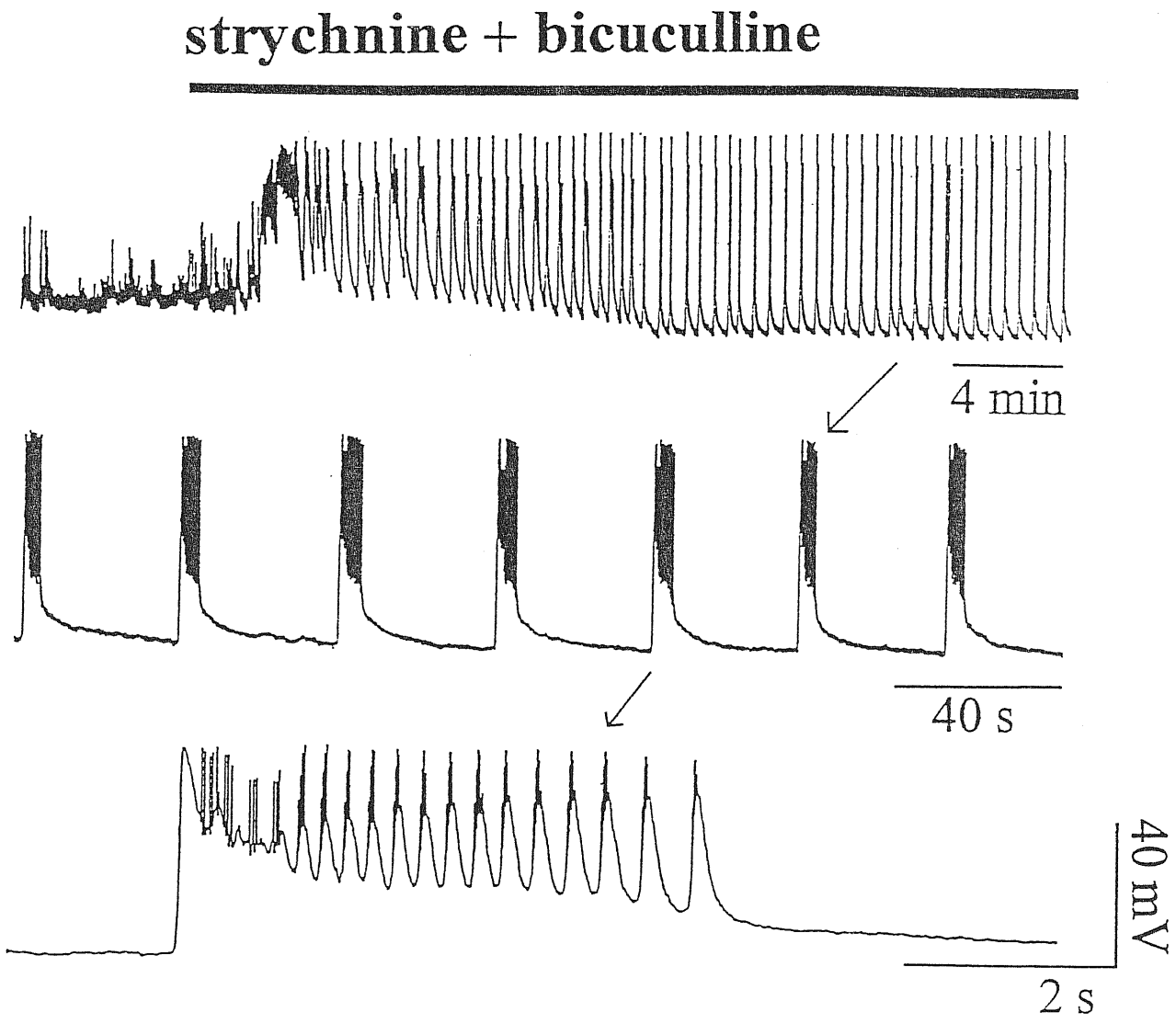

Fig R.4. *Effects of simultaneous application of strychnine and bicuculline.*

Coapplication of strychnine and bicuculline converts control-solution spontaneous activity of a motoneuron into paroxysmal, large amplitude depolarizing events that occur irregularly in the early phase of coapplication. This activity spontaneously turns into a persistent, regular rhythm after 10 minutes application (top trace). A portion of such regular bursting activity (see arrow) is presented at faster timescale in the middle trace. A further expansion (bottom trace) illustrates the typical structure of an individual burst (indicated by arrow), that comprises an initial depolarization followed by a plateau phase and by several intraburst oscillations. Resting potential: -73 mV.

phase of the intraburst oscillations and occasionally during the rapid depolarization that initiated a burst.

On average, a sample of 45 intracellular experiments provided the following values for spontaneous bursts induced by strychnine and bicuculline: risetime 96±15 ms; peak amplitude 44±12 mV; mean intraburst oscillations frequency 3.7±2.1 Hz (range 1-7 Hz); cycle period 29±12 s; burst duration 6.7±2.5 s; CVc=15±8 % and CVd=13±10 %. The low values obtained for the coefficients of variation confirm the more regular occurrence and duration of these events in comparison with the bicuculline-induced bursts. No significant differences related to rat age were found for these values within the tested age range (P0-P12).

Ventral root recordings during rhythmic bursting

Intracellular recordings provided information about rhythmic bursting in individual motoneurons but did not clarify whether this activity took place synchronously in different motoneurons. In order to test whether bursting occurred simultaneously in motoneurons innervating one VR, extracellular recordings were performed from lumbar VRs. As shown in fig R.5B, under these conditions bursting could still be detected and (when DC-coupling was used) its appearance was similar to that of intracellular recordings (compare fig R.5A and B). VR recorded bursts appeared rhythmically at a frequency similar to that of intracellularly recorded bursts and were separated by quiescent periods in which no detectable synaptic activity was present. Faster timescale tracings revealed that also the intraburst oscillatory structure of individual bursts was similar to that recorded intracellularly (compare expanded traces on the right in fig R.5A and B). Burst frequency, burst duration and intraburst oscillation frequency measured from ventral root recordings were not significantly different from those obtained with intracellular recordings. Bursting activity could be consistently recorded from any lumbar ventral root (n=6). These results (together with the observation that rhythmic bursts were present in all antidromically identified motoneurons in the presence of strychnine and bicuculline) clearly indicated that not only rhythmic bursts, but also intraburst oscillations took place almost simultaneously in nearly all motoneurons innervating one lumbar ventral root. AC-coupled trace of fig R.5C also show that this kind of filtering

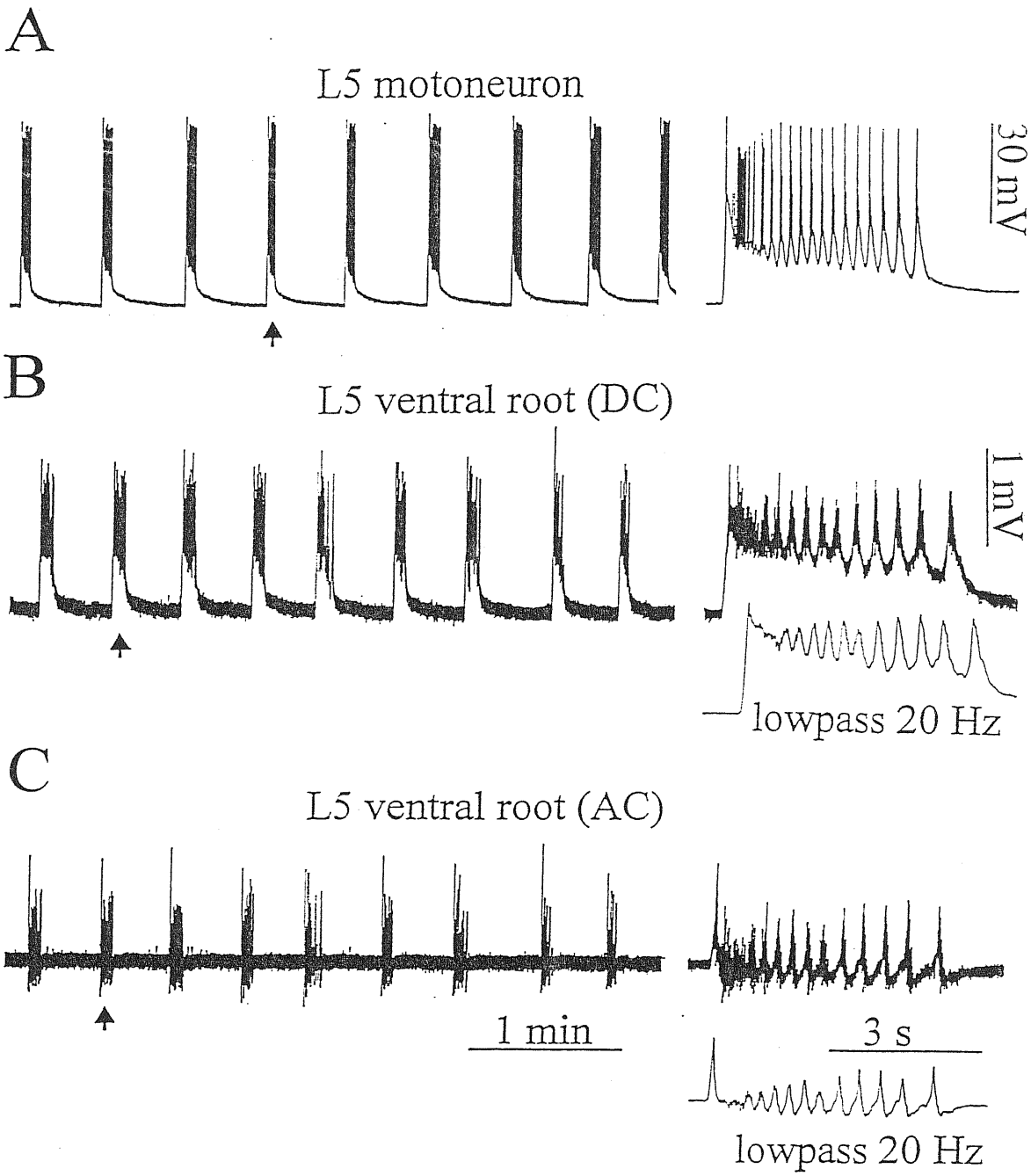

Fig R.5. *Comparison of intracellular and extracellular recordings of bursting activity induced by strychnine and bicuculline.*
A: intracellular traces from L5 motoneuron (resting potential: -75 mV) displaying regular rhythmic bursting characterized by rapid depolarization with superimposed trains of action potentials. A single event (indicated by arrow) is shown on the right with a faster timebase to resolve intraburst oscillatory activity. B: DC-coupled extracellular recording of similar bursting (different preparation from A) from one L5 ventral root. Note similar bursting pattern and structure as observed with intracellular electrode. Traces on the right represent faster timebase records (bottom trace depicts the same event of top trace after 20 Hz lowpass filtering) of the individual burst indicated by arrow. C: AC-coupled VR recording of the same activity depicted in B. Righthand traces show the same single event (faster timebase; the bottom trace is lowpassed at 20 Hz). Note that extracellular recording (either DC or AC coupled) from ventral root provides a reliable method to observe bursting activity.

preserved much of the information about rhythmic bursting and intraburst oscillations (see Methods). With 20 Hz lowpassing filter information about firing activity was lost but slower membrane oscillations were still clearly recognizable (fig R.5B, C). Ventral root recordings were then extensively used to complement intracellular studies, especially in those experiments that required the application of very long protocols.

The degree of synchronicity within different motoneuronal pools was investigated by means of simultaneous recordings from different pairs of ventral roots in the lumbar segments (n=8). Simultaneous recordings from any ipsi- or contralateral pair of lumbar ventral roots revealed that rhythmic activity (including intraburst oscillations) in the disinhibited spinal cord was strongly synchronized in all lumbar motor pools. This phenomenon is illustrated in the examples of fig R.12, 13A, 23B and 27, in which simultaneous recordings from left and right lumbar ventral roots in the presence of strychnine and bicuculline are presented.

Tests for effectiveness of pharmacological block of $GABA_A$ and glycine receptors.

Even if strychnine and bicuculline are known to block inhibitory synaptic transmission in rat motoneurons *in vitro* (Wu et al., 1992), it was important to directly test that in the present experimental conditions inhibitory synaptic processes were blocked throughout the spinal network. This was assessed by experiments performed with VR recordings.

Bicuculline (20 μM) and strychnine (1 μM) were first tested for their ability to prevent the inhibitory action of exogenously-applied glycine or GABA (in concentrations known to inhibit motoneurons strongly; Wu et al., 1992) on polysynaptic reflexes (elicited in L5 VR by electrical stimulation of the homologous ipsilateral DR). DR stimulations were continuously delivered at 8 s intervals, in order to avoid excessive frequency-dependent depression of the reflex (Lev-Tov and Pinco, 1992). Glycine (0.5 mM) caused a strong reduction in reflex peak amplitude and area (fig R.6A). On average, in 3 preparations such a glycine application significantly ($p<0.0001$) decreased polysynaptic reflex peak amplitude by 37 ± 21 % and area by 64 ± 18 %. These effects were readily reversed on wash out (fig R.6A). Subsequent application of 1 μM strychnine caused an increase in reflex peak amplitude (37±15 %) and area (52±25 %) with the appearance of time-

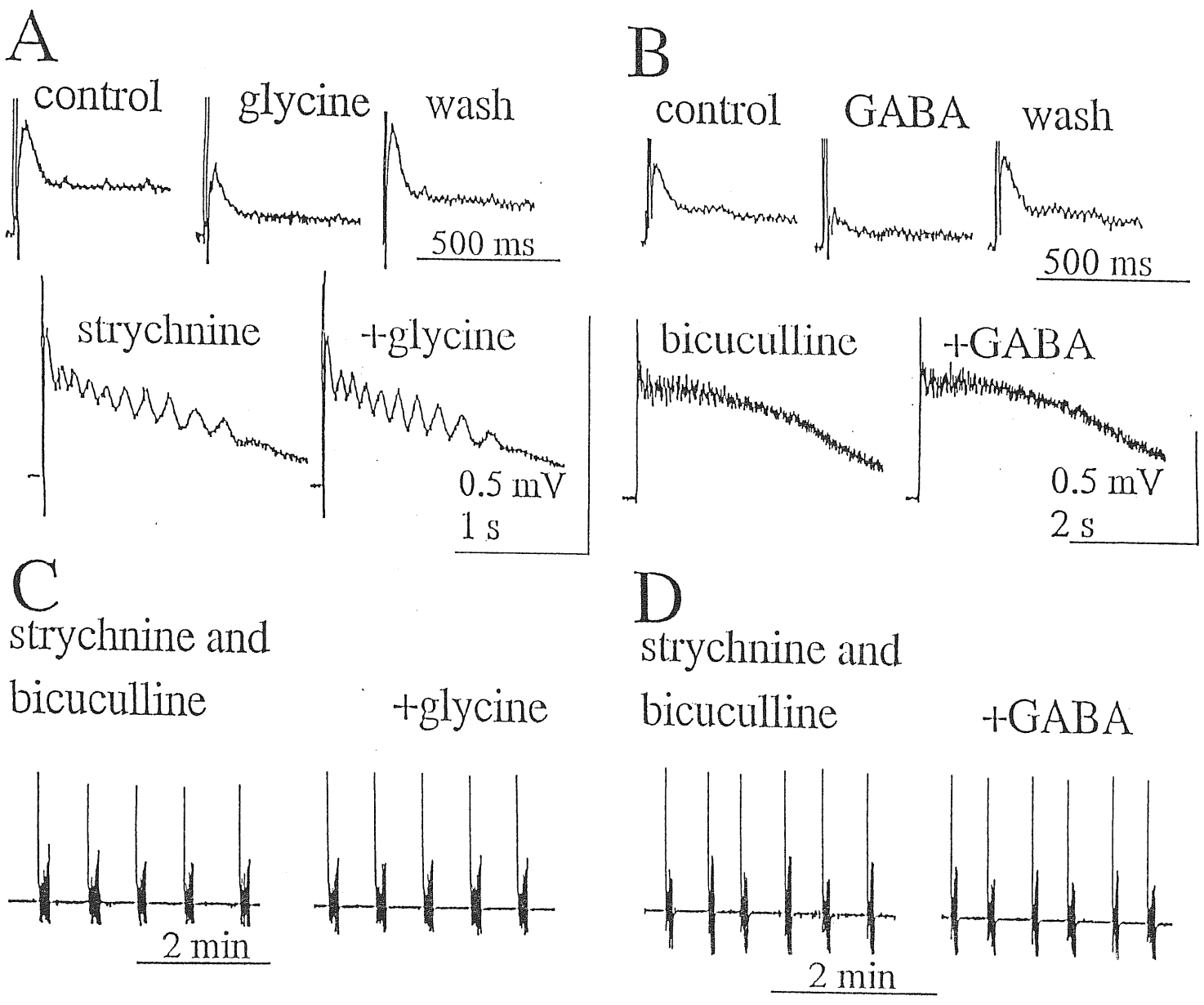

Fig R.6. *Effects of glycine or GABA on reflex activity and bursting.*
A, top: DC records of polysynaptic reflex activity elicited by DR stimulation (0.1 ms duration; 1/8 s frequency) before (control), during (glycine) or after (wash) application of 0.5 mM glycine. Responses are averaged records of ten traces. Those in glycine solution are taken two min after the start of glycine superfusion; wash indicates ten min after glycine washout. Bottom: strychnine (1 μM) enhanced reflex amplitude and induced oscillatory patterns. This effect was not sensitive to glycine (0.5 mM; same preparation as above). B (different preparation from A), top: DC records of polysynaptic reflex activity elicited as described in A before, during or after application of 1 mM GABA. Bottom: bicuculline (20 μM) enhanced reflex activity and prevented the effect of GABA. All responses are averaged records of ten traces and were recorded in the presence of CGP 52 432 (10 μM) to block $GABA_B$ receptors. C: AC-coupled records of spontaneous bursting activity (same preparation as in A) induced by co-application of strychnine (1 μM) and bicuculline (20 μM); glycine (0.5 mM) has no depressant action confirming that glycine receptors are effectively blocked. D, comparable records (same preparation as in B) showing the lack of depressant action of GABA (1 mM) on bursting activity induced by strychnine and bicuculline (in the presence of CGP 52 432), indicating that $GABA_A$ receptors are effectively blocked.

locked oscillations at 4-8 Hz (see example in fig R.6A). In the presence of strychnine, application of 0.5 mM glycine failed to affect reflex amplitude, area or oscillations. The effects of GABA application on dorsal root evoked reflex before and after application of bicuculline were tested in the presence of 10 μM CGP 52 432 in order to avoid involvement of $GABA_B$ receptors. Under these conditions (n=3), 1 mM GABA significantly ($p<0.0001$) and reversibly reduced reflex peak amplitude by 54 ±11 % and area by 88±19% (see example in fig R.6B). Subsequent application of 20 μM bicuculline increased reflex peak amplitude by 64±13 % and reflex area by 440±110 % but, unlike strychnine, it did not elicit slow, rhythmic oscillations. In the presence of bicuculline, application of 1 mM GABA failed to affect reflex peak amplitude or area (fig R.6B).

After induction of spontaneous bursting by co-application of strychnine and bicuculline to the same preparations, 0.5 mM glycine failed to affect burst frequency or duration (fig R.6C, similar data were obtained on three preparations). GABA (1 mM) was equally ineffective on bursting frequency or duration in the presence of strychnine, bicuculline and CGP 52 432 (n=2; fig R.6D). Prolonged application (>30 min) of CGP 52 432 (10 μM) *per se* did not block bursting induced by strychnine and bicuculline in 4/4 preparations, thus showing that $GABA_B$ receptor activation was not necessary for this kind of rhythmogenesis.

These results were confirmed by the observation that, once rhythmic bursts were induced by 1 μM strychnine and 20 μM bicuculline, progressive increases in strychnine concentration up to 10 μM had no effect on burst frequency or duration. On the other hand, when the non-competitive $GABA_A$ antagonist picrotoxin (100 μM) was coapplied with 1 μM strychnine (in the absence of bicuculline), rhythmic bursts similar to those elicited by bicuculline and strychnine were always observed. Under these conditions (n=4) burst frequency, burst duration and their coefficients of variation were not significantly different from those measured in the preparations treated with strychnine and bicuculline. Similarly, during the course of the experiment replacing bicuculline with picrotoxin (in the continuous presence of strychnine) did not alter the bursting pattern established with bicuculline and strychnine at the start of the recording session (n=2). When co-applied with strychnine, 1 mM penicillin (another $GABA_A$ antagonist) was also

able to induce rhythmic bursts similar to the one elicited by bicuculline and strychnine (n=2).

All together these results showed that in the rat isolated spinal cord $GABA_A$ and glycine receptors were fully blocked by the concentrations of strychnine and bicuculline used in the present study and that under these conditions rhythmogenesis should be based on mechanisms independent of these receptors as well as of $GABA_B$ receptors.

Manipulations of motoneuron membrane potential during rhythmic bursting

Mammalian motoneurons posses membrane properties that can allow these cells to amplify and prolong synaptic signals by generation of plateau potentials (Schwindt and Crill, 1984; Kiehn, 1991; Hultborn and Kiehn, 1992). In order to assess whether such intrinsic motoneuron membrane properties were involved in rhythmic burst generation and to examine the voltage sensitivity of such events, we performed intracellular manipulations of the membrane potential in the presence of strychnine and bicuculline either in current-clamp or in voltage-clamp conditions.

Typical results obtained under current-clamp conditions are illustrated in the example of fig R.7. In this case, varying the membrane potential (which was -70 mV without current injection) from -80 to -60 mV (by -0.51 or +0.8 nA steady DC current, respectively) decreased the amplitude of all components of the burst while individual bursts and their intraburst oscillations were unchanged in duration and frequency (fig R.7 A). Results from the same cell are quantified in the graphs of fig R.7 showing amplitude (C), interburst interval and burst duration (D), and mean oscillation period (E) plotted against membrane potential. On a sample of 4 motoneurons the relation between burst amplitude and motoneuron membrane potential was also found to be approximately linear over -50 to -90 mV range without concomitant changes in burst or oscillation frequency. When depolarizing or hyperpolarizing current steps (2 s) were applied to the motoneuron during a burst, they changed the amplitude but not the timecourse of the oscillations (fig R.7 B). Application of slowly depolarizing ramps (30 mV/s from resting membrane potential to -40 mV) or of 0.1-2s depolarizing current steps during the quiescent periods always failed to generate bursts.

Under voltage clamp conditions the dependence of bursting activity on membrane potential was also explored as illustrated in fig R.8. In this case, voltage activated potassium currents and fast sodium currents were reduced by intracellular application of CsCl and N-methyl-lignocaine-iodide (QX222), respectively. Such application was performed by filling the electrodes with 3 M CsCl plus 0.3 mM QX222. After impalement, motoneurons were current-clamped for 10-20 min, until they lost the ability to generate antidromic action potentials, and then voltage-clamped. After application of bicuculline and strychnine, the I-V relation obtained with 0.5 s long voltage steps from a holding potential of -60 mV during quiescent periods showed a nearly linear behaviour over a wide range of membrane potential (Fig R.8 B). Fig R.8 A shows the effects of changing the holding membrane potential from -60 to 0 or +20 mV on bursting currents. At negative holding potential a burst was detected as an inward current with an oscillatory structure (depicted on a faster time base in the right hand side tracings of fig R.8 A) similar to the one observed in current clamp experiments. This pattern of activity was absent at 0 mV and returned essentially unchanged but with opposite polarity at +20 mV. Similar data were replicated four times. Fig R.8C shows that the relation between the peak amplitude of burst current and the holding membrane potential (varied in 20 mV increments maintained for ≥3 min) was relatively linear with an apparent current reversal at 0 mV. Fig R.8 also shows that, unlike burst amplitude, burst duration and interburst interval (D), as well as mean intraburst oscillation period (E) were not affected by changes in holding potential. Similar results were obtained in 3 cases.

All together these results indicated that the motoneuron membrane properties did not play a major role in shaping bursting activity, that rather appears to result from massive, synchronized excitatory synaptic events characterized by an approximately linear voltage-dependence with reversal potential near 0 mV.

Effects of ventral root stimulation during rhythmic activity.

In the presence of strychnine and bicuculline, stimulation of one VR during intraburst quiescent periods always elicited an antidromic action potential in the corresponding motoneuron (n=6); the amplitude and timecourse of the evoked spike were similar to those observed before application of strychnine and bicuculline. However (in marked

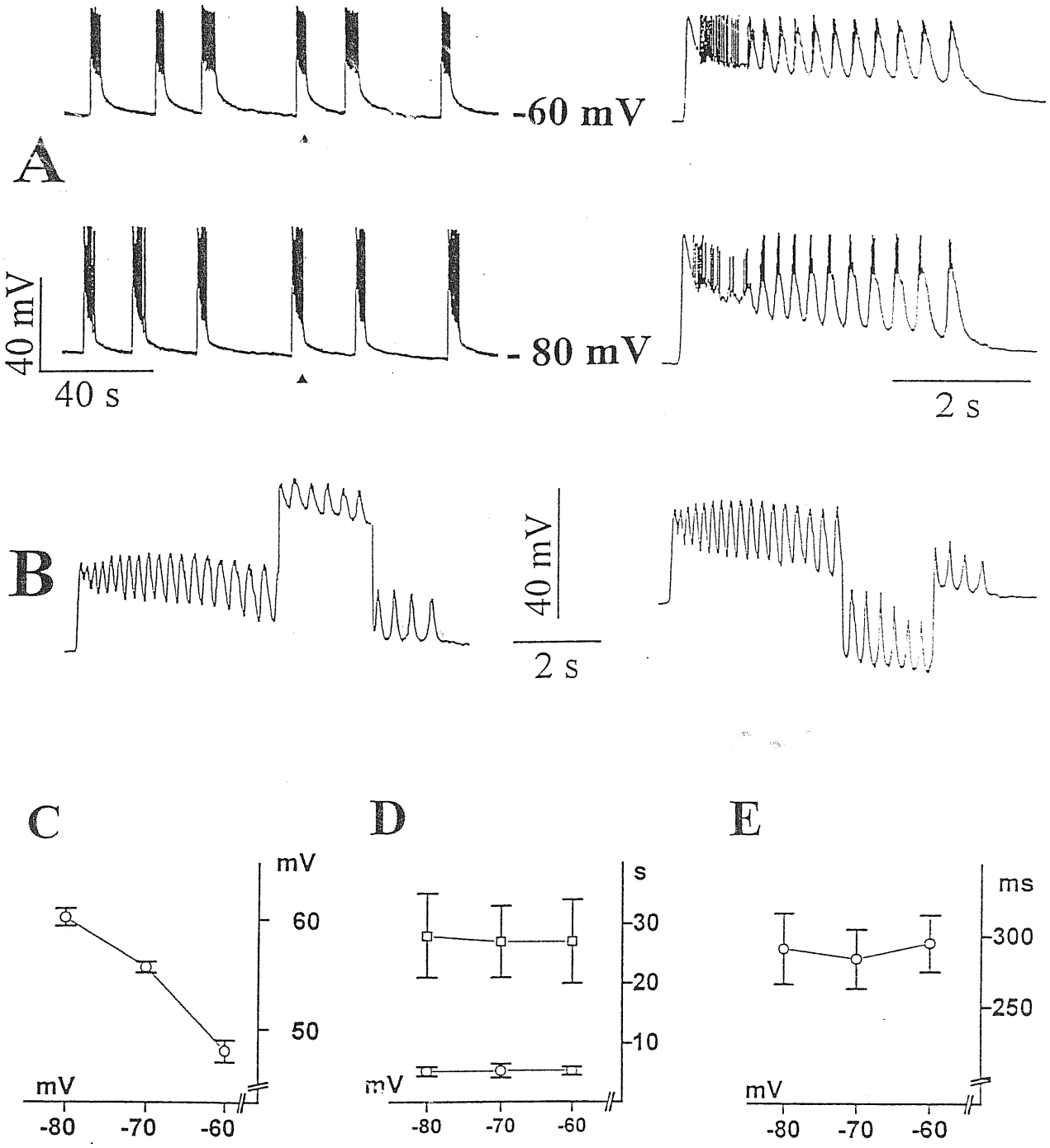

Fig R.7. *Sensitivity of bursts to membrane potential changes in current clamp conditions.*

Under current clamp conditions frequency of bursts and of associated oscillations remains the same at -60 or -80 mV membrane potential while their amplitude grows at the more hyperpolarized value (A). Traces on the right depict faster timebase bursts (marked by a filled triangle on the left hand trace). At -80 mV resting potential current steps (± 0.4 nA; 2 s) applied during the oscillatory phase of the burst change the amplitude but not the frequency of oscillations (B). Tracings in B are not DC mounted and are filtered at 15 Hz to remove spike activity which compounds oscillations (different cell from A,B). Plots illustrate the voltage dependence of peak amplitude (C), of interburst interval (D, squares) and burst duration (D, circles), and of mean intraburst oscillation period (E) for the cell in A. Datapoints in plots C-E refer to the mean of individual responses measured over >4 min for each level of membrane potential.

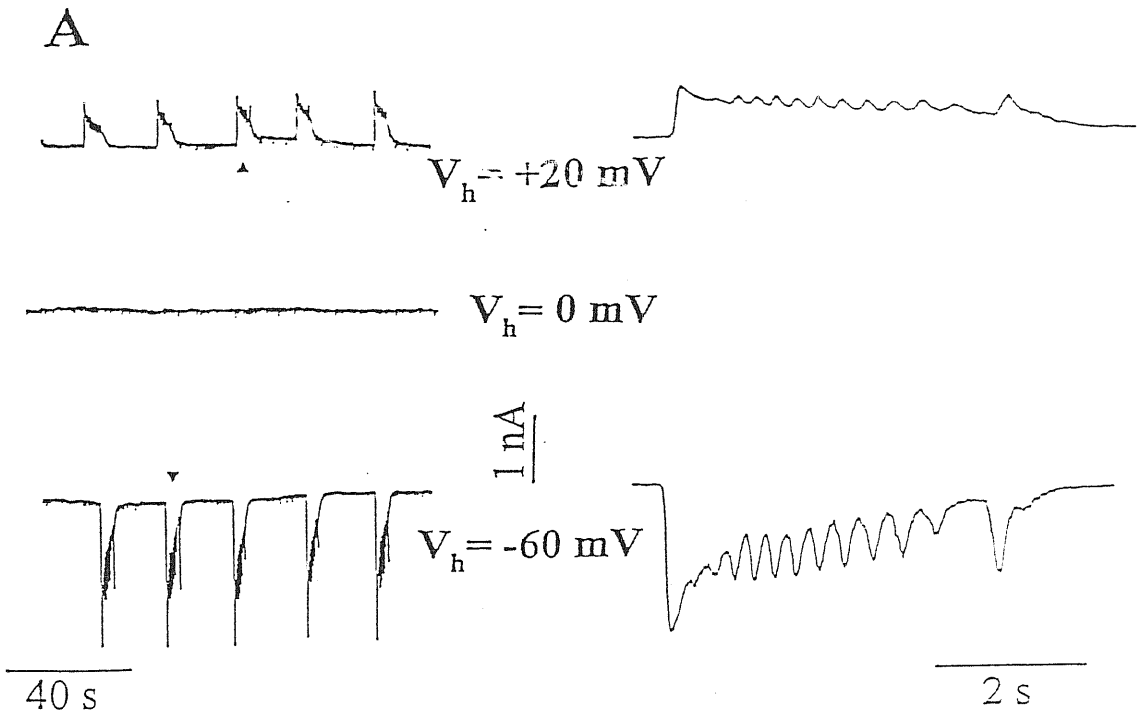

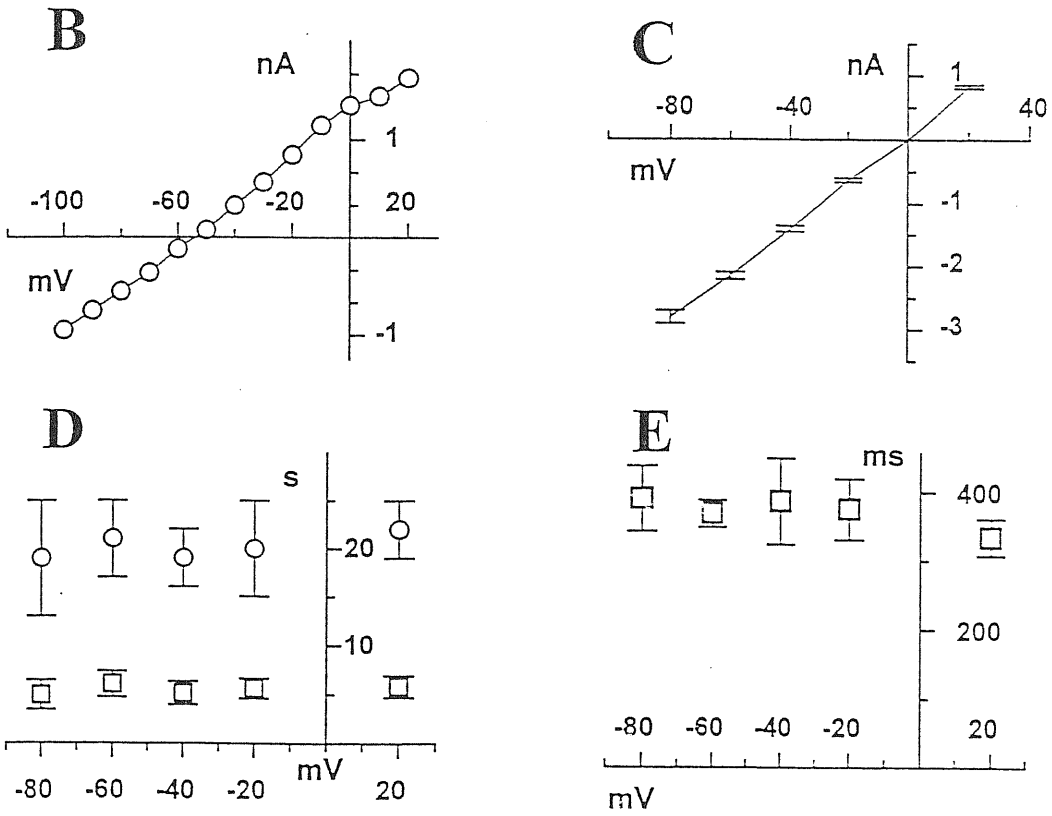

Fig R.8. *Sensitivity of bursts to membrane potential changes in voltage clamp conditions.*
A: bursting currents are outward at +20 mV holding potential (V_h), disappear at 0 mV V_h and are inward at -60 mV V_h. Expanded timebase traces on the right hand side illustrate the timecourse of individual bursts (indicated by filled triangles on the left hand traces) at +20 mV and -60 mV V_h. Cell recorded with an electrode containing caesium and QX-222. Plots illustrate the steady state current-voltage relation (B; no leak subtraction was performed), the voltage dependence of burst peak amplitude (C), of interburst interval (D, circles) and burst duration (D squares), and of mean intraburst oscillation period (E). The data shown in C-E are measured individually for each burst and then averaged over a period > 3 min for each V_h level.

contrast with DR stimulation, see below text of the relative subheading) single or repetitive (with frequency up to 2 Hz) stimulation of a lumbar VR always failed to elicit a burst or to affect bursting timecourse. This situation is illustrated in the experiment of fig R.9, in which a series of three VR stimuli (0.5 Hz) was delivered at different phases during the quiescent interval. These data show that synchronous firing of a population of motoneurons was not able to trigger bursting activity and (together with those exposed in the previous subheading) suggest that, in the presence of strychnine and bicuculline, motoneurons behave as output elements that synchronously receive a massive, rhythmic synaptic input from a premotoneuronal network.

Sensitivity of rhythmic bursting to agents that interfere with synaptic transmission.

The observation that bursts were network-driven events prompted to test the effects of several agents that, acting on different molecular target, are expected to interfere with excitatory synaptic transmission. As mentioned above, bursting currents reversed polarity near 0 mV and displayed an approximately linear voltage dependence (fig R.8A,C). These results suggested a possible implication at the level of the motoneuronal membrane of glutamate-mediated synaptic transmission and in particular of non-NMDA receptors (whose gating is voltage independent; Mayer and Westbrook, 1987). In order to check the involvement of glutamate receptors within the rhythmogenic network, selective antagonists of NMDA or non NMDA receptors were bath-applied in the presence of strychnine and bicuculline.

The non NMDA glutamate receptor antagonist CNQX (20 μM) blocked rhythmic bursting in 4/4 preparations. An example of CNQX-induced bursting suppression is shown in fig R.10. In this case in the earlier phase of CNQX application burst duration decreased, with reduction in the number of intraburst oscillations; bursting was subsequently fully suppressed by CNQX. Recovery from CNQX effects was only partial and difficult to observe.

Application of the NMDA receptor antagonists APV (20 μM) or CPP (10 μM) blocked bursting activity in 4/12 preparations. In the remaining 8 preparations, in the presence of APV or CPP regular rhythmic bursting persisted, although with markedly reduced frequency (on average the cycle period increased by 85±43%; $p<0.0001$) and increased

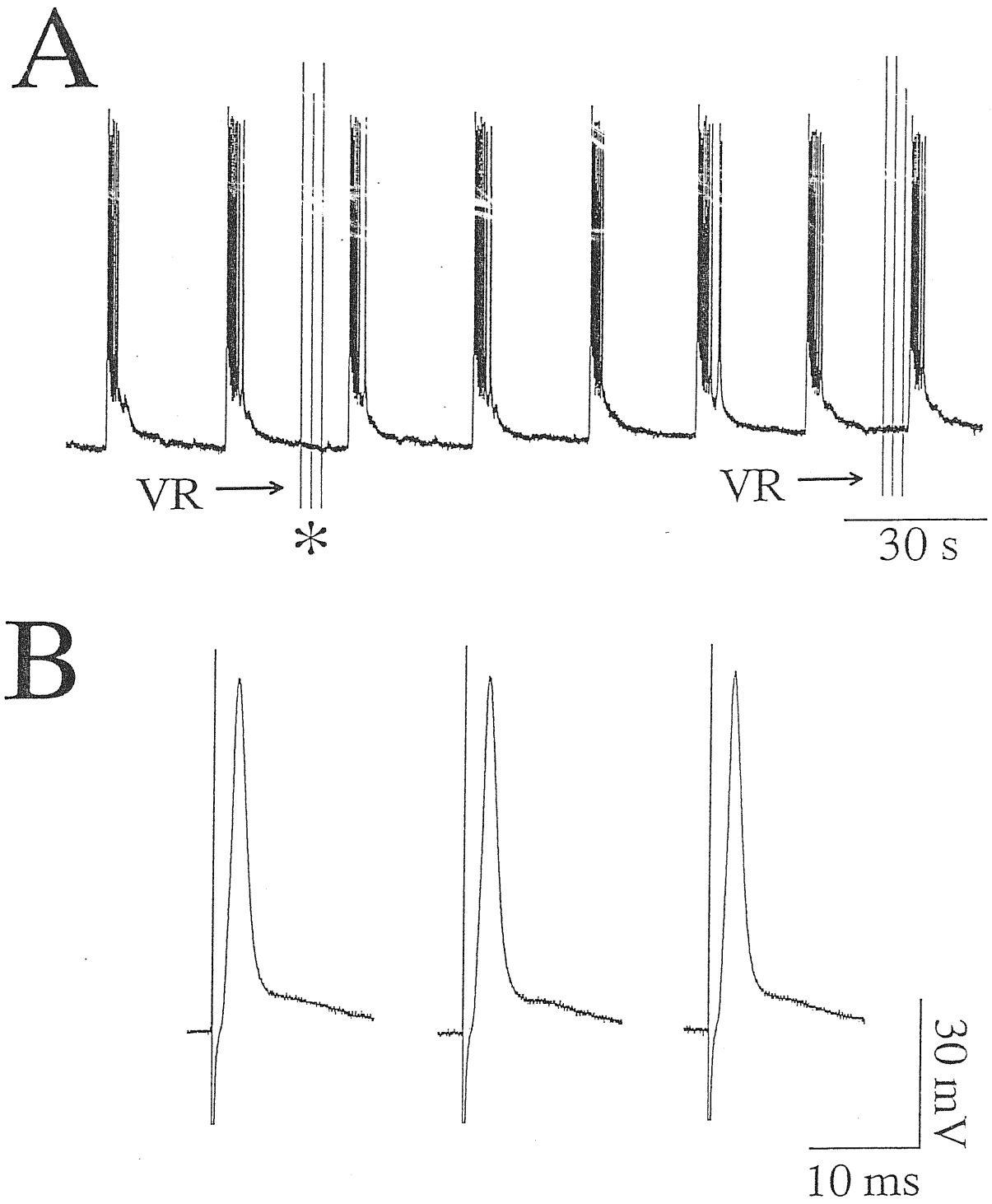

Fig R.9. *Antidromic spikes do not affect spontaneous bursting.*

A: Arrowed VRs indicate antidromic stimuli (4×T stimulation) to L5 ventral root during spontaneous bursting induced by strychnine and bicuculline. Such stimuli always evoked action potentials but failed to elicit bursting activity. Artefacts are clipped by sampling frequency. Asterisk denotes those responses shown as individual action potential at faster time base in B. Membrane potential during quiescent periods was -65 mV. Note that regardless of the timing of the antidromic firing during bursting cycle there was no alteration in spontaneous bursting activity.

burst duration (on average by 110±32 %; p<0.0001). When bursts persisted in the presence of CPP, their peak amplitude was significantly reduced (by 30±12 %. P<0.0001). The two effects of NMDA receptor antagonists are illustrated in fig R.11A (that depicts a full block of bursting by CPP) and fig R.11B (that shows a case in which bursting was slowed down by CPP). In both cases the effects of APV or CPP could be reversed on washout. These data show that glutamatergic synaptic transmission played a central role in bursting activity and that both NMDA and non NMDA receptor subtypes were activated during rhythmic network operation; however, in the majority of preparations rhythmic activity could still be expressed after block of NMDA receptors, while activation of non NMDA receptors was always required in the presence of strychnine and bicuculline.

Application of the voltage activated sodium channel blocker tetrodotoxin (1 μM; n=4) or of the calcium channel blocker cadmium (50 μM; n=4) fully suppressed bursting activity, indicating that action potential generation and calcium-mediated synaptic release were both necessary for rhythmogenesis in the disinhibited spinal cord.

Bursting activity in low-chloride solution

Since $GABA_A$ and glycine receptor channels in the neonatal rat spinal cord are selectively permeant to Cl^- (Gao and Ziskind-Conhaim, 1995), it was interesting to compare the effects of pharmacological block of these receptors with those caused by reduction of the extracellular Cl^-. This manipulation is expected to shift the equilibrium potential for this ion toward more positive values (according to Nerst equation; Hille, 1994) and thus to reduce or reverse chloride-mediated synaptic currents (Feldman and Smith, 1989). In low-chloride solution, GABA and glycine gated channels are then expected to loose at least in part their inhibitory action. Fig R.12 illustrates an experiment in which a spinal cord preparation was superfused with low-chloride solution (see methods for composition). This treatment *per se* induced spontaneous rhythmic bursting that appeared synchronously in left and right ventral roots with cycle period of 65±20 s and burst duration of 18±5 s. These effects were reversible on wash-out. Further coapplication of strychnine and bicuculline evoked bursting characterized by a

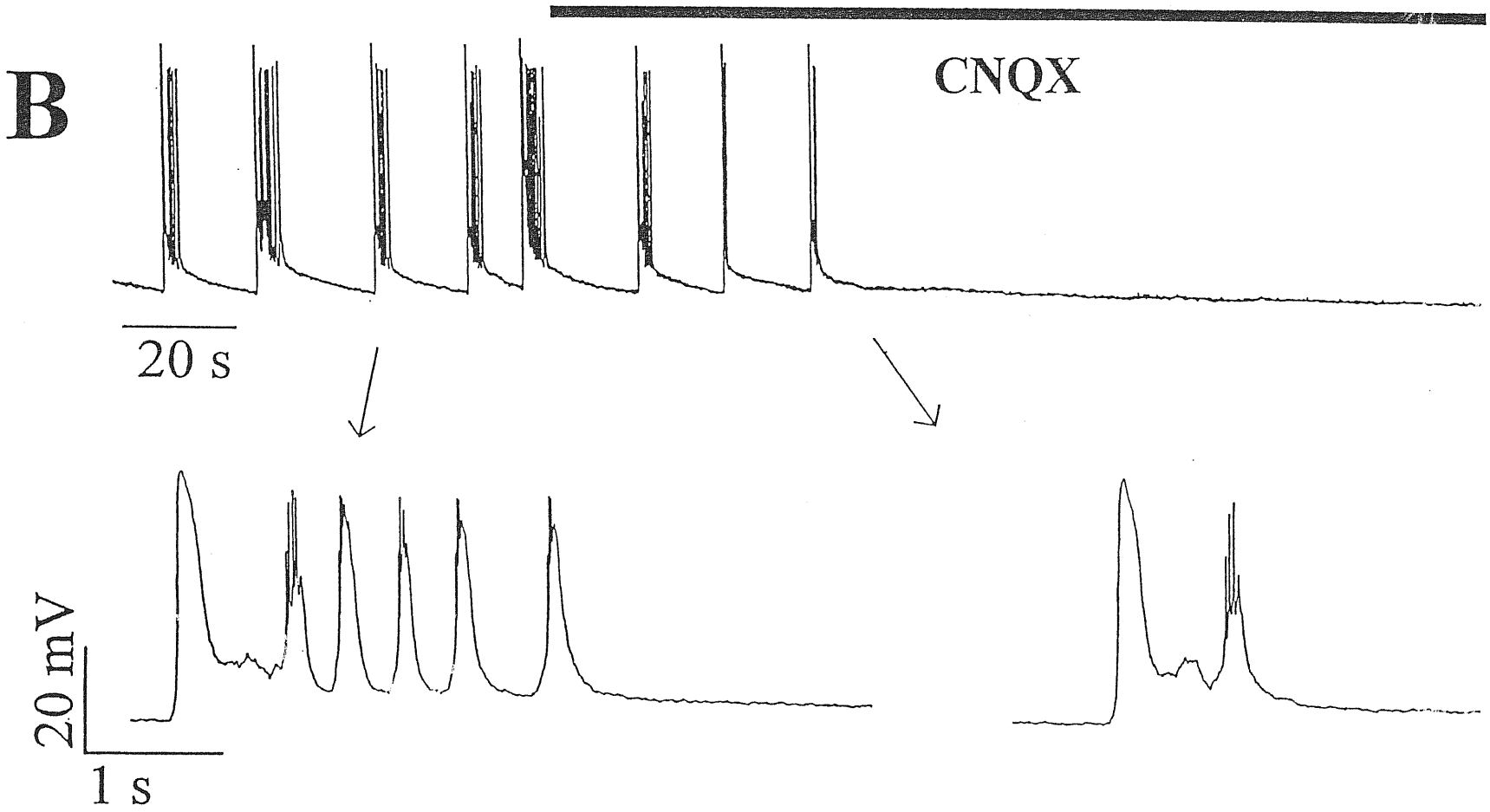

Fig R.10. *Block of bursting activity by CNQX.*

Application of 20 μM CNQX fully abolished rhythmic bursts induced by strychnine and bicuculline. As indicated by faster timebase tracings corresponding to events marked by arrows, there is progressive reduction in the late components of the burst before full antagonism takes place. Resting potential :-80 mV.

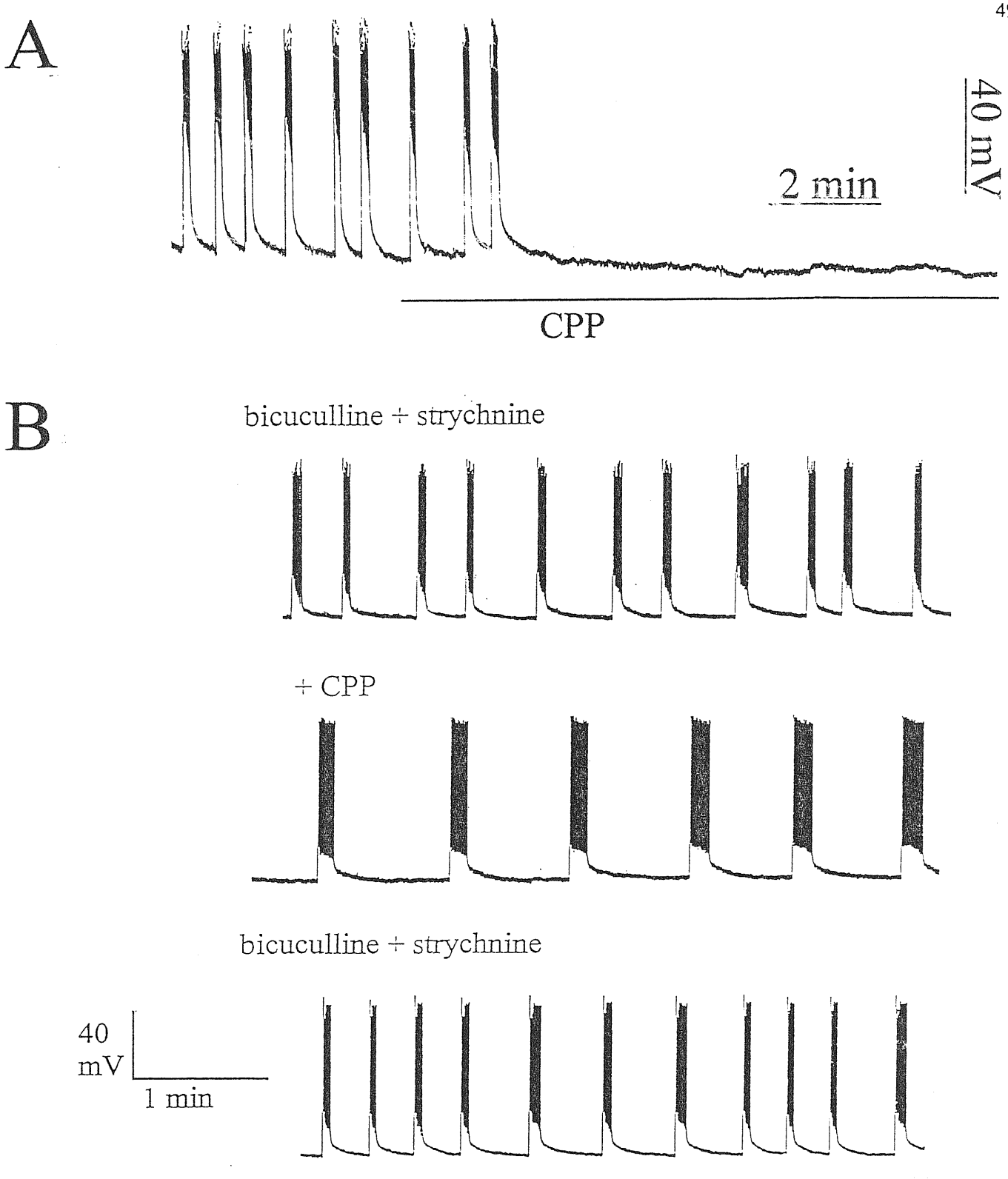

Fig R.11. *Different effects of CPP on bursting activity.*

A illustrates an experiment in which application of CPP (10 μM) fully abolishes bursting activity induced by strychnine and bicuculline. Resting potential: -70 mV. In another preparation (B) prolonged (> 30 min) application of CPP only produces a marked decrease in burst frequency (and a concomitant increase in burst duration). Resting potential: -68 mV. The effects of CPP are easily reversed on washout, as shown in B (bottom trace).

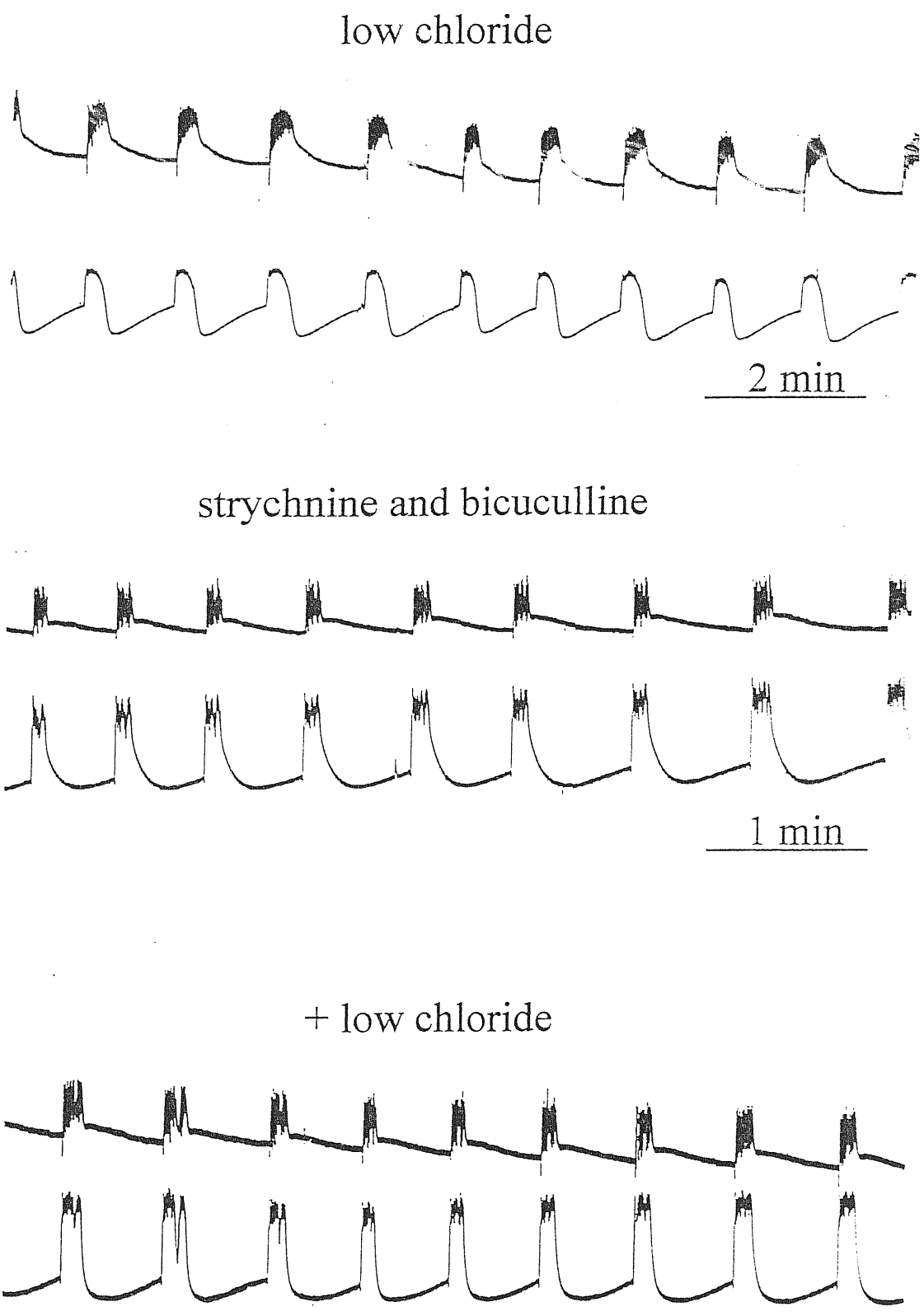

Fig R.12. *Effects of low chloride solution.*
Simultaneous recordings from left (top) and right (bottom) L5 VRs show that application of low chloride solution (top tracings) elicits spontaneous, synchronous rhythmic bursting in motoneurons. In the same preparation, coapplication of strychnine and bicuculline (after washout of low chloride solution) elicits rhythmic bursts with larger frequency (middle traces; note that timescale of top traces is different from middle and bottom traces). Under these conditions, application of low chloride solution failed to affect bursting timecourse (bottom traces). DC-coupled extracellular recordings.

significantly smaller cycle period (35±13 s; $p<0.0001$) and burst duration (8±4 s; $p<0.0001$). In the presence of strychnine and bicuculline, application of low-chloride solution did not induce significant changes in bursting activity. Similar results were found in 3 preparations. These results suggest that superfusion of the spinal cord with low-chloride solution induced a condition that was similar to complete pharmacological block of $GABA_A$ and glycine receptors (since rhythmic bursting was present) but distinct from it (since burst frequency was markedly lower). On the other hand, full block of chloride-permeable synaptic channels by strychnine and bicuculline was confirmed by the observation that in the presence of these agents large changes in chloride concentration failed to elicit any effects on bursting activity.

6. Pharmacological modulation of rhythmic bursting by NMDA or 5-HT.

Several pharmacological agents have been shown to induce locomotor-like patterns in the neonatal rat spinal cord (Kudo and Yamada, 1987; Cazalets et al, 1992; Cowley and Schmidt, 1994b). In particular, NMDA and 5-HT are routinely used to induce fictive locomotion (Sqalli-Houssaini et al, 1993; Kjærulff and Kiehn 1996). Furthermore, locomotor-like patterns display a marked frequency-dependence on the concentration of these agents (Cazalets et al, 1992). In order to compare the pharmacological sensitivity of rhythmic bursting in the absence of synaptic inhibition with that of fictive locomotion, these agents were also tested for their ability to modulate rhythmogenesis in the disinhibited spinal cord.

NMDA

Application of NMDA (up to 10 μM) was found to exert a strong accelerating action on rhythmic bursts in the disinhibited spinal cord. A representative example of these effects is shown in fig R.13, in which left and right L5 ventral roots were simultaneously recorded. In this preparation, after rhythmic bursts were induced by strychnine and bicuculline, application of NMDA increased burst frequency and decreased burst duration in a dose-dependent manner. Increasing NMDA concentrations were cumulatively applied at about 10 min intervals after rhythm stabilisation. The largest

NMDA dose compatible with bursting was 10 μM (in this case cycle period was reduced to 1.3±0.1 s and burst duration to 0.13±0.02 s). The effects of NMDA on cycle period and burst duration are quantified in plots of fig R.13B. As shown in the right-hand side panels of fig R.13A, intraburst oscillations were preserved with 2.5 and 5 μM NMDA, even if their number progressively decreased (consequently to burst duration reduction) and ultimately disappeared with 10 μM NMDA which converted bursts into single-discharge events. On a sample of 4 preparations, application of 5 μM NMDA (in the presence of strychnine and bicuculline) significantly decreased cycle period (by 75±10 %, corresponding to a 4 fold increase in burst frequency) and burst duration (by 59±18 %). In 2 intracellular experiments these effects were associated with a motoneuron depolarization of 7±5 mV.

5-HT

Application of 5-HT had effects similar to that NMDA on bursting activity. An example of the dose-dependent acceleration of strychnine and bicuculline-induced bursting by 5-HT is illustrated by the intracellular experiment of fig R.14: in this case at 5 μM concentration 5-HT elicited a slight and non significant decrease in cycle period without any apparent effect on resting potential (-76 mV). Doubling the 5-HT dose induced a small depolarization (2 mV) and a reduction of the cycle period. At 30 μM concentration a three-fold decrease in the cycle period was observed together with a membrane depolarization of 10 mV. These reductions in cycle period at 10 and 30 μM were accompanied by a concomitant reduction in burst duration. In each case the action of 5-HT was reversible on washout (shown for the two lower doses by records at the start of each subsequent trace). The expanded traces in Fig R.14B show the timecourse of individual bursts before and after 30 μM 5-HT application. In the presence of 5-HT not only the burst duration was clearly shortened but the typical oscillatory structure was almost eliminated. Graphs in Fig R.14C quantify the dose-dependence of 5-HT action on burst frequency (left) or duration (right). On average for this neuron, 5-HT (30 μM) significantly ($P< 0.0001$) increased burst frequency by 237±66 % (corresponding to a 70 % reduction in cycle period) and decreased burst duration by 70±3 % ($P<0.0001$).

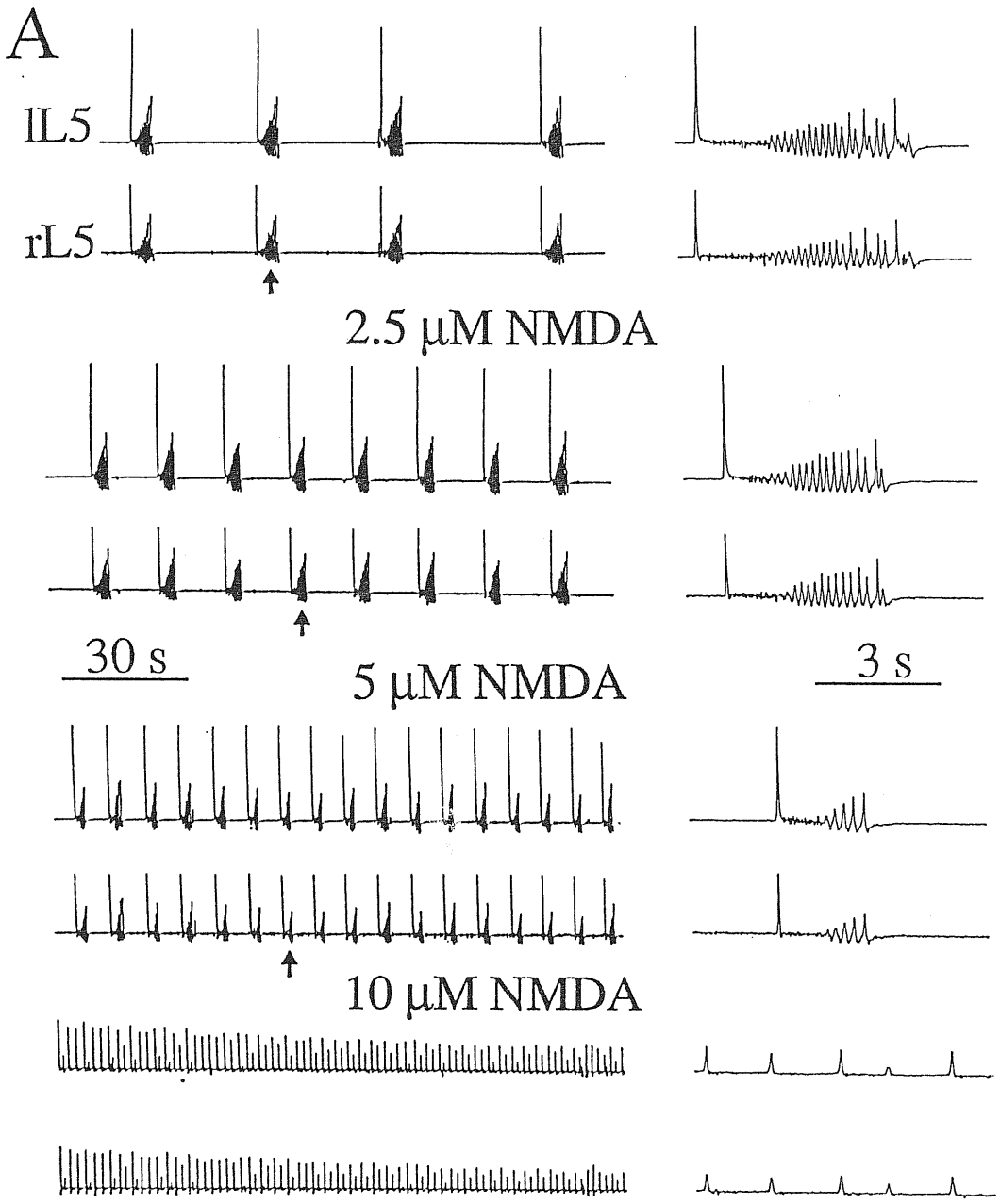

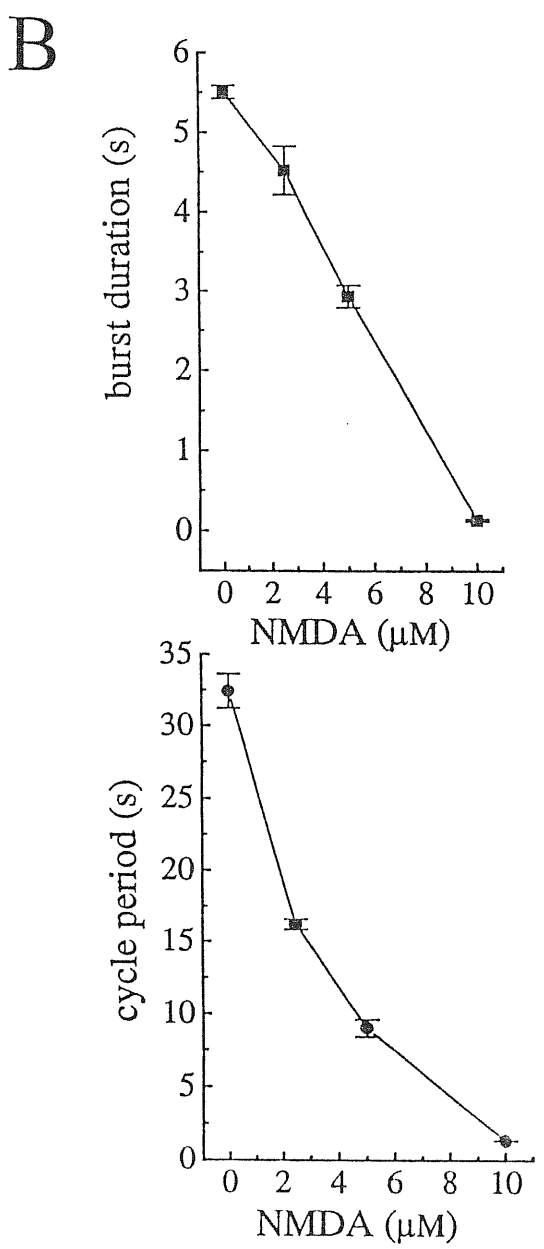

Fig R.13. *Dose-dependent action of NMDA on bursting activity induced by strychnine and bicuculline.*
A, pair of AC-coupled tracings (left and right L5 ventral root; lL5 and rL5; 20 Hz lowpass filtering) in strychnine and bicuculline solution (top) and following application of NMDA at the concentrations shown above tracings. Right hand side panels show faster time base records of individual bursts (arrows) to depict intraburst oscillations. Note progressive acceleration of bursting activity by NMDA with concomitant decrease in burst duration. B, plot of NMDA concentration *versus* burst duration (top) or cycle period (bottom). Each datapoint was calculated over a period of at least 5 min for the preparation shown in A.

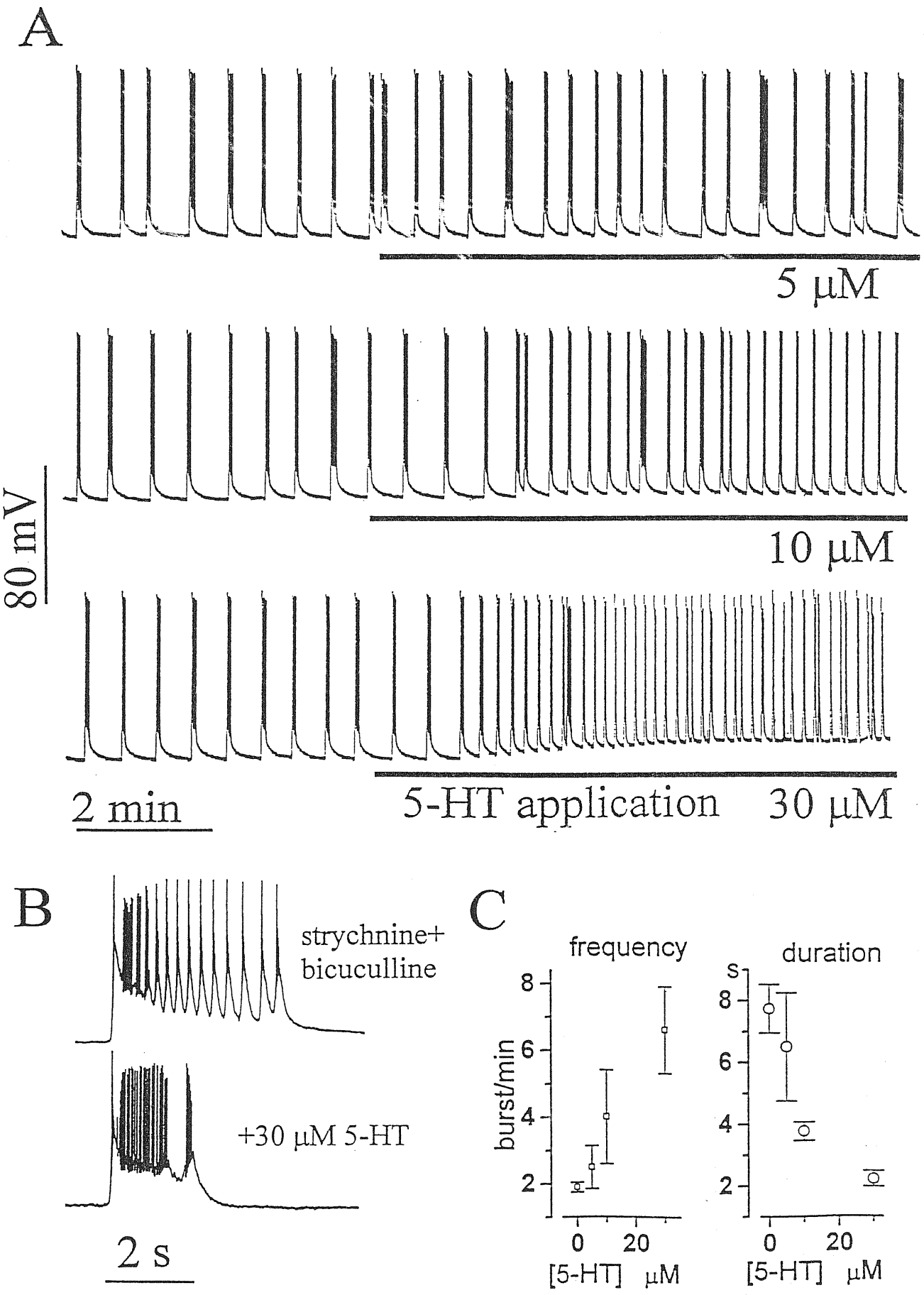

Fig R.14. *Dose-dependent action of 5-HT on bursting activity induced by strychnine and bicuculline.*
A: tracings showing the accelerating effect of 5-HT (applied sequentially at the three concentrations shown above traces) on bursting activity induced by bicuculline and strychnine. The 5-HT applications are indicated by the horizontal bars. Washout of 5-HT between successive doses is >15 min. Resting membrane potential: -76 mV. B: Change in the burst structure induced by 5-HT. Same cell as in A but shown at faster timebase. Note shortening of burst episode and disappearance of slow oscillations. Voltage calibration in A applies to B as well. C: plots of burst frequency (left; squares) or burst duration (right; circles) versus 5-HT concentration. Datapoints are means of individual responses measured for > 4 min on the same cell shown in A and B.

Similar data were obtained from 5 preparations. On average, with 10 μM 5-HT burst frequency was significantly ($P<0.0001$) increased by 107±70 % (corresponding to a 52 % reduction in cycle period) and burst duration was decreased by 51±4 % ($P<0.0001$). At 5 μM 5-HT only slight and non significant effects were observed. In the presence of 5-HT plus strychnine and bicuculline bursting activity was always expressed synchronously within lumbar VRs.

7. Effects of changes in extracellular potassium

Extracellular and intracellular potassium concentrations determine the reversal potential E_k (that can be calculated by means of the Nerst equation; Hille, 1994) for the transmembrane currents mediated by this ion. E_k in turn affects neuron resting membrane potential, that can be approximately predicted by the Goldman-Hodgkin-Katz equation (Hille, 1994). Thus, increasing extracellular potassium concentration is expected to shift E_k toward a more positive value and thus to produce a depolarization in nerve cells.

Fictive locomotion (induced by 5-HT and NMDA) frequency has been shown to be accelerated in a dose-dependent manner by increasing extracellular potassium concentration in the 2-6 mM range (Sqalli-Houssaini et al, 1993). In order to compare this behaviour with that of the rhythmogenic networks in the disinhibited spinal cord, we tested the effects of changing external potassium concentration in the presence of strychnine and bicuculline. Fig R.15 illustrates the effects of increasing external potassium concentration from 1 to 8 mM (see Methods section for solution procedure) under these conditions. A strong dependence of bursting frequency on potassium concentration was observed. Burst frequency was 0.4±0.2 burst/min at 1 mM potassium concentration; 0.9±0.2 burst/min at 2 mM; 1.9±0.8 burst/min at 4 mM; 4.6±0.9 burst/min at 8 mM. All these values were significantly different ($P<0.001$). These changes were accompanied by a dose dependent decrease in burst duration, that was 7.2±0.5 s at 1 mM and 1.8±0.4 s at 8 mM ($P<0.001$). Similar results were obtained in 3 preparations.

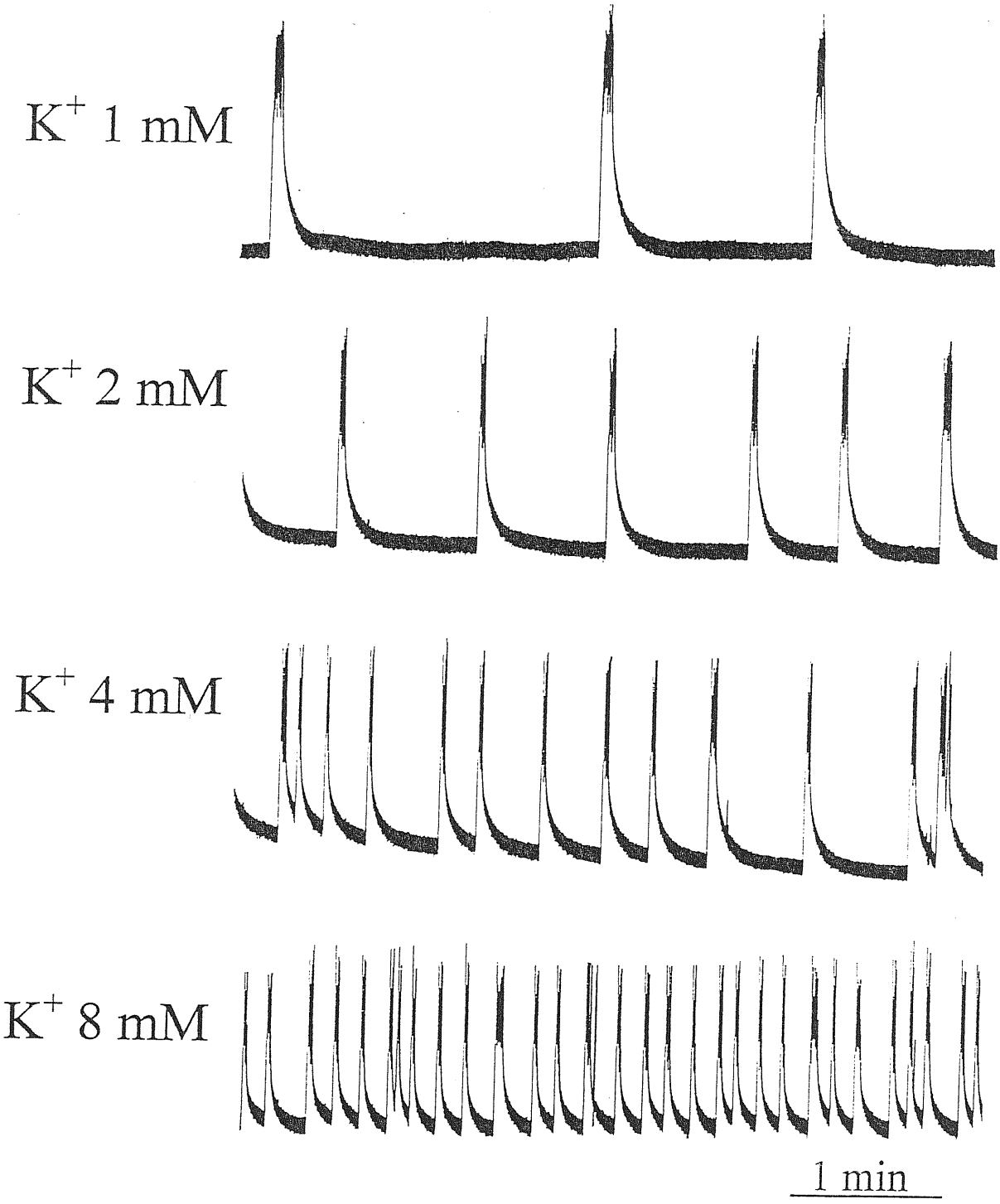

Fig R.15. *Effects of changes in external potassium concentration on bursting activity.*
Spontaneous activity in the presence of strychnine and bicuculline is recorded from left L5 VR in the presence of 1, 2, 4 or 8 mM external potassium. Rhythmic bursts are present throughout while their frequency increases more than tenfold when this concentration changes from 1 to 8 mM. DC-coupled extracellular recordings.

8. Effects of cyclothiazide on the neonatal rat spinal cord in control solution and after block of synaptic inhibition

Desensitization (i.e. a decrease in receptor responsiveness in the continuous presence of an agonist) is a prominent feature of glutamate receptors (Mayer and Westbrook, 1987, Trussel and Fischbach, 1989). In particular, non NMDA glutamate receptors are known to undergo a rapid and profound desensitization. This receptor class can be divided into two subgroups, namely kainate-activated receptors and AMPA-activated receptors (Mayer and Westbrook, 1987; Partin et al, 1993). AMPA-preferring receptor desensitization is selectively blocked by cyclothiazide (Partin et al, 1993; Patneau et al, 1993; Yamada and Tang, 1993). In addition to this effect, cyclothiazide has also been reported to facilitate presynaptic glutamate release (Diamond and Craig, 1995; Barnes-Davies and Forsythe 1995; Isaacson and Walmsley, 1996). Nevertheless, non NMDA receptor-mediated responses are usually much more increased by cyclothiazide than NMDA receptor-mediated ones; this is perhaps due to a concomitant postsynaptic depressant action of cyclothiazide on NMDA receptors, that can counterbalance and mask increased glutamate release (Diamond and Craig, 1995). Since glutamate receptor-mediated synaptic transmission had been found to play a major role in bursting activity of the disinhibited spinal cord, it was of interest to investigate the effects of cyclothiazide on rhythmic activity induced by strychnine and bicuculline. Because the action of this agent had not been previously studied in the rat spinal cord, we preliminarily investigated with intracellular recordings the impact of cyclothiazide on spontaneous and evoked synaptic activity in control solution on 35 motoneurons.

Cyclothiazide effects on AMPA responses in control solution

Application of cyclothiazide (25 μM) did not produce significant changes in resting membrane potential or input resistance of motoneurons (n=35). The action of cyclothiazide on AMPA receptors was tested by bath application of AMPA in the absence or in the presence of cyclothiazide. Fig R.16A shows an example of the action of AMPA on a motoneuron before or after addition of cyclothiazide (25 μM). In this case AMPA elicited a slowly developing depolarization (5.9 mV) which was so potentiated (11.6 mV) in the presence of cyclothiazide that it reached firing threshold. On average 1

μM AMPA produced sustained depolarizations which slowly reached a plateau of 7.8±3.0 mV (n=5). The delayed onset of these responses was probably due to the restricted access of AMPA to motoneurons found at variable depths from the surface of the spinal cord. In all cases recovery from AMPA depolarizations was complete within 6 min from washout. In the same cells cyclothiazide (25 μM; 15 min) strongly enhanced the peak amplitude of 1 μM AMPA responses (16.8 ± 7.6 mV equivalent to an increase of 110±41 % over control; $p<0.05$). The duration of 1 μM AMPA-induced depolarizations (measured as the time during which the membrane potential was ≥ 10% of peak amplitude attained) was also increased in the presence of 25 μM cyclothiazide (+73±70%; $p<0.005$). After washout of cyclothiazide (total exposure time was 30-40 min) recovery was always very poor. In order to test whether cyclothiazide effects were at least in part produced by a direct action on motoneuron membrane, AMPA application was also performed in the presence of tetrodotoxin, that was used to abolish action potentials thus isolating synaptically the impaled motoneuron. Fig R.16B depicts data taken from a cell bathed in 1μM tetrodotoxin (TTX) solution. In this example AMPA (2 μM) induced a slow depolarization (12.5 mV) which was enhanced (15.8 mV) following administration of cyclothiazide without any detectable increase in baseline noise (in contrast to the case in control solution, see fig R.16A). On average, in the presence of TTX, AMPA (2 μM) still evoked a depolarizing response (15±5 mV; n=3) which, in the presence of cyclothiazide, was largely increased both in its plateau amplitude and duration (+109±44 % and +49±29 %, respectively).

Application of 0.1 mM glutamate, the endogenous transmitter acting on AMPA receptors, depolarized motoneurons (7±4 mV; n=4). In 2/4 cells, 25 μM cyclothiazide produced a clear potentiation of such responses (+100±50 %) with no change observed for the remaining two cells. The more variable action of cyclothiazide in the case of bath-applied glutamate was presumably due to the fact that this amino acid acted via various receptor classes and was also removed by uptake systems (Mayer and Westbrook, 1987). The selectivity of cyclothiazide towards AMPA receptors was assessed by examining its effects on depolarizing responses evoked in control solution by NMDA (15 μM; n=3; 7±3 mV) or GABA (1 mM; n=5; 13±3 mV). In both cases cyclothiazide did not produce

significant changes in these responses even when they were evoked in the presence of TTX.

Cyclothiazide effects on evoked synaptic potentials

Electric stimulation of dorsal root fibres elicited subthreshold EPSPs which comprised mono and polysynaptic responses as indicated by their irregular time course with overlapping synaptic events (see examples of fig R.2D,E). In order to depress polysynaptic components of recorded EPSPs and to facilitate analysis of the effects of cyclothiazide, all experiments were thus carried out in the continuous presence of 1 mM mephenesin, an agent routinely used to reduce polysynaptic contribution to DR-evoked motoneuronal responses (Fulton and Walton, 1986a; Lev-Tov and Pinco, 1992). Fig R.17 (top) shows examples of several superimposed EPSPs (observed after >20 min exposure to mephenesin) characterized by their smooth timecourse. Under these conditions EPSPs displayed a latency (from the stimulus artefact to the foot of the EPSP) of 7.4±1.6 ms, a relatively fast 10-90 % rise time (3-9 ms) and a decay which could be fitted with a single exponential function. In order to prevent frequency dependent modulation of the EPSPs, afferent fibres were stimulated at 60 s intervals (Lev-Tov and Pinco, 1992). In 8/12 cells cyclothiazide treatment brought the EPSP to firing threshold even if there was no detectable change in membrane potential or input resistance at rest. Nevertheless, in a number of neurones it was possible to observe the action of cyclothiazide on EPSPs without intervening contamination by spike activity, a situation which allowed us to retain the same stimulation intensity and duration used before application of cyclothiazide. Ongoing synaptic activity and possibility of large changes in EPSP amplitude leading to spike activity following cyclothiazide treatment prevented a systematic analysis of EPSPs at various stimulation intensities and prompted the use of relatively strong stimuli, able to evoke synaptic responses clearly discernible from baseline noise. Attempts (n=3) were made to remove any contamination of evoked EPSPs by inhibitory potentials. However, application of 1 μM strychnine plus 25 μM bicuculline in the presence of mephenesin always led to irregular bursting activity which prevented EPSP measurement. In one further case it was however possible to measure

evoked EPSPs using 1 μM strychnine in control and cyclothiazide solution. The results taken from this series of EPSPs were the same as those when cyclothiazide was applied in control ACSF. Fig R.17 (top) shows an example of a cell in which a large enhancement in the amplitude of the EPSPs versus its respective control was clearly noticed (together with increased spontaneous activity shown as time-unlocked, low amplitude events). Systematic analysis, performed on 4 motoneurons, allowed quantification of the enhancing effects of cyclothiazide (see histograms of Fig R.17). In the presence of 25 μM cyclothiazide, both peak amplitude and area of EPSPs were significantly ($P<0.001$) increased in each cell tested and on average they amounted to 30±18 and 52±23 % rises, respectively. Monoexponential decay time constants. averaging 30.6±10.0 ms in control solution, were not significantly changed in the presence of cyclothiazide (36.9±12.6 ms).

Cyclothiazide effects on spontaneous activity in control solution

In control solution spontaneous synaptic activity of motoneurons, which comprised events mainly due to spike-dependent release of neurotransmitters from local neurones. consistently increased in frequency after application of 25 μM cyclothiazide (see tracings of Fig R.18). This phenomenon was systematically analyzed in 6 motoneurons. The frequency of events exceeding a preset amplitude threshold (five times the standard deviation of baseline noise, usually ≈1 mV above resting membrane potential) was increased in all cases after 10 min of cyclothiazide application (196±87 % of control: n=6). Nevertheless, closer inspection of the data revealed a dishomogenous response pattern. In fact, in 3 cells, large amplitude (10-20 mV) event frequency was strongly increased (858 ± 562 % of control), while small amplitude (5-10 mV) event frequency was reduced (72 ± 26 % of control), so that the mean amplitude was larger in cyclothiazide (the cell in fig R.18A presented this kind of behaviour, as demonstrated by the amplitude histograms beside the raw data). In the other 3 cells, however, the small and intermediate amplitude event frequency was proportionally more increased, so that the mean amplitude was unchanged or even reduced. The latter case is illustrated in the histograms of fig R.18B. Only for one motoneuron (the one of fig R.18A) the decay of

spontaneous events could be fitted by an exponential function since in all other cases complex synaptic responses often overlapped the decay phase. In the example of fig R.18A, a single exponential provided adequate fitting of the decay with a time constant of 13.2±1.8 ms in control solution and 18.8±2.0 ms (n=24; P<0.001) in the presence of cyclothiazide. Application of 1 μM TTX fully blocked all synaptic activity, thus confirming the difficulty of detecting miniature events in mammalian motoneurons recorded with sharp microelectrode (Redman, 1990).

Another important effect of cyclothiazide was to induce the progressive appearance of strong, prolonged bursting activity (see fig R.19A), detectable in 14/17 cells, after about 10 min exposure to this drug. These bursts were defined analogously to those observed in the presence of strychnine and bicuculline, but only bursts with a duration ≥ 0.5 s were included for analysis, in order to reject simple EPSPs. Bursting activity was poorly dependent on resting membrane potential in terms of amplitude, duration and frequency, as indicated by the experiment of fig R.19A in which four different levels of resting membrane potential were attained by injecting steady current into the cell. In this case, bath application of 1 mM GABA elicited a depolarizing response when the motoneuron was held at -84 mV and a hyperpolarizing response when it was held at -68 (fig R.19B), suggesting that reversal potential for GABA receptors was intermediate between these values in this motoneuron that had been impaled for over 30 min with a KCl-filled electrode. In both cases, during GABA application the bursting activity was actually inhibited (see fig R.19B). Neither the peak amplitude (fig R.18C) nor the duration (fig R.18D) of bursts was particularly sensitive to membrane potential variations in the -63 to -93 mV range. Such a result suggests that bursting activity was not an intrinsic property of the recorded cell but it was probably generated via the interneuronal network, consistently with the observation that 1 μM TTX fully blocked bursting activity. The poor dependence of burst amplitude on motoneuron membrane potential in the tested range suggests that cyclothiazide-induced bursting likely resulted from simultaneous or intermixed activation of excitatory and inhibitory synaptic conductances.

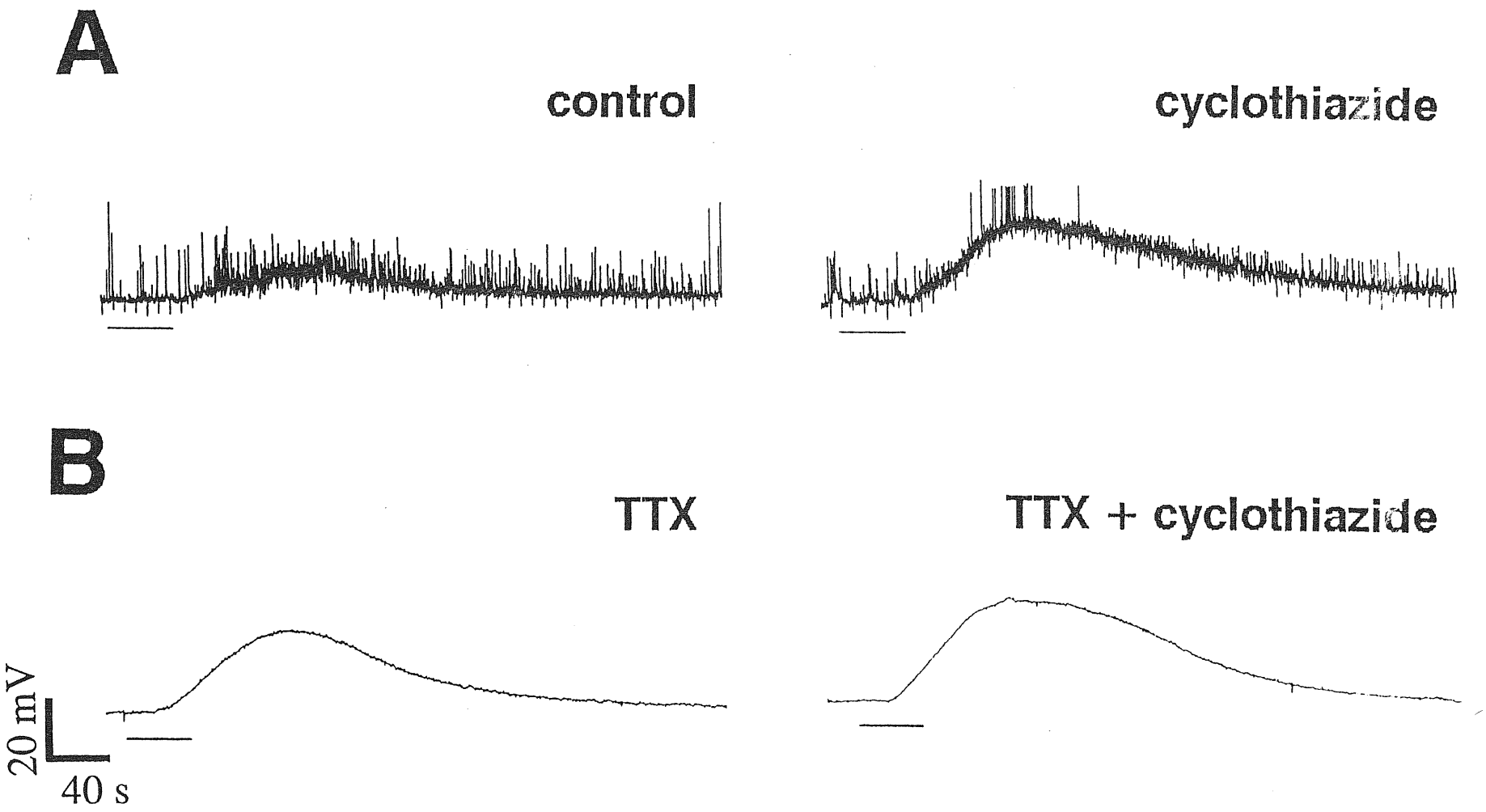

Fig R.16. *Effects of cyclothiazide on AMPA-mediated depolarizations.*

A: control motoneuronal depolarization to 1 μM AMPA (horizontal bar) from resting membrane potential of -82 mV. Upward deflections represent spontaneous synaptic activity. Downward deflections are hyperpolarizing electrotonic potentials (induced by -0.1 nA current pulses). Following 15 min application of cyclothiazide (25μM) the response to the same application of AMPA is strongly potentiated in amplitude and duration.
B: in the presence of TTX (1μM) AMPA (2 μM) evoked membrane depolarization which is largely potentiated by cyclothiazide; resting membrane potential -84 mV (different cell from A).

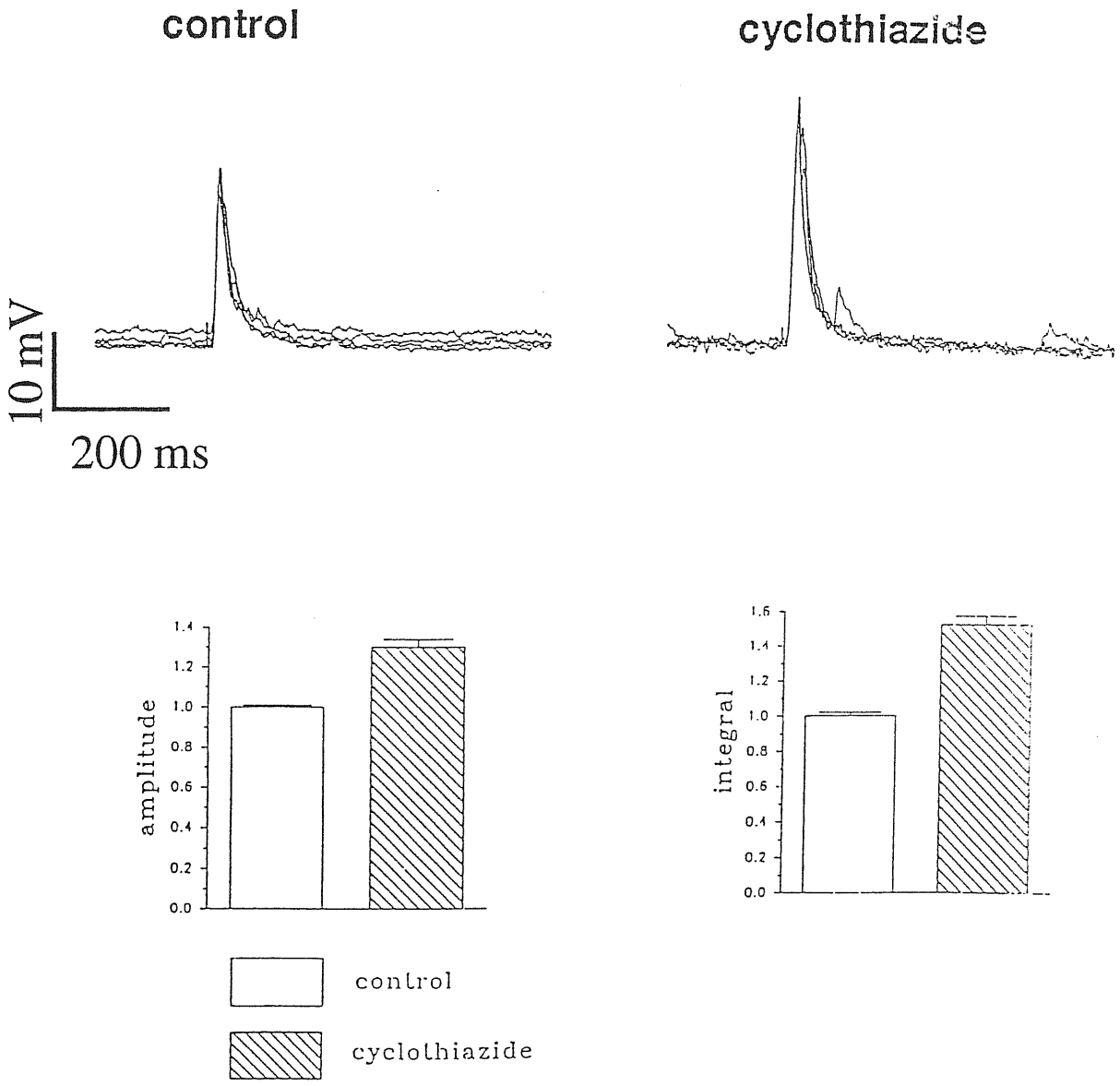

Fig R.17. *Effects of cyclothiazide on evoked EPSPs.*

Top panel: four superimposed EPSPs in control (left) or 25 μM cyclothiazide (right) solution. EPSPs were evoked by low intensity (4 V) stimulation of corresponding dorsal root at 60 s intervals (to avoid frequency dependent changes in synaptic transmission). Note increase in peak amplitude and area of EPSPs in the presence of cyclothiazide while the time constant of decay is unchanged. Resting membrane potential: -78 mV. Bottom panel: histograms of EPSP amplitude (left; mV) or area (right; mV*ms) in control solution (open bars, n=22) or in the presence of cyclothiazide (crosshatched bars, n=20). Data are normalized to the mean values obtained in control conditions for each of 4 cells.

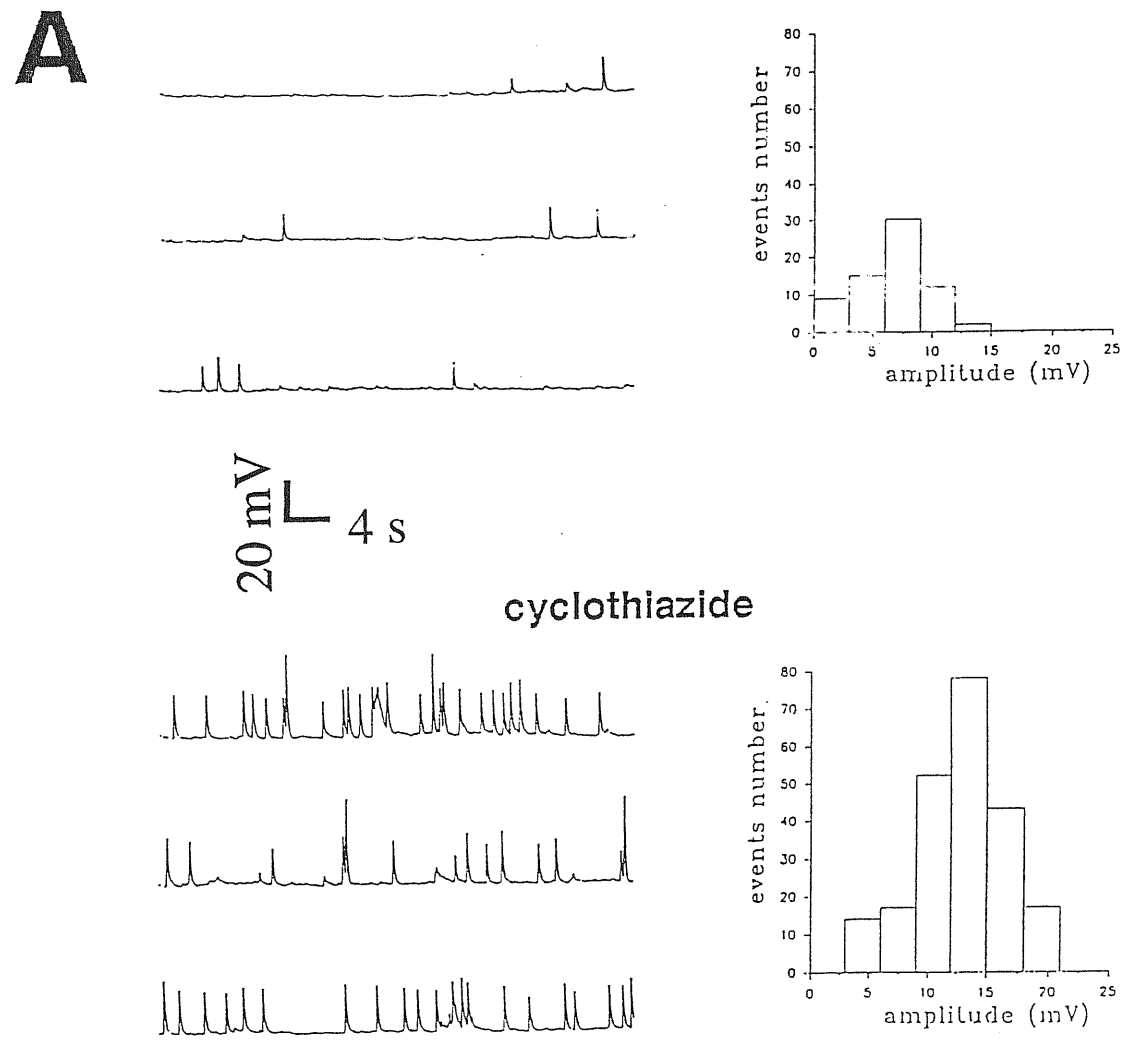

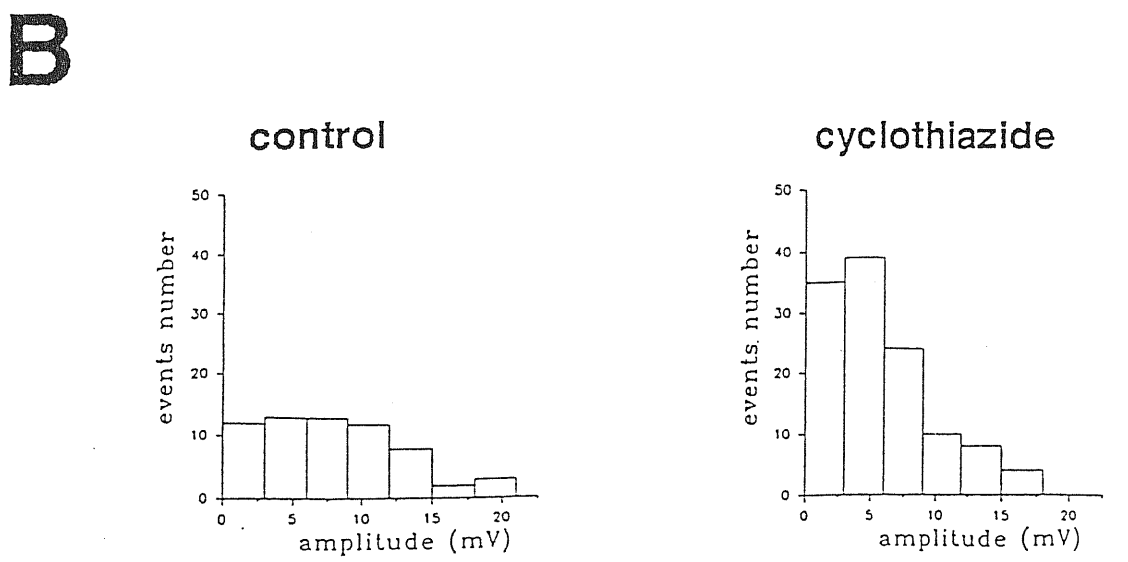

Fig R.18. *Effect of cyclothiazide on spontaneous synaptic activity.*
A (top): continuous sample tracings of spontaneous events in control conditions. Histogram of their distribution is shown in the right hand plot. Note prevalence of events in the range between 5-10 mV. A (bottom): similar tracings from the same cell after 15 min application of cyclothiazide display increased frequency and amplitude of synaptic activity, which is quantified in the right hand side histogram. Note prevalence of events in the range between 10-20 mV. Resting membrane potential: -85 mV. B: Histograms of distribution (in a different motoneuron) of spontaneous events in the absence (left) or in the presence (right) of cyclothiazide (25 μM). Note the increased number of events in the presence of cyclothiazide. In this cell the majority of events was between 0 and 10 mV both in control and in the presence of cyclothiazide. Resting membrane potential: -85 mV.

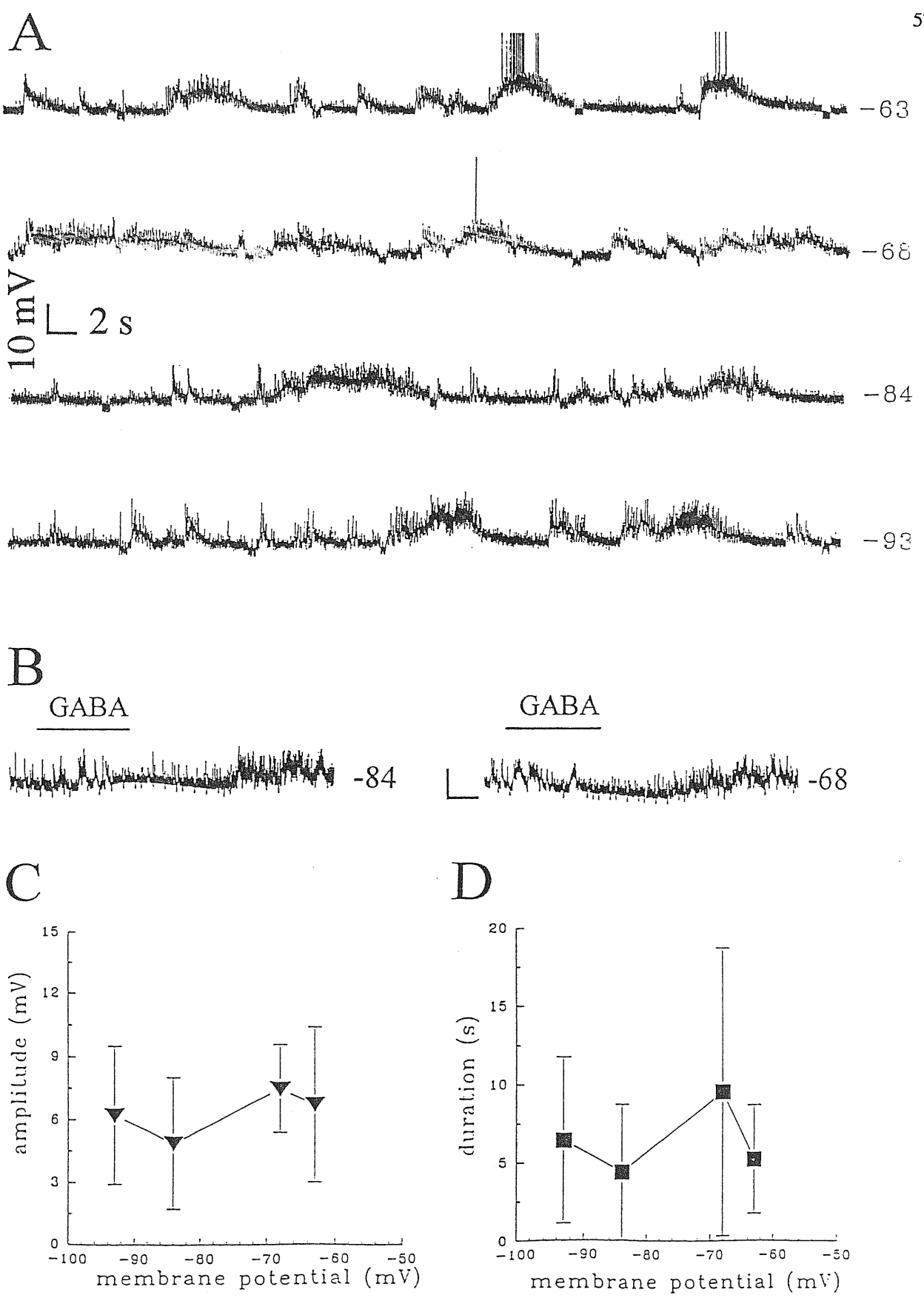

Fig R.19. *Bursting activity evoked by cyclothiazide.*
A: Consecutive traces characterized by repetitive bursting activity, often with superimposed spikes (truncated) and large synaptic events of variable amplitude and duration. These phenomena appear after 10 min exposure to 25 µM cyclothiazide. Membrane potential was changed from -63 to -93 mV (as shown by values alongside traces) by direct current injection. No significant reduction in amplitude and duration of spontaneous bursts is found. B: Application of GABA (1 mM) at two different membrane potentials (indicated by values alongside tracings) produced either depolarization or hyperpolarization during which bursting activity was suppressed. Downward deflections are hyperpolarizing electrotonic potentials (induced by -0.1 nA current pulses). Calibration bars: 27 mV, 40 s. C: Plot of membrane potentials versus burst amplitude. D: plot of membrane potentials versus duration of spontaneous burst. Measurements for C and D are taken over 2 min epochs.

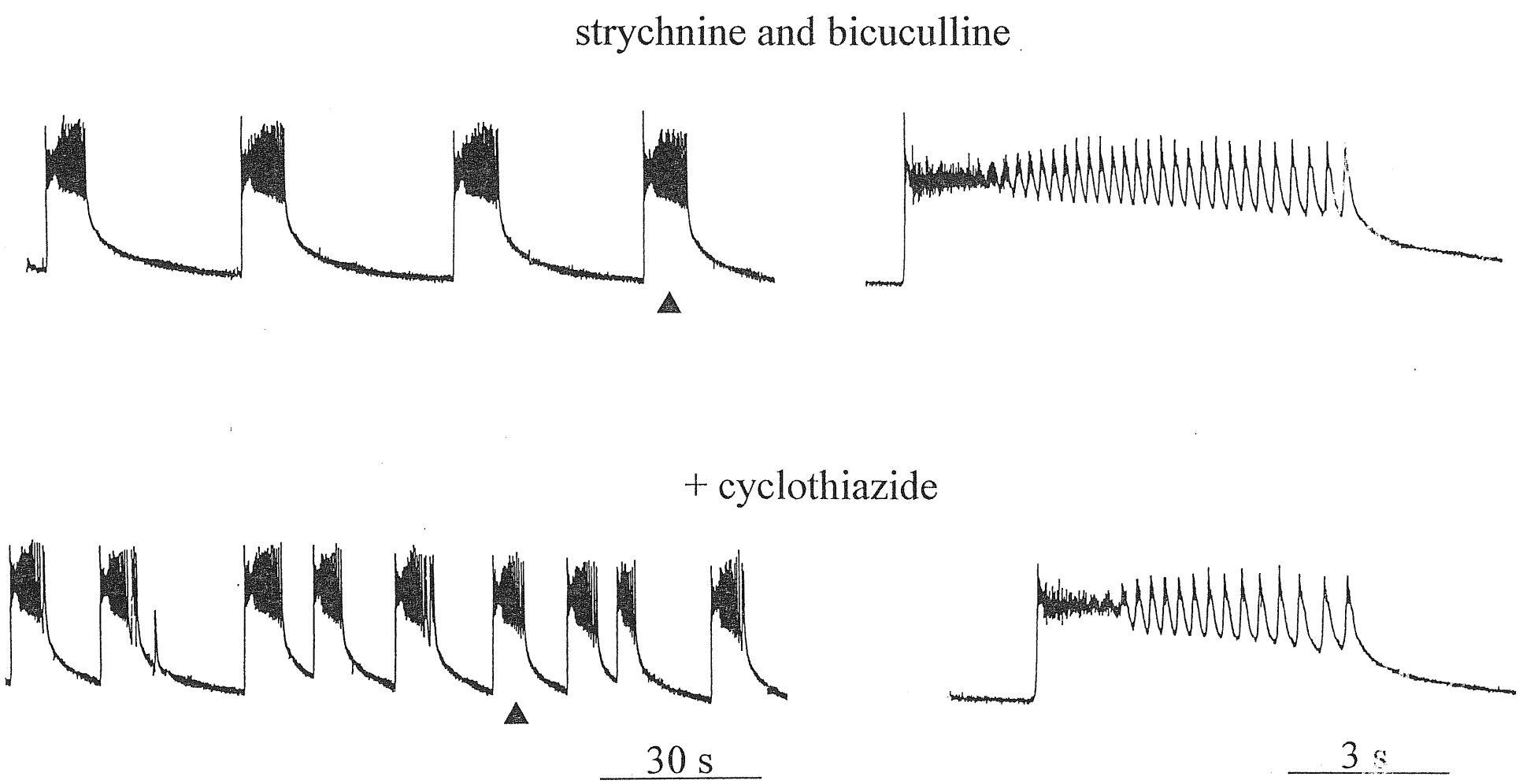

Fig R.20. *Effects of cyclothiazide on bursting activity.*
Rhythmic bursting activity (recorded from right L5 VR in the presence of strychnine and bicuculline; top traces) is accelerated by bath application of cyclothiazide (bottom traces). Faster timescale traces on the right illustrate the individual bursts marked by triangles in left traces. Burst duration decreases in the presence of cyclothiazide but typical intraburst oscillatory structure is preserved.

Cyclothiazide effects on bursting activity in the presence of strychnine and bicuculline

Fig R.20 illustrates the typical effects of 25 μM cyclothiazide applied to the spinal cord in the presence of strychnine and bicuculline. Rhythmic bursting persisted in the presence of cyclothiazide, with increased frequency and decreased duration; furthermore the bursting pattern regularity decreased in the presence of cyclothiazide. On a sample of 4 preparations, cyclothiazide induced the following changes: cycle period decreased by 53±16 % ($P<0.001$); burst duration decreased by 26±13 % ($P<0.005$); CVc increased by 42±12 % ($P<0.05$); CVd increased by 65±34 % ($P<0.05$). As shown in the expanded traces of fig R.20, the oscillatory intraburst structure was preserved in the presence of cyclothiazide. Thus, when non NMDA glutamate receptors responses were potentiated by cyclothiazide the generation of stereotypic bursts in the disinhibited spinal cord was still possible, but the mechanism responsible for their regular rhythmic onset was impaired.

Since cyclothiazide had been found to boost responses mediated by AMPA preferring glutamate receptors and accelerate strychnine plus bicuculline-induced bursting, we tested whether application of this agent could somehow counteract the action of NMDA receptor antagonism in the disinhibited spinal cord. For this purpose, cyclothiazide (25 μM) was applied to preparations in which previous application of CPP (10 μM) had been found to block rhythmic bursting completely (n=3). Cyclothiazide, applied after CPP effects had been washed out, produced burst acceleration (fig R.21), as previously described (see fig R.20). In the presence of cyclothiazide, re-application of CPP failed to block rhythmic activity or to significantly affect its timecourse (as shown in fig R.21) in all preparations tested. Thus, in preparations in which rhythmogenic networks were impaired by NMDA receptor antagonism, bursting ability was recovered when AMPA glutamate receptor activity was boosted by cyclothiazide. Furthermore, the present evidence rules out the possibility that NMDA receptor-dependent pacemaker neurons played a major role in this kind of rhythmogenesis, since the operation of these cells should have been blocked in the presence of NMDA receptor antagonists.

9. Reversal of bursting activity blockade by non NMDA receptor antagonist.

These findings raised a question about bursting blockade by non NMDA receptor antagonist. Is this block insurmountable or, like the case of NMDA antagonism, can it be reversed by increasing the excitability of the rhythm-generating network? To clarify this issue, 5-HT, that is known to depolarize spinal neurons (Takahashi and Berger, 1990) and that has been found to accelerate bursting in the presence of strychnine and bicuculline (see above) was applied to the disinhibited spinal cord in the presence of CNQX, after bursting activity had been fully blocked by this antagonist (n=4). In 3/4 preparations a low dose of 5-HT (≤10 μM) was sufficient to restore rhythmic bursting in the presence of CNQX. This phenomenon is illustrated in the example of fig R.22 in which block of bursting by CNQX was reversed by 5μM 5-HT. Under these conditions burst amplitude was reduced, average burst frequency was similar to that observed in the presence of strychnine and bicuculline alone (about 1.6 burst/min) and rhythmic pattern regularity (that was poor in the absence of CNQX) was markedly increased. In the remaining preparation application of 5-HT (up to 30 μM) failed to restore bursting.

When NMDA and non NMDA receptors were simultaneously blocked by CPP and CNQX in the disinhibited spinal cord, it was impossible to restore bursting activity with even when high doses (up to 100 μM) of 5-HT were added to the bathing solution (n=4).

10. Testing possible membrane mechanisms involved in rhythmogenesis

The experimental findings so far described showed that rhythmic bursting in the disinhibited spinal cord was driven by a premotoneuronal network that required glutamate receptor-mediated synaptic transmission for its operation and that was strongly modulated by external application of NMDA and 5-HT. Nevertheless, the mechanisms responsible for generation of a very regular rhythm in the absence of synaptic inhibition were still to be clarified. In order to cast light on possible mechanisms implicated in this activity, a study was performed on 39 spinal preparations to test the role of three ionic membrane mechanism that are potentially involved in rhythmogenesis:

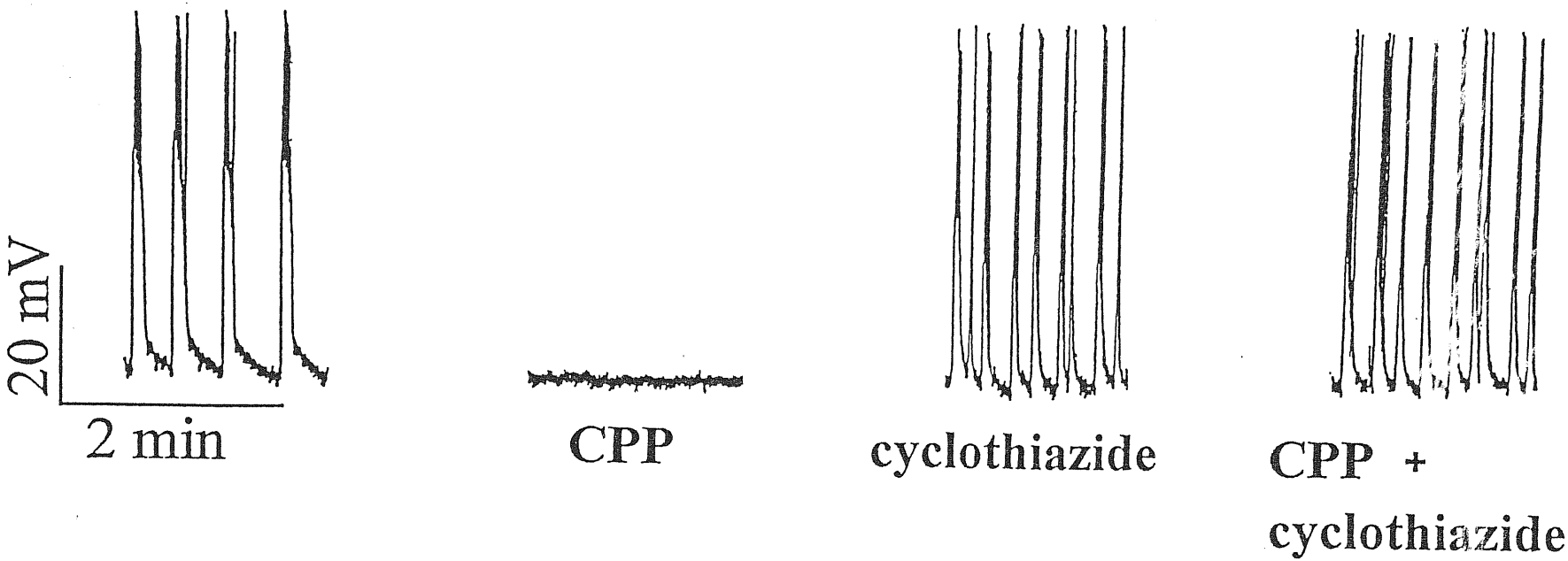

Fig R.21. *Effects of CPP on bursting activity in the presence of cyclothiazide.*

In the presence of bicuculline and strychnine (left hand side panel) spontaneous bursts are suppressed by CPP in this preparation, recover after CPP washout (not shown) and increase in frequency after addition of cyclothiazide to the bicuculline and strychnine solution; in the presence of cyclothiazide, subsequent application of CPP does not abolish bursting anymore. All data from the same neuron at -80 mV resting potential.

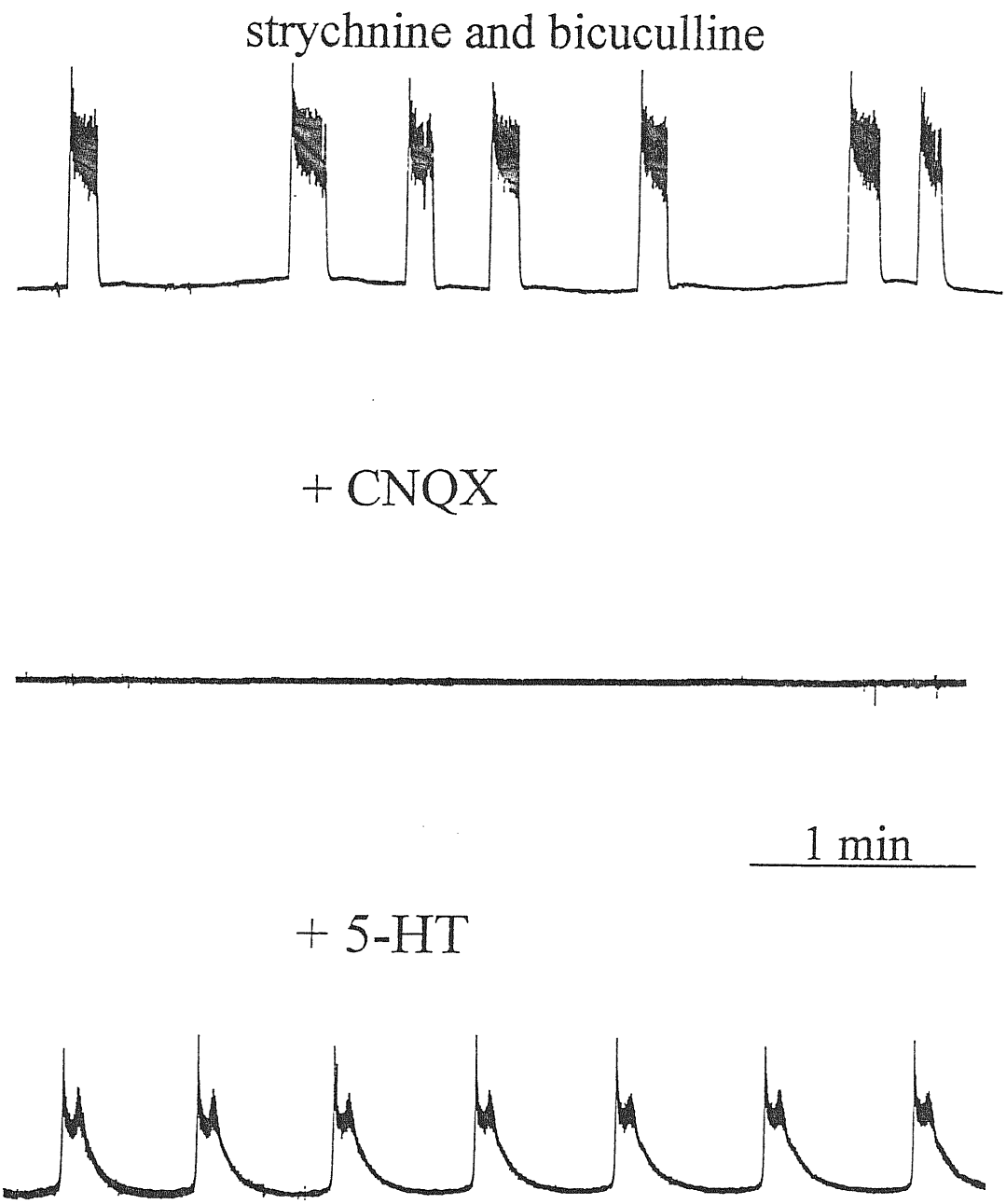

Fig R.22. *Bursting blockade by CNQX is reverted by 5-HT.*

Spontaneous bursting in the presence of strychnine and bicuculline (top) is fully abolished by CNQX application (10 μM). Subsequent application of 5-HT (5 μM) in the presence of CNQX elicits spontaneous rhythmic bursts. Recordings from left L5 VR.

a) the slow calcium activated potassium conductance selectively blocked by apamin (Sah 1996); in the lamprey spinal cord pharmacological suppression of this conductance prolongs cycle period and duration of bursts induced by NMDA (El Manira et al 1994). In this case the apamin-sensitive calcium-activated potassium conductance(s), is thought to be gradually activated during a burst (due to calcium entry in spinal neurons) and to contribute to burst termination in the lamprey (El Manira et al 1994). It is reasonable to hypothesize that a calcium influx also takes place in interneurons during long-lasting depolarizing bursts in the disinhibited spinal cord. This influx could activate calcium-dependent potassium conductances that would exert a hyperpolarizing action on spinal neurons; this process could cause a decrease in neuronal excitability and contribute to burst termination. In order to test this possibility, apamin was bath-applied during rhythmic bursting in the absence of synaptic inhibition.

b) the slow inward rectifier conductance, that in the thalamus gives rise to intrinsic neurons oscillations through a dynamical interplay with a low threshold calcium current (McCormick and Pape 1990). An analogous inward rectifier conductance was found in the neonatal rat spinal cord and is blocked by extracellular application of caesium (Takahashi, 1990b). A mechanism similar to the one producing thalamic oscillations could be in principle involved also in the generation of rhythmic bursts or intraburst oscillations. This possibility was tested by extracellular application of caesium to the disinhibited spinal cord.

c) the electrogenic sodium pump, that produces a long lasting hyperpolarization of hippocampal neurons during recovery from glutamate-induced depolarization (Thompson and Prince, 1986) and whose electrogenic activity is required for spacing intrinsic bursts induced by NMDA in midbrain neurons (Johnson et al, 1992). A recent modelling study (Li et al 1996) has also indicated that such a pump activity is important to support numerically simulated bursting. We hypothesised that the long-lasting depolarization characterizing a burst in the disinhibited spinal cord would result in a progressive dissipation of sodium and potassium ionic gradients (due to massive sodium influx and potassium efflux through synaptic and voltage-activated channels); increase in intracellular sodium and extracellular potassium concentration would in turn produce a strong activation of the electrogenic sodium pump, that would generate an outward

current expected to decrease excitability and eventually terminate a burst. The activity of the electrogenic sodium pump is selectively blocked by extracellular application of either oubain, strophanthidin or potassium-free solution. (Horisberger et al. 1991; Glynn, 1993). These pharmacological tools were then separately tested in the disinhibited spinal cord.

Effects of apamin

The action of apamin (0.4 μM) was tested on rhythmic bursting of the disinhibited spinal cord in 6 preparations; examples of these experiments are illustrated with either intracellular (fig R.23A) or extracellular recording from left and right L5 ventral roots (fig R.23B): unlike the case of the lamprey spinal cord, in all preparations tested apamin largely decreased cycle period and burst duration (on average by 46±10 % and by 47±14 %, respectively; $p< 0.001$), as also illustrated by the histograms in fig R.25A. Expanded timebase tracings on the right hand side of fig R.23A and B show that intraburst oscillations persisted even if their number was usually diminished due to reduction in burst duration (fig R.23A, B). In the presence of apamin bursts and intraburst oscillations still appeared synchronously in left and right L5 ventral roots (fig R.23 B). The effects of apamin (which were not reversible for >2 hour washout) were not associated with any change in motoneuron resting membrane potential as indicated by intracellular experiments (n=3). Other pharmacological agents able to block slow calcium activated potassium conductances are muscarinic agonists (Schwindt et al. 1988; Storm, 1990). Carbachol (10 μM) was tested on the rhythmic pattern of the disinhibited spinal cord. Pooled data (see histograms in fig R.25B) indicate that this agent significantly ($p<0.001$) reduced cycle period (by 64±16 %) and burst duration (by 55±19 %; n=5) in manner analogous to that observed with apamin. The present results showed that in the rat spinal cord block of slow calcium activated potassium conductances accelerated bursting without changing its intrinsic characteristics. It is thus clear that, unlike lamprey spinal cord, in the rat disinhibited spinal cord these conductances do not play a specific role in burst termination. Burst acceleration can be likely explained by tonic depolarization

caused by block of slow calcium activated potassium conductances on spinal interneurons.

Effects of caesium

Typical effects of caesium application (4 mM) on rhythmic bursting of the rat spinal cord are illustrated in fig R.24A with recordings from one L5 ventral root. While burst frequency was unaffected by this agent, burst duration was significantly increased as shown also with the faster timebase responses on the right hand side of fig R.24A. Individual oscillations became gradually longer within the burst episode while they had similar duration prior to the application of caesium. The action of caesium was reversed after 20 min washout (see bottom traces in fig R.24A). Similar effects were also detected with intracellular recording (fig R.24B; different preparation from A) which indicated that caesium increased burst duration by 80 %. In this cell caesium application caused a resting membrane potential hyperpolarization of 9 mV. Neither repolarizing (via intracellular current injection) the cell to its initial resting potential (-70 mV) nor depolarization up to -55 mV membrane potential changed the action of caesium on burst duration. Similar results were obtained from 8 preparations with either intracellular (n=3) or ventral root recordings (n=5). On average, burst duration was increased to 170±47 % of control ($p<0.001$) while burst cycle period was not significantly affected, as illustrated by the histograms in fig R.25C. In intracellular recordings, caesium application produced an average hyperpolarization of 7±4 mV. While these findings outline a contribution of a caesium sensitive inward current to the control of burst length (see Discussion), it seems that the predominant mechanism responsible for burst generation remained elusive.

Pharmacological inhibition of the electrogenic sodium pump

Three different methods to block the electrogenic sodium pump activity, namely application of ouabain, or strophanthidin or omission of extracellular potassium (Horisberger et al. 1991; Glynn, 1993), were tested in the presence of strychnine plus bicuculline-induced spinal bursting. Fig R.26 illustrates the effects of ouabain (10 μM) on an intracellularly recorded motoneuron. In this example, in the presence of strychnine

and bicuculline, the resting membrane potential was -70 mV and spontaneous bursts took place at regular intervals (top row of fig R.26). Single antidromic stimulation (during quiescent periods) evoked an action potential with 75 mV amplitude (right hand side panel). Such a stimulation did not influence subsequent bursts. After a latency of approximately 5 min from the start of ouabain application, the motoneuron membrane potential slowly depolarized and, after 15 min in the presence of ouabain, it reached -64 mV when bursts appeared irregularly and had highly variable duration, since events lasting tens of seconds coexisted with short discharges (see middle tracing of fig R.26). At this stage a full antidromic spike could still be evoked although of reduced amplitude (63 mV) owing to depolarization (see right hand side middle tracing). After 20 min application (see bottom tracings of fig R.26), the motoneuron membrane potential declined to -50 mV and the antidromic spike amplitude was 38 mV. This phase was characterized by long quiescent periods that were interrupted by spontaneous bursts of irregular duration so infrequently to make impractical any quantitative analysis of residual events. In order to check the viability of the spinal network under these conditions, dorsal root stimuli (of intensity sufficient to activate polysynaptic pathways) were delivered during quiescent periods and were found to evoke long lasting bursts similar to the ones appearing spontaneously, as illustrated in the bottom row of fig R.26. Further exposure to ouabain slowly led to suppression of electrical excitability. Similar results were obtained from 8 spinal cord preparations recorded either intracellularly (n=4) or extracellularly from left and right L5 ventral roots (n=4) in which, in the presence of ouabain, irregular bursts appeared synchronously. These effects could not be reversed on ouabain washout.

Analogous data were obtained with bath application of strophanthidin (4 μM), another selective blocker of the electrogenic sodium pump, as illustrated by simultaneous recordings from left and right L5 ventral roots in fig R.27. After a latency of 6-10 min from the beginning of strophanthidin application, regular rhythmic bursts (induced by strychnine and bicuculline; see pair of top tracings of fig R.27 for control condition) were gradually converted into chaotic activity (shown at 30 min in the pair of middle tracings), characterized by bursts of variable duration and unpredictable onset, similar to those observed in the presence of ouabain. Like the case of regular bursts observed in the

presence of strychnine and bicuculline only (top tracings), even this chaotic activity (middle tracings) appeared synchronously in left and right ventral roots. Further exposure (40 min) to strophanthidin brought about nearly-complete suppression of bursting even if dorsal root stimulation elicited bursts of variable duration. Recovery from strophanthidin was observed albeit extremely slowly; regular rhythmicity returned only after 2-3 hour washout (bottom row of fig R.27). Similar results were obtained in 4 preparations in which ventral root recording was preferred to intracellular one in order to perform continuous long lasting monitoring of burst suppression and recovery.

When normal solution was replaced by potassium-free solution (n=4 or n=3 preparations for extra or intracellular recording, respectively), changes in the spontaneous bursting pattern (evoked by strychnine and bicuculline) started after approximately 20 min and developed fully after 40-60 min as exemplified in fig R.28A for an AC-coupled recording from L5 right ventral root. Large control bursts (top trace) were converted into short episodes of variable amplitude and interposed with small and brief spontaneous events without any ordered pattern (middle). Return to control solution (with strychnine and bicuculline) gradually re-established bursting patterns after 40 min washout (bottom). Fig R.28B shows similar changes developing in an intracellularly-recorded motoneuron (-72 mV resting potential) in which the regular bursting pattern was replaced by irregular activity of shorter duration and with spontaneous fluctuations in baseline potential (-81 mV at rest). Recovery required very long washout periods (>40 min) which compromised intracellular recording stability.

Thus, similar effects on bursting activity were observed after application of ouabain. strophanthidin or potassium free solution, suggesting that such effects were effectively due to impairment of the electrogenic sodium pump. Dramatic loss of bursting pattern regularity in the presence of electrogenic sodium pump blockade while the spinal network was still able to produce (irregular) long lasting bursts, strongly suggests that the activity of the electrogenic sodium pump was an essential pacemaker mechanism within rhythmogenic networks. In the Discussion section a model based on reciprocal excitation between neurons and on the electrogenic sodium pump dynamics is considered for its ability to produce rhythmic bursts and intraburst oscillations through rhythmic

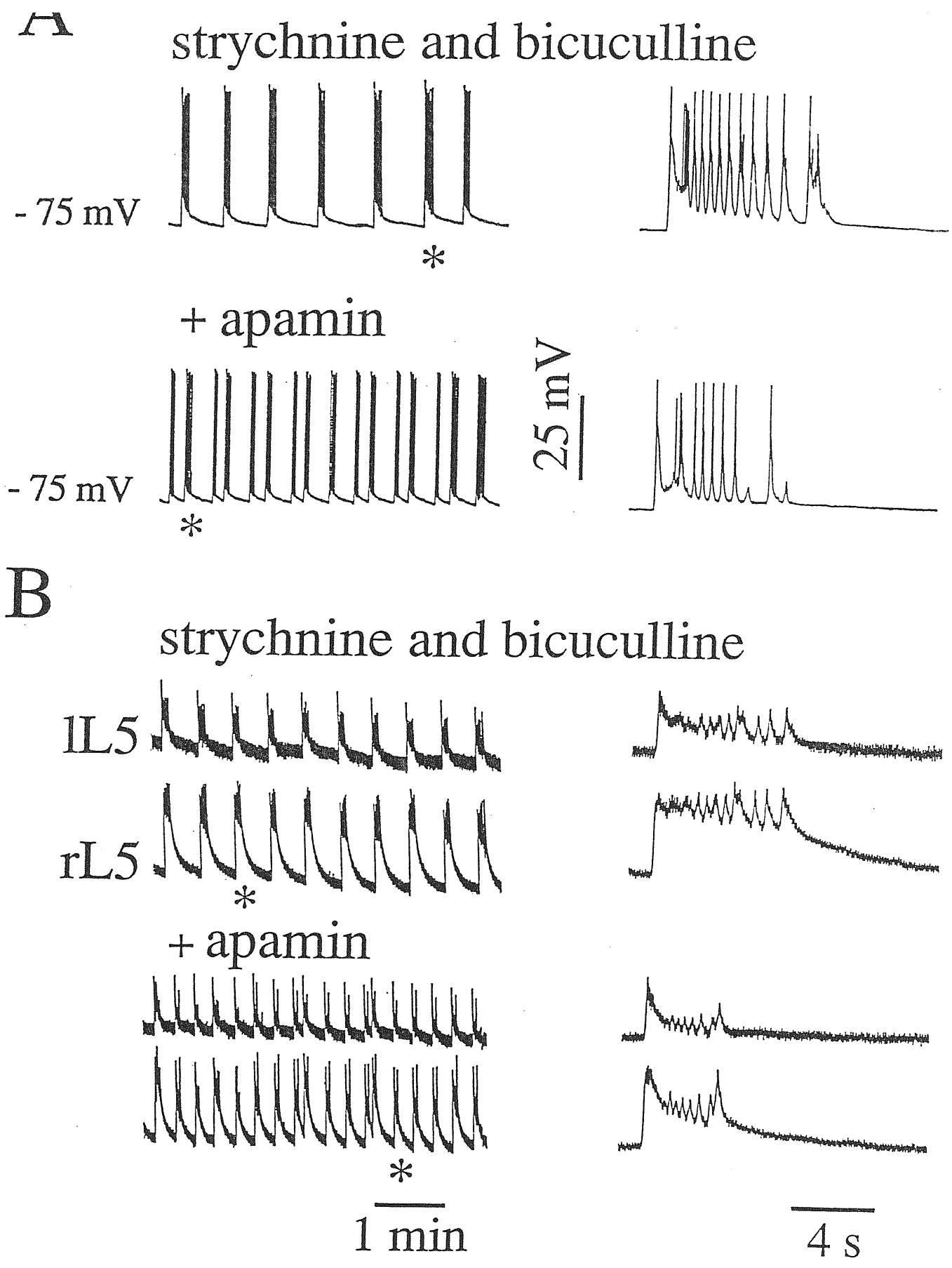

Fig R.23. *Spontaneous rhythmic bursting evoked by strychnine and bicuculline in the isolated spinal cord of the neonatal rat is affected by bath-applied apamin (0.4 μM).*
A: intracellular recordings from a lumbar motoneuron displaying regular bursting (a single bursting episode, marked by asterisk, is expanded on the right hand side to reveal intraburst oscillatory structure) in the presence of strychnine and bicuculline (top tracing) and following 20 min application of apamin. Note decrease in cycle period and burst duration. Value alongside traces are membrane potentials at rest. B: comparable data recorded from left (l) and right (r) L5 ventral roots (different preparation from A) at slow (left) or fast (right) timebase. Asterisks denote expanded burst episodes. Note similarity of extracellular records to intracellularly-recorded responses and analogous action of apamin which reduces cycle period and burst duration synchronously in both lumbar roots.

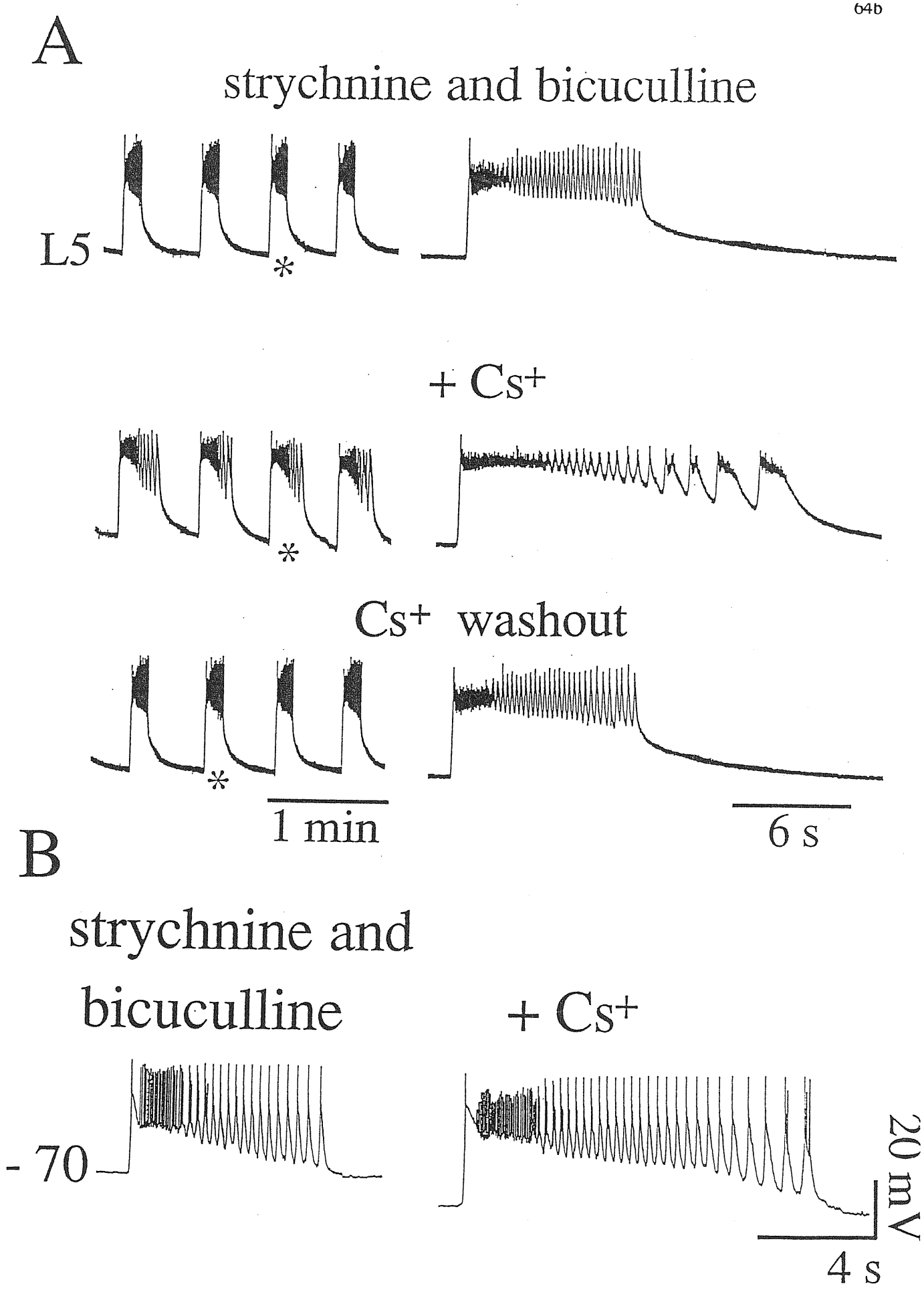

Fig R.24. *Effects of extracellularly applied caesium (4 mM) on strychnine and bicuculline-induced bursting.*
A: extracellular recording from L5 ventral root before (top), after 20 min application of Cs^+ (middle) and after 20 min washout (bottom). Right hand side responses are expanded events marked by asterisks. Note large prolongation of individual bursts with enhanced oscillatory activity. B: intracellular recording from lumbar motoneuron (different preparation from A) showing individual bursts before (left) and after application of Cs^+ (right). Note similarity to effects recorded extracellularly, and associated with 9 mV hyperpolarization from -70 mV initial resting potential.

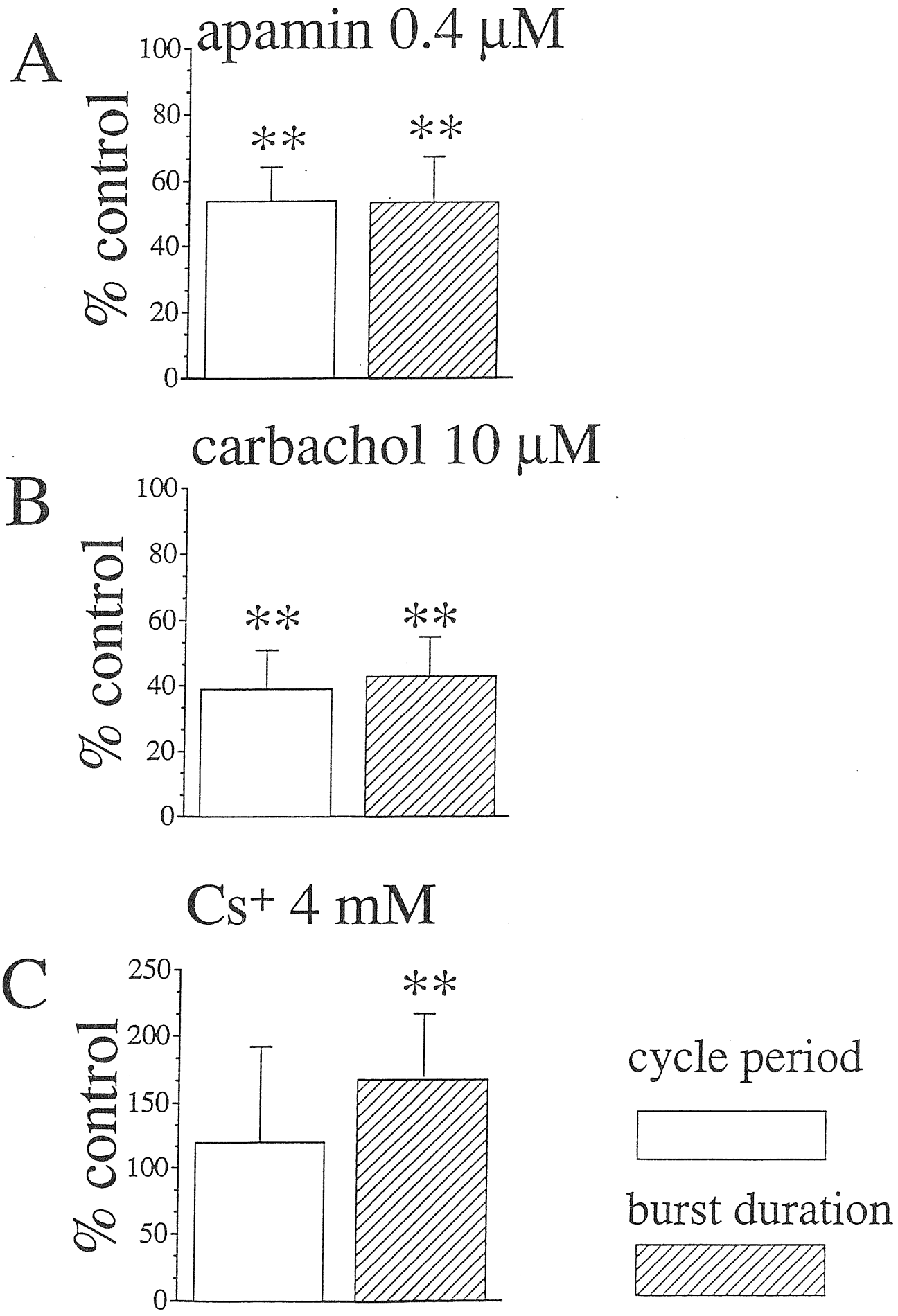

Fig R.25. *Histograms of effects of apamin (A), carbachol (B) and caesium (C) on cycle period and burst duration.*

Data are expressed as % of control bursts. Double asterisks denote statistically significant effect ($p<0.001$). Number of experiments are indicated in the text.

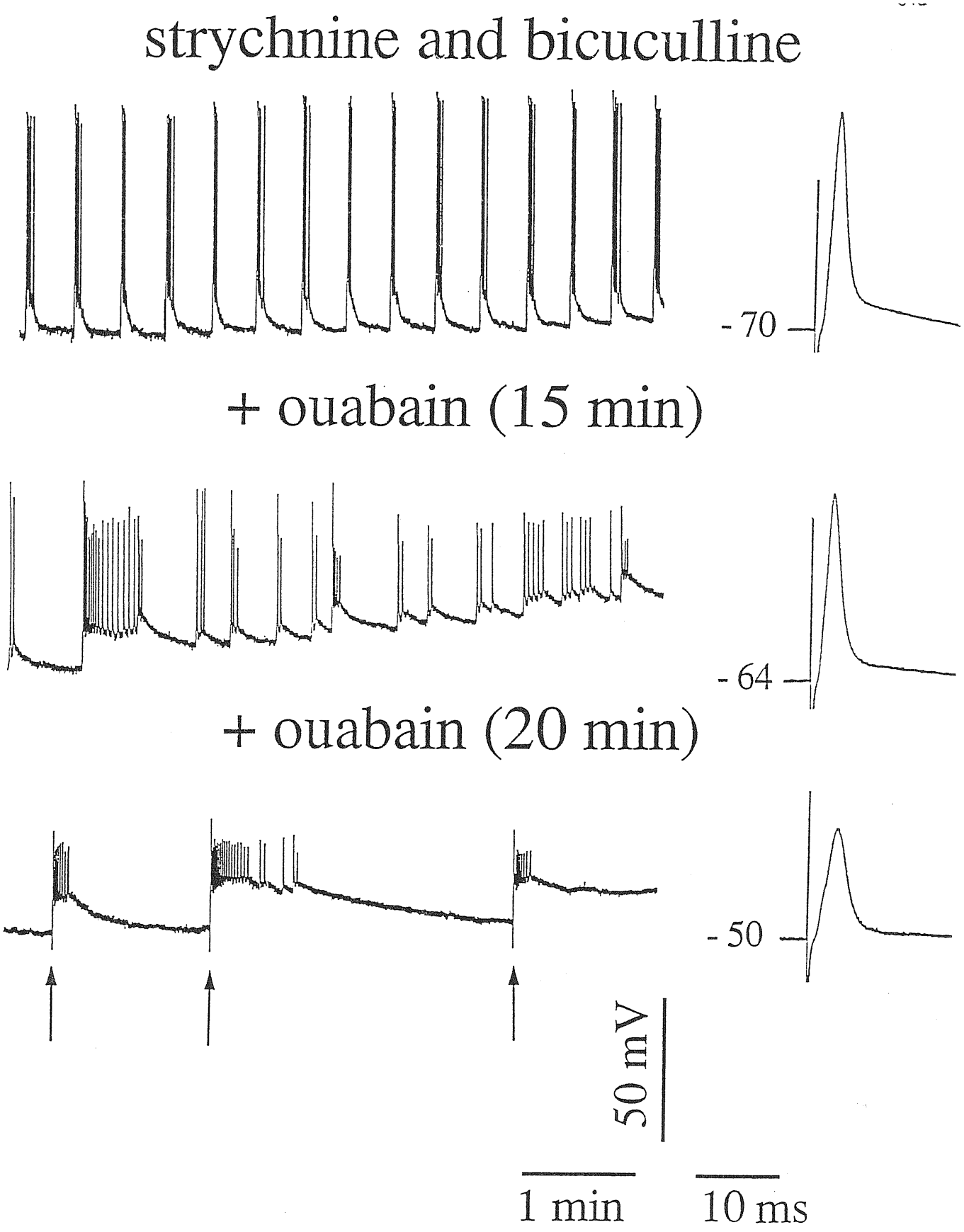

Fig R.26. *Action of ouabain (10 μM) on strychnine and bicuculline induced bursting.*
Top: control bursts (displayed at slow speed) with alongside averaged (n=5) antidromic spike from -70 mV resting potential. Middle: after 15 min application of ouabain membrane potential is depolarized to -64 mV (corresponding to the end of trace) with strong disruption of burst rhythmicity and structure. Antidromic spike is reduced in amplitude but still present. Bottom: bursts evoked by single pulses applied to segmental dorsal root (see arrows) 20 min after the start of ouabain application which has by now suppressed spontaneous rhythmicity. Antidromic spike from -50 mV resting potential is shown on the right.

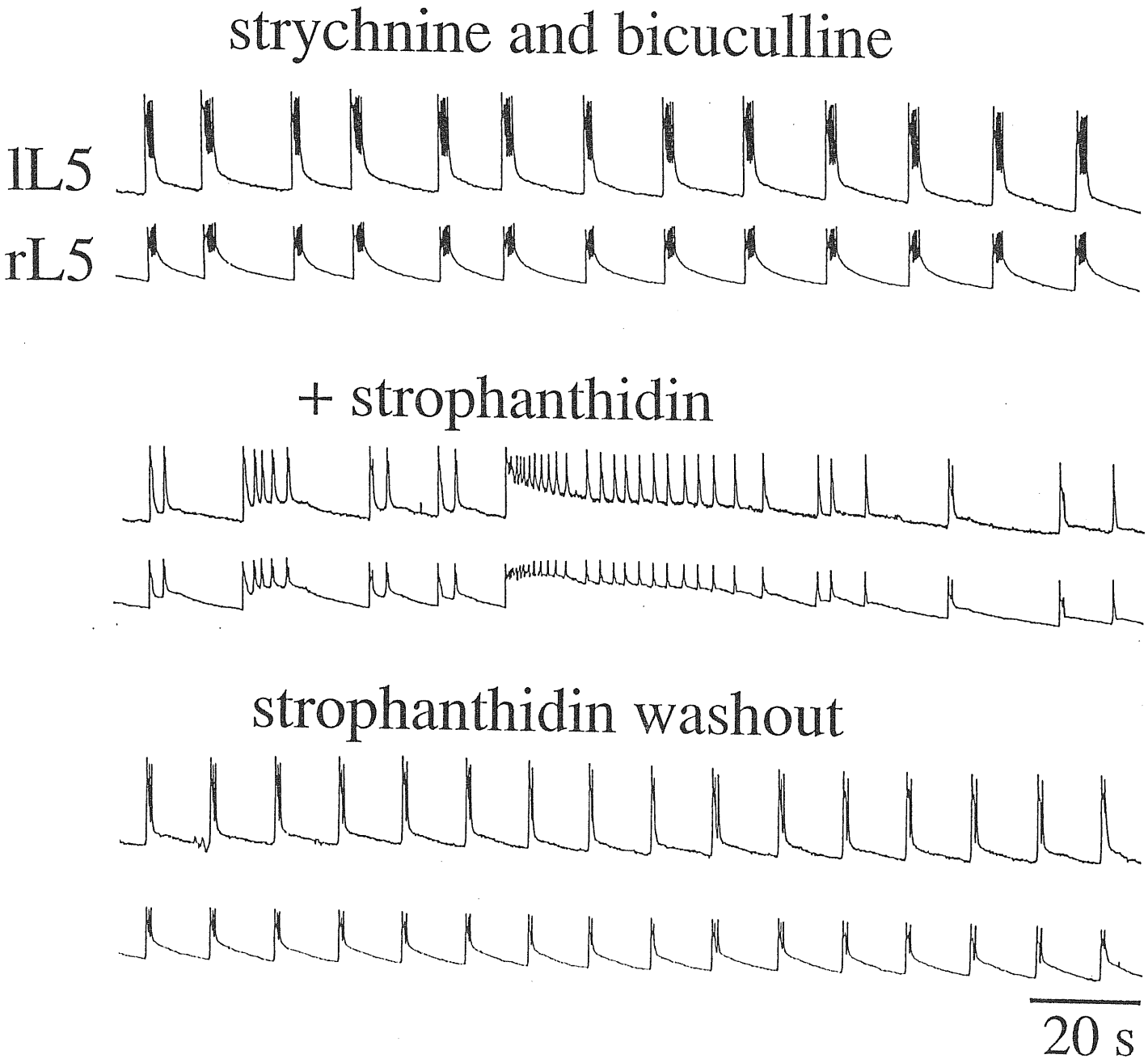

Fig R.27. *Effects of strophanthidin (4 μM) on strychnine and bicuculline induced bursting.*
For each pair of responses traces are extracellular recordings from left and right ventral roots. Top: control bursting; middle: after 30 min application of strophanthidin; bottom: after 2 h washout. Note severe disruption of bursting induced by strophanthidin with partial recovery on wash. Uncoordinated paroxysmal activity retains synchronous appearance in both ventral roots.

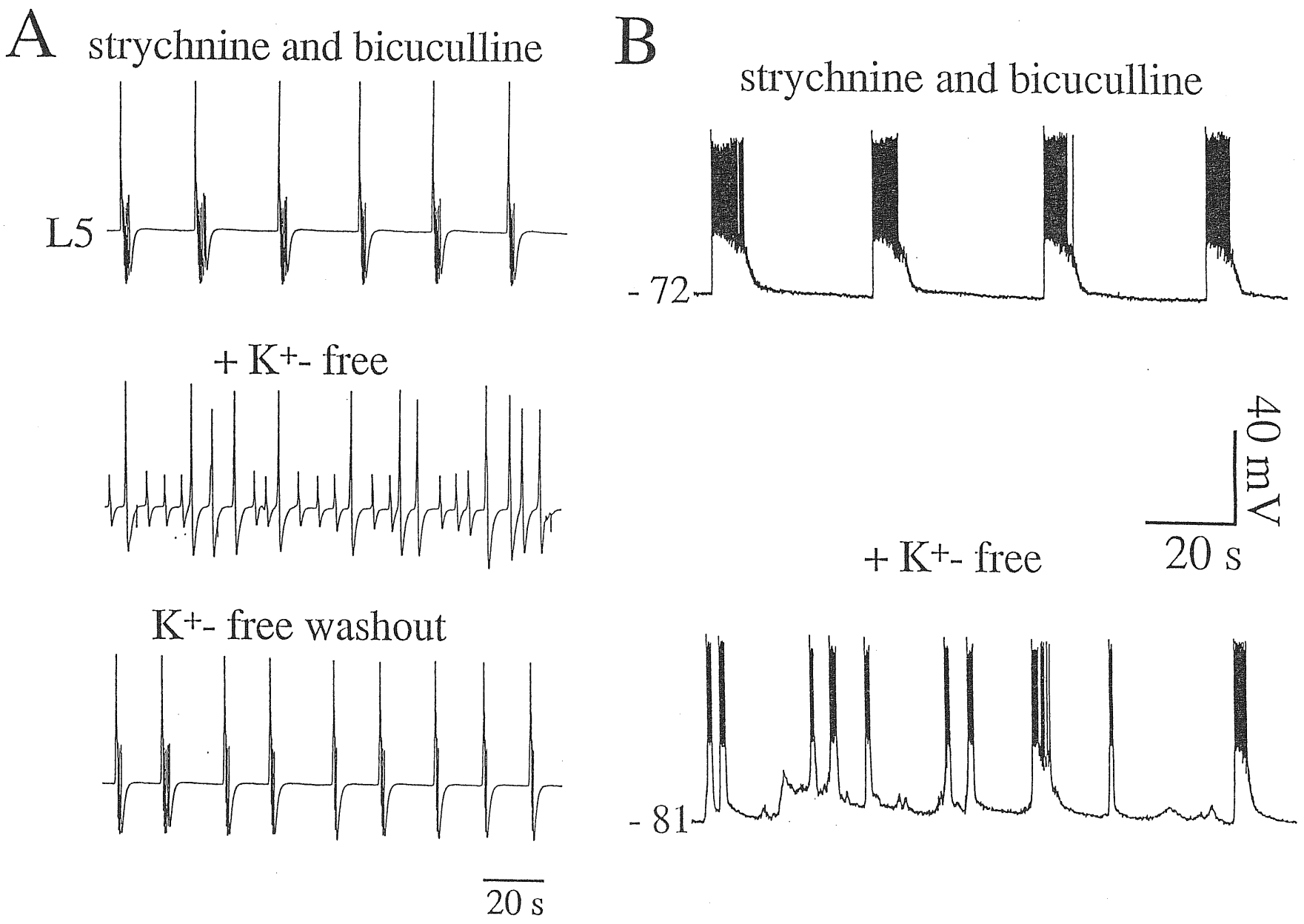

Fig R.28. *Effects potassium-free solut on strychnine bicuculline indu bursting.*
A: extracellu recording (AC-coupl lowpass filtered) control bursting (tc after 40 min in K^+-f solution (middle) after 40 min return control strychnine bicuculline medium. N reversible disruption bursting activity. intracellular records spontaneous burst before (top) following 25 application of K^+-f solution. Note membr hyperpolarization v disruption of burst activity comprising lar amplitude eve interposed with irregu baseline fluctuations.

activation and inactivation of voltage dependent conductances and progressive activation of the electrogenic sodium pump during a burst.

11. Modulation of rhythmic bursting by DR or VL afferent fibres.

An interesting question is whether the rhythmogenic network responsible for rhythmic bursting in the presence of strychnine and bicuculline is accessible to external synaptic inputs and to what extent such inputs are able to modulate its operation as one might expect for a network capable of expressing appropriate responses to behavioural requisites (Marder and Calabrese 1996). Since in the mammalian spinal cord rhythmogenic networks controlling patterned motor activity (locomotion, scratching, etc.) are modulated by sensory inputs and descending pathways, it was important to examine whether the bicuculline plus strychnine induced rhythm is similarly susceptible to modulation by such afferent inputs. Hence, a study was undertaken to clarify whether synaptic inputs from DR or ventrolateral (VL) descending fibres could affect rhythmogenesis, whether the characteristics of bursting were modified by afferent signals and whether such a rhythm could be entrained by patterned afferent impulses.

DR and VL stimulations in control solution activate polysynaptic pathways impinging on motoneurons (Pinco and Lev-Tov, 1993a; 1994). In the absence of synaptic inhibition it was of interest to investigate whether, under certain conditions, DR or VL stimulation could activate polysynaptic pathways independently from bursting activity, because these would reveal that such pathways are not part of the rhythmogenic network.

To clarify these issues, intracellular and extracellular experiments were performed on 35 spinal cord preparations in the presence of strychnine and bicuculline, using DR or VL stimulation at intensity between 1 and 4.5×T in order to recruit low threshold fibres (Kiehn et al, 1992; see Methods for stimulation procedures).

Characteristics of intracellularly-recorded bursts

The effects of DR stimulations delivered during spontaneous bursting were firstly studied with intracellular recording from motoneurons. An example of this type of experiment is illustrated in fig R.29A: under current clamp conditions an L5 motoneuron displayed the

typical bursting pattern (top trace) with spontaneous bursts comprising large amplitude intraburst oscillations and action potentials, as shown on the left of the second trace of fig R.29A where part of the record is displayed at higher speed. The interburst period was characterized by synaptic quiescence. The arrow in the top trace of fig R.29A indicates the time when a single stimulus (1.5×T) was delivered to the ipsilateral L5 dorsal root. Such a stimulation evoked a bursting event similar to the spontaneous ones and comprising an equivalent intraburst oscillatory structure, as also illustrated on a faster timescale in the bottom trace of fig R.29A (right). The dorsal root stimulation did not disrupt the regular pattern induced by strychnine and bicuculline but merely reset it, since the interval between the stimulus and the onset of the subsequent spontaneous burst was similar to the spontaneous cycle period which then resumed its regular rhythm. Comparable data were obtained from 5 intracellular experiments (in 4 different preparations) in which single DR stimulations were delivered at different phases of the cycle (during the quiescent period). Dorsal root stimulation reset the spontaneous rhythm regardless of its timing after the end of the previous spontaneous burst. To assess quantitatively this phenomenon, the interval between the onset of an evoked burst and the onset of the following spontaneous one was plotted as a function of the time between the end of the preceding spontaneous burst and the stimulus (fig R.29 B; n=5). The slope coefficient of the regression line of these data was not significantly different from zero. Furthermore, the average interval between the stimulus and the onset of the next spontaneous burst (25.3±3.3 s) was not significantly different from the average spontaneous cycle period (28.2±2.3 s; measured for >3 min before stimulation). CVc or CVd values measured over 3 min before stimulation were not significantly different from corresponding values measured over 3 min after stimulation (CVc=17±6% and 15±5%; CVd= 10±4% and 12±4%).

The sensitivity of bursts to stimulation strength (range between 1×T and 4×T) was next tested. In the presence of strychnine and bicuculline the threshold for postsynaptic potentials (PSPs) did not change with respect to the one found in control solution; nevertheless, even a PSP at or just above threshold was always followed (after a certain latency) by a burst. This is exemplified in fig R.29C in which the fast traces display the short-latency PSP and the initial component of the bursting episode. While amplitude,

duration or structure of evoked bursts did not depend on pulse intensity (data not shown), the burst time-to-peak (from stimulus artefact to initial peak of evoked burst) was strongly related to the stimulus strength as illustrated by the intracellular record in Fig R.29C (different preparation from Fig R.29A). A single 1.1×T stimulation (note downward deflection representing stimulus artefact and delivered after ≥15 s quiescence) elicited, first, a short latency (<10 ms) small amplitude PSP (amplitude=2.1 mV) which was followed by a burst peaking at 265 ms. Under the same conditions, increasing stimulation intensity to 1.3 or 1.7×T decreased the burst time-to-peak to 206 or 129 ms, respectively, while the PSP grew in amplitude from 11.2 to 21.3 mV without latency change. With 3.4×T stimulation, the burst peaked at 94 ms so that it became indistinguishable from the PSP. On the other hand, as previously mentioned, single or repetitive stimulations of one (or more) VR at intensity up to 10×T applied during quiescent periods did not trigger or affect bursting (see fig R.9 and related text).

Entrainment at different frequencies

Repetitive stimulation protocols often led to unstable recording conditions which made unsuitable the use of the intracellular technique for this type of study. Bursting entrainment was further investigated by means of VR recordings.

Entrainment of bursting was defined as the ability of a periodic external stimulus to elicit bursts on a 1:1 basis. The effects of repetitive DR stimuli delivered at various intervals were first tested. Fig R.30 illustrates one example in which left L5 VR activity was recorded during stimulation (at different periods) of the ipsilateral L5 DR. Spontaneous bursting (top trace) took place with a cycle period of 25.4±.1.8 s and a burst duration of 2.8±0.5 s. Individual bursts comprised several intraburst oscillations, as shown in the expanded trace (on the right) of the arrowed event (on the left). An example of entrainment is shown in the middle trace of Fig R.30. In this case stimuli were delivered at 10 s intervals and 3×T intensity. Each stimulus was followed by an evoked burst similar to the spontaneous ones but significantly ($P<0.01$) reduced in duration (on average 2.1±0.3 versus 2.8±0.5 s, see also expanded trace on the right). For this preparation the minimum period at which entrainment was possible was 2 s (not shown).

Bottom row of Fig R.30 shows that, while 1 s period stimulation failed to elicit bursting, spontaneous bursting activity (with frequency similar to the one observed prior to stimulations) rather unexpectedly returned in the presence of DR pulses (the latter are seen as fast upward deflections). When this type of stimulation ceased, spontaneous bursting persisted with an apparently unperturbed timecourse. The expanded trace in bottom row of Fig R.30 (right) shows that at 1 s interval DR stimuli, despite the absence of bursting entrainment, still elicited depolarizing reflexes (lasting ≥200 ms) as indicated by the time-locked responses which were still present even during spontaneous bursts and seemed to be minimally influenced by the underlying burst. At the same time, bursts maintained a timecourse similar to the one recorded in the absence of stimulations and were not time-locked with the electrical stimuli. Similar results were obtained from 25 preparations using in each case stimuli of fixed intensity (3×T) delivered to one L5 DR while recording from the ipsilateral L5 VR. The lowest interval of stimulation able to support entrainment was in the range of 2-5 s (see histogram of Fig R.31B) with an average value of 2.8±.0.8 s. Spontaneous bursting which recommenced despite the 1 s stimulus interval occurred with a period of 21.1±6.8 s, a value not significantly different from the one in the absence of stimuli (24.7±4.5 s) although the CVp was larger (24.5±10.8 versus 10.4±8.9 %) during such a stimulation.

We next explored the longest stimulus interval able to induce 1:1 entrainment of spontaneous bursting. An example of this approach is illustrated in Fig R.31A in which a spontaneous cycle period of 26.6±1.5 s (recorded from right L5 VR) was first observed (top record). When DR stimulation was delivered at 30 s intervals (see middle trace of fig R.31A), each pulse evoked a burst followed by a spontaneous one that preceded the next evoked event. Bottom trace of fig R.31A shows comparable data with an interstimulus interval of 40 s. Thus, in neither case the stimulation period was able to entrain bursting. In this preparation the maximum period for one-to-one entrainment was 20 s, corresponding to a situation in which bursts never appeared spontaneously during stimulation. This maximum stimulus period for entrainment was lower than the period for spontaneous bursting. Values for the largest interval of stimulation are illustrated by the histogram of Fig R.31C (n=15 preparations), with an average value of 19.5±3.8 s.

Collectively, these data show that entrainment was possible over a relatively wide range of stimulation periods (typically between 2 and 20 s) and that at shorter stimulation intervals, the activity of the burst generator was separated from that of the interneurons participating in the polysynaptic (DR-evoked) motoneuronal reflex.

Side-to-side coordination during DR entrainment

As previously shown, in the absence of synaptic inhibition spontaneous rhythmic bursts and intraburst oscillations took place simultaneously on both sides of the cord. In order to verify whether such a synchronicity was preserved during repetitive DR stimulation, we recorded bilaterally from pairs of homologous VRs while stimulating one DR at the same segmental level. An example is illustrated in Fig R.32. In this case, stimulations (2×T) were applied to left L5 DR while recording from left and right L5 VRs. At 5 s stimulation period, evoked bursts comprised 3-5 intraburst oscillations, that appeared simultaneously on both sides of the cord (top tracings). At 1 s stimulation period (bottom tracings), bursts could not be entrained (see also fig R.30) and appeared simultaneously on both sides. Under these conditions DR stimulation evoked a depolarizing reflex from the ipsilateral VR, but was almost ineffective on the contralateral VR, as indeed observed even before adding strychnine and bicuculline (records not shown). Similar results were obtained with bilateral recording from L5, L4 or L3 VRs in 4 preparations. These data suggest strong, bilateral coupling of the rhythm generating network since bursts could not be restricted to one side only even by DR stimuli strongly asymmetrical in their ability to generate PSPs.

Dependence of burst duration on stimulation period

Since each preparation could be entrained by DR stimulation within a wide range of periods, the question then arises whether within this range burst duration and intraburst structure were also affected. This issue was explored in experiments like the one depicted in Fig R.33A. This preparation could be entrained between 15 and 2 s stimulation interval (intensity=3×T) and records pertaining to 10, 5 and 2 stimulation periods are shown from top to bottom of fig R.33A. At 10 s stimulus period (top of fig

R.33A), evoked bursts lasted 4.1±0.4 s and comprised 9-13 intraburst oscillations (note that fast downward deflections are spike activity of ventral roots). At 5 s stimulus period burst duration was 2.1±0.2 s with 4-7 intraburst oscillations. At 2 s stimulus period, burst duration was reduced to 1.1±0.1 s and bursts comprised only 3 discernible oscillations. These changes in burst duration were statistically significant ($P<0.01$) although they were not accompanied by significant changes in burst amplitude. Analogous results were obtained from 15 preparations. The average dependence of burst duration on stimulation period is plotted in Fig R.33B, where data are normalized with respect to the burst duration measured, in each experiment, for 10 s stimulation period. It is apparent that burst duration decreased over a five-fold range when stimulation period was decreased, thus allowing the network to return earlier to the quiescent state when temporally closer stimuli were delivered.

Dependence of entrainment on stimulation strength

We also investigated whether the range of stimulation period which supported entrainment depended on the stimulus strength. An example of this type of experiment is illustrated in Fig R.34. Fig R.34A shows left L5 VR responses induced by single pulses applied to the ipsilateral L5 DR at 1×T or 4×T in control solution before application of strychnine and bicuculline. While 1×T stimulation elicited a slight depolarizing response (0.12 mV amplitude), 4×T stimulation not only produced a larger depolarization (0.24 mV) but also a fast, large-amplitude biphasic response presumably due to motoneuron action potentials. After establishing spontaneous bursting with strychnine and bicuculline (not shown), both stimulus strengths (at constant 10 s period) were able to entrain bursts (Fig R.34B) which possessed similar amplitude, duration and intraburst oscillatory structure, as also illustrated in the expanded traces of Fig R.34C. Like the case of a single DR stimulus (see fig R.29 C), only the time-to-peak of bursts depended on stimulation strength, as shown by the fast timescale tracings of Fig R.34D: with 1×T stimulation the initial peak was reached after 70-80 ms, while with 4×T stimulation it was reached after 25-35 ms. In the latter case a fast biphasic response similar to that observed in control solution was also present.

When the stimulation period was decreased, major differences between the effects of 1×T and 4×T stimulations emerged. These are illustrated in Fig R.35A (same preparation as in fig R.34). In the upper trace 1×T stimuli (2 s period) could not entrain rhythmic activity, even if each stimulation generated a depolarizing reflex (duration ≥200 ms). Lower trace of fig R.35A shows the effect of increasing stimulation intensity to 4×T: in this case entrainment at 2 s period was possible as each pulse evoked a burst (lasting on average 1.25 ± 0.05 s). These results are summarized in fig R.35B in which the lowest limit for the stimulation period capable of burst entrainment was plotted against values for stimulation intensity (1-4.5×T range). It appears that with 1×T intensity, entrainment was possible only at periods ≥ 10s; between 1×T and 2.5×T values the lowest period at which entrainment was observed decreased from 10 s to 2 s and reached a steady state level for intensities higher than 2.5×T. Conversely, changes in stimulus strength did not alter the largest value of stimulus period able to support entrainment (data not shown). Similar results were obtained in two other preparations These results indicate that during closely spaced pulses the efficacy of DR pathways in triggering a burst episode was critically dependent on the stimulation intensity.

Entrainment with VL stimulation

In order to analyze whether entrainment of the spontaneous rhythm in the disinhibited cord was restricted to DR stimulations we also investigated the effects of VL stimulations. In control solution these pulses (0.1 ms) evoked short latency (3-4 ms) synaptic responses comprising a depolarizing component (with superimposed spike activity when stimulus intensity was >3×T) decaying biexponentially. These responses are similar to those previously reported for motoneuronal EPSPs evoked by VL stimulation (see for example Elliott and Wallis, 1993). In order to avoid excessive stimulation, pulse intensity was usually fixed at 3×T. In the presence of bicuculline and strychnine a single VL stimulus evoked a burst similar to the spontaneous ones and reset the spontaneous rhythm (data not shown) in the same fashion as previously found with single pulses applied to a DR (see fig R.29). These observations prompted testing an extended range of VL stimulus periods to find out their entrainment ability. Fig R.36 depicts the effect of three different stimulating periods on a preparation with stable

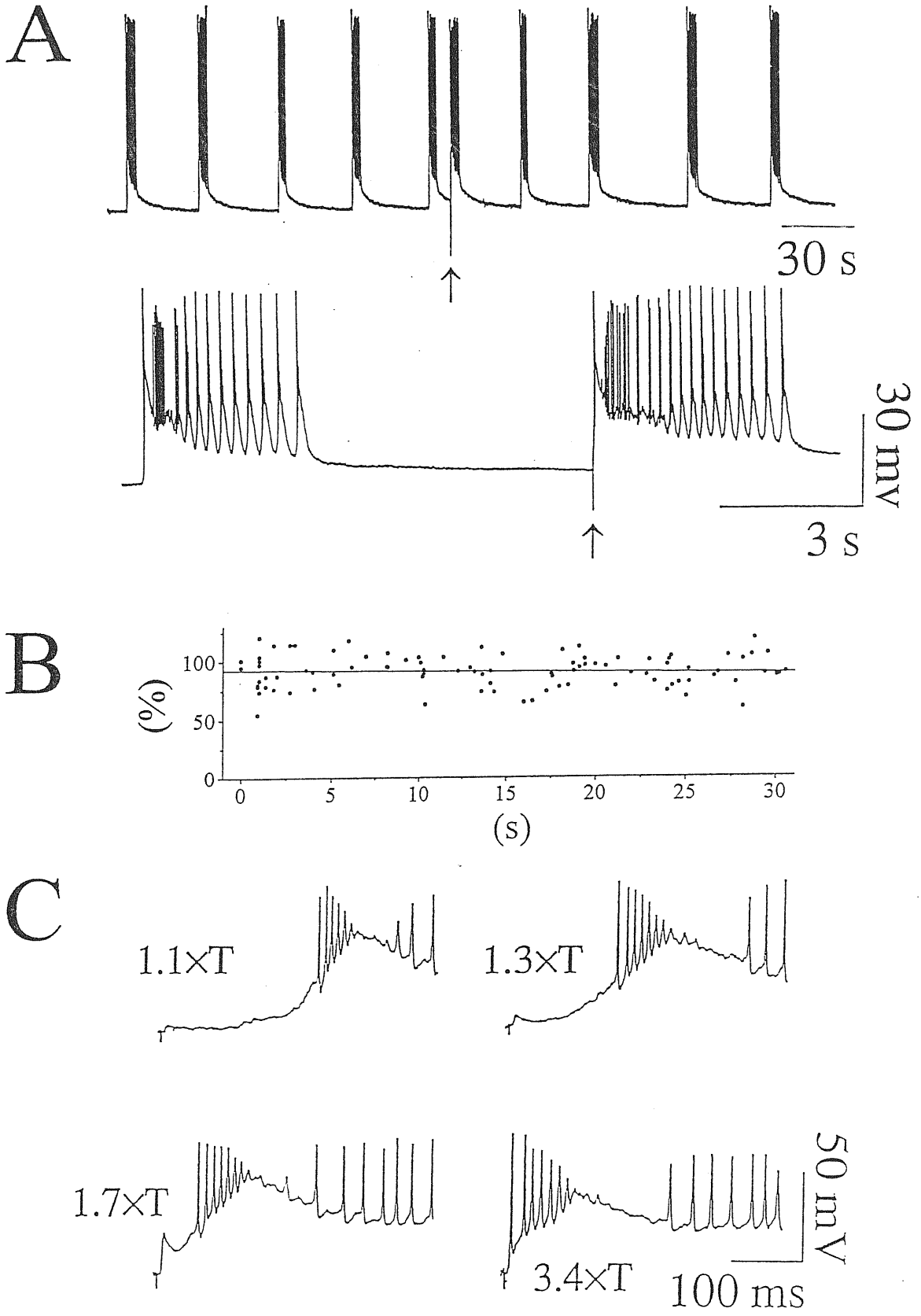

Fig R.29. *Effect of DR stimulation on spontaneous bursting recorded intracellularly from lumbar motoneuron.*
A, top: spontaneous bursts occurring in the presence of strychnine and bicuculline are reset by a single DR pulse (1.5×T; applied at the time indicated by arrow) which induces a bursting episode. Note that, after this event, bursting recommences with similar period as before. Bottom: expanded timebase trace of two individual bursts either arising spontaneously (left, immediately before electrical pulse) or evoked by DR stimulus (right). Note similar structure and duration of evoked and spontaneous events. Resting potential=-71 mV. B: scatter plot of the interval between the end of the preceding spontaneous burst and the stimulus (abscissa) versus the interval between the stimulus and the first spontaneous burst (ordinate, data are normalized with respect to the mean of interburst interval for spontaneous bursting in each cell, n=5). The horizontal line is the regression line fitted to the data. C (different cell from A): fast timebase records of responses elicited by DR pulses of varying intensity (indicated in terms of T values) and comprising initial synaptic potential followed by burst with latency progressively reduced up to fusion with early synaptic response (bottom row, right). Resting potential=-74 mV.

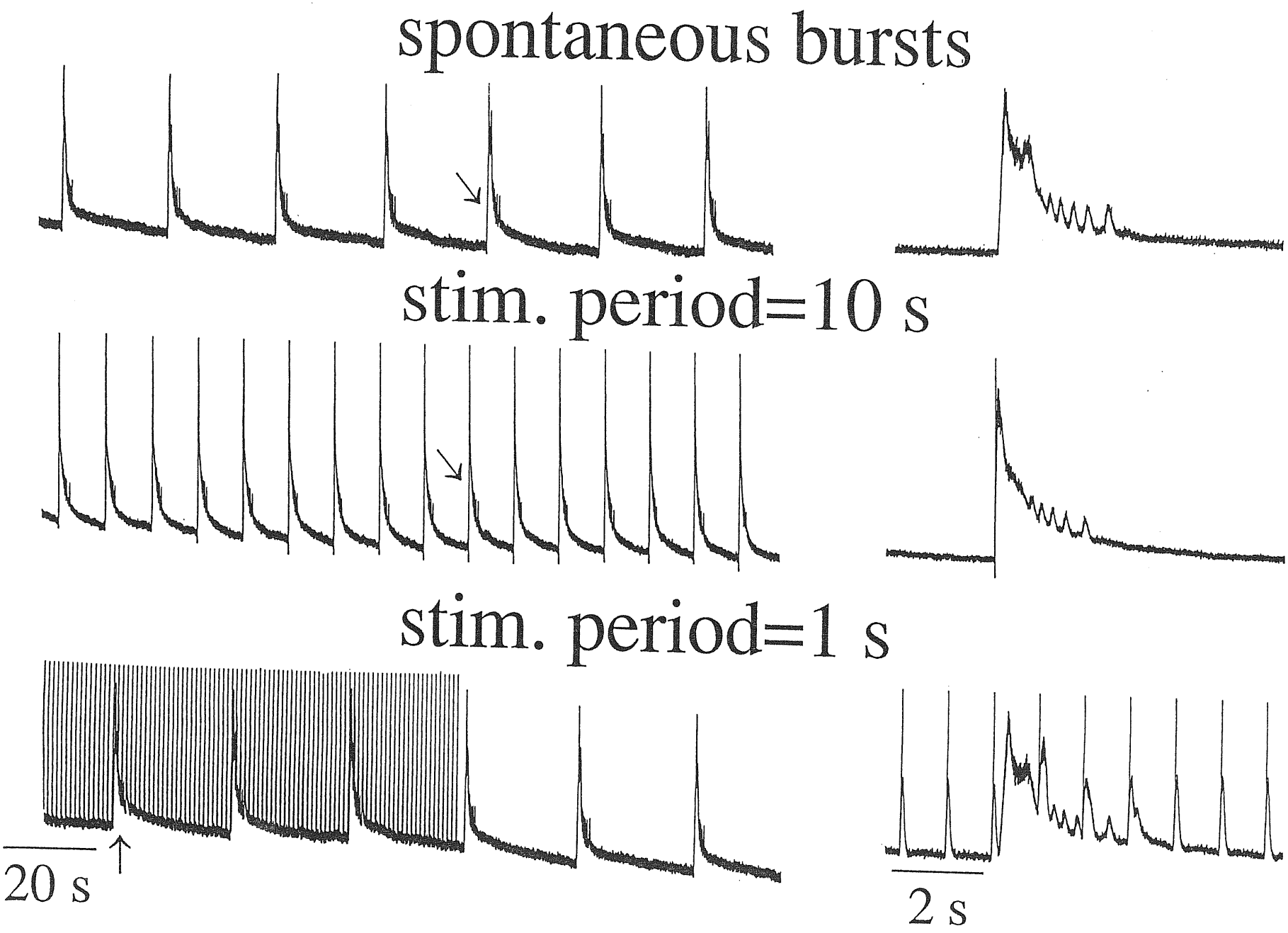

Fig R.30. *Effects repetitive stimuli applied L5 DR (at various perio on bursting recorded fr L5 VR.*

Top trace: spontanec bursts occurring in t presence of strychnine a bicuculline. The eve indicated by arrow displayed at 10 times fas speed on the right hand sic Note intraburst oscillatc structure. Middle trace: 1 entrainment of bursts by I pulses (10 s period); eve marked by arrow is display at faster speed on the rig hand side. Evoked bursts a of shorter duration wh retaining oscillatc structure. Bottom trac failure to entrain bursts DR stimuli at 1 s peri (these are indicated by t sharp, evenly-spaced upwa deflections): spontaneo bursts return desp electrical pulses and pers after end of electric stimulation. Right hand si panel shows at faster spe the reflex activity induced 1 s period pulses and o independent spontaneo burst during which evok synaptic responses contin to be preser

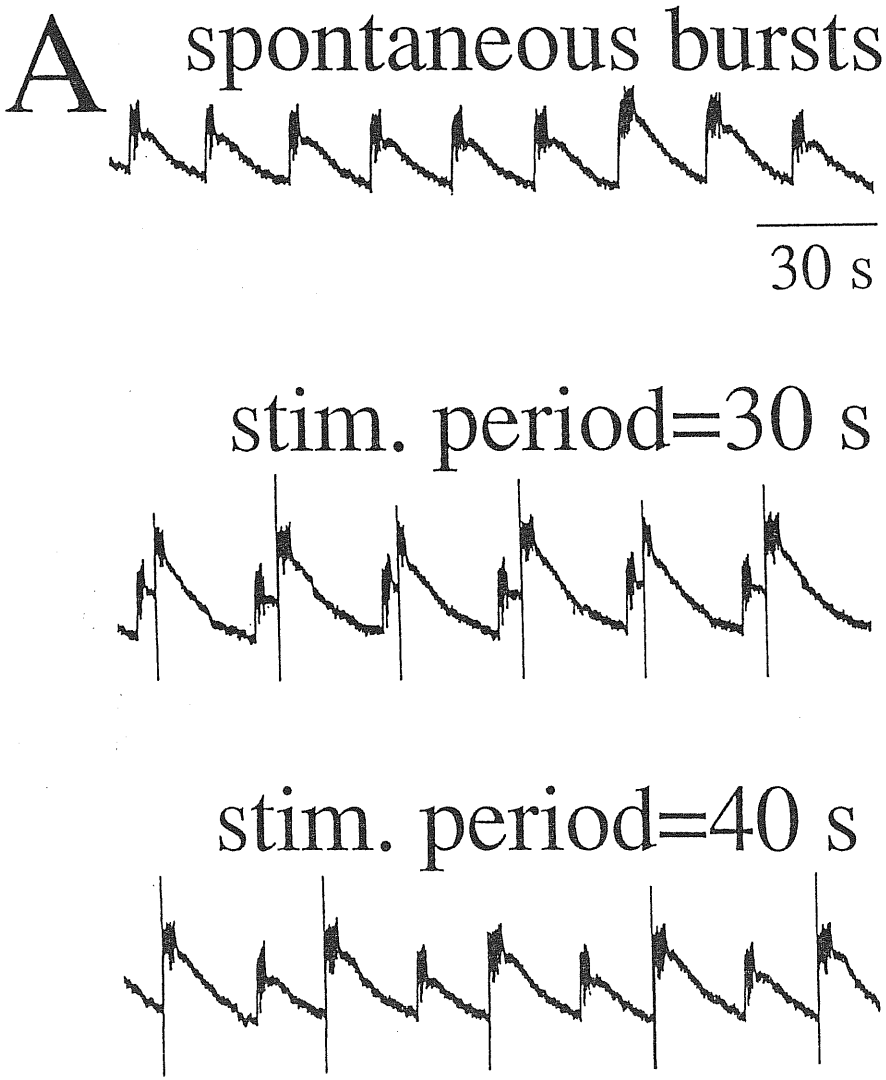

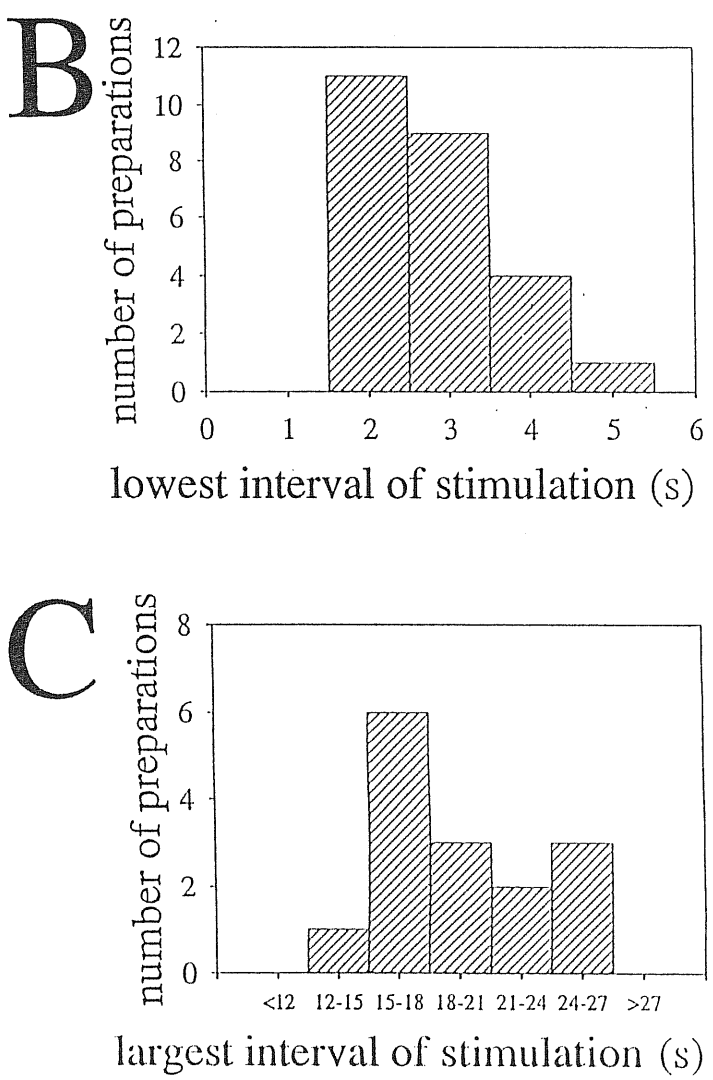

Fig R.31. *Effects of high perioc stimulation of DR fibres or bursting induced by strychnine and bicuculline.*

A, top: right L5 VR record o spontaneous bursts; middle electrical pulses (30 s period are repetitively applied to the ipsilateral L5 DR to coincide with early decay phase o spontaneous bursts. Electrically evoked bursts are preceded by stimulus artefacts. Note that thi low period of stimulation fail to elicit 1:1 entrainment since spontaneous events coexist with evoked ones; bottom: simila results are obtained at 40 stimulation period. B distribution of the lowes stimulation period capable o supporting entrainment over 2 preparations. C: distribution o the largest period of stimulatio capable of supporting entrainment over 1 preparations.

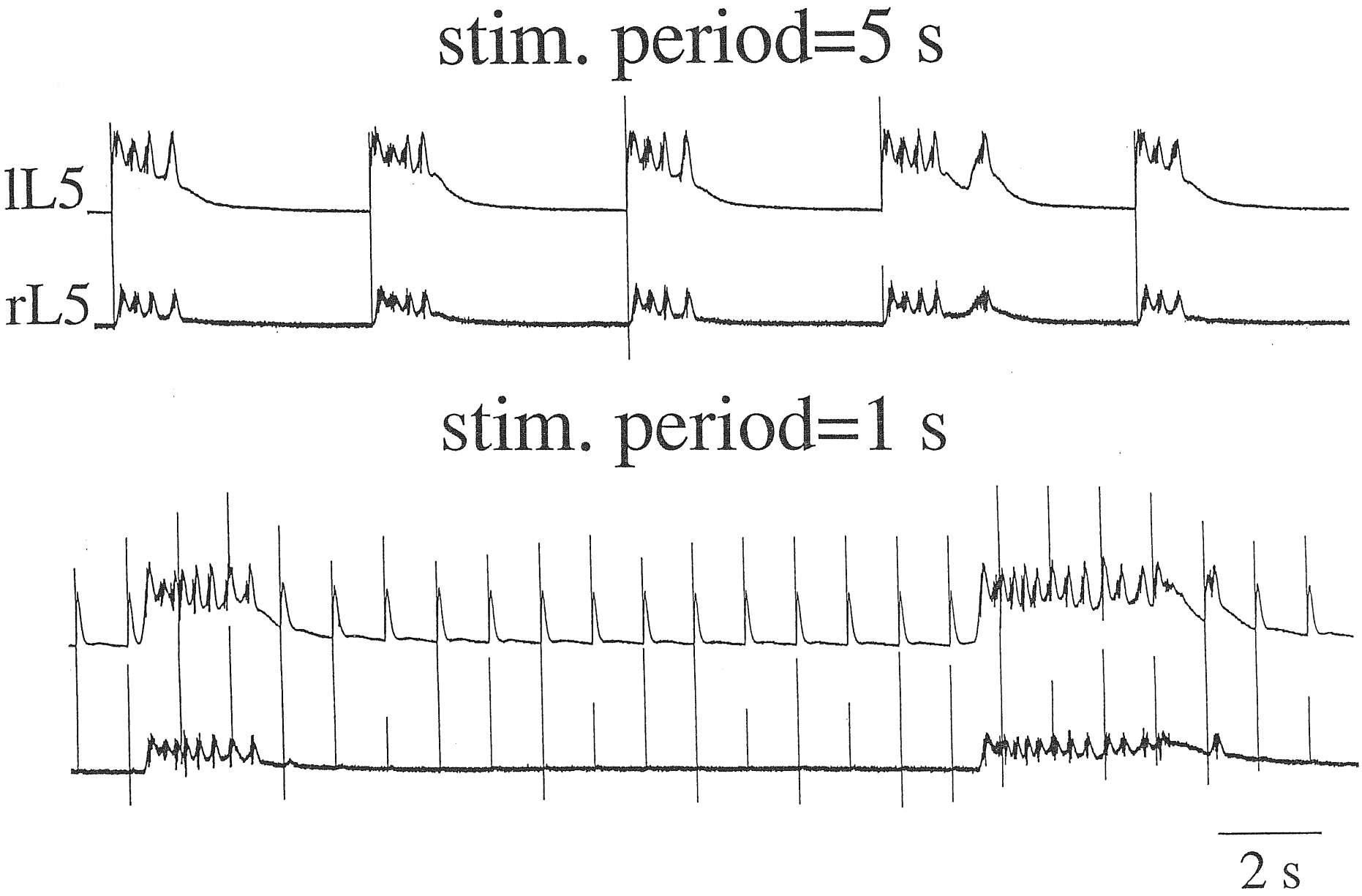

Fig R.32. *Bilateral recording of bursting activity at two different stimulation periods.*
Top: simultaneous recording from left (l) and right (r) L5 VRs showing 1:1 entrainment of bursting by left L5 DR stimuli applied every 5 s. Bottom with similar protocol but lower stimulation period (1 s) burst entrainment fails while electrical pulses elicit reflexes detected only from lL5 VR. Note that spontaneous bursts and their intraburst oscillations appear simultaneously in both VRs.

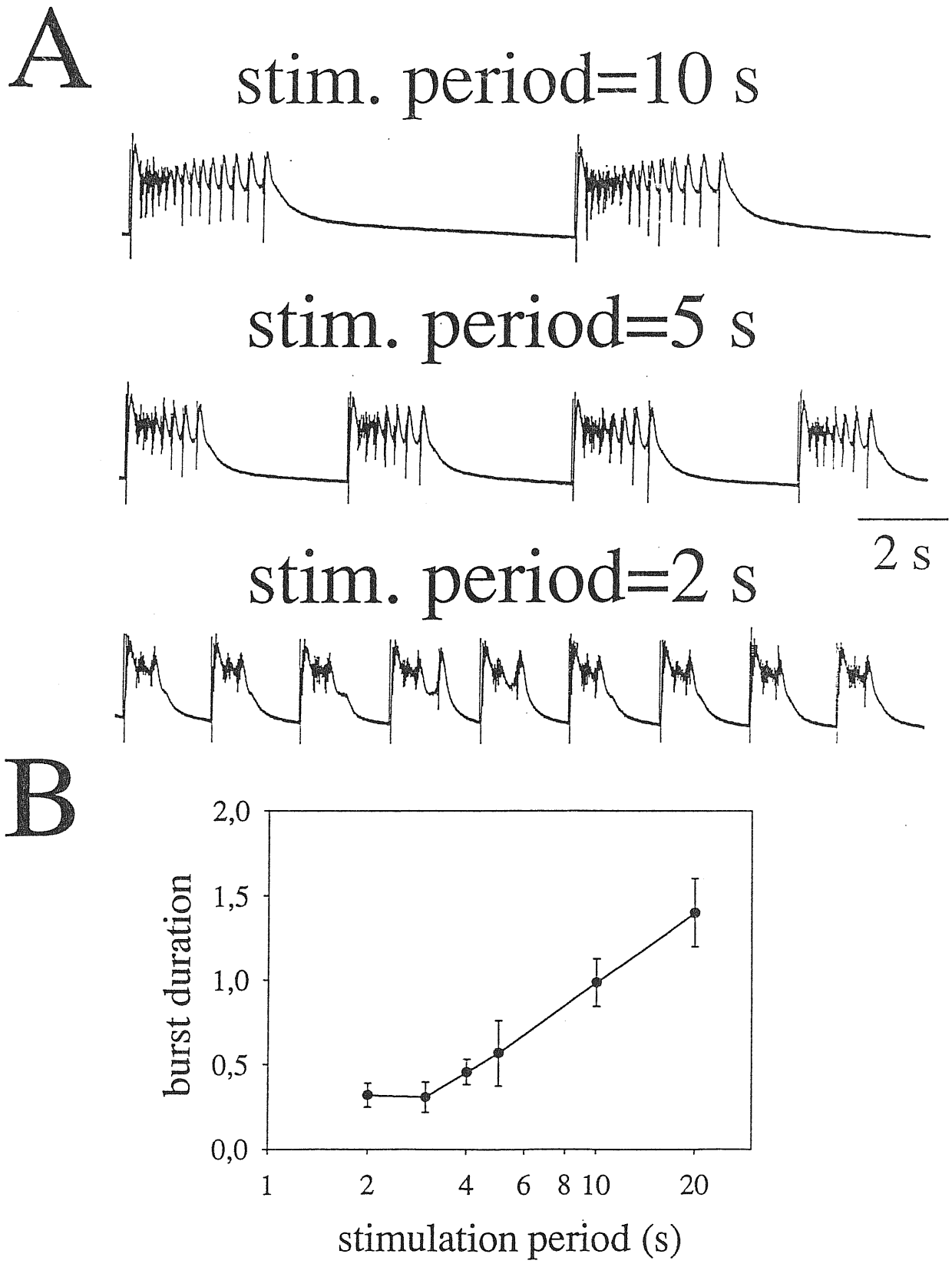

Fig R.33. *Dependence of burst duration on stimulation period.*
A, top: bursts entrained by 10 s period of DR stimulation. Biphasic stimulus artefacts at the beginning of each burst are closely preceded by short, upward calibration steps (0.5 mV). Fast downward deflections during burst oscillations are summated spike responses of motoneurons. Middle: halving the stimulation period produces a reduction in burst duration of approximately 50 %. Bottom: 2 s period of stimulation still produces 1:1 entrainment of bursts which become short event of about 1 s duration but retaining their oscillatory structure. B: graph of stimulation period (log scale; s) versus burst duration normalized with respect to response observed in each preparation with 10 s period of stimulation. Data are from 25 preparations.

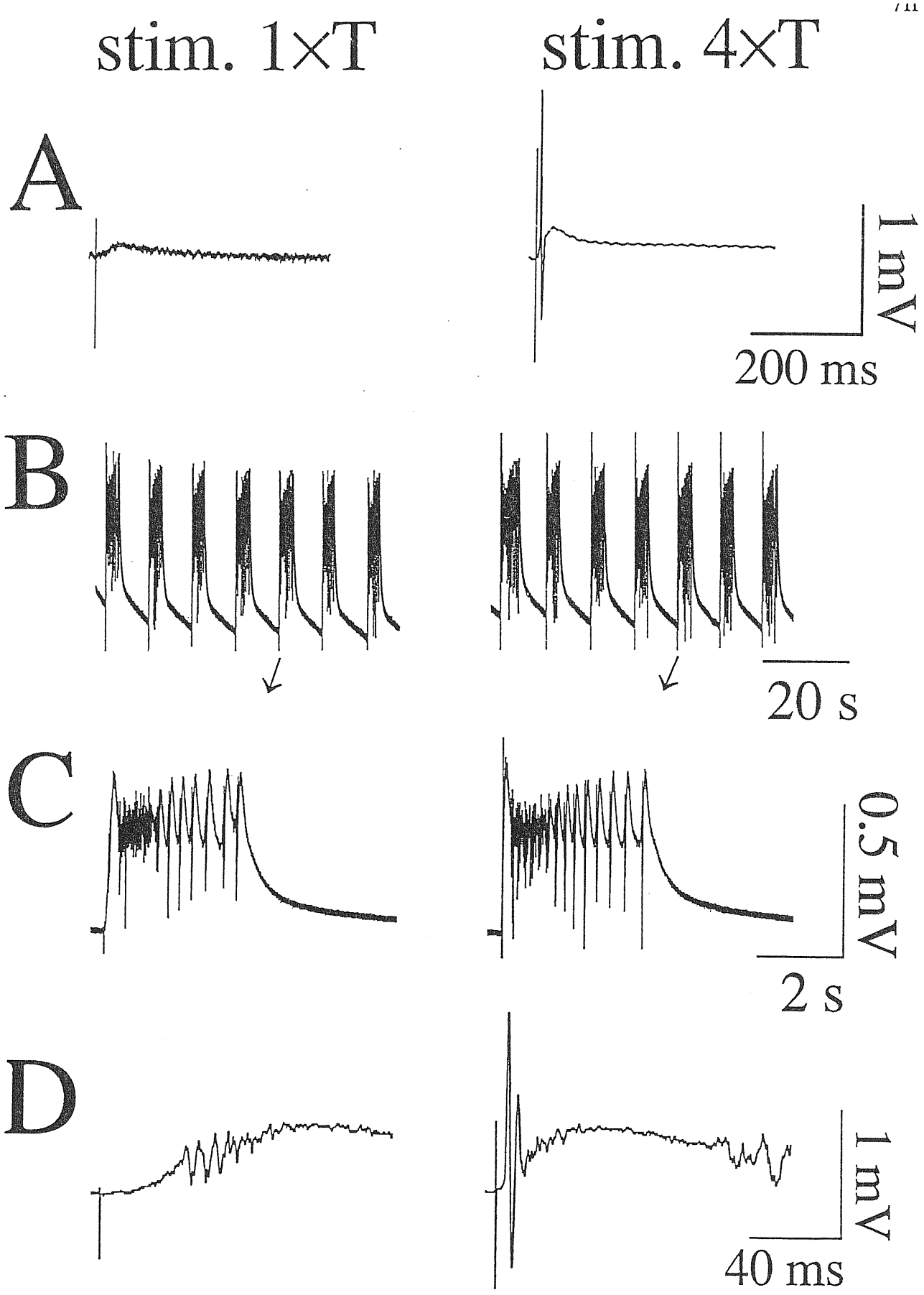

Fig R.34. *Effects of changes in stimulus intensity on the ability to entrain bursts.*
A: in standard solution (without addition of strychnine and bicuculline) a just threshold (1×T; left) or 4×T (right) pulse to L5 DR evokes small synaptic response or larger event with spike activity (see biphasic event during early part of response). Responses are averages of 5 recordings in each instance. B: in the presence of strychnine and bicuculline 1×T or 4×T stimulation (10 s period) produces 1:1 entrainment of bursting. C: faster records of event marked by arrows in B indicate similar oscillatory structure of evoked bursts. Voltage calibration refers to panels B and C. D: on an even faster timebase the early component of the evoked bursts depicted in C is displayed. Note that stronger pulse elicits response of shorter latency and with earlier spike activity.

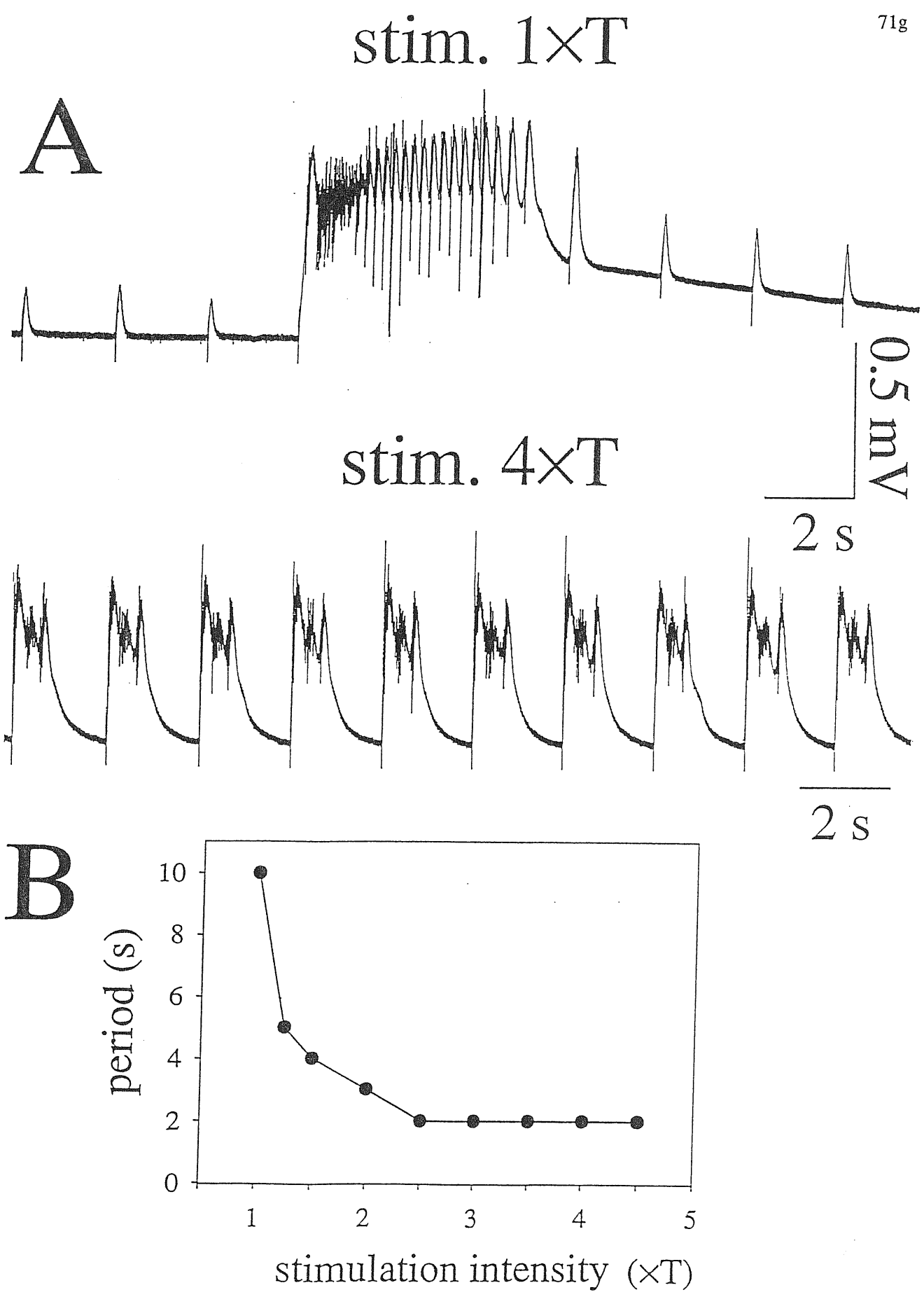

Fig R.35. *Different stimulus intensity shows differential ability to induce burst entrainment.*
A, top: at 2 s stimulation period a weak pulse intensity (1×T before addition of strychnine and bicuculline) fails to support burst entrainment; a spontaneous burst develops during repetitive electrical stimulation (large downward deflections are spike activity of motoneurons); bottom: at the same stimulation period as above increase in pulse strength (4×T) supports 1:1 entrainment of bursts. B: graph of stimulus intensity (expressed as multiples of threshold, T, obtained before adding strychnine and bicuculline) of DR electrical pulses versus the lowest period of stimulation which allows burst entrainment. All traces are from the same preparation shown in fig R.34.

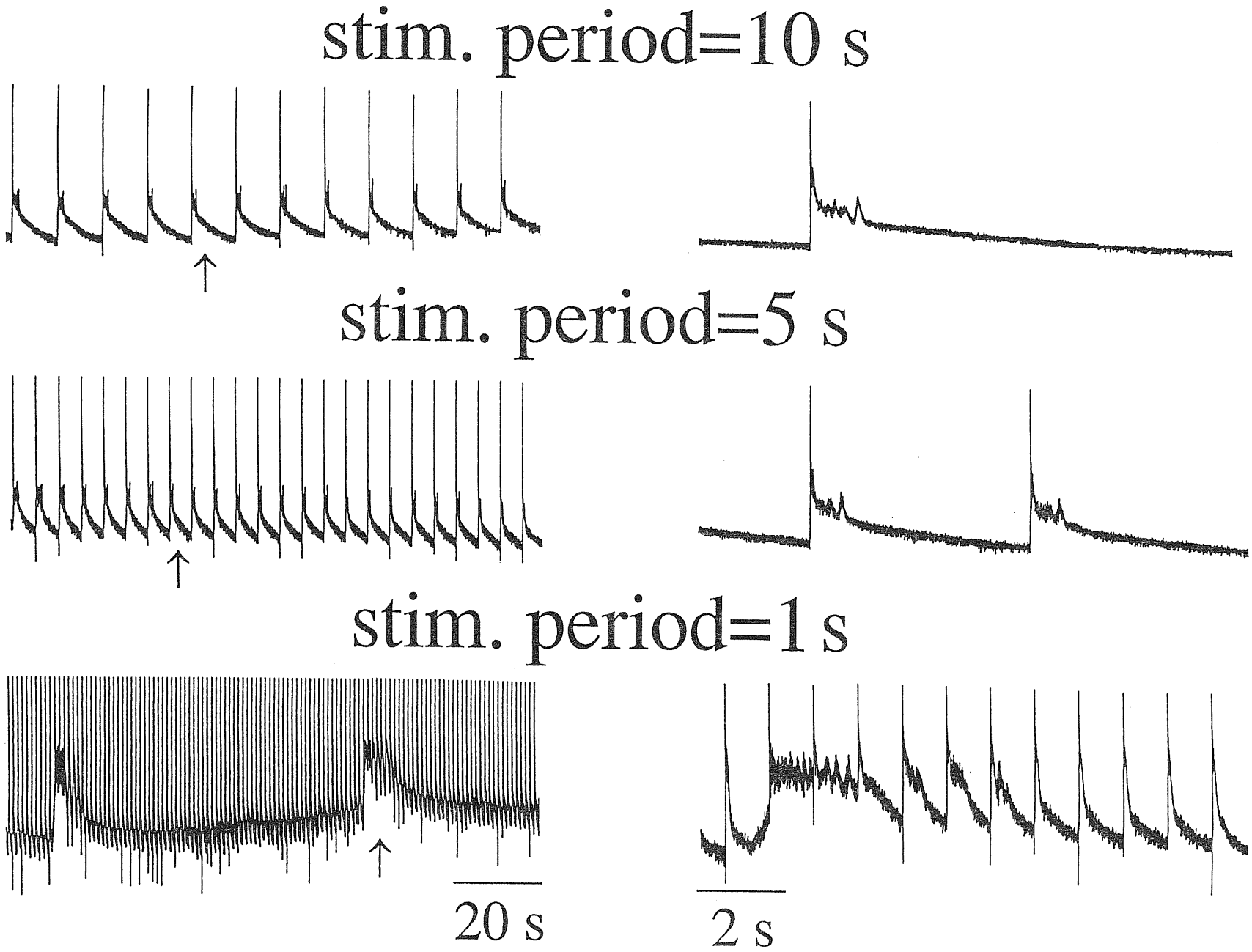

Fig R.36. *Effects of VL stimulation on bursting induced by strychnine and bicuculline.*
Top: 1:1 entrainment of bursting by 10 s period of stimulation. Faster record of event indicated by arrow is shown on the right. Middle: 1:1 entrainment persists with VL stimulation at 5 s period. Evoked bursts are further reduced in duration. Events corresponding to arrow are displayed on a faster timebase on the right. Bottom: failure of entrainment by 1s period stimulation (large upward deflections) while spontaneous bursts re-emerge. Burst marked by arrow is also shown on a faster timebase on the right; note that this event is independent from evoked synaptic responses (time-locked with stimulus artefacts). Recordings from left L5 VR.

spontaneous bursting (average cycle duration= 26.0±5.2 s; burst duration=3.2±0.8 s; recorded from left L5 VR). The top trace of fig R.36 shows that pulses at 10 s interval fully entrained bursting on an 1:1 basis while the evoked burst duration (1.9±0.3s) was significantly reduced with respect to the spontaneous one ($P<0.01$). One individual burst (marked by vertical arrow) is displayed on the right at expanded time scale to indicate that burst structure was preserved. The middle trace of fig R.36 shows that a train of 5 s interval stimuli induced entrainment and significantly reduced ($P<0.01$) burst duration to 1.0±0.2 s (see also faster right hand trace of recording marked by arrow). The lower trace of fig R.36 represents the effect of 1 s interval stimuli: in this case the stimulation did not elicit a burst, but only a polysynaptic reflex (lasting 640±80 ms) similar to the one recorded in the absence of strychnine and bicuculline (duration=480±70 ms). Despite the continuous application of VL pulses at 1 s interval, spontaneous bursts still occurred (although at slower rate in this example). The arrowed sample trace of fig R.36 is shown on the right-hand side at faster speed which allows to observe that the burst started just between two stimuli.

Similar data were obtained from 8 preparations, in which the minimum period of VL stimulation (at 3×T intensity) able to support entrainment was 2-5 s (average=2.9±1.0 s). In 4 cases in which VL stimulation at 1 s period was tested, it induced ventral root responses similar in shape and duration (123±34 %) to the ones obtained prior to strychnine and bicuculline. During such a stimulation, spontaneous bursts developed with an average cycle period of 31.2±11.8 s, not significantly different from that measured in the absence of stimuli (26.3±6.8 s), even if in the former conditions the CVp was larger, namely 20.0±7.3 % versus 11.7±7.4 %. In 7 preparations the largest interval of stimulation able to support 1:1 entrainment was found to be on average 20.2±2.9 s.

Like the case of DR stimulations, decreasing the stimulus interval of VL pulses reduced burst duration: in fact, the normalized duration of evoked bursts was changed from 1.5±0.3 to 0.25±0.12 when the stimulus interval was reduced from 20 to 2 s (normalization was carried out with respect to data with 10 s stimulation period).

In two further preparations we investigated whether the range of stimulation periods for which entrainment was possible depended on pulse strength. Results were similar to the ones obtained with DR stimulations (*cf.* fig R.35). In both cases the lowest stimulation

period that caused entrainment was 2 s when pulse strength was ≥3×T whereas with 1×T stimulation intensity the lowest stimulation period was 10 s.

12. Effects of selective lesions on rhythmic bursting

As mentioned in the Introduction section, the issue of localization of the rhythmogenic activity responsible for locomotion in the neonatal rat spinal cord is a complex one and still not definitely resolved; in fact, some authors claimed that such a network is strictly localized to the upper lumbar segments (L1/L2; Cazalets et al, 1995) while others suggested that rhythmogenic ability is distributed along the rostrocaudal axis (Kjærulff and Kiehn, 1996). In the case of the chick embryo preparation Ho and O'Donovan (1993) have shown that both caudal and rostral segments of the lumbosacral cord can generate this rhythmic activity and that neurones localized in the ventrolateral part of the ventral horns are sufficient for the generation of motoneuronal bursting. Moreover, they showed that during spontaneous motor episodes two different mechanisms are responsible for burst frequency and burst duration and that these mechanisms can be affected separately by experimental lesions. As shown in the former subheading, in the disinhibited spinal cord repetitive stimulation of afferent synaptic inputs at intervals shorter than 2 s revealed disconnection between polysynaptic reflex pathways and burst generator activity. These data suggest that, under these conditions, rhythmogenesis was produced by a specialized spinal network. An investigation was then carried out to cast light on the localization of the rhythmogenic networks in the disinhibited spinal cord by means of selective lesions including removal of segments, progressive hemisectioning and ablation of dorsal horn tissue.

Lesions were performed on 37 spinal preparations with a small piece of razor blade after observing control responses: data were normally collected following a 15 min stabilization period after each lesion. Various types of lesion were produced: they consisted of a) gradual cutting along the midline (sagittal plane cutting) thus yielding two hemisected preparations, b) transverse sectioning (coronal plane cutting, thus eliminating spinal cord segments) or c) cutting through a frontal plane yielding hemicords with ventral horns only. The latter preparation was further divided along a sagittal plane to produce a quadrant in which only one ventral horn was present. At the end of each

experiment preparations were fixed with tissue freezing medium, sectioned and stained as described in the Methods section.

Ablation of rostral or caudal segments

In order to investigate whether the networks localized to L1/L2 lumbar segments are necessary for the rhythmic activity evoked by strychnine and bicuculline, we recorded bilaterally from L5 ventral roots before and after ablation of the spinal cord segments rostral to L3 (the lesion is schematically shown in fig R.37 A, left). Fig R.37 shows that bursting persisted in both L5 ventral roots; rhythmic activity was also maintained in the L2 ventral root (that is above the transection level) with frequency and duration not significantly different from intact preparation. In 6/6 preparations rhythmic bursts (with intraburst oscillations) persisted at the same frequency in the caudal segments after this lesion (compare in fig R.37 A, top and bottom tracings taken from the same spinal cord before and after surgical ablation). The average values for cycle period from 6 preparations confirmed the lack of change after removal of the upper spinal segments (fig R.37 B, left). Burst duration became slightly shorter, as indicated by the right-hand side records at faster time sweep (fig R.37 A). This phenomenon was however not statistically significant as shown by the histograms from 6 preparations (fig R.37 B, right). These data clearly demonstrated that in the disinhibited spinal cord both rostral (L1-L2) and caudal (L3-L5) lumbar segments posses a similar rhythmogenic ability. It seemed also of interest to explore the minimum number of segments necessary to support bursting. In four cases the portion of the cord localized caudal to L6 was subsequently removed without change in burst frequency and duration. Furthermore, a tissue block containing only L4 and L5 segments (n=3) generated bursts (recorded from L5 ventral root) of more irregular nature as indicated by their elevated coefficient of variation for the cycle period (on average 75% vs 12% in the intact cords). Burst duration was on average decreased by 59% with respect to the intact preparations. A block of tissue comprising the L5 segment only (n=3) displayed irregular and infrequent spontaneous bursts occurring on average at 7.3±3.7 min interval and lacking intraburst oscillations (burst duration was 3.3±2.6 s).

Sagittal sectioning of the spinal cord

Since the present pattern consists of simultaneous bursting of homologous ventral roots, we tested whether side-to-side neural connections at different segmental levels were necessary to maintain synchronicity. To this end we first performed progressive hemisectioning from the caudal part of the cord (as indicated by dotted lines at the top of fig R.38 A), while recording from left and right L5 ventral roots. Fig R.38 A shows that, even when the cord was bisected up to L4 or L2 (termed type I or II lesion, respectively) rhythmic bursts still took place simultaneously in L5 ventral roots. Similar results were obtained in 4 preparations. In the example of fig R.38 A sagittal hemisectioning also produced shortening of individual burst duration. This phenomenon was however not statistically significant when data from 4 preparations were pooled together (see below). The average values observed for burst frequency and burst duration are illustrated in the plots of fig R.39A, in which the type I and II lesions are grouped as caudal hemisection protocol (open columns). While burst frequency and burst duration were not significantly affected by these lesions, the coefficient of variation of the cycle period (but not the one of burst duration) was largely increased (+ 168 %) after type II lesion. Thus, such a lesion affected the regularity of burst onset without any concomitant change in burst duration regularity. When the cord was further split up to L1 level, complete synchronicity was maintained in 2/4 preparations. Further splitting up to thoracic level resulted in burst desynchronization in all cases.

Analogous results were observed when the hemisection was performed starting from the rostral end of the cord (rostral hemisection protocol; n=4). In this case bursts still took place simultaneously in L5 ventral roots even when the cord was split down to L6 (type III lesion) or to S2 (type IV lesion), as shown in fig R.38 B. The effects of these lesions on the average values of cycle period and burst duration are plotted in fig R.39 B. Even in this case no significant changes were observed in these values but the coefficient of variation of the cycle period was largely increased after lesions III and IV (+531 % and +590 %, respectively). Moreover, burst duration appeared to decrease after each lesion although this effect was not statistically significant. Further splitting of the spinal cord resulted in partial or complete loss of synchronicity in all cases. Thus, side-to-side

connections localized more than 3 segments apart from L5 level (either rostrally or caudally) are sufficient to maintain rhythmic bursts synchronous in L5 ventral roots.

Complete hemisection of the spinal cord was performed on 4 intact preparations. In all cases rhythmic bursting in left and right L5 ventral roots persisted without synchronicity. In two cases the two halves displayed different burst frequency and duration (see fig R.38C) while in the other two ones burst frequency and duration were similar for the left and right sides, although no longer temporally locked together. Plots of fig R.39C (obtained by pooling all data from both sides of each preparation) show that in addition to a strong increase in the coefficient of variation of cycle period, complete hemisection caused a significant reduction in burst duration. These data demonstrate that each side of the spinal cord possessed the neural substrate necessary to produce rhythmic activity in the presence of strychnine and bicuculline.

Effects of dorsal horn ablation

After dorsal horn removal from the chick embryo spinal cord the remaining network, localized in the ventral horns, is still able to perform coordinated rhythmic activity (Ho and O'Donovan, 1993). In order to test whether in the neonatal rat spinal cord ventral horn networks were able to generate rhythmic activity in the absence of synaptic inhibition, we recorded from L5 ventral roots before and after a frontal section which removed the dorsal horns and the central canal area from spinal cord preparations comprising lumbosacral segments. In 5 such preparations histological examination of stained sections confirmed that only the laminae localized ventrally to the central canal had been left (see example in fig R.40 B). In all these cases, rhythmic bursts were still observed in lesioned preparations as illustrated by a representative example in fig R.40 A. While the cycle period was unaffected by dorsal horn removal, a significant reduction in burst duration was consistently observed even if intraburst oscillations were still detectable. Average values of cycle period and burst duration before and after dorsal horns ablation are plotted in Fig R.40C.

Rhythmic activity in isolated ventral horns

In 4 preparations exposed to strychnine and bicuculline rhythmic bursting was studied after surgical removal of dorsal horns plus one ventral horn which left an isolated spinal cord quadrant. Such a lesion, performed on a preparation consisting of 4-5 lumbosacral segments, was confirmed histologically on transversal slices of the tissue (see example in Fig R.41 B). Fig R.41 A illustrates recordings from L5 ventral root before and after this procedure. Rhythmic bursts were still present after lesion, their frequency was larger than in control, while their duration decreased. Similar results were observed in the other preparations. The average values for cycle period and burst duration are plotted in fig R.41 C. In all cases burst frequency increased after this lesion with a concomitant decrease in burst duration. Both effects were statistically significant (fig R.41 C). The oscillatory structure of bursts, typical of intact preparations, was always lost after this lesion and bursts were converted from multi-component events (lasting on average about 7 s) to shorter (1-3 s) single discharges (fig R.41 A).

Sensitivity of lesioned preparations to 5-HT and NMDA

In fully hemisected spinal cords and in preparations consisting of isolated ventral horns application of 5-HT (10 μM) or NMDA (5 μM) in the presence of strychnine and bicuculline always resulted in a concomitant increase of burst frequency and decrease of burst duration, similarly to what observed in intact spinal cord (see fig R.13 and related text for NMDA effects, and fig R.14 and related text for 5-HT effects on intact preparations). In the presence of 5-HT, cycle period and burst duration were significantly ($p<0.0001$) decreased by 40±11 % and by 53±15 %, respectively, in hemisected cords (n=3) and by 59±10 % and 37±9 %, respectively, in dorsal horn-ablated preparations (n=3). In the presence of NMDA, cycle period and burst duration were significantly ($p<0.0001$) decreased by 45±16 % and by 56±10 %, respectively, in hemisected cords (n=2) and by 62±9 % and 43±13 %, respectively, in dorsal horn-ablated preparations (n=3). In isolated ventral quadrants (in which bursts were reduced to single-discharge events) cycle period was significantly ($p<0.0001$) decreased by NMDA or 5-HT (by 62±21 % and by 55±18 %, respectively, n=3). In these

preparations, however, burst duration was not significantly affected by these agents. This situation is illustrated in the example of Fig 42 A: in the presence of strychnine and bicuculline alone, regular rhythmic bursts were recorded from L5 ventral root of an isolated ventral horn. These events were less than 2 s in duration and lacked intraburst oscillations which were replaced by a plateau with sustained action potential firing (as indicated by thickening of tracing during burst; right hand side panels of Fig R.42 A). Application of 5 μM NMDA produced a strong increase in burst frequency (310 %) but failed to affect burst duration significantly (see plots of Fig R.42 B). The faster tracings of individual bursts shown in right hand side panels of Fig R.42 A also indicate that there was no alteration in intraburst structure in the presence of NMDA. These results suggest that two different mechanisms could underlie burst triggering and burst structure. The second mechanism was probably lost after surgical isolation of a single ventral quadrant, resulting in brief and unstructured bursts, while the mechanism responsible for burst onset was still present. As a consequence, pharmacological manipulations with 5-HT or NMDA were able to affect burst triggering only.

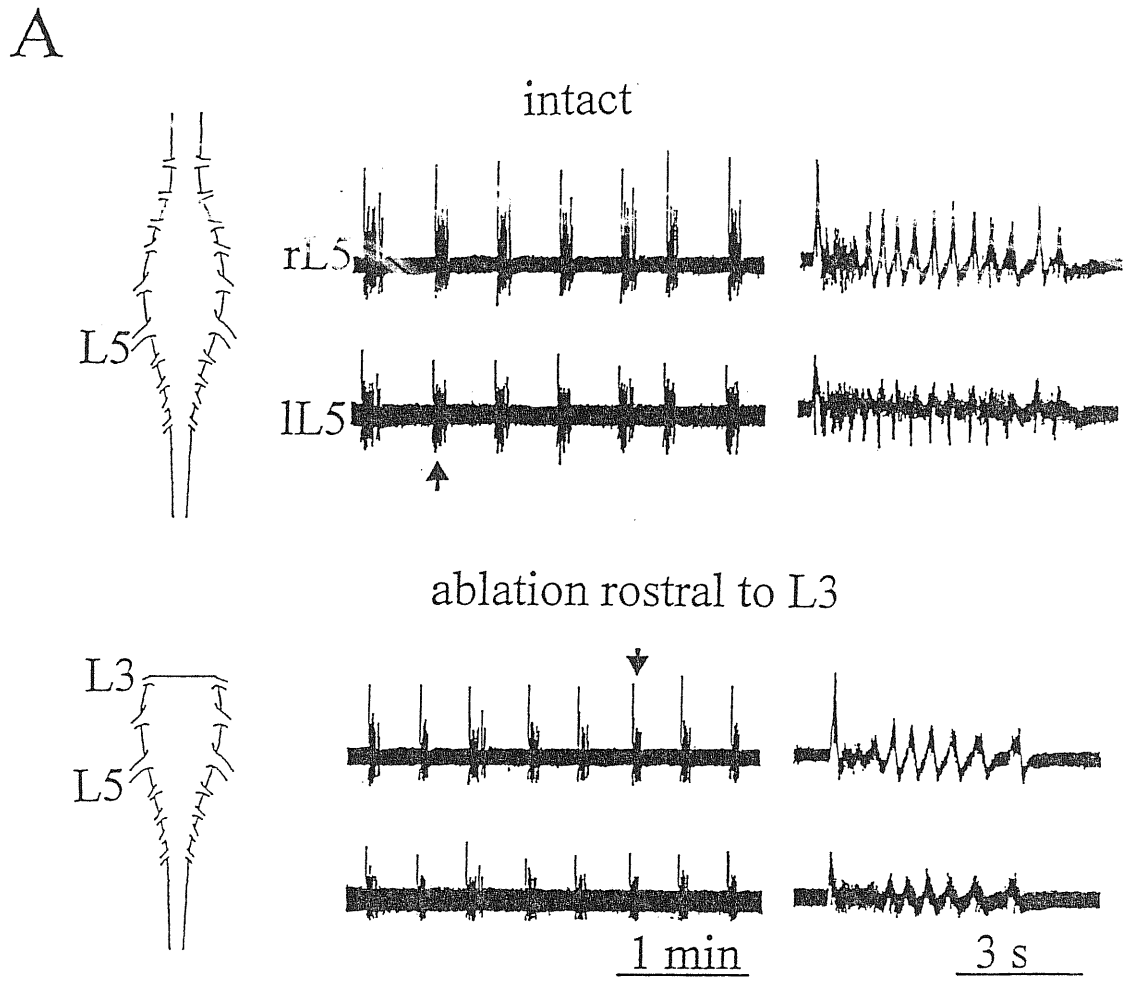

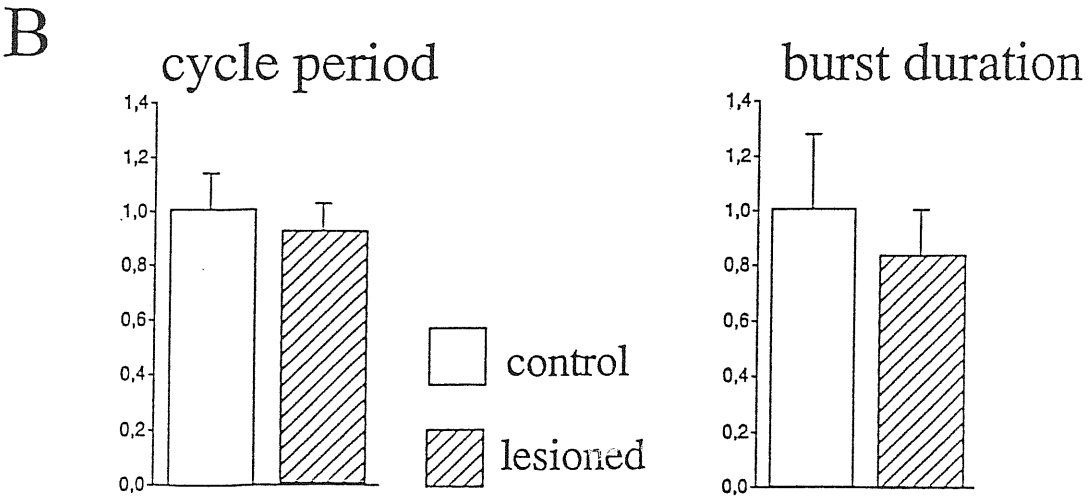

Fig R.37. *Effect of cross sectioning the spinal cord at L3 level on bursting activity.*
A, AC-coupled sample records of bursting induced by strychnine and bicuculline in an isolated preparation (intact) and after removal of the cord region rostral to L3 (see schematic diagram on the left hand side). Righthand traces are faster records of arrowed events. B, histograms of cycle period (left) or burst duration (right) calculated from 6 preparations before (open columns) or after (hatched columns) this type of lesion. In this and subsequent figures (unless otherwise indicated) data are normalized with respect to control values prior to the lesion.

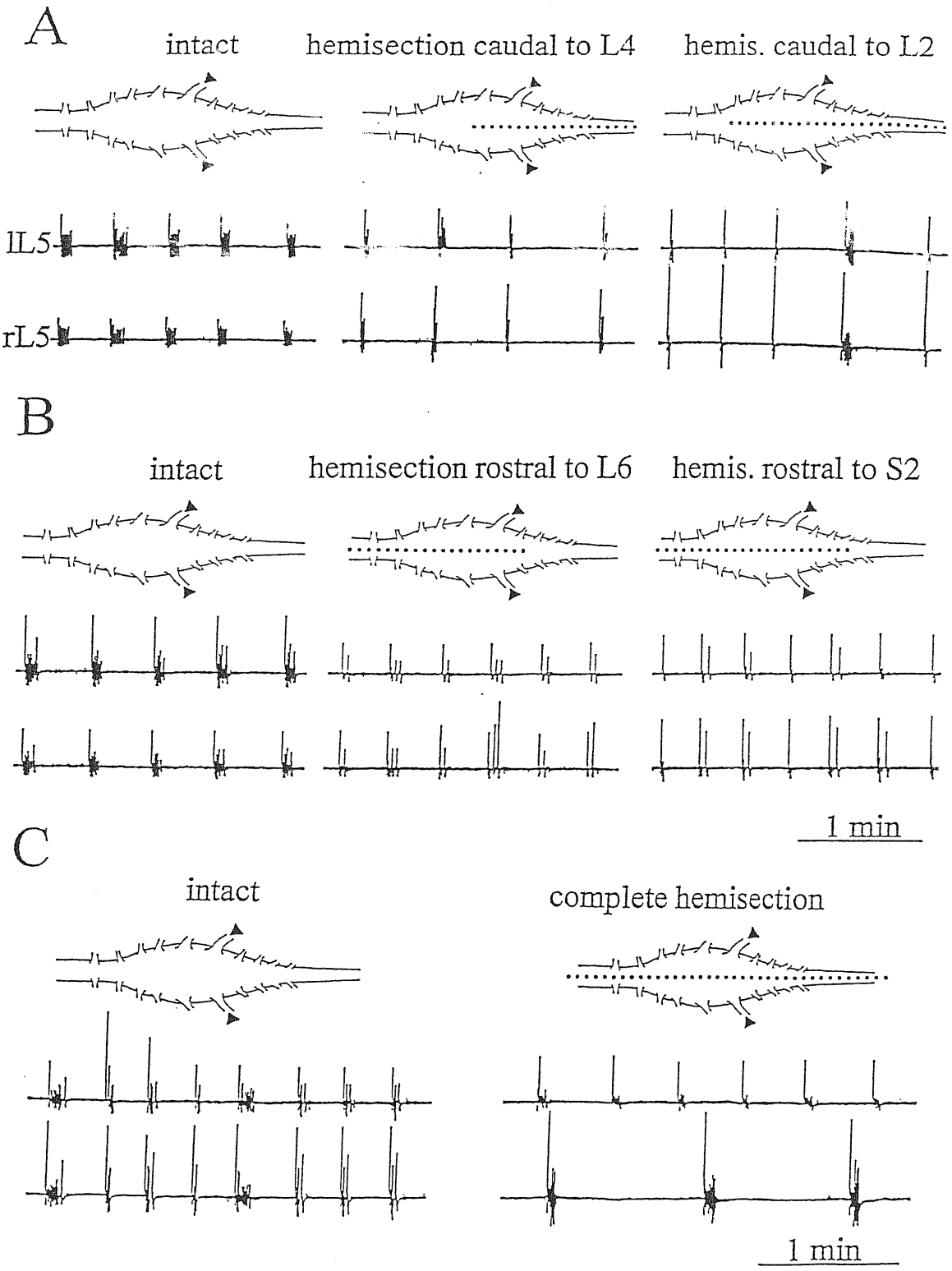

Fig R.38. *Effects of sagittal hemisectioning of the spinal cord on bursting activity.*
A, AC-coupled tracings (from left and right L5 ventral roots marked by filled triangles; 20 Hz lowpass filtering) of bursting activity from the isolated preparation (intact; left) and after two types of lesion bisecting the cord from the caudal end up to L4 (middle) or to L2 (right). Schemes of these lesions are shown above corresponding traces. Synchronized bursting (with shorter burst duration) persists after these lesions. B, similar tracings from a preparation in which the bisectioning was started from the rostral end down to L6 (middle) or S2 (right) as indicated by schemes above traces. Also in this case bilateral synchronicity of L5 bursting is preserved. C, example of bursting activity from a preparation before (left) and after (right) complete hemisectioning of the spinal cord. The latter procedure leads to alteration in the frequency of bursting for each root, loss of synchronicity between the left and right ventral roots, and shorter burst duration.

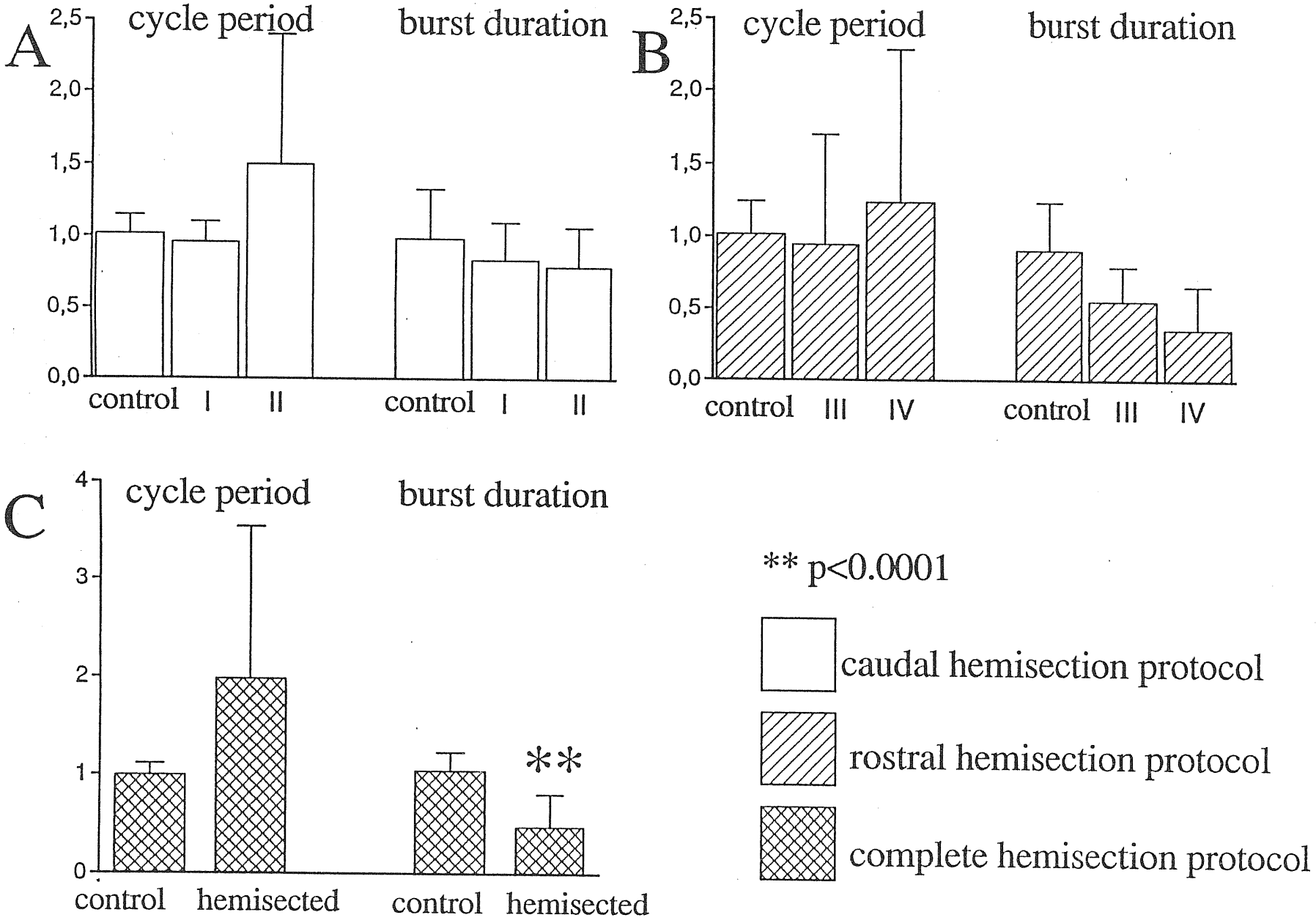

Fig R.39. *Histograms of changes in cycle period and burst duration after partial or complete hemisection of the spinal cord.*
A, B and C represent three lesion protocols, namely hemisectioning from the caudal end (open columns), from the rostral end (hatched columns) or complete hemisection (cross hatched columns). Data are averages from 4 preparations for each protocol. The extent of hemisectioning in A and B is indicated as I, II, III or IV (see results for further details): note that, when hemisectioning splits a considerable length of the cord (type II or IV lesions), there is an increase in the standard deviation of cycle period (reflecting increased variability of burst frequency) even if average values do not differ significantly. Complete hemisectioning (C) largely increases the variability of the cycle periods and significantly (P<0.0001; double asterisks) reduces burst duration.

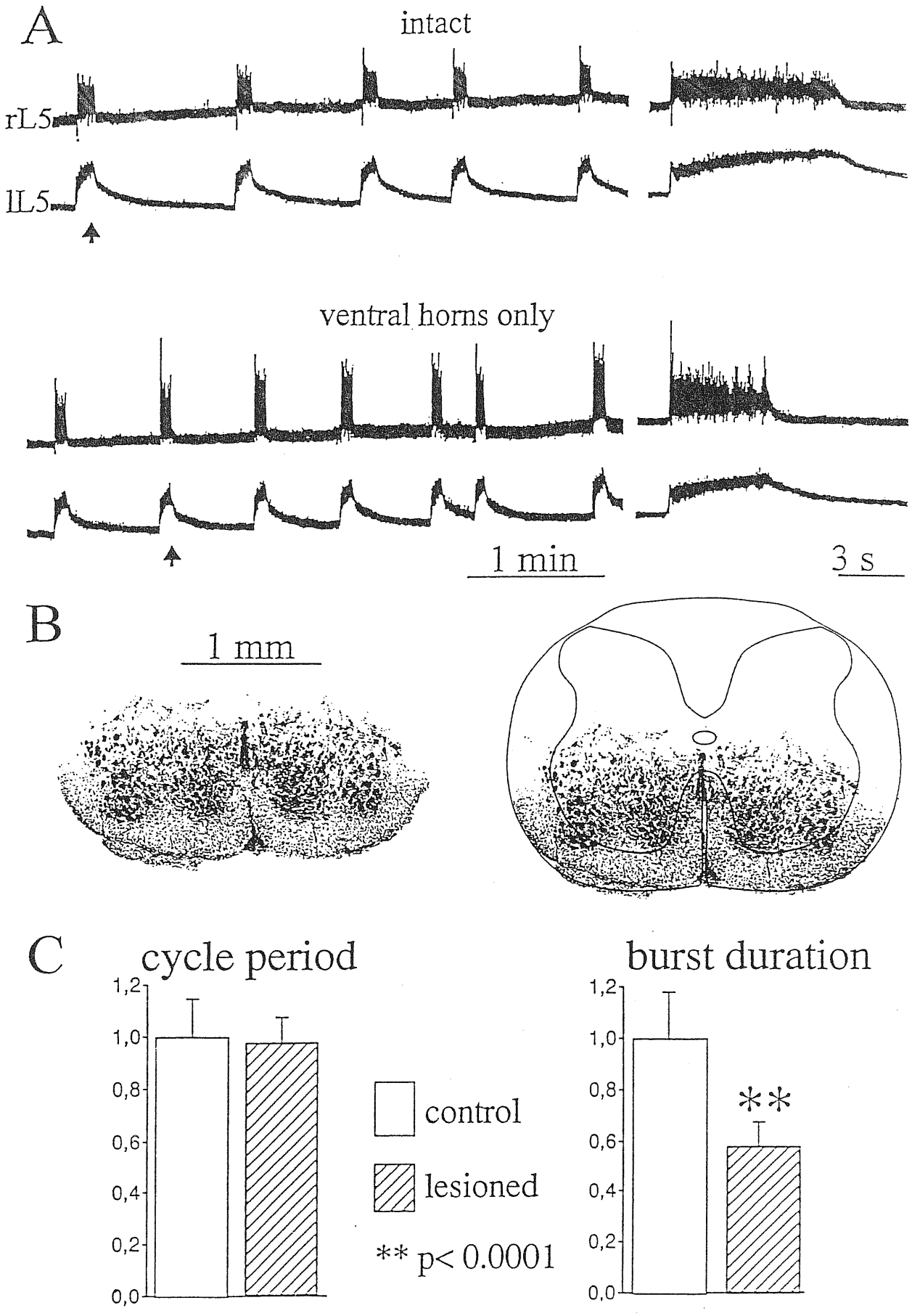

Fig R.40. *Effect of ablation of dorsal horns on bursting activity.*
A, DC-coupled records of bursting activity from L5 ventral roots before (intact; top) and after frontal section (ventral horns only; bottom) which removes dorsal horns and area below midline (see stained section of this preparation in B, either alone or within the schematic contours of the spinal cord). Right hand traces are shown with a faster time base to depict individual burst (arrows) timecourse. Note that this procedure shortens burst duration. C, histograms of normalized cycle periods (left) and burst duration (right) for unlesioned (open columns) or lesioned (hatched colums) preparations (n=4). Burst duration is significantly decreased (P<0.0001; double asterisks).

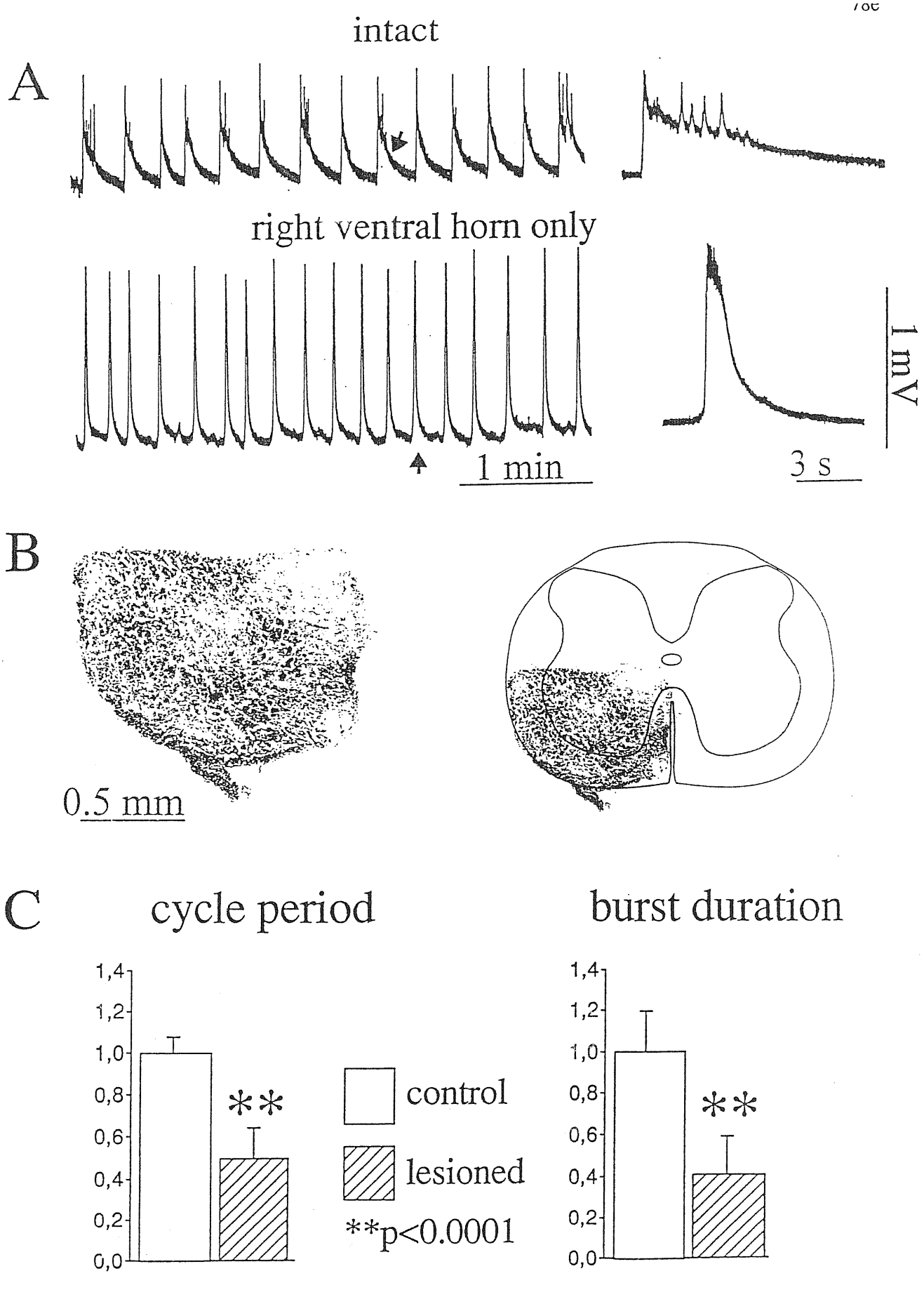

Fig R.41. *Bursting activity in an isolated ventral horn quadrant.*
A, DC-coupled tracings (from right L5 ventral root) in isolated preparation (intact; top) and after surgical isolation (bottom) of a ventral quadrant. The latter is shown in B histologically either alone or within the idealized contours of the spinal cord. Responses indicated by arrows are shown on the right hand side of A on a faster time base. C, histograms of cycle period (left) or burst duration (right) for unlesioned (open columns) or lesioned (hatched columns) preparations (n=4). Double asterisks indicate P<0.0001.

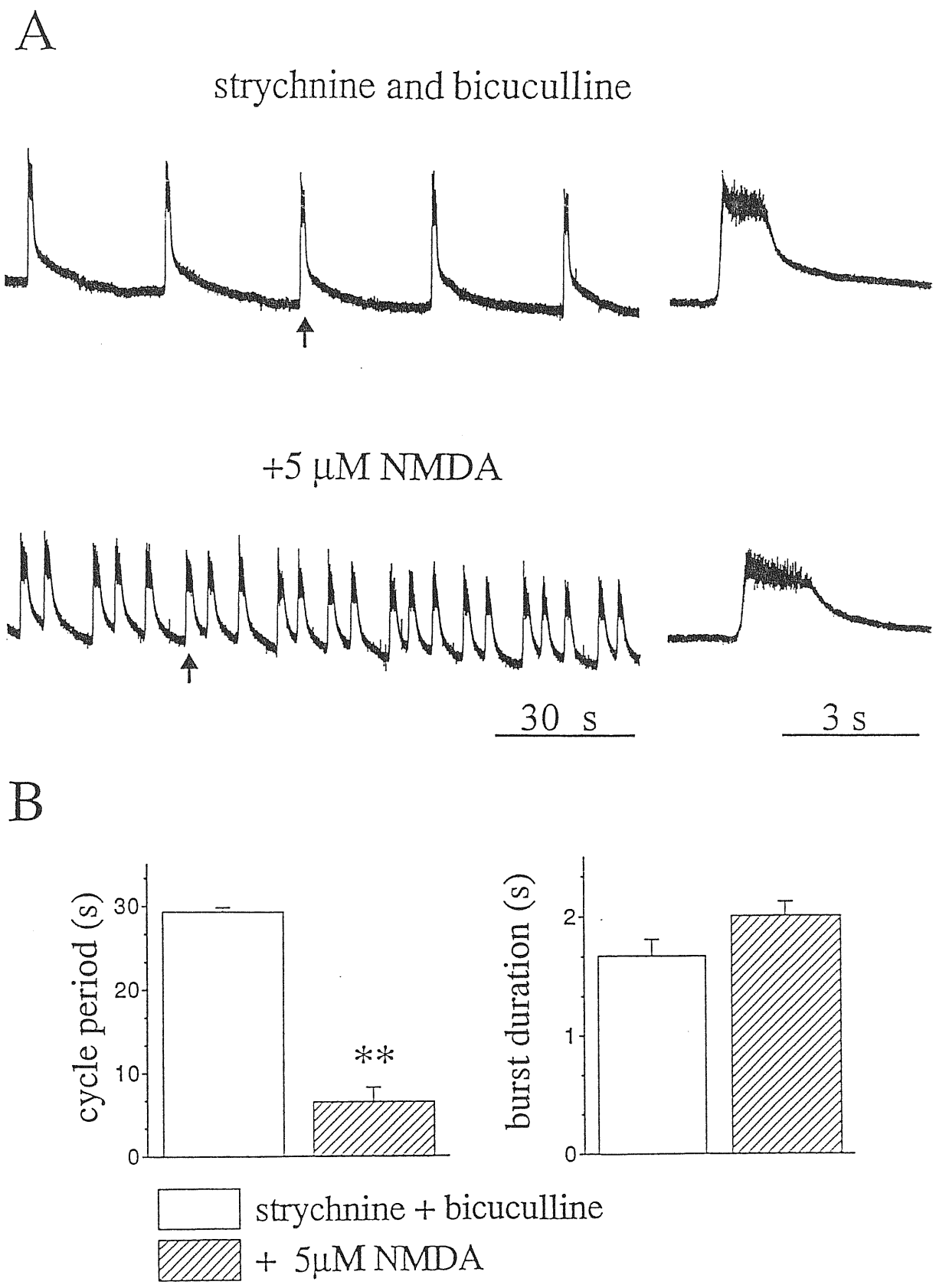

Fig R.42. *Sensitivity of bursting to NMDA in a ventral quadrant preparation.*
A, DC-coupled tracings of bursting activity from left L5 ventral root in a ventral quadrant preparation (for details see Fig R.41 legend) in strychnine and bicuculline solution (top) to which NMDA (5 μM) is then added (bottom). Right hand side traces are shown with faster time base. Note increase in burst frequency in the presence of NMDA.
B, histograms of cycle period (s; left) or burst duration (s; right) in strychnine plus bicuculline solution (open columns) or after addition of NMDA (hatched columns). Data are means of values observed during 5 min periods. Asterisks indicate statistically significant difference ($P<0.0001$).

DISCUSSION

The principal finding of the present study is the novel demonstration that in the neonatal rat spinal cord pharmacological block of synaptic inhibition evokes spontaneous rhythmic bursts in lumbar motoneurons, characterized by a frequency of about 2 events/min and by a burst duration of about 7 s. This activity persisted as long as pharmacological block was present and was expressed synchronously by all motoneurons innervating VRs at lumbar level. Under these conditions, rhythmic bursts were strongly accelerated in a dose-dependent manner by NMDA, 5-HT or by increasing extracellular potassium concentration. Rhythmic activity in the disinhibited spinal cord was entrained on a one-to-one basis within a ten-fold range of frequencies by repetitive activation of DR or VL afferent inputs. Regular rhythmic bursting was still expressed by a reduced preparation comprising only few spinal segments deprived of the dorsal horn tissue. Rhythmogenic ability was maintained also by an isolated ventral quadrant, although in this case burst duration was markedly reduced.

Preliminary electrophysiological tests performed on motoneurons (including pharmacological sensitivity of DR evoked responses to glutamate receptor antagonism, frequency-dependent depression of such responses and antidromic action potentials elicited by electrical activation of VR fibres) were fully consistent with previous reports (Fulton and Walton 1986a; Lev-Tov and Pinco 1992; Pinco and Lev-Tov 1993a) obtained from the neonatal rat spinal cord; these data confirm that the spinal preparations were in normal conditions during the present experiments.

1. Efficacy of block of synaptic inhibition.

Rhythmic bursts were consistently observed after co-application of strychnine and bicuculline, at concentrations (1 and 20 μM, respectively) that are known to block

$GABA_A$ and glycine receptors (DeFeudis and Somoza 1977; Moehler and Okada 1977; Becker et al. 1988; Schneider and Fyffe, 1992). These receptors are selectively permeable to chloride ions and are the main mediators of inhibitory processes in the mammalian spinal cord (Young and Macdonald, 1983; Davidoff and Hackman, 1984). In the rat, these receptors are known to exert an inhibitory action within the spinal networks starting from embryonic day 19. In fact, beyond this developmental stage pharmacological block of either $GABA_A$ or glycine receptors results in strong potentiation of the polysynaptic responses elicited in motoneurons by DR stimulation (Wu et al, 1992). The acquisition of inhibitory properties by glycine and GABA receptors at E19 is thought to coincide with a shift towards negative values of chloride reversal potential of spinal interneurons (Nishimaru et al, 1996);

The expression of a spontaneous regular rhythm in the presence of pharmacological block of inhibitory processes is important from a theoretical point of view because, as discussed in the Introduction section, many models of spinal rhythmogenesis rely upon synaptic inhibition (Grillner et al, 1991; Dale, 1995). Therefore, although findings in other preparations indicated that strychnine and bicuculline at the concentrations used in the present experiments were effective in blocking glycine and $GABA_A$ receptors, it was important to test whether such receptors were actually blocked in the spinal networks under these conditions. Several results indicated that this condition was fulfilled for both receptors during rhythmic bursting. Exogenous application of high doses of either GABA (in the presence of the $GABA_B$ antagonist CGP 52 432) or glycine strongly depressed DR-evoked reflexes in control solution; in the presence of either bicuculline or strychnine, DR-evoked reflexes were strongly increased in amplitude and duration with respect to control, but GABA or glycine, respectively, failed to affect these responses. Furthermore, in the presence of strychnine, bicuculline and CGP 52 432, rhythmic bursts were not affected by exogenous application of glycine or GABA. Thus, in the presence of the respective antagonists, $GABA_A$ or glycine receptors were not activated by high doses of exogenously applied agonists, that were able to strongly depress polysynaptic activity in control solution. These findings were supported by the observation that bath-application of another $GABA_A$ antagonist, picrotoxin (100 μM), together with strychnine, elicited rhythmic bursting identical to that elicited by bicuculline and

strychnine. It is therefore unlikely that bursting could result from non specific effects of bicuculline on molecular targets different from $GABA_A$ receptors, because such effects would not be reproduced by the non competitive $GABA_A$ receptor antagonist picrotoxin. In the case of glycine receptors, selective antagonists different from strychnine are not commonly available; however, rhythmic bursting was unaffected when strychnine concentration was increased from 1 to 10 μM (in the presence of bicuculline). This observation confirms that block of glycine receptors was already complete at 1 μM, and argues against non specific effects of strychnine, that would have been expected to increase when strychnine concentration changed from 1 to 10 μM.

The observation that block of $GABA_B$ receptors *per se* did not produce major changes in rhythmic bursting induced by strychnine and bicuculline demonstrates that activation of this receptor type, that is involved in presynaptic inhibition in the spinal cord (Stuart and Redman, 1992), was not required for such an activity.

Co-application of strychnine and bicuculline was necessary for regular rhythmic bursts to take place. When bicuculline alone was applied to the rat cord it elicited bursting activity highly irregular in onset and duration. Strychnine *per se* did not elicit spontaneous bursting in the majority of preparations, although a burst-like event could be evoked under these conditions by DR stimulation. In the cat in vivo, spontaneous network-driven bursts can be evoked by strychnine (Fuortes and Nelson 1963; Schwindt and Crill 1981). This difference with the neonatal rat spinal cord in vitro might be explained by the lesser functional role of the glycinergic system at 0-10 days (Paton and Richter 1995) although the glycine receptor sensitivity to strychnine is the same as in the adult (Becker et al. 1988). An alternative explanation is that during in vivo experiments the spinal cord might receive synaptic inputs from sensory afferents and/or supraspinal regions; similarly to DR stimulation in vitro, these afferent inputs could trigger bursting in the presence of strychnine. Longer bursting events are observed in the cat in vivo in the presence of penicillin, an agent that can interfere with GABAergic transmission (Schwindt and Crill 1984). As discussed below, the motoneuronal mechanisms involved in this activity appear different from those observed in the rat spinal cord. However, the incomplete understanding of penicillin effects makes a direct comparison with the present findings difficult.

Bursting dependence on strychnine and bicuculline is also different from the one observed in embryonic slices of rat spinal cord, in which rhythmic behaviour can be consistently observed after block of glycine receptors, while a more variable behaviour is elicited by $GABA_A$ antagonism (Streit, 1993).

While strychnine or bicuculline largely increased dorsal root-evoked reflex activity, only strychnine caused the appearance of 4-8 Hz time-locked neuronal oscillations. These oscillations are similar to the ones intrinsic to the spontaneous bursts in strychnine and bicuculline solution and, as they were absent during the irregular bursting elicited by bicuculline alone, presumably imply a particular role for glycinergic inhibition in the decay phase of polysynaptic excitatory responses. Similarly, Cowley and Schmidt (1995) have shown that application of strychnine (but not of bicuculline) during fictive locomotion evokes 4-8 Hz packets of synchronized intraburst discharges. In organotypic slices EPSPs clusters also appear at 5 Hz frequency during strychnine-induced bursts (Streit, 1993). Thus, it seems likely that this kind of oscillatory behaviour specifically arose from block of glycinergic inhibition in the neonatal rat spinal cord.

Experiments were performed to study the effects of low chloride solution on spontaneous activity of motoneurons. This experimental condition is obviously different from pharmacological block of inhibition because in low chloride solution $GABA_A$ and glycine receptors can open in response to their agonists, even though their reversal potential is expected to be strongly shifted towards a more positive value, thus reducing (or suppressing) the inhibitory action of such receptors. Application of low chloride solution elicited spontaneous rhythmic bursts characterized by a slower frequency with respect to those evoked by strychnine and bicuculline. While the reason of such a difference in bursting timecourse is still to be clarified, these data confirm that interference with chloride-mediated inhibition specifically resulted into the expression of a rhythmic behaviour in the neonatal rat spinal cord. Furthermore, when low chloride was applied in the presence of strychnine and bicuculline, it failed to produce any detectable effect on bursting activity, thus showing that chloride permeable synaptic channels were effectively blocked in the presence of the antagonists.

2. Role of motoneurons in bursting activity.

Spontaneous activity of neonatal rat motoneurons was characterized by a highly irregular pattern of low-amplitude depolarizing synaptic potentials, that in some preparations tended to form randomly-appearing clusters of activity. It is possible that part of these depolarizing events were mediated by $GABA_A$ or glycine receptors. In fact, the chloride reversal potential of rat motoneurons (unlike interneurons) has been reported to remain positive to resting membrane potential for up to 10 days of age (Takahashi, 1984, Wu et al, 1992). Furthermore, impalement with a KCl-filled electrode could have caused loading of the intracellular space by chloride, thus shifting the reversal potential toward a more positive value. While a systematic investigation of motoneuron reversal potential was not the aim of the present study, we found that under these impalement conditions exogenous GABA application usually produced depolarizing responses in lumbar motoneurons at normal resting potentials. In contrast to bicuculline application, that converted motoneuronal activity into paroxysmal bursting, strychnine application strongly reduced the number of spontaneous low-amplitude depolarizing synaptic events. Therefore, it is possible that these events were mediated by glycine. An alternative explanation is that, regardless of the receptors mediating such depolarizing events at the level of the motoneuron membrane, strychnine application could have dramatically changed the activity of the network impinging on motoneurons, thus reducing the genesis of low amplitude events at premotoneuronal level and allowing the appearance of larger amplitude events.

In the presence of strychnine and bicuculline the spontaneous activity of motoneurons turned into an extremely regular bursting pattern. Under these conditions bursts were characterized by a stereotypic structure, with large amplitude membrane potential oscillations (with an average frequency of about 4 Hz) developing during each individual burst, that lasted, on average, for about 7 s. An important question is whether active motoneuronal membrane properties played a role in the genesis of these events by giving rise to intrinsic oscillation mechanisms or bistable behaviour, as described for other spinal preparations (Hultborn and Kiehn, 1992; Grillner et al, 1991; see also Introduction section). Alternatively, burst and intraburst oscillations could have been mainly mediated in motoneurons by massive synaptic events. Several lines of evidence strongly argue in

favour of the second possibility. An intrinsic membrane mechanism giving rise to bistable behaviour or plateau potentials is expected to be based upon a dynamic balance between voltage-dependent conductances (Schwindt and Crill, 1984; Hultborn and Kiehn, 1992; McCormick and Pape, 1990); changing the resting potential by several mV under current-clamp conditions would be expected to affect such balance and its timecourse dramatically. Furthermore, voltage-clamping the membrane at different holding potentials should prevent the operation of such an intrinsic mechanism. In contrast to these predictions, large changes in motoneuron membrane potential either under current-clamp or voltage-clamp conditions always failed to affect burst or intraburst oscillation timecourse. In the present experiments, by using intracellularly applied caesium and QX 222 to minimize voltage-activated sodium and potassium currents, it was possible to obtain an apparently adequate voltage-clamp of burst currents which were events typically slow and thus sufficiently resolved by the single electrode voltage-clamp method. Under these conditions the amplitude of burst currents was approximately linearly related to membrane potential and reversed at 0 mV. Similarly, under current-clamp conditions burst amplitude decreased when motoneuron membrane was depolarized. These findings indicate that bursts were generated by large synaptic events resulting in rhythmic activation of excitatory receptors on motoneuron membrane. In this sense the present phenomenon is therefore substantially different from motoneuronal bursting induced in the cat in vivo by penicillin, in which prolonged depolarizations were synaptically triggered but were maintained by activation of motoneuronal voltage-dependent inward conductances (Scwindt and Crill, 1984).

The striking absence of detectable spontaneous activity during the interburst period suggest that, in the presence of strychnine and bicuculline, excitatory interneurons impinging on motoneurons remained at subthreshold level until they were suddenly synchronized to discharge together in the presence of strychnine and bicuculline. The observation that bursts and intraburst oscillations took place synchronously on both sides within lumbar segments is consistent with the notion that all components of these events were network-driven.

Did motoneurons contribute to rhythmogenesis or did they behave just as output elements of the system? The second hypothesis is strongly favoured by the findings that

repetitive VR stimulations delivered during interburst quiescent intervals consistently elicited antidromic action potentials in the impaled motoneuron (and presumably in a large population of motoneurons) but, in sharp contrast to DR stimulation, always failed to evoke a burst or to affect bursting timecourse. Rhythmic activity therefore appears to be produced by a premotoneuronal network, whose activity was strongly synchronized throughout the lumbar cord and whose synaptic drive impinged on motoneurons giving rise to rhythmic bursts.

Since under voltage-clamp conditions burst currents were inward at negative holding potentials, reversed polarity at positive potentials and disappeared near 0 mV, it seems likely that they were mainly generated by synapses electrotonically near the recording electrode and displaying homogeneous sensitivity to the imposed level of membrane potential. In particular, the burst reversal potential was similar to the one of excitatory synaptic currents mediated by glutamate (Mayer and Westbrook 1987). The linear dependence of burst amplitude on membrane potential suggests that these events were not mainly mediated by NMDA receptors on the motoneuron membrane, since in the presence of extracellular magnesium NMDA receptor-mediated responses are expected to show a strong non-linear voltage dependence (Mayer and Westbrook 1987). Since NMDA receptor antagonists had important effects on bursting activity (see following subheading), it is feasible that the role of these receptors was mainly played at the level of the premotoneuronal network. At motoneuronal level, non NMDA glutamate receptors (that are not usually voltage dependent; Mayer and Westbrook 1987) could therefore have played a major role. The non NMDA receptors antagonist CNQX blocked bursting activity in the disinhibited spinal cord. This finding, however, does not allow to discern whether the action of CNQX took place at the level of the premotoneuronal network, at the level of motoneuron membrane or both. The observation that in the presence of CNQX rhythmic bursts could be restored by 5-HT, although with reduced amplitude, suggests that motoneuronal sensitivity to the rhythmic synaptic drive was not fully abolished by CNQX, and that in the absence of 5-HT this agent actually blocked the operation of the premotoneuronal rhythmic network and not only its action on motoneurons. At the level of the motoneuron membrane, identification of other

excitatory receptor mechanisms directly involving in mediating rhythmic synaptic drive will require local application of selective antagonists.

As described in the Methods section, bursts were usually followed by a long afterdepolarization, that often persisted up to the onset of the following burst. The origin of this event was not clarified in the present study. Nevertheless, since an inward current corresponding to such an event was not observed under voltage-clamp conditions at any holding potential, it appears that such a phenomenon was not generated by the same synapses giving rise to bursting currents.

3. Role of glutamate receptors in the rhythmogenic network.

Rhythmic ability in the presence of glutamate receptor antagonists

Since in the presence of tetrodotoxin or of the calcium channel blocker cadmium rhythmic bursting was suppressed it is clear that action potential mediated synaptic transmission was necessary for this activity. Glutamatergic synaptic transmission was found to play a major role in the disinhibited spinal cord. As discussed above, non NMDA receptors were necessary for the network operation in the presence of strychnine and bicuculline alone, although rhythmic bursting resumed in the presence of CNQX with low doses of 5-HT, an agent known to increase excitability of spinal neurons (Takahashi and Berger, 1990). Antagonists of NMDA receptors, in turn, slowed down but did not suppress rhythmic activity in the majority of preparations. Furthermore, even in those preparations in which such an antagonism eliminated bursting, rhythmic activity resumed in the presence of cyclothiazide, an agent that was shown to be able to boost non NMDA glutamatergic synaptic transmission in the neonatal rat spinal cord. Preliminary experiments have also shown that 5-HT (5-20 μM) can counteract the effects of NMDA receptor antagonists on disinhibited rhythmic activity (Bracci, Ballerini and Nistri, unpublished data). One possible explanation of these data is that, in the presence of 5-HT or cyclothiazide, glutamate release strongly increased within the rhythmogenic network and that such an increase could have partially surmonted the blocking action of NMDA or non NMDA antagonists. Nevertheless, this possibility is unlikely since such antagonists were used at concentrations known to fully block synaptic responses

mediated by respective receptors in the spinal cord (Pinco and Lev-Tov, 1993a); furthermore, bath application of AMPA (1 μM) or NMDA (10 μM), that produce very strong firing activity in motoneurons in control solution, elicit no effect in the presence of non NMDA or NMDA antagonists, respectively (Beato et al, 1997). Therefore, a more probable explanation is that during block of non NMDA or NMDA receptors the network operation could still be sustained by residual excitatory processes, provided that the neuronal excitability was increased. Therefore, these data indicate that both NMDA and non NMDA receptors supported the operation of the rhythmic network, and that such an operation could persist, under conditions of increased excitability, as long as at least one of the two receptor classes was functionally intact. In fact, in the simultaneous presence of both NMDA and non NMDA antagonists, rhythmic activity was never observed despite application of large doses of 5-HT; these data also suggest that other excitatory synaptic processes not mediated by glutamate were unable to sustain rhythmic activity regardless of the level of neuronal excitability. When glutamate-mediated excitatory synaptic transmission was unperturbed, AMPA receptors appear to be the predominant class to sustain rhythmic activity.

Interestingly, in another study similar results were found for fictive locomotion induced by 5-HT in the same preparation. In this case, locomotor-like activity could still be expressed in the presence of either NMDA or non NMDA receptor antagonists, provided that the 5-HT dose was increased with respect to control conditions (Beato et al, 1997).

The role of glutamate receptors in the disinhibited spinal cord is somewhat different from that played in the hippocampal bursting induced by block of $GABA_A$ receptors (glycine is not a major inhibitory transmitter in hippocampus). In fact, in this preparation although bursting requires AMPA receptors, NMDA receptor antagonism only impairs the late phase of bursts (Brady and Swann, 1986; Traub et al, 1993).

Effects of cyclothiazide on motoneuronal activity

The effects of cyclothiazide, an agent known to attenuate AMPA receptor desensitization (Partin et al, 1993; Patneau et al., 1993; Yamada and Tang, 1993) and to favour glutamate release (Diamond and Craig, 1995; Isaacson and Walmsley, 1996; Barnes-Davies and Forsythe 1995), were investigated in the rat spinal cord in order to

evaluate the effects of boosting AMPA receptor responses on motoneuron activity before and after block of synaptic inhibition. Potentiation by cyclothiazide has been reported to be limited to non NMDA glutamate receptors, since a concomitant postsynaptic depression of NMDA receptors would compensate facilitatory presynaptic effects (Diamond and Craig, 1995). In the neonatal rat spinal cord, cyclothiazide was found to increase motoneuronal responses to AMPA while NMDA responses were unaffected by this agent, either in the presence or in the absence of TTX. These data suggest that under the present conditions motoneuronal NMDA receptors were not strongly depressed by cyclothiazide. On the other hand, the persistence of the cyclothiazide-induced potentiation of AMPA effects in TTX solution suggests that at least in part cyclothiazide effect was taking place at the level of the motoneuron membrane AMPA receptors. On motoneurons, cyclothiazide also largely enhanced dorsal root-evoked EPSPs in amplitude and area. A gradual build-up of excitation developed leading to intense, network-driven bursting activity. These data are compatible with the proposed mechanism of action of cyclothiazide on glutamate release and on AMPA receptor desensitization (a process that may develop fast enough to attenuate the peak amplitude of glutamatergic responses; Colquhoun et al, 1992; Trussel et al, 1993). The decay time constant of evoked synaptic currents has been found to be increased by cyclothiazide at certain synapses (Trussel et al, 1993; Rammes et al, 1994). In the present experiments cyclothiazide increased both the amplitude and the decay time constant of spontaneous EPSPs in those preparations in which individual synaptic events could be distinguished (and their decay could be fitted exponentially). These data might suggest that desensitization played an important role in the decay of glutamatergic EPSPs on motoneurons. Nevertheless, the decay time constant of DR evoked EPSPs was not usually changed by cyclothiazide. Although in the present experiments interneuronal activity was strongly depressed by mephenesin, DR stimulation probably activated mono and oligosynaptic pathways. In fact, due to increased spontaneous synaptic activity in the presence of cyclothiazide, a relatively strong intensity stimulation was used in order to obtain evoked responses clearly distinguishable from baseline noise. Under these conditions, even if desensitization was controlling the decay of glutamatergic EPSPs in the spinal cord, the duration of DR evoked EPSPs might have

been determined by activation of complex synaptic pathways including inhibitory interneurons, rather than by simple decay of monosynaptic glutamatergic events. This view is supported by the observation that, despite the presence of mephenesin, in the presence of strychnine and bicucuilline DR evoked responses were converted into long burst-like events, therefore preventing an analysis in terms of amplitude and decay time constant.

In the presence of cyclothiazide the excitation of any spinal neuron receiving glutamatergic inputs would be expected to be boosted, leading to a modification in the whole network activity. It is not obvious *a priori* if this should produce generalized bursting activity because inhibitory interneurons also receive glutamatergic inputs (Headley and Grillner, 1990) and might thus balance excessive excitation. In practice, after application of cyclothiazide virtually all motoneurons displayed an increase in the frequency of depolarizing spontaneous events. As previously mentioned, an important effect of cyclothiazide was to cause spontaneous bursting of motoneurons. The poor dependence of the burst duration and frequency on membrane potential indicates that they were likely driven by a premotoneuronal network; since burst amplitude was also poorly dependent on membrane potential it is likely that bursts were characterized by intermixed activation of excitatory and inhibitory inputs to the motoneuron membrane. Unlike NMDA or 5-HT induced patterns (Cazalets et al, 1992), cyclothiazide induced bursting was irregular in onset and duration, suggesting that regular rhythmogenesis cannot simply arise from a potentiation of non NMDA glutamate receptor responses throughout the spinal networks. In the disinhibited spinal cord cyclothiazide accelerated bursting activity while markedly decreasing the regularity of cycle period and burst duration. Under these conditions, burst structure was essentially preserved. These data suggest that AMPA receptor desensitization was not required for generating bursts and intraburst oscillations. On the other hand, control of regular rhythmicity of the bursting pattern by spinal networks appear to require normal operation of glutamatergic transmission, since it was impaired under conditions in which AMPA receptor-mediated responses were shown to be increased and glutamate release is also expected to be favoured (Diamond and Craig, 1995; Barnes-Davies and Forsythe 1995; Isaacson and Walmsley, 1996). Interestingly, as mentioned above, in the presence of cyclothiazide

NMDA receptor antagonists failed to affect bursting frequency or duration. Since in the absence of cyclothiazide NMDA receptors responses are characterized by kinetics much slower than non NMDA receptors (Jonas and Spruston, 1994), and since the two receptor types are thought to be colocalized in spinal synapses (Kullmann, 1994), it is possible that in the presence of cyclothiazide prolongation of AMPA receptor-mediated responses could have compensated shortening of glutamatergic responses previously induced by NMDA receptor antagonists.

4. Mechanisms underlying rhythmogenesis.

As discussed in the Introduction section, two cellular mechanisms that have been proposed to underlie spinal pattern generation are based on reciprocal inhibition and/or intrinsic pacemaker neurons (Grillner et al, 1991, 1995; Hochman et al, 1994a; Kiehn et al 1996). It is clear that reciprocal inhibition, that is expected to be mediated by glycine and/or GABA receptors (Grillner et al, 1991; Cowley and Schmidt, 1995), cannot account for rhythmogenesis in the disinhibited spinal cord. As far as pacemaker neurons are concerned, interneurons and motoneurons provided with intrinsic oscillatory properties have been described in the rat spinal cord (Hochman et al, 1994a, 1994b). The ability of these cells to produce a rhythmic behaviour was found to be critically dependent on the activation of NMDA receptors on their membrane by exogenously applied NMDA. Since in the present conditions rhythmic activity could always persist in the presence of NMDA receptor antagonists, provided non-NMDA receptor responses were potentiated by cyclothiazide, it is evident that NMDA-dependent pacemaker neurons were not necessary for this activity. These data prompted the investigation of alternative mechanisms potentially involved in rhythm generation in the absence of synaptic inhibition. Several membrane mechanisms potentially involved in rhythmic behaviour were tested in the presence of strychnine and bicuculline.

Role of apamin-sensitive conductances

In the lamprey spinal cord apamin-sensitive potassium conductances were reported to be activated by intracellular calcium entry and thus to contribute to neuron repolarization

and termination of intrinsic oscillations induced by NMDA (El Manira et al 1994), although the function of these conductances in controlling fictive swimming remains controversial (Meer and Buchanan 1992). Rat lumbar motoneurons also possess a sustained calcium-dependent potassium current (Takahashi 1990a). Nevertheless, in the disinhibited spinal cord apamin sensitive conductances did not play a role similar to that reported for lamprey. In fact, apamin reduced burst duration, instead of increasing it as described in the lamprey, and increased burst frequency, suggesting that such conductances were not the main burst-terminating factor. Carbachol, which is supposed to block the slow calcium-dependent potassium current (Schwindt et al. 1988; Sah 1996), induced analogous effects. The origin of apamin and carbachol effects is presently unclear. As discussed in the following subheading, many agents known to depolarize spinal neurons were found to accelerate bursting in the disinhibited spinal cord. It is possible to hypothesize that the increase in burst frequency observed in the presence of apamin or carbachol could have been due to a tonic depolarization of rhythmogenic interneurons induced by suppression of calcium-activated potassium conductances. This issue remains however speculative since apamin failed to depolarize motoneurons and a direct test of apamin effect on interneurons was not possible in the present experimental conditions.

Role of caesium-sensitive conductances

An inward conductance activated by hyperpolarization, characterized by slow kinetics of activation and de-activation and suppressed by extracellular caesium has been described in several CNS cells including rat motoneurons, where it contributes to resting potential (Takahashi, 1990b). In the disinhibited rat spinal cord caesium application did not suppress bursting or intraburst oscillations but produced an increase in burst duration without significantly affecting burst frequency. These results suggest that burst and intraburst oscillations were not generated by a mechanism similar to that described in thalamic neurons, where intrinsic oscillations take place due to a dynamic interplay between caesium-sensitive, inward rectifier conductances and low threshold calcium conductances (McCormick and Pape, 1990). Nevertheless, caesium-sensitive currents appear to be involved in burst termination since burst duration was markedly increased

by caesium. A possible mechanism for this kind of action is discussed below. Since burst termination was delayed but not suppressed by caesium, it is also clear that other factors in addition to caesium-sensitive currents were involved in burst termination. Consistently with previous observation (Takahashi, 1990b), intracellular recordings revealed that motoneurons were hyperpolarized in the presence of caesium; this finding shows that also in the presence of strychnine and bicuculline caesium sensitive inward conductances were significantly activated at resting potential.

Role of the electrogenic sodium pump

Several findings obtained in other CNS preparations stimulated testing the role of the electrogenic sodium pump in the disinhibited spinal cord. In hippocampal neurons such a pump can produce a large amplitude hyperpolarization following a glutamate-induced depolarization similar in amplitude and duration to the present spinal bursts (Thompson and Prince, 1986). Furthermore, the electrogenic sodium pump has been recently shown to play an important role in the repolarizing phase of intrinsic oscillations induced by NMDA in midbrain dopamine neurons (Johnson et al, 1992; Li et al 1996) and a strong activation of the electrogenic sodium pump resulting in a hyperpolarizing current can also take place during seizures in cortical neurons (Ayala et al, 1970). These data suggested that such a pump could also have played a role in the present rhythmic phenomenon. In fact it was possible to hypothesize that, like in the case of hippocampal neurons depolarized by glutamate, a burst was accompanied in rhythmogenic interneurons by a massive influx of sodium and that such an influx could have markedly increased the pumping rate (Thomas, 1972; Thompson and Prince, 1986). Such an electrogenic process in turn, would be expected to affect the network behaviour. In the disinhibited spinal cord, where rhythmicity was preserved in the presence of apamin or caesium, pharmacological block of the electrogenic sodium pump by ouabain, strophantidin or potassium-free solution always produced a profound disruption of the rhythmic pattern, so that burst duration and interburst intervals became extremely irregular and unpredictable. While ouabain effects were irreversible (Canessa et al 1992), during strophanthidin wash-out bursting activity slowly returned to a regular rhythm. potassium-free experiments gave similar results although with much slower onset (>40

min), presumably due to the buffering ability of spinal cells that can long counteract depletion of extracellular potassium (Czeh et al, 1988). A comparably slower action of the potassium-free solutions *vs* ouabain in blocking a delayed hyperpolarization of spinal neurons mediated by the sodium pump activity has also been observed by Davidoff and Hackman (1980). In the present study, after 1 h exposure to potassium-free solution, bursts were converted into single discharges of variable amplitude, lacking any intraburst structure and appearing at irregular intervals. It should be noted that, even if ouabain eventually led to loss of motoneuron excitability, disruption of rhythmic bursting was observed long before such a loss took place and under conditions in which DR stimulation could still elicit bursting events of variable duration. These data suggest that when the electrogenic sodium pump was pharmacologically blocked the network still possessed the ability to generate large-amplitude bursting events but lacked the ability to control duration and periodicity of such events. Therefore it appears that the electrogenic sodium pump played a major role in pacing rhythmic activity. The possibility that loss of rhythm regularity could be due to non specific effects on molecular targets different from the electrogenic sodium pump is unlikely since similar effects were obtained separately by blocking the electrogenic pump by three pharmacological tools acting through different molecular mechanisms on the same substrate (Horisberger et al. 1991; Glynn, 1993).

While it is reasonable to assume that, as observed in other preparations, the electrogenic sodium pump in the disinhibited spinal cord contributed to repolarize spinal interneurons after their ionic gradients had been dissipated, a more specific interpretation of the data so far described in terms of cellular mechanisms will require some assumptions regarding the rhythmogenic factors in the disinhibited spinal cord. In fact, any tentative explanation of the experimental findings is complicated by the observation that, as discussed above, rhythmic activity appeared to be produced by a premotoneuronal network, while experimental access was limited to motoneurons.

A tentative model for rhythmogenesis in the absence of synaptic inhibition.

The observation that rhythmic behaviour observed in the neonatal rat spinal cord after pharmacological block of synaptic inhibition cannot be easily explained by reciprocal

inhibition or intrinsic pacemaker neurons, and the prominent role of the electrogenic sodium pump stimulated the formulation of a tentative model that could account in qualitative terms for some of the experimental findings. In this framework it will be hypothesised here that a burst was a synchronous event in the disinhibited spinal cord. This hypothesis implies that all elements of the premotoneuronal rhythmogenic network underwent a burst simultaneously, performing all together rhythmic depolarizations similar in timecourse to that observed in motoneurons. This view is supported by the strong degree of synchrony of bursting activity over several lumbar segments. It is therefore unlikely that bursting could result from a circuit in which excitation travelled along certain neuronal pathways, thus activating motoneurons "en passant", a hypothesis that is also hardly compatible with long quiescent intervals observed (Streit, 1996). Further support to the assumption that bursts took place synchronously in the rhythmogenic network arises from comparison with data obtained in the hippocampal slice, where block of synaptic inhibition by application of the $GABA_A$ antagonist picrotoxin elicits rhythmic bursts that are similar to those described in the present study because they comprise a first depolarizing shift followed by several intraburst oscillations (that are termed "secondary bursts"), as shown in the example of fig I.8 of the Introduction section. In hippocampal slices bursts and intraburst oscillations have been found to take place synchronously in pyramidal neurons even though separated by considerable distances (Traub et al, 1993; Taylor et al, 1995).

For hippocampal bursting it has been proposed that in the absence of synaptic inhibition, rapid spread of excitation is generated by recurrent excitatory connections of CA3 pyramidal neurons, so that a burst can be initiated by firing activity of a few cells, or even of a single neuron (Miles and Wong, 1983; Traub et al, 1993). While the synaptic organization of the interneuronal networks in the neonatal rat spinal cord is still unknown, it is tempting to speculate that a similar recurrent excitatory connectivity could have underlain spinal bursting as well. Under this assumption it is feasible that synchronous excitation could be induced by an autoregenerative, positive-feedback process in which firing activity of mutually interconnected interneurons produces synaptic depolarization in the same population of cells; such a depolarization, in turn, will increase neuronal excitability thus inducing further firing activity and so on. This kind of

positive feedback is proposed here to underlie the initial depolarization that characterize burst onset and the depolarizing phases of the following intraburst oscillations. In this perspective, an important question concerns the factors determining termination of mutual excitation process and consequent repolarization of network elements. For hippocampal bursting it has been proposed that during mutual excitation of pyramidal neurons an increase in intracellular calcium may activate an outward potassium current, that in turn may gradually decrease neuron excitability thus terminating the depolarizing process (Traub et al, 1993). In the present experiments apamin or carbachol application failed to prolong burst or intraburst oscillations. It cannot be excluded, however, that other potassium conductances activated by calcium and insensitive to these agents (Sah, 1996) could have played a role in terminating mutual excitation. Another possible determinant of the repolarization process is voltage-dependent inactivation of fast sodium conductances (Hille 1994). In fact, it is likely that depolarization of interneurons should have gradually inactivated their sodium channels, thus reducing the amplitude of action potentials and eventually preventing their generation. This phenomenon could have contributed to mutual excitation termination; consequent shutting off of excitatory synaptic conductances would have determined neuron repolarization. During the repolarizing phase sodium channels inactivation is expected to be gradually removed, thus allowing neurons to resume their firing ability. If a sufficient number of cells started firing at a certain time during the repolarization phase, mutual excitation would be triggered again and a new intraburst oscillation would begin. While a direct verification of the role of sodium channels inactivation will require recordings from rhythmogenic interneurons, this view is supported by the observation that in motoneurons the depolarizing phase of the intraburst oscillations was characterized by a series of few action potentials whose amplitude gradually decreased when depolarization increased, while firing activity was usually absent during the repolarizing phase, as shown in fig D.1. Regardless of the factors responsible for mutual excitation termination and repolarization, it could be argued that this kind of process should give rise to persistent oscillations at constant frequency. Nevertheless, within each burst oscillations decreased in frequency and eventually terminated. This observation suggests that during a burst an additional process decreasing interneuron excitability could have gradually developed. A

possible candidate for such a process would be an outward current gradually activated during each burst. It is proposed here that such a current could have been generated by the electrogenic sodium pump, that produces an outward current by extruding approximately three Na^+ for every two K^+ taken in (Post et al, 1967) and is highly sensitive to internal sodium, with pumping rate approximately proportional to intracellular sodium concentration (Thomas, 1972). As mentioned above, in CA1 pyramidal neurons focal glutamate application, giving rise to depolarizing events comparable in amplitude and duration to spinal bursts, was followed by electrogenic sodium pump-induced afterhyperpolarizations > 10 mV that persisted for tenths of s (Thompson and Prince, 1986). In the disinhibited spinal cord bursts were mainly mediated by glutamatergic inputs; it is therefore reasonable that during a burst a strong sodium influx took place in spinal neurons through cation-permeable glutamate receptors and through voltage-activated sodium-permeable channels. Like in hippocampal neurons, this influx could have gradually activated the electrogenic sodium pump in spinal interneurons, thus producing an outward current responsible for decrease in oscillation frequency and eventually for burst termination. In this case one would expect that bursts should have been followed by an afterhyperpolarization in the elements of the rhythmogenic network. In motoneurons a similar afterhyperpolarization was not observed. Nevertheless, it must be considered that spinal interneurons have a soma diameter much smaller than motoneurons (Lev-Tov and O'Donovan 1995) and therefore a larger surface-to-volume ratio. Thus, assuming the same membrane density of glutamate receptors with the same degree of activation during a burst, interneurons would have undergone a much larger increase in sodium concentration than motoneurons during such an event. This increase in sodium concentration, in turn, could have produced an increase in pumping rate, that would have persisted until the normal sodium concentration was reached. The resulting outward current could have underlain burst termination and maintenance of long quiescent periods between bursts. This view is supported by the fact that the duration of electrogenic sodium pump-induced afterhyperpolarization in hippocampal neurons is comparable to quiescent intervals in the disinhibited spinal cord. As suggested by Thompson and Prince (1986), the afterhyperpolarization mediated by the electrogenic sodium pump can be considered as a

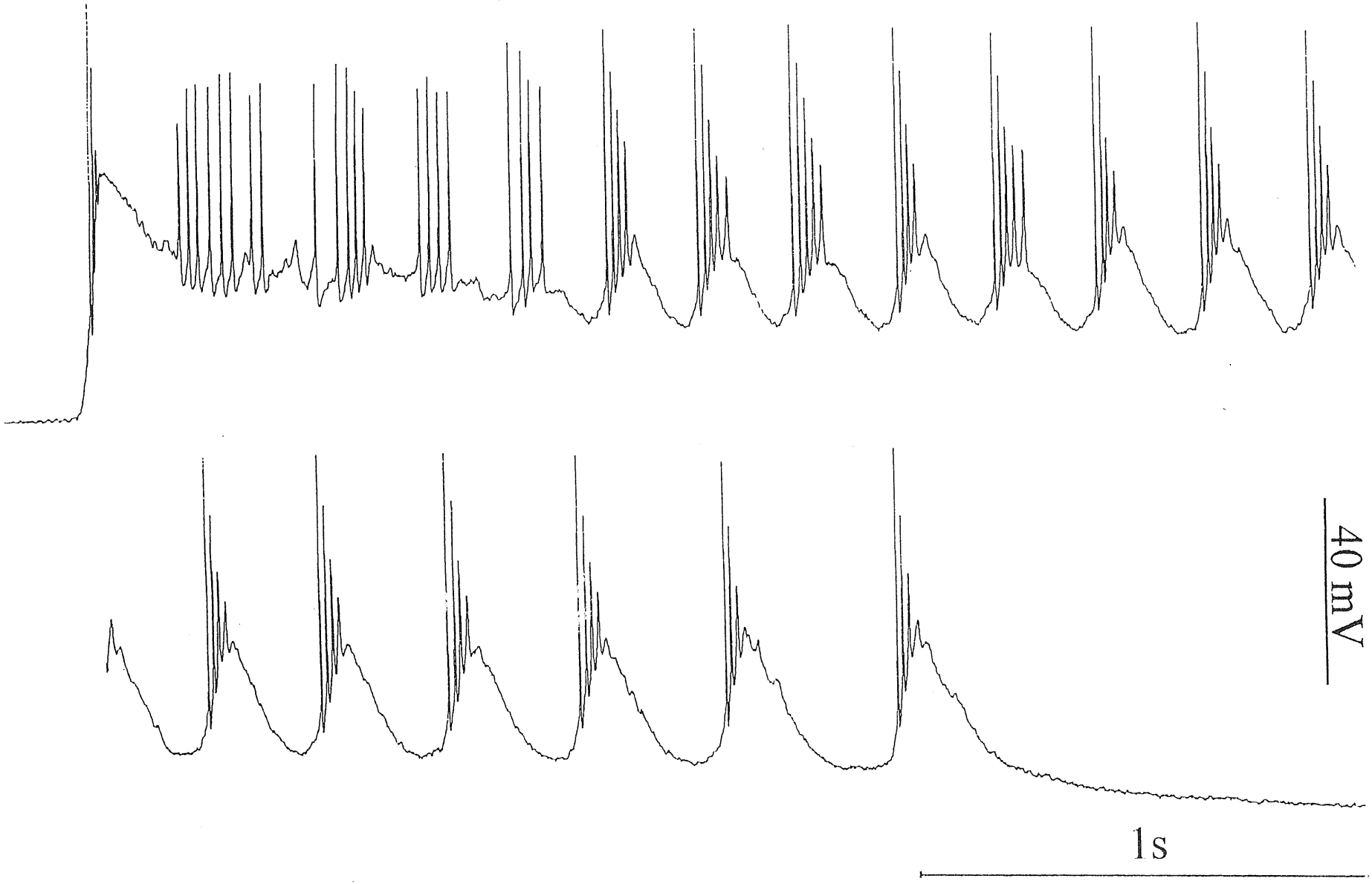

Fig D.1. *Generation of action potentials in a motoneuron during a burst.* A typical burst recorded intracellularly in a lumbar motoneuron under current-clamp conditions (resting potential was -72 mV) is presented at a fast timescale at which individual action potential amplitude can be evaluated. Note that firing activity is present during the depolarizing phase of each intraburst oscillation and that spike amplitude strongly decreases when such events are generated at more depolarized potential levels.

self-regulating process since it will spontaneously terminate when sodium concentration is restored. In the disinhibited spinal cord recovery from such an afterhyperpolarization could have allowed some element of the rhythmogenic network to resume their firing ability thus triggering a new burst.

Another factor contributing to shift the net membrane current in outward direction could have been slow de-activation of caesium-sensitive inward rectifying conductances. In fact, caesium application strongly prolonged burst duration. Caesium-sensitive, hyperpolarization-activated cationic conductances that are open at resting membrane potential in motoneurons (Takahashi, 1990b), could have become slowly de-activated during a burst, due to persistent depolarization. A similar process is known to underlie repolarization of intrinsic oscillations in thalamic neurons, in which the depolarizing phase is due to activation of low-threshold calcium conductances (McCormick and Pape, 1990). Similarly, in the disinhibited spinal cord, de-activation of inward rectifying conductances could have produced a net hyperpolarizing influence contributing, together with electrogenic sodium pump activity, to burst termination.

Another factor potentially involved in intraburst oscillation frequency decrease and in burst termination is synaptic depression, as proposed by Streit (1993) for rat embryo organotypic slices and by Chub and O'Donovan (1996) for the chick embryo spinal cord. In the neonatal rat spinal cord synapses impinging on motoneurons from DR afferents or interneurons are well known to undergo a profound frequency-dependent synaptic depression, that can persist for intervals as long as 60 s (Lev-Tov and Pinco, 1992; Streit et al. 1992). In organotypic slices in which bursting activity is induced by strychnine or bicuculline, involvement of synaptic depression in burst termination has been suggested by several observations. In this preparation bursts are separated by quiescent intervals and are detected on motoneurons as repetitive clusters of EPSPs appearing at a frequency of about 5 Hz. The amplitude of such EPSP clusters has been shown to decline during an individual burst with a timecourse similar to that of EPSPs evoked by repetitive focal stimulation of interneurons. Furthermore, burst duration and amplitude of the first (and larger) EPSP of either spontaneous or evoked bursts have been found to be positively correlated to duration of the quiescent interval preceding the burst. These data has suggested that burst length is determined by an activity-dependent buildup of

synaptic depression in the spinal networks; such a buildup is in fact expected to require less time if a burst initiates when synaptic efficacy is still recovering from previous activity. Since burst duration is not correlated to the duration of the following quiescent interval, it also appears that burst initiation is not determined by recovery from synaptic depression (Streit, 1993). In the intact spinal cord, burst amplitude was remarkably constant for a given preparation and did not depend on the duration of the preceding quiescent interval both for spontaneous or evoked bursts. Nevertheless, saturation of synaptic receptors on the motoneuron membrane during a burst could have masked synaptic depression, that is considered to be mainly due to presynaptic factors (Lev-Tov and Pinco, 1992; Streit et al, 1992). A consistent correlation between burst duration and the preceding interburst interval was not found during spontaneous bursting. Furthermore, it was possible to elicit a burst of normal amplitude and duration as early as 0.5 s after termination of the preceding spontaneous burst. A strong correlation between burst duration and stimulation period (in the range 2-20 s) was always found when bursts were driven by repetitive activation of DR or VL fibres. The reason of the discrepancy between the effects of single or repetitive stimulation on evoked burst duration are presently unclear. Collectively, these findings do not rule out the possibility that synaptic depression played a role in burst termination, although, unlike organotypic slices, direct evidence for such a role is not currently available for the neonatal rat spinal cord. Since agents able to interfere selectively with synaptic depression are not currently available, testing this hypothesis will require experimental access to the rhythmogenic network.

Regardless of the cellular mechanisms responsible for burst termination, these data indicate the rhythmogenic network was not in an absolutely refractory state after the end of a burst. Strong reduction of burst duration during repetitive stimulation supports the view that accumulation of certain "state variables" intrinsic to the rhythmogenic network (such as intracellular sodium concentration, de-activation of inward rectifier conductances or synaptic depression) occurred during a burst and was responsible for its termination when such variables reached certain "high" critical levels. Recovery from accumulation of these state variables should have taken place during the quiescent periods, so that these variables returned to their "low" values before the onset of the next burst. If the network was forced by repetitive external inputs to generate a new burst

before complete recovery occurred, burst duration was reduced because the state variables had not returned to the "low" values and therefore they reached more rapidly the "high" critical values at which network operation was impaired.

A final verification of the present model, as well as of any other model of spinal pattern generation will be possible only when the rhythmogenic network is identified in terms of its cellular elements and its synaptic organization and when a number of its elements can be recorded simultaneously.

5. Pharmacological modulation of rhythmic bursting.

Rhythmic bursting in the disinhibited spinal cord was accelerated in a dose-dependent manner by NMDA, 5-HT and increases in extracellular potassium concentration. While these manipulations act through different cellular mechanisms, they are all expected to depolarize spinal neurons thus increasing their excitability (Mayer and Westbrook, 1987; Takahashi and Berger, 1990; Sqalli-Houssaini et al, 1993). In all cases, burst acceleration was accompanied by a marked reduction in burst duration. As discussed in a later subheading, these observation are of functional significance since the frequency of locomotor patterns elicited in the same preparations by 5-HT or NMDA also depends on the concentration of these agents (Cazalets et al, 1992; Beato et al, 1997); furthermore, fictive locomotion induced by neurochemicals is accelerated in a dose-dependent manner by increasing extracellular potassium concentration (Sqalli-Houssaini et al 1993).

The reason why these agents accelerated bursting activity in the disinhibited spinal cord is still to be determined. A tentative explanation in qualitative terms can be found in the framework of the model proposed in the previous subheading for rhythmogenesis in the absence of synaptic inhibition; in this case it has been hypothesized that after a quiescent period a new burst will be triggered when some elements of the network resume firing after termination of the hyperpolarization induced by the electrogenic pump (and possibly by other factors). It is feasible that when neuron excitability was increased by agents such as 5-HT, NMDA or high potassium, interneurons tended to start firing action potential earlier during the quiescent period. Therefore, such a firing activity could have triggered a burst before extrusion of sodium excess was complete. In this case, in the presence of one of the accelerating agents, at the onset of each burst internal sodium concentration

would have been larger than in the presence of strychnine and bicuculline alone. As a consequence, sodium concentration would have reached more rapidly the critical value at which the activity of the electrogenic sodium pump is strong enough to terminate a burst. This kind of process could then account for concomitant reduction of burst duration and cycle period observed in the presence of 5-HT, NMDA or high potassium. In this way the effects of depolarizing agents on the network operation would have been similar to those of repetitive stimulations, with the difference that in the former case an early burst triggering signal would have been generated by elements intrinsic to the rhythmogenic network instead of arising from extrinsic synaptic inputs.

6. Entrainment of rhythmic bursting by afferent synaptic inputs.

DR or VL fibre stimulation entrained spontaneous bursting within a wide range of periods (usually 2-20 s). Decreasing the stimulus interval to <2 s led to loss of entrainment with unexpected return of spontaneous bursts (identical to those found in the absence of stimulation) superimposed with electrically evoked reflexes.

DR stimulus intensities just above threshold for short-latency synaptic responses were sufficient to elicit a burst virtually identical to spontaneous ones. Single pulses merely reset the bursting pattern which then resumed its normal activity; in this case increasing pulse intensity from 1 to 4×T progressively reduced burst latency with no change in burst amplitude or structure. Since a single juxta-threshold DR stimulus delivered during the quiescent period generated a spontaneous-like burst, it appears that a relatively small synaptic input could re-activate burst generation. These property are consistent with the view that bursts were produced by an autoregenerative mechanism that needed a small triggering input to start its operation that was then self-sustained for a given time. Shorter latencies produced by increasing stimulus strength might be explained by the larger number of neurons recruited by stronger afferent input activation, resulting in a faster build-up of mutual excitation through the network.

With repetitive stimulation at periods comparable with (or larger than) the spontaneous cycle period, a spontaneous burst regularly developed after each evoked one at the same interval observed in the absence of stimulation. This finding suggests that a burst (either spontaneous or evoked) activated a mechanism that kept the network silent for about 30

s (but was readily overcome by afferent synaptic inputs). As mentioned above, active extrusion of sodium appear as a likely candidate for this self-regulating mechanism.

Like spontaneous ones, evoked bursts were always simultaneously observed on both sides of the spinal cord. Since longitudinal hemisection of the spinal cord preserved rhythmic activity in right and left halves, the present experiments confirm that, although each hemicord possessed an autonomous rhythm generating network, these networks were strongly coupled in the intact, disinhibited spinal cord.

Lowering the stimulation period (at constant intensity) entrained bursts which became progressively shorter without changes in their amplitude. The cellular mechanisms giving rise to this phenomenon have been discussed above in the light of the proposed model for pattern generation in the absence of synaptic inhibition. From a functional point of view, this property demonstrates the strong plasticity of the rhythmogenic network that enabled it to follow relatively fast external inputs on a 1:1 basis without altering the burst peak amplitude. Such a behaviour is somehow opposite to frequency-dependent depression observed in control solution for DR-evoked EPSPs, in which repetitive stimulation strongly decreases amplitude but not duration of motoneuronal responses (Lev-Tov and Pinco, 1992). It is interesting that bursts never fused together to generate an ictal-like sustained depolarization as described for feline spinal motoneurons in vivo in which, unlike rat motoneurons in vitro, intrinsic postsynaptic conductances also play a major role (Schwindt and Crill 1984).

In the neonatal rat spinal cord in vitro, when the pulse period was below 2 s, the scenario suddenly changed since polysynaptic reflexes were still present in VRs, entrainment ceased and spontaneous bursting (independent from stimulation) resumed. These data were obtained with fixed stimulus intensity through the range of stimulation periods. In the range 1-2.5×T, bursts evoked by strong pulses retained essentially the same structure as those elicited by weak pulses although they remained entrained even at much lower stimulus periods. In other words, an increase in stimulus intensity reduced the ability of bursts to escape entrainment. Further increases in stimulus strength did not change entrainment. It is noteworthy that comparable data were also observed when stimulating the VL tract, indicating that the possibility to entrain bursting was not a peculiarity of DR fibres. The current data can be explained by postulating the existence of afferent

polysynaptic pathways (subserving reflex activity recorded from motoneurons) distinct from a spontaneously active rhythmogenic network (fig D.2). The presence of a distinct rhythmogenic network can be inferred from the present data showing spontaneous bursting recommencing independent from polysynaptic reflex activity at low stimulation periods. Hence, it is proposed that in the absence of inhibition rhythmogenesis was not a common property of the whole spinal circuitry, but was generated by a specialized network. Since DR or VL stimulation could drive bursting activity, it is clear that such a rhythmogenic network should receive mono or polysynaptic excitatory inputs from DR and VL afferent fibres. In the framework of the model proposed for rhythmogenesis, a burst was generated when such a synaptic input was strong enough to elicit firing activity in a sufficient number of elements of the rhythmogenic network, thus triggering the mutual excitation process. An idealized diagram of simplified connections in the disinhibited spinal cord is shown in fig D.2. According to this scheme the DR and VL afferents, via mono or polysynaptic pathways involving interneurons (Int), are distributed to the motoneuron pool (MN) as well as to the rhythmogenic network. This arrangement can thus account for burst entrainment and resetting by electrical stimulation of DR or VL fibres. Since closely-spaced stimuli to DR or VL afferents could not entrain bursts, they were therefore deemed unable to drive the rhythmogenic network, whose activity was expressed as re-emergence of spontaneous bursts with superimposed reflexes.

The question then arises why entrainment failed at periods below 2 s. This might be due to either an intrinsic inability of the rhythmogenic network to follow fast stimuli or a decreased strength of the synaptic inputs impinging on the rhythmogenic network: in the latter case the afferent input would have been unable to bring rhythmogenic network neurons to spike threshold and thus to trigger burst generation. Such a decrease might be explained by postulating frequency-dependent depression of the synapses linking fibre afferents to the rhythmogenic network. As far as the monosynaptic DR-evoked reflex is concerned, synaptic depression is known to occur at stimulation intervals lower than 60 s (Lev-Tov and Pinco, 1992). Indirect support for a role of synaptic depression in the present experiments comes from the observation that the lowest entrainment period was further reduced when the stimulus strength was raised, thus presumably recruiting a larger number of fibres which compensated for diminished synaptic efficacy. VL-evoked

monosynaptic EPSPs of motoneurons do not however display frequency dependent depression (Pinco and Lev-Tov 1994). Hence, either VL fibres impinging on rhythmogenic network have properties different from those reaching motoneurons, or part of VL and DR afferents impinge on a common interneuronal target (see postulated projection indicated by dashed lines in Fig. 2) that in turns sends frequency-sensitive connections to the rhythmogenic network. The latter hypothesis is supported by the finding that VL descending tracts share some common targets with DR afferents both in cat (Maxwell and Jankowska, 1996) and in rat (Antal et al. 1996) spinal cord.

7. Localization of the rhythmogenic networks in the disinhibited spinal cord.

Selective lesions of the neonatal rat spinal cord have revealed that: 1) removal of segments rostral to L3 had no effects on burst frequency and duration although more than two segments were necessary to preserve regular rhythmicity; 2) gradual midsagittal splitting of the spinal cord from the caudal end increased the variability of burst frequency but not of burst duration; 3) gradual midsagittal splitting from the rostral end had similar effects on burst variability and tended to reduce burst duration; 4) bilateral synchronicity between the activity of the two L5 ventral roots persisted even when connections cross remained intact only at a distance of several segments (either rostrally or caudally); 5) after complete separation of the spinal cord into left and right hemicords, both sides continued to perform independently rhythmic bursting at different rates, even if this lesion increased burst frequency variability and decreased burst duration; 6) ablation of the tissue dorsal to the central canal did not affect burst frequency but resulted in reduction of burst duration; 7) while the characteristic structure of bursts with several oscillations was usually retained following the above-mentioned lesions, in the case of the ventral quadrant preparation bursts were converted into simple single-discharge events at higher frequency. These data show that the rhythmogenic network was distributed along the longitudinal axis at lumbar level in the disinhibited spinal cord and that the minimal neuronal network necessary for this rhythmic activity was contained within a single ventral quadrant spanning over few lumbar segments. Data obtained with gradual midsagittal hemisections show that, although left and right hemicords individually possessed the ability to generate rhythmic bursts, the whole disinhibited

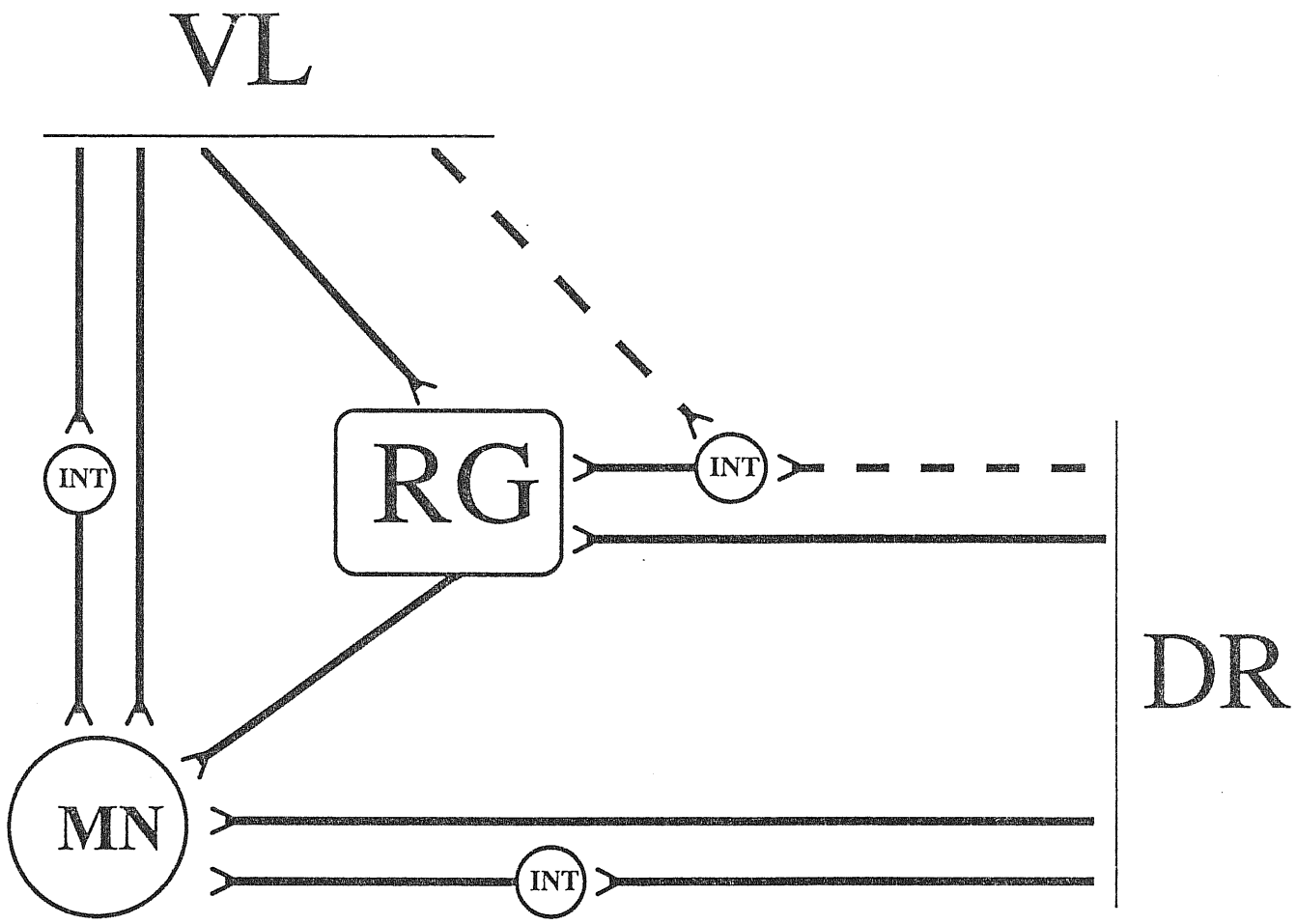

Fig D.2. *Idealized scheme of minimal synaptic connections able to account for spontaneous bursting and its entrainment in the presence of strychnine and bicuculline.*
It is postulated that VL tracts project to motoneurons (MN) (via mono and polysynaptic pathways), to the rhythm generator (RG) and to an unidentified pool of excitatory interneurons (Int). Similar arrangements are presumed to exist for the DR afferents activated by relatively small intensity, short duration electrical shocks. The dashed lines indicate the more hypothetical nature of those projections which are postulated only as one possible explanation to account for the similar loss of entrainment at low periods of stimulation observed with DR or VL stimulation. The scheme should simply be considered as an operational diagram for the most parsimonious explanation of spontaneous bursting and entrainment. Note that, due to pharmacological block of Cl^--mediated inhibition, inhibitory interneurons are omitted from the scheme.

spinal cord behaved as a strongly coupled oscillator even when large part of side-to-side connections were eliminated. These data suggest that a rhythm generating network corresponding to the one presented in fig 1.2 could be contained in each ventral horn and distributed along all the lumbar segments of the cord.

Either longitudinal hemisection or removal of dorsal horns resulted in decreased burst duration (while bursts preserved their oscillatory structure), while the cycle period was not significantly different from the unlesioned preparation. In the isolated ventral quadrant, burst were extremely short and lacked intraburst oscillations; in this case cycle period was also significantly shorter than in the intact cord. These data suggest that burst duration critically depended on the dimensions of the rhythmogenic network. It is possible that during dorsal horns ablation part of the ventral horn tissue was also damaged. Therefore, even if rhythmic ability was confined to ventral horns, part of the rhythmogenic network could have been removed by dorsal horns ablation. Combination of this lesion with midsagittal hemisection, that *per se* reduced burst duration, gave rise to an isolated ventral quadrant and further reduced the dimension of the network by eliminating side-to-side connections. Consistently, in the isolated ventral quadrant burst duration was shorter than with one of the other two lesions.

In organotypic cultures of the rat spinal cord, in the presence of strychnine or bicuculline tangential lesions have been shown to affect separately burst duration and burst frequency (Streit, 1996). In that case burst frequency and burst duration tend to decrease when part of the tissue is removed, although in certain cases a decrease in frequency can be accompanied by an increase in burst duration. These data has suggested that burst initiation could be due to periodic activation of some spontaneously active cells, while burst duration could be determined by reverberation of activity in the rest of the network (Streit, 1996). In this light, removal of a portion of spontaneously active cells would decrease burst frequency, while removal of a part of the reverberating network would decrease burst duration. In the intact cord, selective lesions did not decrease burst frequency. In the model proposed in the previous subheadings it is assumed that each intraburst oscillation began when some elements of the rhythmogenic network resumed firing during the repolarizing phase of the preceding oscillation. In this model these neurons play a role similar to that proposed by Streit for spontaneously active cells in

organotypic slices, although in the present case it is not possible to establish whether such a role was played by a particular class of cells or by any element of the rhythmogenic network. If we assume that neurons able to trigger a new oscillation were distributed across the rhythmogenic network, it must be expected that a reduction in the size of such a network would decrease the probability that a new oscillation is generated; as a consequence, number of intraburst oscillations and burst duration would also be reduced. Under the assumption that a strong sodium influx took place during each burst, this implies that in a lesioned preparation, due to reduced duration each burst should have been accompanied by a less conspicuous accumulation of intracellular sodium. This would be expected to decrease the time required for sodium extrusion and therefore the duration of the quiescent intervals and cycle period. Such a reduction in cycle period was observed in the isolated ventral quadrant, but not in the hemisected or dorsal horn-ablated preparations. Nevertheless, it should be considered that a decrease in the number of neurons able to trigger mutual excitation is also expected to decrease the probability that a new burst is initiated after a quiescent period, and this phenomenon could have compensated the shorter time required for sodium extrusion.

In the isolated ventral quadrant, bursts were reduced to a single-discharge event without intraburst oscillations. These data suggest that in such a preparation the probability of the rhythmogenic network to be excited again after the initial depolarization was extremely low. On isolated spinal cords or lesioned preparations in which intraburst oscillations were still present, 5-HT or NMDA always produced a concomitant decrease in cycle period and burst duration. In the case of isolated ventral quadrants these drugs only enhanced burst frequency without changing burst duration. These findings are consistent with the observation that in intact preparations 5-HT or NMDA decreased burst duration by lowering the number of intraburst oscillations rather than decreasing their duration, that was poorly affected by these agents (see fig R.13 and R.14 of the Results section). Similarly, in the isolated ventral quadrant in which bursts were reduced to a single oscillation, their duration, unlike their frequency, was not affected by 5-HT or NMDA.

8. Possible functional relevance of rhythmic bursting in the absence of synaptic inhibition.

A very important issue concerns the relation between rhythmic activity in the absence of synaptic inhibition and other patterns that can be observed in the same preparation under different pharmacological conditions and are more directly related to motor activities of the animal in vivo. As discussed in the Introduction section, several agents can induce rhythmic bursts in the neonatal rat spinal cord, including 5-HT, NMDA and their combination (Cazalets et al, 1992; Sqalli-Houssaini et al, 1993; Rossignol and Dubuc, 1994; Kjærulff and Kiehn 1996; Cowley and Schmidt, 1997). Although these patterns are characterized by alternating activity of left and right lumbar ventral roots at various segmental levels, recordings from nerves of extensor and flexors hindlimb muscles have revealed that 5-HT- but not NMDA- induced patterns include flexor-extensor alternation, as expected for a locomotor-like activity (Cowley and Schmidt, 1994b, 1997; Kiehn and Kjaerulff, 1996). In addition to this difference between NMDA and 5-HT induced patterns, lesion studies have suggested that 5-HT-sensitive rhythmogenic networks are located rostrally to L1/L2 segments (Cowley and Schmidt, 1997, Cazalets et al, 1995), while NMDA-sensitive rhythmogenic networks are also present in more caudal lumbar segments (Cowley and Schmidt, 1997). In partial contrast to these findings, Kjaerulff and Kiehn (1996) have reported that a combination of 5-HT and NMDA can induce alternating activity also in a few isolated caudal lumbar segments (L2-L6). It is still to be clarified whether alternating rhythmic activities observed under different pharmacological conditions are generated by spinal networks using different rhythmogenic mechanisms (a view favoured by Cowley and Schmidt, 1997) or whether they are produced by the same spinal oscillator(s), in which different phase-couplings can be induced by different agents (as proposed for lower animal species by Harris-Warrick and Marder, 1991). The present findings raise an additional related question, namely whether synchronous rhythmic bursting induced by strychnine and bicuculline was generated by the same neural oscillators activated by 5-HT or/and NMDA in control solution or whether synchronous and alternating activities are produced by independent neural mechanisms. The experimental findings obtained in the present study do not allow a definite answer to this important issue. Nevertheless, a number of pharmacological and

anatomical analogies between synchronous rhythmic bursting in the absence of synaptic inhibition and alternating patterns can be underlined. Alternating pattern frequency has been shown to be positively correlated to either 5-HT or NMDA concentration (Cazalets et al, 1992; Beato et al, 1997); Cazalets et al (1992) have reported that in the presence of 5-HT (25-100 μM), alternating burst period vary between 13 and 6 s, while in the presence of NMDA (10-40 μM) it changes between 3.5 and 1 s. With lower doses of 5-HT (2.5-30 μM), Beato et al (1997) have reported that alternating burst period varies in the range 8-3 s. In the presence of strychnine and bicuculline spontaneous cycle period was markedly larger with respect to these values. Nevertheless, synchronous bursting was easily accelerated in a dose-dependent manner by either 5-HT or NMDA up to frequencies overlapping those observed with these agents in control solution (see fig R.13 and R.14 of Results section). Furthermore, like alternating patterns induced by 5-HT plus NMDA (Sqalli-Houssaini et al, 1993), rhythmic bursts in the absence of synaptic inhibition were accelerated in a dose-dependent manner by increasing extracellular potassium, and their period was <10 s at 8 mM potassium concentration in the absence of any other excitatory agent. Another common feature of synchronous bursting and 5-HT-induced alternating patterns is that, like disinhibited rhythmic activity, 5-HT patterns appear to rely on glutamatergic transmission but they can still be expressed in the presence of either NMDA or non NMDA receptor antagonists provided that neuronal excitability is increased (Beato et al, 1997). As far as lesion studies are concerned, it must be noted that the anatomical distribution of the rhythmogenic networks in the disinhibited spinal cord is similar to that of the networks generating alternating patterns in response to 5-HT plus NMDA. In fact, such patterns can still be expressed after ablation of dorsal horns or after midsagittal hemisection and are generated by a segmentally distributed network (Kjaerulff and Kiehn, 1996). A similar laminar and segmental distribution was also found for the spinal networks generating flexor-extensor alternating patterns in the chick embryo (Ho and O'Donovan, 1993).

On the basis of these analogies, it is tempting to speculate that rhythmic bursts in the disinhibited spinal cord could have been generated by the same spinal oscillators that give rise to alternating behaviours in the presence of 5-HT or NMDA. It has been proposed that the spinal network responsible for rhythmic limb movements is composed by a

number of oscillators (termed "unit burst generators"), each driving one or few synergist muscles acting on a given joint (Grillner, 1981). According to this view, different phase-coupling of such oscillators might give rise to disparate rhythmic patterns underlying relevant rhythmic behaviours. In the neonatal rat spinal cord, it has been suggested that left-right and extensor-flexor oscillators are linked by inhibitory and excitatory connections acting in parallel, since alternating patterns evoked by excitatory agents can be converted into synchronous ones by application of either strychnine or bicuculline (Cowley and Schmidt, 1995; 1997). A similar transformation from alternating to synchronous patterns following application of inhibitory amino acids antagonists have also been reported in other preparations, including lamprey and chick embryo spinal cord (Hagevik and McClellan, 1994; Sernagor et al, 1995). The present findings, obtained in the presence of a complete block of inhibitory processes, might suggest that synaptic inhibition is not required for the intrinsic operation of the spinal oscillators, that could be composed by purely excitatory networks. In the absence of synaptic inhibition, excitatory links between various spinal oscillators would be prevalent, resulting in a strong in-phase coupling across the cord. On the other hand, in control solution inhibitory connections between oscillators would tend to prevail, giving rise to left-right (and in some cases extensor-flexor) alternation.

Furthermore, it is possible that an extrinsic inhibitory control is exerted on spinal oscillators, as suggested by Cazalets et al (1994). Suppression of such an inhibitory control by strychnine and bicuculline could then explain why in the presence of these antagonists spontaneous rhythmicity did not require the presence of excitatory agents, that instead are needed to produce alternating patterns in the presence of synaptic inhibition.

9. Conclusions

The present study has investigated synchronous rhythmic activity that appears spontaneously in neonatal rat motoneurons when chloride-mediated synaptic inhibition is pharmacologically blocked throughout the cord. The findings that the collective behaviour of spinal neurons, far from becoming chaotic under this conditions, turns into an extremely regular pattern that can be strongly modulated by several chemical agents

also implicated in locomotor activity and is preserved after ablation of large portions of neuronal tissue, enlighten a non obvious feature of spinal networks and can provide new insight into the complex field of spinal pattern generation. The present experiments have addressed several issues concerning rhythmogenesis in the absence of synaptic inhibition, that appears to be driven by a premotoneuronal network in which glutamatergic transmission plays an essential role; on the basis of the experimental findings a tentative explanation of such a behaviour in terms of mutual excitation of a kernel of spinal interneurons has also been proposed here. Nevertheless, an exhaustive understanding of spinal pattern generation (either in the absence or in the presence of synaptic inhibition) in terms of cellular and network mechanisms will require development of new experimental approaches, that are expected to identify the neural substrate of rhythmic activity and its synaptic organization.

The physiological implications of the present findings remain to be determined. In particular, it will be essential to clarify whether this activity is generated by the same oscillators involved in the generation of other spinal patterns (in particular locomotor ones), a view that is favoured but certainly not demonstrated by the present findings. The observation that the network generating such a behaviour can be easily entrained by rhythmic afferent synaptic inputs and can adapt the duration of its output to external input frequency is of potential interest to the field of the interaction between sensory and supraspinal afferent fibres and spinal pattern generation.

Apart from functional implications, block of synaptic inhibition provides a large experimental simplification of the overwhelming and poorly understood complexity of spinal circuitries, and therefore supplies a pharmacological tool to investigate those properties of the spinal networks that rely upon excitatory connections only and that can be masked by synaptic inhibition in control solution.

REFERENCES

Alford S, Sigvaardt KA and Williams TL. GABAergic control of rhythmic activity in the presence of strychnine in the lamprey spinal cord. Brain Res (1990) 506, 303-306.

Antal M, Petko' M, Polgar E, Heizmann CW, and Storm-mathisen J. Direct evidence of an extensive gabaergic innervation of the spinal dorsal horn by fibers descending from the rostral ventromedial medulla. Neuroscience (1996) 73, 509-518.

Arshavsky Y, Orlovsky GN, Panchin YV, Roberts A and Soffe SR. Neuronal control of swimming locomotion: analysis of the pteropod mollusc Clione and embryos of the amphibian Xenopus. TI NS. (1993) 16, 227-33.

Atsuta Y, Garcia-Rill E and Skinner RD. Control of locomotion in vitro: I. Deafferentation. Somatosens Motor Res (1991) 8, 45-53.

Ayala GF, Matsumoto H and Gumnit RJ. Excitability changes and inhibitory mechanisms in neocortical neurons during seizures. J Neurophysiol (1970) 33, 73-85.

Bal T and McCormick DA. What stops synchronized thalamocortical oscillations? Neuron (1996) 17, 297-308.

Bal T, von Krosigk M and McCormick DA. Synaptic and membrane mechanisms underlying synchronized oscillations in the ferret lateral geniculate nucleus in vitro. J Physiol (1995) 483, 641-63.

Baldissera F, Hultborn, H and Illert M. Integration in spinal neuronal systems. In VB Brooks (ed), Handbook of Physiology, Section 1: The Nervous System, Vol II, Motor Control. APS (1981) 509-595.

Barbeau H end Rossignol S. Initiation and modulation of the locomotor pattern in adult chronic spinal cat by noradrenergic, serotonergic and dopaminergic drugs. Brain Res (1991) 546, 250-260.

Barnes-Davies M and Forsythe ID. Pre- and postsynaptic glutamate receptors at a giant excitatory synapse in rat auditory brainstem slices. J Physiol (1995) 488, 387-406.

Beato M, Bracci E and Nistri A. Contribution of NMDA and non-NMDA glutamate receptors to locomotor pattern generation in the neonatal rat spinal cord. Proc Roy Soc (1997) In Press

Becker CM Hoch W and Betz H. Glycine receptor heterogeneity in rat spinal cord during postnatal development.*EMBO Journal* (1988) 7, 3717-3726.

Brady RJ and Swann JW. Ketamine selectively suppresses synchronized after-discharges in immature hippocampus. Neurosci Lett (1986) 341, 143-149.

Bragin A, Jando G, Nadasdy Z, Hetke J, Wise K, and Buzsaki G. Gamma (40-100 Hz) oscillation in the hippocampus of the behaving rat. J Neurosci (1995) 15, 47-60, 1995 Jan.

Brodal A. Neurological anatomy in relation to clinical medicine. 3td ed. New York, Oxford University Press (1981).

Brown TG. The intrinsic factors in the act of progression in the mammal. Proc Roy Soc London B (1911) 84, 308-319.

Burke R. Spinal Cord: Ventral Horn. In The Synaptic organization of the brain, G M Shepherd ed, Oxford University Press (1990) p. 88-132.

Canessa CM, Horisberger JD, Louvard D and Rossier BC. Mutation of a cysteine in the first transmembrane segment of Na,K-ATPase α subunit confers ouabain resistance. EMBO J (1992) 11, 1681-1687.

Cazalets JR, Borde M, Clarac F. Localization and organization of the central pattern generator for hindlimb locomotion in newborn rat. J Neurosci (1995) 15, 4943-51.

Cazalets JR, Sqalli-Houssaini Y and Clarac F. GABAergic inactivation of the central pattern generators for locomotion in isolated neonatal rat spinal cord. J Physiol (1994) 474, 173-81.

Cazalets JR, Borde M and Clarac F. The synaptic drive from the spinal locomotor network to motoneurons in the newborn rat. J Neurosci (1996) 16, 298-306.

Cazalets JR, Sqalli-Houssaini Y and Clarac F. Activation of the central pattern generators for locomotion by serotonin and excitatory amino acids in neonatal rat. J Physiol (1992) 455, 187-204.

Chub N and O'Donovan MJ. Homeostatic regulation of rhythmic neural output in the developing chick spinal cord. Soc Neurosci Abs (1996) 22, 1377.

Cohen AH and Harris-Warrick RM. Strychnine eliminates alternating motor output during fictive locomotion in the lamprey. Brain Res (1984). 293, 164-167.

Colquhoun D, Jonas P and Sakmann B. Action of brief pulses of glutamate on AMPA/Kainate receptors in patches from different neurones of rat hippocampal slices. J.Physiol (1992) 458, 261-287.

Contreras D and Steriade M. Spindle oscillation in cats: the role of corticothalamic feedback in a thalamically generated rhythm. J Physiol (1996) 490, 159-79.

Cowley KC and Schmidt BJ. A comparison of motor patterns induced by N-Methyl-D-Aspartate, acetylcholine and serotonin in the in vitro neonatal rat spinal cord. Neurosci Lett (1994b) 171, 147-150.

Cowley KC and Schmidt BJ. Effects of inhibitory amino acids antagonists on reciprocal inhibitory interaction during rhythmic motor activity in the in vitro neonatal rat spinal cord. J. Neurophysiol (1995) 74: 1109-1117.

Cowley KC and Schmidt BJ. Regional distribution of the locomotor pattern-generating network in the neonatal rat spinal cord. J Neurophysiol (1997) 77, 247-259.

Cowley KC and Schmidt BJ. Some limitations of ventral root recordings for monitoring locomotion in the in vitro neonatal rat spinal cord. Neurosci Lett (1994a) 171, 142-146.

Czèh G, Obih JCA and Somjen GG. The effect of changing extracellular potassium concentration on synaptic transmission in isolated spinal cords. Brain Research (1988) 446, 50-60.

Dale H, Feldberg W and Vogt M. Release of acetylcholine at voluntary motor nerve endings. J Physiol (1936) 86, 353-380.

Dale N and Gilday D. Regulation of rhythmic movements by purinergic neurotransmitters in frog embryos. Nature. (1996) 383, 259-63.

Dale N and Roberts, A. Excitatory amino acid receptors in xenopus embryo spinal cord and their role in the activation of swimming. J Physiol (1984) 348, 527-543.

Dale N. Experimentally derived model for the locomotor pattern generator in the Xenopus embryo. J Physiol (1995) 489, 489-510.

Davidoff RA and Hackman JC. Hyperpolarization of frog primary afferent fibres caused by activation of a sodium pump. J Physiol (1980) 302, 297-309.

Davidoff RA and Hackman JC. Spinal inhibition. In: Handbook of spinal cord; Davidoff RA ed (1984) pp 385-459, Dekker, NY.

DeFeudis FV and Somoza E. density of GABA-receptors in rat cerebral cortex measured with bicuculline-methiodide in the presence of Na^+ and other inorganic ions. Gen Pharmac (1977) 8, 181-187.

Diamond JS and Craig EJ. Asynchronous release of synaptic vesicles determines the time course of the AMPA receptor-mediated EPSC. Neuron (1995) 15, 1097-1107.

Di Francesco D, Ferroni A, Mazzanti M and Tromba C. Properties of the hyperpolarizing-activated current (i_f) in cells isolated from the rabbit sino-atrial node. J Physiol (1986) 377, 61-68.

Dichter MA (ed) Mechanisms of epileptogenesis. New York Plenum Publishing Corporation (1988).

Douglas JR, Noga BR, Dai X and Jordan LM. The effects of intrathecal administration of excitatory amino acids agonists and antagonists on the initiation of locomotion in the adult cat. J Neurosci (1993) 13, 990-1000.

Drew T and Rossignol S. Functional organization within the medullary reticular formation of the intact unanaesthetized cat I. Movements evoked by microstimulation. J Neurophysiol (1990) 64, 767-781.

Eccles JC, Fatt P and Koketsu K. Cholinergic and inhibitory synapses in a pathway from motor-axons collaterals to motoneurons. J Physiol (1954) 126, 524-562.

Eccles JC. The excitatory responses of spinal neurons. In: Physiology of spinal neurons. Eccles JC and Schadé JP editors, Elsevier Publishing Company (1964).

Edgerton VR, Grillner S, Sjostrom A and Zangger P. Central generation of locomotion in vertebrates. In: Neural Control of Locomotion, Herman R Grillner S and Sjostrom A Zangger P eds. New York: Plenum Press (1976) p. 439-464.

El Manira A, Tegner J, and Grillner S. Calcium-dependent potassium channels play a critical role for burst termination in the locomotor network in lamprey. J Neurophysiol (1994) 72, 1852-61.

Elliott P, and Wallis DI. Glutamatergic and non-glutamatergic responses evoked in neonatal rat lumbar motoneurons on stimulation of the lateroventral spinal cord surface. Neuroscience (1993) 56, 189-197.

Engel AK, Konig P, Kreiter AK, Schillen TB and Singer W. Temporal coding in the visual cortex: new vistas on integration in the nervous system. Trends Neurosci (1992) 15, 218-26.

Feldman JL and Smith JC. Cellular mechanisms underlying modulation of breathing pattern in mammals. Ann NY Acad Sci (1989) 437, 114-130.

Forssberg H and Grillner S. The locomotion of the acute spinal cats injected with clonidine i.v. Brain Res (1973) 50, 184-186.

Fulton B and Walton K. electrophysiological properties of neonatal rat motoneurons studied in vitro. J Physiol (1986a) 370, 651-678.

Fulton B and Walton K. Ionic mechanisms underlying the firing properties of rat neonatal motoneurons studied in vitro. Neurosci (1986b) 19, 669-683.

Fuortes MGF and Nelson PG. Strychnine: its action on spinal motoneurons of cat. Science (1963) 140, 806-808.

Gao BX and Ziskind-Conhaim L. Development of glycine- and GABA-gated currents in rat spinal motoneurons. J Neurophysiol (1995) 74, 113-21.

Garcia-Rill E, Skinner RD and Fitzgerald JA. Chemical activation of the mesencephalic locomotor region. Brain Res (1985) 330, 43-54.

Gelfand IM, Orlovsky GN and Shik ML. Locomotion and scratching in tetrapods. In: Neural Control of Rhythmic Movements in Vertebrates, Cohen AH, Rossignol S and Grillner S eds, John Wiley and Sons Press, 1988, p. 167-199.

Glynn, IM. All hands to the sodium pump. J Physiol (1993) 462, 1-30.

Green CS and Soffe SR. Transitions between two different motor patterns in Xenopus embryos. J Comp Physiol A (1996) 178, 279-91.

Grillner S, Deliagina T, Ekeberg O, el Manira A, Hill RH, Lansner A, Orlovsky GN and Wallen P. Neural networks that co-ordinate locomotion and body orientation in lamprey. Trends Neurosci (1995) 18, 270-9.

Grillner S, Wallen P and Brodin L. Neuronal network generating locomotor behaviour in lamprey. Annu Rev Neurosci (1991) 14, 169-199.

Grillner S. Control of locomotion in bipeds, tetrapods, and fish. In: Handbook of Physiology, The Nervous System, Motor Control, VB Brooks ed. Am Physiol Soc (1981) 1179-1236.

Hablitz J.J Picrotoxin-induced epileptiform activity in the hippocampus: role of endogenous versus synaptic factors. J Neurophysiol (1984) 51: 1011-1027.

Hagevik A and McClellan AD. Coupling of spinal locomotor networks in larval lamprey revealed by receptor blockers for inhibitory amino acids: neurophysiology and computer modeling. J Neurophysiol (1994) 72, 1810-29.

Harris-Warrick RM and Marder E. Modulation of neural networks for behavior. Annu Rev Neurosci (1991) 14, 39-57.

Headley PM and Grillner S. Excitatory amino acids and synaptic transmission: the evidence for a physiologicsl function. TIPS (1990) 11, 205-210.

Hille B. Ionic channels of excitable membranes (second edition). Sinauer Associates Inc., Massachusetts (1994).

Ho S and O'Donovan MJ. Regionalization and intersegmental coordination of rhythm-generating networks in the spinal cord of the chick embryo. J Neurosci (1993) 13, 1354-71.

Hochman S, Jordan LM and Schmidt BJ. TTX-resistant NMDA receptor-mediated voltage oscillations in mammalian lumbar motoneurons. J Neurophysiol (1994b) 72, 2559-62.

Hochman S., Jordan, LM & MacDonald JF. N-Methyl-D-Aspartate receptor-mediated voltage oscillations in neurons surrounding the central canal in slices of rat spinal cord. J Neurophysiol (1994a) 72, 565-577.

Horisberger JD, Lemas V, Kraehenbühl JP and Rossier BC. Structure-function relationship of Na,K-ATPase. (1991) Ann. Rev. Physiol. 53, 565-584.

Hultborn H and Kiehn O. Neuromodulation of vertebrate motor neuron membrane properties. Curr Opin Neurobiol (1992) 2, 770-775.

Hunt CC. Relation of function to diameter in afferent fibres of muscle nerves. J Gen Physiol (1954) 38, 117-131.

Hwa GGC, Avoli M, Olivier A, and Villemure JG. Bicuculline-induced epileptogenesis in the human neocortex maintained in vitro. Exp Brain Res (1991) 83, 329-339.

Isaacson JS and Walmsley B. Amplitude and time course of spontaneous and evoked excitatory postsynaptic currents in bushy cells of the anteroventral cochlear nucleus. J Neurophysiol (1996) 76, 1566-71.

Jefferys JG, Traub RD and Whittington MA. Neuronal networks for induced "40 Hz" rhythms. Trends Neurosci (1996) 19, 202-208.

Johnson SW, Seutin V, North RA. Burst firing in dopamine neurons induced by N-methyl-D-aspartate: role of electrogenic sodium pump. Science (1992) 258, 665-667.

Jonas P and Spruston N. Mechanisms shaping glutamate-mediated excitatory postsynaptic currents in the CNS. Curr. Opin. Neurobiol.(1994) 4, 366-372.

Katz PS. Neurons, Networks and Motor Behavior. Neuron (1996) 16, 245-253.

Kiehn O and Kjaerulff O. Spatiotemporal characteristics of 5-HT and dopamine-induced rhythmic hindlimb activity in the in vitro neonatal rat. J Neurophysiol (1996) 75, 1472-82.

Kiehn O, Iizuka M and Kudo N. Resetting from low threshold afferents of N-methyl-D-aspartate-induced locomotor rhythm in the isolated spinal cord-hindlimb preparation from newborn rats. Neurosci Lett (1992) 148, 43-6.

Kiehn O, Johnson BR and Raastad M. Plateau properties in mammalian spinal interneurons during transmitter-induced locomotor activity. Neuroscience (1996) 75, 263-273.

Kiehn O. Plateau potentials and active integration in the 'final common pathway' for motor behaviour. Trends Neurosci (1991) 14, 68-73.

Kjærulff O and Kiehn O. Distribution of networks generating and coordinating locomotor activity in the neonatal rat spinal cord in vitro. A lesion study. J Neurosci (1996). 16, 5777-5794.

Kjaerulff O, Barajon I and Kiehn O. Sulphorhodamine-labelled cells in the neonatal rat spinal cord following chemically induced locomotor activity in vitro. J Physiol (1994) 478, 265-73.

Kriellaars DJ, Brownstone RN, Noga BR and Jordan, LM. Mechanical entrainment of fictive locomotion in the decerebrate cat. J Neurophysiol (1994) 71, 1-13.

Kudo N and Yamada T. N-methyl-D,L-aspartate-induced locomotor activity in a spinal cord-hindlimb preparation of the newborn rat studied in vitro. Neurosci Lett (1987) 75, 43-48.

Kudo N, Ozaki S and Yamada T. Ontogeny of rhythmic activity in the spinal cord of the rat. In Neurobiological basis of human locomotion, pp 127-136 (Shimamura M, Grillner S and Edgerton V editors), Japan Scientific Societies Press (1991).

Kullmann DM. Amplitude fluctuations of dual-component e.p.s.c.s in hippocampal pyramidal cells: implications for long-term potentiation. Neuron (1994) 12, 1111-1120.

Kuypers HG. Anatomy of the descending pathways. In: Handbook of Physiology, Section 1: The Nervous System, Vol II, Motor Control, Brooks VB ed, Am Physiol Soc (1981) p. 597-666.

Landmesser LT and O'Donovan MJ. Activation patterns of embryonic chick hindlimb muscles recorded in-ovo and in an isolated spinal cord preparation. J Physiol (1984) 347, 189-204.

Lee KH and McCormick DA. Abolition of spindle oscillations by serotonin and norepinephrine in the ferret lateral geniculate and perigeniculate nuclei in vitro. Neuron (1996) 17, 309-21.

Lee WL and Hablitz JJ. Effect of APV and ketamine on epileptiform activity in the CA1 and CA3 region of the hippocampus. Epilepsy Res (1990) 6, 87-94.

Lev-Tov A and O'Donovan MJ. Calcium imaging of motoneuron activity in the en-bloc spinal cord preparation of the neonatal rat. J Neurophysiol (1995) 74, 1324-1334.

Lev-Tov A and Pinco M. In vitro studies of prolonged synaptic depression in the neonatal rat spinal cord. J Physiol (1992) 447, 149-69.

Li YX, Bertram R and Rinzel J. Modeling N-methyl-D-aspartate-induced bursting in dopamine neurons. Neuroscience (1996) 71, 397-410.

MacLean JN, Hochman S and Magnuson DS. Lamina VII neurons are rhythmically active during locomotor-like activity in the neonatal rat spinal cord. Neurosci Lett (1995) 197, 9-12.

Magnuson DS, Schramm MJ, and Maclean JN. Long-duration, frequency dependent motor responses evoked by ventrolateral funiculus stimulation in the neonatal rat spinal cord. Neurosci Lett. (1995) 192, 97-100.

Marder E, and Calabrese RL. Principles of rhythmic motor pattern generation. Physiol Rev (1996) 76, 687-717.

Matthews-Bellinger J and Salpeter MM. Distribution of acetylcholine receptors at frog neuromuscolar junctions with a discussion of some physiological implications. J Physiol (1978) 279, 197-213.

Maxwell DJ, and Jankowska E. Synaptic relationship between serotonin-immunoreactive axons and dorsal horn spinocerebellar tract cells in the cat spinal cord. Neuroscience (1996) 70, 247-253.

Mayer ML and Westbrook GL. The physiology of excitatory amino acids in the vertebral central nervous system. Prog Neurobiol (1987) 28, 197-276.

McCormick AD and Pape HC. Properties of a hyperpolarization-activated cation current and its role in rhythmic oscillation in thalamic relay neurons. J. Physiol (1990) 431, 291-318.

Meer DP and Buchanan JT. Apamin reduces the late afterhyperpolarization of lamprey spinal neurons, with little effect on fictive swimming. Neurosci Lett (1992) 143, 1-4.

Merlin LR, Taylor GW and Wong RK. Role of metabotropic glutamate receptor subtypes in the patterning of epileptiform activities in vitro. J Neurophysiol (1995) 74, 896-900.

Miles R and Wong RKS. Single neurones can initiate synchronized population discharge in the hippocampus. Nature (1983) 306, 371-373.

Miles R, Wong RKS and Traub RD. Synchronized afterdischarges in the hippocampus: contribution of local synaptic interaction. Neuroscience (1984) 12, 1179-1189.

Moehler H and Okada T. GABA receptor binding with ^{3}H (+) bicuculline-methiodide in rat CNS. Nature (1977) 267,65-67.

Moore LE, Hill RH and Grillner S. Voltage-clamp frequency domain analysis of NMDA-activated neurons. J Exp Biol (1993) 175:59-87.

Nishimaru H, Iizuka M, Ozaki S and Kudo N. Spontaneous motoneuronal activity mediated by glycine and GABA in the spinal cord of rat fetuses in vitro. J Physiol (1996) 497, 131-143.

Nistri A. Spinal cord pharmacology of GABA and chemically related amino acids. In: Handbook of the Spinal Cord, Vol 1 Pharmacology, pp 45-104. Ed. RA Davidoff. Dekker: NY (1983).

Otsuka M and Konishi S. Electrophysiology of mammalian spinal cord in vitro. Nature (1974) 252, 733-734.

Partin KM, Patneau DK, Winters CA, Mayer ML and Buonanno A. Selective modulation of desensitization at AMPA versus kainate receptors by cyclothiazide and concanavalin A. Neuron (1993) 11, 1069-1082.

Patneau K.D, Vyklicky LJr and Mayer ML. Hippocampal neurones exhibit cyclothiazide-sensitive rapidly desensitizing responses to kainate. The J Neurosci (1993) 13, 3496-3509.

Paton JFR and Richter DW. Role of fast inhibitory synaptic mechanisms in respiratory rhythm generation in maturing mouse. J Physiol (1995) 484, 505-521.

Paxinos G and Watson C. The rat brain in stereotaxic coordinates. (1986) Second edition. Academic Press, NY.

Pearson KG and Rossignol S. Fictive motor patterns in chronic spinal cats. J Neurophysiol (1991) 66, 1874-1887.

Perrins R and Roberts A. Cholinergic and electrical synapses between synergistic spinal motoneurones in the Xenopus laevis embryo. J Physiol (1995) 485, 135-44.

Pinco M and Lev-Tov A. Modulation of monosynaptic excitation in the neonatal rat spinal cord. J Neurophysiol (1993b) 70, 1151-1158.

Pinco M and Lev-Tov A. Synaptic excitation of alpha-motoneurons by dorsal root afferents in the neonatal rat spinal cord. J Neurophysiol (1993a) 70, 406-17.

Pinco M. Lev-Tov A. Synaptic transmission between ventrolateral funiculus axons and lumbar motoneurons in the isolated spinal cord of the neonatal rat. J Neurophysiology (1994) 72, 2406-2419.

Post RL, Albright CD and Dayani K. Resolution of pump and leak components of sodium and potassium ion transport in human erythrocytes. J Gen Physiol (1967) 50, 1201-1220.

Pratt CA and Jordan LM. Ia inhibitory interneurons and Renshaw cells as contributors to the spinal mechanisms of fictive locomotion. J Neurophysiol (1987)7, 56-71.

Rammes G, Parsons C, Muller W, Swandulla D. Modulation of fast excitatory synaptic transmission by cyclothiazide and GYKI 52466 in the rat hippocampus. Neurosci Lett (1994) 175, 21-24.

Redman S. Quantal analysis of synaptic potentials in neurones of the central nervous system. Physiol.Rev (1990) 70, 165-198.

Rexed B. Some aspects of the cytoarchitectonics and synaptology of the spinal cord. In: Organization of the spinal cord, JC Eccles and JP Shadé eds. Progress in Brain Research vol 11. Elsevier Publishing Company, Amsterdam (1964) 58-92.

Rexed B. The cytoarchitectonic organization of the spinal cord in the cat. J Comp Neurol (1952) 96, 415-495.

Roberts A, Tunstall MJ and Wolf E. Properties of networks controlling locomotion and significance of voltage dependency of NMDA channels: stimulation study of rhythm generation sustained by positive feedback. J Neurophysiol (1995) 73, 485-95.

Robinson GA and Goldberger ME. The development and recovery of motor function in spinal cats II. Pharmacological enhancement of recovery. Exp Brain Res (1985) 62. 387-400.

Rossignol S and Dubuc R. Spinal pattern generation. Curr Opinion in Neurobiol (1994) 4, 894-902.

Rossignol S. Neural control of stereotypic limb movements. In: Handbook of Physiology, Section 12, LB Rowell and JT Sheperd eds. Am Physiol Soc (1996) 173-216.

Sah P. Ca^{2+}-activated K^{+} currents in neurons: types, physiological roles and modulation. Trends Neurosci. (1996) 19, 150-154.

Schneider SP and Fyffe RE. Involvement of GABA and glycine in recurrent inhibition of spinal motoneurons. J Neurophysiol (1992) 68, 397-406.

Schotland JL and Grillner S. Effects of serotonin on fictive locomotion coordinated by a neural network deprived of NMDA receptor-mediated cellular properties. Exp Brain Res (1993) 93, 391-8.

Schwindt PC and Crill WE. The spinal cord model of experimental epilepsy. In: Electrophysiology of Epilepsy, PA Schwartzkroin and HV Wheal eds, Academic Press London (1984) p. 219-251.

Schwindt PC and Crill WE. Voltage clamp study of cat spinal motoneurons during strychnine-induced seizures. Brain Res (1981) 204, 226-230.

Schwindt PC, Spain WJ, Foehring, RC, Chubb MC and Crill WE. Slow conductances in neurons from cat sensorimotor cortex in vitro and their role in slow excitability changes. J Neurophysiol (1988). 59, 450-467.

Sernagor E, Chub N, Ritter A and O'Donovan MJ. Pharmacological characterization of the rhythmic synaptic drive onto lumbosacral motoneurons in the chick embryo spinal cord. J Neurosci (1995) 15, 7452-64.

Sherrington CS. Decerebrate rigidity and reflex coordination of movements. J Physiol (1898) 22, 319-332.

Shik ML, Severin FV and Orlovsky GN. Control of walking and running by means of electrical stimulation of the mid-brain. Biophysics (1966) 11, 756-765.

Sivilotti L and Nistri A. GABA receptor mechanisms in the central nervous system. Progr Neurobiol. (1991) 36, 35-92.

Smith JC and Feldman JL. In vitro brainstem-spinal cord preparations for study of motor systems for mammalians respiration and locomotion. J Neurosci Meth (1987) 21, 321-333.

Smith JC, Feldman JL and Schmidt BJ. Neural mechanisms generating locomotion studied in mammalian brainstem-spinal cord preparation in vitro. FASEB J (1988) 2, 2283-2288.

Soffe SR. Motor patters for two distinct rhythmic behaviors induced by excitatory amino acids antagonists in the Xenopus embryo spinal cord. J Neurophysiol (1996) 75, 1815-1825.

Soffe SR. Two distinct rhythmic motor patterns are driven by common premotor and motor neurons in a simple vertebrate spinal cord. J Neurosci (1993) 13, 4456-69.

Sqalli-Houssaini Y, Cazalets JR and Clarac F. Oscillatory properties of the central pattern generator for locomotion in neonatal rats. J Neurophysiol (1993) 70, 803-13.

Steriade M, Amzica F and Contreras D. Synchronization of fast (30-40 Hz) spontaneous cortical rhythms during brain activation. J Neurosci (1996) 16, 392-417.

Steriade M, Contreras D, Amzica F. Synchronized sleep oscillations and their paroxysmal developments. Trends Neurosci (1994) 17, 199-208.

Steriade M, McCormick DA and Sejnowski TJ. Thalamocortical oscillations in the sleeping and aroused brain. Science (1993) 262, 679-85.

Storm JF. Potassium current in hippocampal pyramidal cells. Progress in Brain Research (1990) 83, 161-183.

Streit J, Lüsher C and Lüsher HR. Depression of postsynaptic potentials by high frequency stimulation in embryonic motoneurons grown in spinal cord slice cultures. J Neurophysiol. (1992) 68, 1793-1803.

Streit J. Mechanisms of pattern generation in co-cultures of embryonic spinal cord and skeletal muscle. Intern J Dev Neurosci (1996) 14, 137-48.

Streit J. Regular oscillations of synaptic activity in spinal networks in vitro. J Neurophysiol (1993) 70, 871-8.

Stuart, GJ and Redman SJ. The role of $GABA_A$ and $GABA_B$ receptors in presynaptic inhibition of Ia EPSPs in cat spinal motoneurons. J Physiol (1992) 447, 675-692.

Taal W and Holstege JC. GABA and glycine frequently colocalize in terminals on cat spinal motoneurones. Neuroreport (1994) 5, 2225-2228.

Takahashi T and Berger AJ. Direct excitation of spinal motoneurones by serotonin. J Physiol (1990) 423, 63-76.

Takahashi T. Inhibitory miniature synaptic potentials in rat motoneurons. Proc Roy Soc Biol (1984) 221, 103-109.

Takahashi T. Inward rectification in neonatal rat spinal motoneurons. J Physiol (1990b) 423, 47-62.

Takahashi T. Membrane currents in visually identified motoneurons of neonatal rat spinal cord. J. Physiol (1990a) 423, 27-46.

Taylor GW, Merlin LR and Wong RKS. Synchronized oscillations in hippocampal CA3 neurons induced by metabotropic glutamate receptor activation. J Neurosci (1995) 15, 8039-8052.

Tegner J, Matsushima T, El Manira A and Grillner S. The spinal GABA system modulates burst frequency and intersegmental coordination in the lamprey: differential effects of GABAA and GABAB receptors. J Neurophysiol (1993) 69, 647-57.

Thomas RC. Intracellular sodium activity and and the sodium pump in snail neurons. J Physiol (1972) 220, 55-71.

Thompson SM and Prince DA. Activation of electrogenic sodium pump in hippocampal CA1 neurons following glutamate-induced depolarization. J Neurophysiol (1986) 56, 507-522.

Traub RD, Miles R, and Jefferys JGR. Synaptic and intrinsic conductances shape picrotoxin-induced synchronized after-discharges in the guinea-pig hippocampal slice. J Physiol (1993) 461, 525-547.

Traven HG, Brodin L, Lansner A, Ekeberg O, Wallen P and Grillner S. Computer simulations of NMDA and non-NMDA receptor-mediated synaptic drive: sensory and supraspinal modulation of neurons and small networks. J Neurophysiol (1993) 70, 695-709.

Trussel LO and Fischbach GD. Glutamate receptor desensitization and its role in synaptic transmission. Neuron (1989) 3, 209-218.

Trussel LO, Zhang S and Raman IM. Desensitization of AMPA receptors upon multiquantal neurotransmitter release. Neuron (1993) 10, 1185-1196.

Wall MJ and Dale N. A slowly activating $Ca^{(2+)}$-dependent K^+ current that plays a role in termination of swimming in Xenopus embryos. J Physiol (1995) 487, 557-72.

Wikstrom M, Hill R, Hellgren J and Grillner S. The action of 5-HT on calcium-dependent potassium channels and on the spinal locomotor network in lamprey is mediated by 5-HT1A-like receptors. Brain Research. (1995) 678, 191-9.

Wu WL, Ziskind-Conhaim L and Sweet MA. Early development of glycine- and GABA-mediated synapses in rat spinal cord. J Neurosci (1992) 12, 3935-45.

Yamada KA and Tang C. Benzothiadiazides inhibit rapid glutamate receptor desensitization and enhance glutamatergic synaptic currents. J Neurosci (1993) 13, 3904-3915.

Young AB and Macdonald RL. Glycine as a spinal cord neurotransmitter. In Handbook of the spinal cord, vol. 1, Davidoff RA ed (1983) pp 1-44. Dekker, New York.

Figure index